

**Spatial structure and temporal dynamics
of an intertidal population
of the marine ecosystem engineering worm
Lanice conchilega
(Pallas, 1766)**

Renata M. S. Alves

**Spatial structure and temporal dynamics of an intertidal
population of the marine ecosystem engineering worm
Lanice conchilega (Pallas, 1766)**

ISBN: 978-90-8256-111-1

Ghent University
Faculty of Sciences
Biology Department
Marine Biology Research Group
Campus Sterre S8
Krijgslaan 281
9000 Gent, Belgium

Cover design and photo: Renata M. S. Alves
Cover illustration: Danae Kapasakali
Thesis layout: Renata M. S. Alves
Printed by: Reproduct nv
Voskenslaan 205, 9000 Gent



Academic year 2017-2018

Publicly defended on December 15th, 2017

Co-authors for one or more chapters:

Magda Vincx, Carl Van Colen, Tjeerd J. Bouma, Marijn Rabaut, Jean-Marc Guarini,
Jan Vanaverbeke, Bart De Smet, Cornelis Stal, and Alain De Wulf.

To cite published work reprinted in this thesis, please refer to the original publications as mentioned in the beginning of each chapter.

To cite this thesis, please use the following format:

Alves, R. (2017). Spatial structure and temporal dynamics of an intertidal population of the marine ecosystem engineering worm *Lanice conchilega* (Pallas, 1766). Ghent University, PhD thesis, 238pp.



Spatial structure and temporal dynamics of an intertidal population of the marine ecosystem engineering worm *Lanice conchilega* (Pallas, 1766)

Renata Mamede da Silva Alves

Promoters:

Prof. Ann Vanreusel

Prof. Jean-Marc Guarini

Prof. Magda Vincx

Prof. Tjeerd Bouma

Dr. Carl Van Colen

Dr. Marijn Rabaut

Academic year: 2017-2018

This thesis is submitted in partial fulfilment of the requirements for the degree of

Doctor in Science (Marine Sciences).

Composition of the examination board

(* Reading committee / ^P Promoter)

Prof. Olivier De Clerck
Ghent University, Ghent (Belgium) (chairman)

Prof. Tom Moens
Ghent University, Ghent (Belgium) (secretary)

Dr. Tarik Meziane
National Museum of Natural History, Paris (France) (secretary)

Dr. Emma Michaud *
University of Western Brittany, Brest (France)

Prof. Steven Degraer *
Royal Belgian Institute of Natural Sciences, Brussels (Belgium)

Dr. Olivier Beauchard *
Flanders Marine Institute, Oostende (Belgium)

Prof. Jan Vanaverbeke *
Royal Belgian Institute of Natural Sciences, Brussels (Belgium)

Dr. Cornelis Stal *
Ghent University, Ghent (Belgium)

Prof. Ann Vanreusel ^P
Ghent University, Ghent (Belgium)

Prof. Jean-Marc Guarini ^P
University Pierre and Marie Curie, Paris (France)

Prof. Emeritus Magda Vincx ^P
Ghent University, Ghent (Belgium)

Prof. Tjeerd Bouma ^P
Royal Netherlands Institute of Sea Research, Yerseke (Netherlands)

Dr. Carl Van Colen ^P
Ghent University, Ghent (Belgium)

Dr. Marijn Rabaut ^P
Independent expert, Marine and Renewables

Table of contents

(This table of contents is hyperlinked. Click the titles to navigate.)

Acknowledgements	i
Thesis abstract	iii
Summary	v
Sammenvatting	xi
Résumé	xvii
1. General Introduction	1
1.1. Ecosystem engineering	4
1.2. Ecosystem engineering and time scales	10
1.3. Ecosystem engineering and spatial scales	11
1.4. Introducing the sandmason, <i>Lanice conchilega</i>	16
1.5. Temporal aspects of <i>L. conchilega</i> ecosystem engineering	20
1.6. Spatial aspects of <i>L. conchilega</i> ecosystem engineering	21
1.7. Conservation framework and the status of polychaete aggregations	25
1.8. Study site	27
1.9. Research framework and thesis outline	28
2. A case study on the growth of <i>Lanice conchilega</i> (Pallas, 1766) aggregations and their ecosystem engineering impact on sedimentary processes	33
2.1. Abstract	35
2.2. Introduction	36
2.3. Methods	38
2.3.1. Study site	38
2.3.2. Effects of <i>L. conchilega</i> presence on sedimentary processes	39
2.3.3. Spatially-dependent effects of temporal variability in <i>L. conchilega</i> density	42
2.3.4. Effects of abrupt sedimentation on <i>L. conchilega</i>	43
2.4. Results	44
2.4.1. Effects of <i>L. conchilega</i> presence on sedimentary processes	44

2.4.2. Spatially-dependent effects of temporal variability in <i>L. conchilega</i> density	45
2.4.3. Effects of abrupt sedimentation on <i>L. conchilega</i>	48
2.5. Discussion	49
2.5.1. Effects of <i>L. conchilega</i> presence on sedimentary processes	49
2.5.2. Spatially-dependent effects of temporal variability in <i>L. conchilega</i> density	50
2.5.3. Effects of abrupt sedimentation on <i>L. conchilega</i>	52
2.6. Conclusions	52
3. Effects of temporal fluctuation in population processes of intertidal <i>Lanice conchilega</i> (Pallas, 1766) aggregations on its ecosystem engineering	55
3.1. Abstract	57
3.2. Introduction	58
3.3. Methods	60
3.3.1. Study site	60
3.3.2. <i>In-situ</i> surveys	61
3.3.3. Analyses of temporal variation in population density, structure, and secondary production	63
3.4. Results	65
3.4.1. Temporal patterns in tube density and demographic structure	65
3.4.2. Demographic structure and its consequences to ecosystem engineering	68
3.5. Discussion	73
3.5.1. Temporal patterns in tube density and demographic structure	73
3.5.2. Demographic structure and its consequences to ecosystem engineering	76
4. The use of kite aerial photography and low-altitude digital photogrammetry for studying small-scale spatial patterns in intertidal biogenic reefs	79
4.1. Abstract	81
4.2. Background on remote sensing and the Habitats Directive	82
4.3. Study site	84

4.4. Mapping and monitoring methods	85
4.4.1. Aerial image acquisition	85
4.4.2. Image processing, photogrammetric reconstruction, and <i>L. conchilega</i> detection	88
4.5. Outputs from mapping and monitoring	96
4.5.1. Acquisition, processing, and reconstruction	96
4.5.2. Semi-automated detection protocol	100
4.6. Evaluating mapping and monitoring methods	103
4.6.1. Acquisition, processing, and reconstruction	103
4.6.2. Semi-automated detection protocol	106
4.7. Background on the spatial ecology of polychaete aggregations and <i>Lanice conchilega</i>	109
4.8. Methods to assess the temporal evolution of <i>L. conchilega</i> small-scale distribution	112
4.9. Observations on the temporal evolution of <i>L. conchilega</i> small-scale distribution	112
4.10. Discussion on the temporal evolution of <i>L. conchilega</i> small-scale distribution patterns	115
4.11. Conclusions	118
4.11.1. Mapping, detecting, and monitoring	118
4.11.2. Temporal evolution of <i>L. conchilega</i> small-scale distribution patterns	119
5. Preliminary findings of a simulation-based exercise on the role of feeding in modulating <i>Lanice conchilega</i> population dynamics	121
5.1. Abstract	123
5.2. Introduction	124
5.3. Methods	127
5.3.1. Case-study intertidal population	127
5.3.2. Modeled ecological dynamics	129
5.3.3. Parametrisation	134
5.3.4. Model assumptions	137
5.3.5. Sensitivity analyses	138
5.4. Preliminary results and discussion	142
5.4.1. Findings from the sensitivity analyses	142

5.4.2. Model shortcomings	155
5.5. Preliminary conclusions	158
6. General Discussion	159
6.1. Habitat modification through autogenic engineering	162
6.2. Population dynamics and distribution	165
6.2.1. Interactions with hydrodynamic flow	165
6.2.2. Observed patterns and how they may have formed	172
6.2.3. The role of consumer-resource interactions	179
6.2.4. A note on potential mechanisms for spatial pattern formation	180
6.3. Ecological value and current conservation frameworks	180
6.4. Conclusions and future prospects	184
Addendum I: <i>L. conchilega</i> life cycle	191
Addendum II: Digital elevation models per campaign	195
Addendum III: Orthomosaics per campaign	199
Cited literature	203
Publications list	235

Acknowledgements

Five years ago, I left my home in São Paulo and made my way to Belgium to begin what I like to call the adventures to become a doctor in marine sciences. There have been many ups and downs since then, and sharing my life and work between my two international families in Gent and Banyuls-sur-mer has been both frightening and magical. You have introduced an astounding amount of fun and care in between experiments, field campaigns, late night working sessions, and more. Developing this thesis has been a great challenge, and one that I could not have overcome without the help of great people around me. So in this final stretch, I would like to thank you for being a part of this endeavour. I specifically like to thank the MARES program organisers under the guidance of Tim Deprez, Magda Vincx, and Ann Vanreusel, as well as Ghent University, University Paris VI (UPMC), and the Royal Institute for Sea Research (NIOZ) and their efforts to collaborate for this project. My gratitude also goes out to our funders through a MARES Grant (2012-1720/001-001-EMJD) whose financial support made this project possible. Thank you also to my promoters, Prof. Em. Magda Vincx, Dr. Carl Van Colen, Prof. Tjeerd J. Bouma, Prof. Jean-Marc Guarini, Dr. Marijn Rabaut, and Prof. Ann Vanreusel for their guidance, support, and patience. I consider myself a very lucky student for having had six amazing scientists to guide me through the process of developing a doctoral thesis. Your voices and advice will resonate in all of my future endeavours not only professionally but personally as well, thank you. I particularly like to thank Magda, Carl, and Tjeerd for your advice and understanding. Thank you also to the members of the examination committee for all their feedback, which greatly improved the final manuscript as well as giving me plenty of food for thought.

I also want to thank my collaborators at the Geography Department Dr. Cornelis Stal and Prof. Alain De Wulf as well as Annelies Vandenbulcke for guiding me through the wondrous world of remote sensing and geographical information systems. It has been a mind expanding experience and I couldn't be happier to be able to share it with you. Thank you Coen for your guidance in working the RTK GNSS R6s, learning to work PhotoScan, answering a gazillion of questions about ArcGIS and how to do things, as well as help with testing and checking the work and manuscript. I can't wait to continue our collaboration to get the work published, but I must admit I will miss our meetings and which always started with a hug and were always very inspiring. Thank you everyone who helped with the campaigns: Niels Viaene, Bart Beuselinck,

Carl Van Colen, Francesca Pasotti, Nele De Meester, Annamaria Vafeiadou, Liesbet Colson, Michael Dresel, and Rebeca M. S. Alves. This work would not be possible without your help, and which is more, it would not be as memorable to me. Thank you Niels Viaene, Bart Beuselinck, Dirk Van Gansbeke, Annelien Rigaux, Iarre Lafort, and Lara Macheriotou for helping with sample analyses and cohort analyses measurements. I'm also grateful to Nele De Meester, Bart De Smet, and Carl Van Colen for help translating the thesis summary to Dutch, as well as Aless Osterreicher, Thibaud Mascart, and Elise Toussaint for their help with the French translation. I'd also like to thank the FIRE (Fostering Innovative Research based on Evidence) statistical force, in particular Dr. Rosanna Overholser from the Department of Applied Mathematics, Computer Sciences and Statistics, and Emmanuel Abatih for their assistance with the analyses for chapter 2 (2014-098-RHO) and 3 (2016-0027-ENA).

Thank you also to the people who welcomed and supported me in the marine station at Banyuls-sur-mer. Sandrine Fanfard, Mariana Padron, Mareike Volkenandt, and Florence Britton for their friendship, support, advice, as well as help with modelling and programming. Thanks also to all the people who made my time in Banyuls so cheerful and eventful: Stefan Lambert, Belén Quintana, Peter Hofmann, Hugo, Laetitia Dadaglio, Lola Paradinas, Theo, Fanny, Marine, Anaïs Schendekehl, Coco Koedooder, Inne Withouck, and Tara Van Belleghen (a.k.a. Her Royal Highness Pillow Princess Tara Von Belleghem, The First of The Teary Goodbyes, L'Extraordinaire Solo Moments Comme Le Bateau, Brazilian at Heart Chocolate Sprinkler, Protector of the Marine Realm, and Mother of Dinosaurs). Life in Banyuls was amazing mostly because of you, and I will always treasure that time. Thank you also to my "ghentian family": Lua Monteiro and Johan, Francesca Pasotti and Blu, Lara Macheriotou, Nils Luyten, Michael Dresel, Annamaria Vafeiadou, Danae Kapasakali, Christoph Mensens, Alex Sotillo, Tânia Nara, Valentina Filimonova, Sofia Ramalho, EeZin Ong, and Veronica Lo. I can't even begin to describe how important you are to me, or how grateful I am to call you friends. Last, but not least, I want to thank my family. You inspire me to do better and continue moving forward.

Indeed it has been an amazing experience, and so many people have contributed to it. So, if I forgot anyone, I apologise. To everyone, thanks again for being a part of these last 5 years, and consider yourselves hugged (for those who are hug-inclined), and/or kissed (for those who are kiss-inclined).

Sincerely,

A handwritten signature in blue ink, appearing to read 'Luca Monteiro', with a stylized flourish at the end.

Thesis Abstract

Lanice conchilega is an ecosystem engineering polychaete worm. It forms tube aggregations in temperate coastal zones, being particularly abundant in Europe. Tube aggregations engineer sandy-muddy marine sediments by posing as physical barriers which modulate water flow on the sediment surface, increasing local sedimentation and creating distinct micro-habitats within tube arrays for other organisms. Although previous research has greatly contributed to our understanding of how this organism engineers marine sediments, processes pertaining to formation and decay of its aggregations remained unclear. **The main objective of this thesis was to elucidate these processes, in particular, to determine the role of population dynamics on engineering effects and the formation and decay of intertidal *L. conchilega* aggregations.** Experiments were executed exploring the relationships between population dynamics, sedimentation, and mortality (**chapter 2**). Findings revealed that dense aggregations induce locally higher sedimentation and more stable sediments in comparison to bare surfaces. Abrupt sedimentation triggered tube-accretion and may form a positive feedback wherein growing tubes cause further sedimentation, hence contributing to aggregation maintenance. However, abrupt sedimentation of 5-12cm in height may hinder maintenance by increasing population mortality through smothering, which diminishes tube density and undermines further flow modulation. We also assessed temporal patterns in population structure, and investigated how these relate to ecosystem engineering by *L. conchilega* on marine sediments through monthly *in-situ* monitoring of intertidal aggregations (**chapter 3**). This revealed that seasonal population dynamics and demographic composition influence the temporal evolution of *L. conchilega* engineering effects, intensifying in periods of high density (*i.e.* recruitment), and decaying during periods of harsh conditions (*i.e.* winter). We also assessed the temporal evolution, persistence, and longevity of small-scale distribution patterns for intertidal *L. conchilega* aggregations (**chapter 4**). It was found that the formation of small-scale spatial patterns was associated to the aforementioned recruitment periods, prompting the formulation of a hypothetical conceptual model for aggregation formation and decay. We postulate that yearly recruitment in spring and autumn result in population replenishment and the formation of early small-scale spatial patterns. The latter are likely modified by continuing settlement and post-settlement survival giving rise to different small-scale distribution patterns, while

aggregation decay was shown to occur apart from recruitment and likely due to population mortality. Lastly, we explored an alternative conceptual model for spatial-pattern formation in *L. conchilega* aggregations by performing a modelling exercise assessing the role of food availability and assimilation on population dynamics (**chapter 5**). Findings from the exercise suggest that food availability and assimilation are likely to only marginally influence population density dynamics, which seems to be determined largely by the recruitment intensity. This thesis has led us to conclude that spatial-pattern formation in *L. conchilega* aggregations is likely delineated by conditions during settlement and factors influencing post-settlement survival. Since hydrodynamic conditions often influence settlement and recruitment, we suggest that future research focus on the effects of hydrodynamic stress in *L. conchilega* larval settlement and survival at very small spatial scales.

Summary

In 1994, Jones and co-authors penned the term 'ecosystem engineers' to describe organisms that modulate resources to other species by causing state changes in biotic and/or abiotic environmental properties and/or processes. These organisms can have tremendous impact on ecosystems, shaping the environment they live in. One example is the beaver (*Castor sp.*). It constructs dams that interrupt river flow and cause flooding, consequently changing conditions which affect species composition across the landscape. Beavers are considered allogenic engineers, that is, they are organisms that cause change through their actions (in this case dam construction). Other organisms may cause change simply through presence, and in these cases they are called autogenic engineers. Reef-building organisms fall under the latter category, providing complex structures with a myriad of micro-habitats and conditions to other species. The calcareous constructs built by coral reefs, for example, provide such an abundance of resources that they sustain extensive trophic webs and extremely high species richness. Coastal and marine environments have a plethora of organisms that may be considered ecosystem engineers. For example, sting rays create feeding pits that provide shelter, mangrove crabs make burrows that modulate sediment biogeochemistry to microbial communities, and marsh tussocks modulate water flow creating distinct micro-habitats within the canopies for other species. This thesis focused on one case-study of autogenic engineering in the coastal environment, that of the sessile tube-building polychaete *Lanice conchilega*.

Lanice conchilega is a terebellid worm that constructs tube aggregations. These can be considered reefs due to their extensive effects on both biotic and abiotic environmental properties. *Lanice conchilega* aggregations autogenically engineer marine sediments by attenuating water flow as it passes through tube arrays. This affects the sedimentation regime locally and reduces hydrodynamic stress within the aggregations. The changes imposed by *L. conchilega* may result in distinct micro-conditions within an aggregation than that of the surrounding habitats, often sustaining high species richness and abundance. Autogenic effects from *L. conchilega* aggregations can vary across space and time. Aggregations may present patchy distributions, engineering alternating portions of a landscape and increasing spatial heterogeneity. They can also be ephemeral, disappearing in moments of high environmental stress, such as winter. Although previous research has greatly contributed to our understanding of how this organism engineers marine sediments,

several knowledge gaps remained that were addressed in this thesis. These gaps are summarized further, however, an in-depth description of knowledge gaps can be found in **chapter 1** alongside descriptions of our study site and the organism of study. **Our main objective was to elucidate the role of population dynamics on engineering effects and the formation and decay of intertidal *L. conchilega* aggregations.** We focused on an intertidal *L. conchilega* population as a case study, located on the sandy beach of Boulogne-sur-mer (Nord Pas-de-Calais, France). We employed short-term experiments, medium-term monitoring (*i.e.* 1.5 years), remote sensing, and ecological modelling to achieve our main objective. What follows is a summary of the work executed for this thesis.

Previous research employing model simulations suggest that flow attenuation by *L. conchilega* aggregations is a density-dependent process wherein high density aggregations attenuate flow more than low density ones. This relationship is likely nonlinear, that is, flow attenuation should cease to intensify past a density threshold. Nevertheless, a hypothetical mechanism for vertical expansion of *L. conchilega* aggregations was offered by the aforementioned research. High fine sediment deposition from autogenic engineering may trigger tube accretion, causing vertical expansion of an aggregation and further fine sediment deposition. This hypothetical mechanism was explored in **chapter 2**, wherein we investigated the autogenic engineering effects of *Lanice conchilega* aggregations through short-term experiments. Weekly *in-situ* estimations of sedimentary properties revealed that *L. conchilega* aggregations with density ranging between 3 200 and 16 318 ind·m⁻² have significantly different sedimentary properties than bare sand. However, properties did not vary within that density range, indicating that the relationship between flow attenuation and density is nonlinear. *In-situ* monitoring of *L. conchilega* density and several environmental properties for 3 weeks revealed marginally different temporal trends between centre and edges of aggregations following a natural disturbance (*i.e.* storm). This hinted at the presence of gradients within the aggregations that may contribute to the formation of patchy distributions. Lastly, a laboratory experiment revealed significantly higher mortality rates and tube building activity in the presence of sediment deposition between 5cm and 12cm in column height. As such, our findings are in agreement with the previous hypothetical mechanism, suggesting that a positive feedback between sedimentation and tube-building activity may drive vertical expansion. However, the latter may be limited by deposition-induced mortality.

Tube dimensions as well as protruding height above the sediment surface determines autogenic engineering effects from polychaete tube aggregations by modulating their area of flow obstruction. During its development, *L. conchilega* individuals can grow from <1mm to approx. 5-6mm in inner tube diameter. As population dominance shifts from a majority of juveniles to adults, it can be expected that the area of flow obstruction per aggregation will change. As such, population dynamics and demographic structure may impact autogenic engineering effects. Previous research has addressed the relationship between engineering effects and physical characteristics of the tubes with experiments using mimic tubes and ecological modelling. However, there was still a knowledge gap on the role of changing tube dimensions and seasonal density fluctuations as *in-situ* populations had not been considered. This gap was addressed in **chapter 3**, wherein we analysed the seasonal evolution of population dynamics and ecosystem engineering effects of our case-study intertidal population. *In-situ* monitoring lasting 1.5 years revealed two recruitment periods: one in spring (during April) and one in autumn (during September-October). The spring recruitment had higher density of recruits (*i.e.* approx. 30 000 ind·m⁻²) than the one in autumn (*i.e.* approx. 4 000 ind·m⁻²), and this high density was associated to distinct environmental properties. This indicates that demographic processes may be responsible for periods of pronounced ecosystem engineering. Nevertheless, mass mortality severely reduced population density during winter. However, the population persisted, likely due to recruits from other populations, which are associated to short- and long-term population dynamics.

Lanice conchilega frequently displays a patchy or fragmented small-scale distribution, increasing spatial heterogeneity across the landscape which constitutes part of their ecological value. Their tube aggregations expand habitat availability to associated species, enabling an increase in species richness and abundance as previously mentioned. Previous research have focused on population dynamics and ecosystem engineering, but failed to encompass small-scale spatial dynamics. As such, knowledge on the small-scale distribution of *L. conchilega* aggregations is scarce despite its importance. This is likely due in part to difficulties of traditional sampling methods in properly sampling heterogeneous landscapes at the required resolutions (< 1m). To the best of our knowledge, there had not been a thorough characterisation of *L. conchilega* small-scale spatial patterns until the present work. We addressed this gap in **chapter 4**, wherein our case-study population was monitored for 1.5 years using kite aerial photography (KAP) and low-altitude digital photogrammetry to map

their small-scale distribution at ultra-high spatial resolution (*i.e.* approx. 3mm). These mapping methods produced 12 orthomosaics and digital elevation models with very-high resolution and small local errors, enabling accurate measurement taking from the material. However, global large errors hindered analytical change detection, as such, analyses of the temporal evolution of *L. conchilega* small-scale distribution patterns was executed through visual interpretation. These were novel methods that enabled the characterisation of *L. conchilega* small-scale distribution patterns at unprecedented resolution. Further analyses on method performance can be found in chapter 4. Three distribution types were observed during our survey: patches, beds, and interrupted beds. Their differing morphologies indicated distinct mechanisms of formation. Distribution types were formed following recruitment periods, suggesting that pattern formation is a consequence of interactions between larval settlement and hydrodynamic conditions during that period. As such, these interactions are likely responsible for the variance in small-scale distribution types.

Distribution patterns are often a consequence of multiple mechanisms working in tandem. As such, additional mechanisms for spatial pattern formation were also considered during the development of this thesis. These include consumer-resource interactions, wherein the distribution of an organism is dictated by a resource that it requires. *Lanice conchilega* is both a filter- and deposit-feeder, consuming mainly microorganisms from the water column and sediment surface. Previous flume experiments suggest that filter-feeding by *L. conchilega* worms can cause local water column depletion, creating gradients in food concentration that may impact individual worms downstream. Additionally, filter-feeding may be affected by competition for food, as has been shown for *L. conchilega* and the Pacific cupped oyster *Crassostrea gigas* in the Bay of Veys (France). As such, we explored the impact of consumer-resource interactions on population dynamics through a population model in **chapter 5**. A modelling framework was employed due to the complexity of *L. conchilega* feeding ecology, and it analysed potential effects of food limitation and assimilation on population. Preliminary results from the population model simulations suggest only a marginal importance of consumer-resource interactions on adult *L. conchilega* density dynamics. During our study, total density dynamics were mostly influenced by recruitment intensity and subsequent mortality. Thus, our preliminary findings highlighted the importance of recruitment and establishment of juvenile cohorts for total population density dynamics.

The insights gained on *L. conchilega* population dynamics and autogenic engineering through time and space during this thesis work was summarised and integrated in **chapter 6**. The chapter addresses the relationships between population dynamics and autogenic engineering, as well as potential mechanisms of spatial pattern formation. Lastly, it discusses how our findings can support ecosystem-based approaches to conservation, and presents future prospects for research.

In conclusion, our findings support a nonlinear engineering relationship between tube density and flow attenuation, the latter ceasing to intensify past a density threshold of 3 200 ind·m⁻². Sedimentation may indeed contribute to the vertical expansion of *L. conchilega* aggregations, whereas catastrophic sedimentation may not only contribute but also limit it by inducing higher mortality. Density gradients within aggregation may contribute to the formation of patchy distributions by modulating vertical expansion in addition to creating patch-work ecosystem engineering effects across a landscape. However, further research needs to investigate whether significantly distinct densities occur between portions of an aggregation. Population dynamics influence intensity of autogenic engineering creating seasonal cycles of effects by likely modulating the area of flow obstruction. This may also contribute to the formation of patchy distributions in addition to gradients in density between portions of an aggregation. However, it seems more likely that processes pertaining to larval settlement and recruitment have higher importance in the formation of small-scale spatial patterns in *L. conchilega* populated landscapes. We hypothesise that these processes may originate density gradients due to influences from hydrodynamic forcing, and/or enhance them due to adult presence facilitation through attenuation of hydrodynamic forcing. These hypothetical mechanisms may provide guidance to future research.

Samenvatting

Jones en coauteurs definieerden voor het eerst de term 'ecosysteem ingenieurs' in 1994, waarbij ze organismen beschreven die de toegang tot bepaalde bronnen voor andere organismen veranderden door aanpassingen in biotische en/of abiotische omgevingseigenschappen en/of –processen. Deze organismen kunnen een enorme impact hebben op ecosystemen, en vormen zo de omgeving waarin ze leven. Een bekend voorbeeld is de bever (*Castor sp.*), die dammen bouwt die de stroming van rivieren onderbreken, waardoor overstromingen veroorzaakt worden. Deze veranderde condities hebben tot gevolg dat de soortensamenstelling veranderd langsheen dit landschap. Bevers worden 'allogene ingenieurs' genoemd: organismen die veranderingen veroorzaken door hun activiteit (in dit voorbeeld het bouwen van dammen). Andere organismen kunnen simpelweg door hun aanwezigheid veranderingen teweegbrengen. Deze organismen worden 'autogene ingenieurs' genoemd. Rif bouwende organismen behoren tot deze laatste categorie, ze voorzien complexe structuren met een groot aantal micro-habitats en condities voor andere soorten. De kalkstructuren gebouwd door koraal bijvoorbeeld, zorgen voor een rijke hoeveelheid aan bronnen. Hierdoor kunnen ze een hoge biodiversiteit en een uitgebreid voedselnetwerken ondersteunen. Langsheen de kust en in mariene omgevingen vinden we een overvloed aan organismen die kunnen beschouwd worden als ecosysteem ingenieurs. De pijlstaartrog, bijvoorbeeld, creëert voedselputten die bescherming voor andere organismen voorzien. Krabben in mangroves maken gangen die de biogeochemie van sedimenten veranderen, evenals de microbiële gemeenschappen. Marsh-pollen moduleren de waterstroom en creëren verschillende microhabitats tussen grassprietten voor andere soorten. Deze thesis focust op één bepaalde ecosysteem ingenieur langsheen kusten: de sessiele kokerworm *Lanice conchilega*.

Lanice conchilega is een borstelworm van de familie *Terebellidae* die een koker bouwt. Een opeenhoping van deze kokers kan worden beschouwd als een rif omwille van het extensief effect op zowel biotische als abiotische omgevingskenmerken. Aggregaties van *Lanice conchilega* zullen autogeen mariene sedimenten gaan bewerken door de waterstroom te verzwakken wanneer die tussen en boven de kokers passeert. Dit beïnvloedt lokaal de sedimentatie en vermindert de hydrodynamische stress binnen de aggregatie van kokers. Deze veranderingen, bewerkstelligd door *L. conchilega*, kunnen leiden tot verschillende micro-condities

binnen deze aggregaties wat meestal een hogere soortenrijkdom en populatie densiteit vergeleken met de omliggende habitats tot gevolg heeft. Autogene effecten van de aggregaties van *L. conchilega* kunnen variëren afhankelijk van plaats en tijd. De aggregaties kunnen bestaan uit onregelmatige patches, afwisselende delen van het landschap die beïnvloed worden, en een verhoogde ruimtelijke heterogeniteit creëren. De aggregaties kunnen ook tijdelijk zijn, waarbij ze verdwijnen tijdens periodes van hoge omgevingsstress, zoals tijdens de winter. Hoewel eerder onderzoek sterk heeft bijgedragen tot het begrijpen van hoe deze organismen de mariene sedimenten kunnen bewerken, zijn er nog steeds gaten in onze kennis. Deze zullen in deze thesis belicht worden. Een gedetailleerd overzicht over deze kennis lacunes omtrent deze organismen en hun interactie met hun leefomgeving, kan teruggevonden worden in **hoofdstuk 1**, samen met een beschrijving van de studieplaats en de organismen. **Ons belangrijkste doel was de rol van populatiedynamieken op het ingenieurs effect van de kokerworm te verduidelijken en de vorming van de intertidale *L. conchilega* aggregaties in ruimte en tijd te bestuderen.** De focus lag op een intertidale *L. conchilega* populatie op het zandstrand van Boulogne-sur-mer (Nord Pas-de-Calais, Frankrijk). We pasten korte experimenten toe, gecombineerd met middellange termijn monitoring (anderhalf jaar), teledetectie en ecologische modellen om deze doelen te bewerkstelligen. Wat volgt is een samenvatting van deze thesis.

Eerder onderzoek gebruikte simulaties die veronderstelden dat de stroomvermindering, veroorzaakt door de *L. conchilega* aggregaties, een densiteitsafhankelijk proces is, waarbij aggregaties met hoge densiteit de waterstroom meer verzwakken dan aggregaties met lagere densiteit. Echter, dit verband lijkt eerder niet-lineair waarbij de verzwakking van de stroom ophoudt wanneer een bepaalde densiteit bereikt is. Het hierboven vermelde onderzoek stelde eveneens een hypothetisch mechanisme voor de verticale expansie van *L. conchilega* aggregaties voor, namelijk dat de depositie van fijn sediment door autogene ingenieurs de aangroei van kokers kan versnellen, met een verdere verticale expansie van de aggregatie en een verdere depositie van fijn sediment. Deze hypothese werd onderzocht in **hoofdstuk 2**. In dit hoofdstuk werden de autogene ingenieurseffecten van *L. conchilega* aggregaties door middel van korte experimenten bestudeerd. Wekelijkse *in-situ* schattingen toonden aan dat *L. conchilega* aggregaties met densiteiten van 3 200 and 16 318 ind·m⁻² significant verschillende sediment kenmerken vertoonden dan sediment zonder organismen.

xii

Binnen dit dichtheitsbereik verschillen de kenmerken echter niet, wat aantoont dat het verband tussen de verzwakking van de stroom en de dichtheid niet-lineair is. *In-situ* monitoring van *L. conchilega* dichtheiten en omgevingskenmerken gedurende 3 weken, toonde aan dat er kleine tijdelijke verschillen bestaan tussen het centrum en de randen van de aggregaties, wanneer een natuurlijke verstoring (storm) had plaatsgevonden. Dit toont aan dat de aanwezigheid van gradiënten binnen de aggregaties kan leiden tot onregelmatige distributies. Bovendien toonde een laboratoriumexperiment aan dat er significant hogere mortaliteit en snellere kokervorming terug te vinden was wanneer er een sedimentdepositie tussen 5cm en 12cm in kolomhoogte plaats vond. Deze bevindingen bevestigen de eerder vermelde hypothese, en toont aan dat een positieve terugkoppeling tussen sedimentatie en kokervorming kan leiden tot verticale expansie. Dit laatste kan echter wel gelimiteerd worden door een verhoogde mortaliteit ten gevolge van de depositie.

Zowel de dimensies van de koker als de uitstekende hoogte boven het sedimentoppervlak beïnvloeden de ingenieurseffecten van de kokerworm aggregaties, en dit door middel van het beïnvloeden van het areaal waar de waterstroom wordt tegengehouden. Tijdens hun ontwikkeling kunnen *L. conchilega* individuen groeien van <1mm tot ongeveer 5-6mm in diameter. Wanneer populaties veranderen van een dominantie aan juvenielen naar een dominantie aan volwassenen, kan er verwacht worden dat deze het areaal waar de stroom verzwakt wordt, zullen veranderen. Populatiodynamieken en demografische structuur kunnen op deze manier de autogene ingenieurseffecten beïnvloeden. Door middel van experimenten met nekkokers en ecologische modellen toonde eerder onderzoek een verband tussen ingenieurseffecten en fysische kenmerken van de kokers aan. Er ontbreekt echter nog steeds kennis met betrekking tot de rol van veranderende kokerdimensies en seizoensdichtheitsfluctuaties, want *in-situ* populaties werden tot nu toe in deze context niet onderzocht. Dit werd verder bestudeerd in **hoofdstuk 3**, waarin seizoens evoluties van populatiodemografie en de effecten van de ecosysteem ingenieurs van de bestudeerde populatie werden geëvalueerd. *In-situ* monitoring gedurende anderhalf jaar toonde aan dat er twee periodes van rekrutering zijn: één in de lente (april) en één tijdens de herfst (September-Oktober). De rekrutering in de lente leidde tot hogere dichtheiten van rekruten (ongeveer 30 000 ind·m⁻²) vergeleken met deze in de herfst (ongeveer 4 000 ind·m⁻²), en deze hoge dichtheiten waren geassocieerd met sterke veranderingen in sediment eigenschappen. Dit toont aan dat demografische processen verantwoordelijk kunnen zijn voor sterke

ecosysteem ingenieurs effecten. Massale mortaliteit zorgde echter voor een sterke afname in populatiedensiteit tijdens de winter. De bestudeerde populatie kon vermoedelijk overleven door rekruten van andere populaties.

Op kleine schaal vertoont *L. conchilega* frequent een onregelmatig en gefragmenteerde distributie, wat zorgt voor een verhoging van de ruimtelijke heterogeniteit in het landschap. Dit draagt mee bij tot de ecologische waarde van de soort. De kokeraggregaties zorgen voor een uitbreiding van de aanwezige habitats die beschikbaar zijn voor geassocieerde soorten, wat kan leiden tot een verhoging in soortenrijkdom en populatie densiteiten. Eerder onderzoek legde de nadruk op populatiedynamieken en ecosysteem ingenieurs effecten, maar hield meestal geen rekening met ruimtelijke dynamieken op kleine schaal. Kennis omtrent de distributie van *L. conchilega* aggregaties op kleine schaal is nog steeds beperkt voornamelijk doordat traditionele staalname methodes niet toelaten om in heterogene landschappen de verspreiding op een kleine ruimtelijke schaal (< 1m) accuraat te onderzoeken. Voor zover geweten is er geen karakterisatie van ruimtelijke patronen op kleine schaal van *L. conchilega* terug te vinden. Dit werd bestudeerd in **hoofdstuk 4**, waar de studiepopulatie gedurende anderhalf jaar werd gemonitord met behulp van fotografie aan de hand van een vlieger (kite aerial photography, KAP) en digitale fotogrammetrie op lage hoogte. Deze innovatieve methode zorgde ervoor dat de karakterisatie van de verspreiding van *L. conchilega* op een ultrahoge resolutie (*i.e.* ong. 3mm) mogelijk werd. Drie distributietypes werden geobserveerd gedurende dit onderzoek: patches, aggregaties en onderbroken aggregaties. De verschillen in morfologie tonen verschillen in vorming aan. De distributietypes werden gevormd na de rekruteringsperiodes, wat aantoont dat ruimtelijke patronen gevormd worden als gevolg van interacties tussen larvale rekrutering en hydrodynamische condities gedurende deze periode.

Distributiepatronen zijn vaak het gevolg van de wisselwerking tussen verschillende mechanismen. Aanvullende mechanismen voor ruimtelijke patroonvorming werden daarom ook bekeken tijdens deze thesis. Deze omvatten interacties tussen gebruiker en bron, waarbij de distributie van een organisme afhangt van de bronnen die het nodig heeft. *Lanice conchilega* is zowel een filter- als een depositievoeder, waarbij respectievelijk voornamelijk microorganismen vanuit het water en het sediment worden opgenomen. Eerder uitgevoerde experimenten suggereren dat filtervoeding in *L. conchilega* een uitputting van voedsel in de lokale waterkolom kan veroorzaken,

waarbij gradiënten in voedselconcentratie ontstaan, die op hun beurt de overleving en verspreiding van individuen kan beïnvloeden. Bovendien kan het filtervoeden beïnvloed worden door competitie voor voedsel, zoals al aangetoond voor *L. conchilega* en de Japanse oester *Crassostrea gigas* in de baai van Veys (Frankrijk). Om deze reden, onderzochten we in **hoofdstuk 5** de impact van de gebruiker-(voedsel)bron interacties op de dichtheidsdynamieken van *L. conchilega* door middel van een populatiemodel. Omwille van de complexiteit van de voedsel-ecologie van *L. conchilega* werd een modelleerkader gebruikt om de potentiële effecten van voedsel-limitatie en assimilatie op de populatie te analyseren. Voorlopige resultaten van de simulaties van het populatiemodel suggereren een beperkt belang van de gebruiker-bron interacties op dichtheidsdynamieken van adulte *L. conchilega*. Tijdens onze studie werden totale dichtheid dynamieken meestal beïnvloed door de intensiteit van rekrutering en de mortaliteit die hier op volgde. Onze voorlopige resultaten tonen het belang van rekrutering en de ontwikkeling van juveniele cohorten aan voor totale populatie dynamieken.

De inzichten in populatiedynamieken en autogene ingenieur-effecten van *L. conchilega* doorheen de tijd en ruimte werden samengevat en geïntegreerd in **hoofdstuk 6**. Dit hoofdstuk bespreekt het belang van verschillende temporele en ruimtelijke schalen voor de effecten van ecosysteem ingenieurs en hun rol in het bepalen van de distributie van *L. conchilega* op kleine ruimtelijke schaal. Bovendien wordt er bespreekt hoe onze bevindingen kunnen bijdragen tot het behoud van ecosystemen. Mogelijke toekomstige plannen worden tevens besproken.

Als besluit kan gesteld worden dat onze bevindingen een niet-lineair verband tussen kokerdichtheid en stroomvermindering bevestigen. Deze stroomvermindering nam niet meer toe vanaf een dichtheid van 3 200 ind·m⁻². Verder tonen we aan dat sedimentatie inderdaad kan bijdragen tot de verticale expansie van *L. conchilega* aggregaties, maar ook bijdraagt tot een hogere mortaliteit wat verticale expansie kan limiteren. Dichtheidsgradiënten binnen de aggregaties kunnen bijdragen aan de vorming van gefragmenteerde distributies door verticale expansie te beheersen en ongelijke effecten in een landschap te creëren. Toekomstig onderzoek zal moeten aantonen of sterk verschillende dichtheiden effectief voorkomen binnen verschillende delen van een aggregatie. Populatiedynamiek beïnvloedt de intensiteit van autogene engineering en creëert seizoensgebonden variatie in hun effect op mariene sedimenten door het bepalen van het gebied van stromingsobstructie. Dit kan ook

bijdragen tot de vorming van een onregelmatige verspreiding, aanvullend op gradiënten in densiteit tussen delen van een aggregatie. In het bijzonder lijken de processen met betrekking tot de kolonisatie en rekrutering van juvenielen het grootste aandeel te hebben in de vorming van kleinschalige ruimtelijke patronen in landschappen waar *L. conchilega* voorkomt. We veronderstellen dat deze processen dichtheitsgradiënten doen ontstaan als gevolg van de interactie met hydrodynamische invloeden, en/of dat de aanwezigheid van adulte organismen die deze interacties versterken door hydrodynamische invloeden af te zwakken. Deze hypothesen kunnen als leidraad voor toekomstig onderzoek dienen.

Résumé

En 1994, Jones et co-auteurs définirent le terme “ingénieurs d'écosystème” afin de décrire tout organisme capable de moduler l'allocation de ressources à d'autres espèces en changeant les propriétés et/ou processus biotiques et/ou abiotiques de l'environnement. Ces organismes peuvent impacter largement les écosystèmes en modulant leur habitat. Un exemple est le castor (*Castor sp.*). Cette espèce construit des barrages sur des rivières, qui interrompent le flux d'eau et causent des inondations, ayant pour conséquence le changement de conditions environnantes, affectant ainsi la composition des espèces à travers le paysage. Les castors sont considérés des espèces-ingénieur (ou ingénieurs d'écosystème) allogéniques, c'est-à-dire des organismes qui changent l'environnement au travers de leurs actions (dans le cas présent, la construction de barrages). D'autres espèces peuvent causer des changements simplement par leur présence, et sont alors appelées des espèces-ingénieur autogéniques. Les organismes constructeurs de récifs appartiennent à cette dernière catégorie, fournissant une structure complexe présentant une myriade de micro-habitats et conditions à d'autres espèces présentes. Les constructions calcaires engendrées par les récifs coralliens, par exemple, offrent une abondance de ressources capable de maintenir de vastes réseaux trophiques ainsi qu'une biodiversité extrêmement élevée. Les environnements marins et côtiers présentent une pléthore d'organismes pouvant être considérés ingénieurs d'écosystème. Les raies pastenague, par exemple, créent des puits d'alimentation qui servent d'abri; les crabes de mangrove font des terriers qui la biogéochimie du sédiment utilisé par les communautés microbiennes, et les touffes d'herbes en zone marécageuse régulent les flux d'eau, créant ainsi des micro-habitats distincts dans les auvents pour d'autres espèces. Cette thèse se concentre l'étude d'un organisme ingénieur présent en environnement côtier, le polychète Tubicole sédentaire, *Lanice conchilega*.

Lanice conchilega est un ver térebelle qui construit des agrégats de tubes. Ces derniers peuvent être considérés des récifs dus à leurs effets sur les caractéristiques biotiques et abiotiques de l'environnement. Les massifs de *Lanice conchilega* ont un effet d'ingénierie autogénique sur le sédiment marin en atténuant l'écoulement de l'eau lorsqu'elle traverse les réseaux de tubes. Cela affecte localement le régime sédimentaire et réduit le stress hydrodynamique dans ces agrégations. Les changements imposés par *L. conchilega* peuvent entraîner des micro-conditions au

centre de ces agrégats distinctes de celles des habitats environnants, contribuant souvent à la richesse et abondance importance d'espèces. Les effets autogéniques de *L. conchilega* peuvent varier dans le temps et l'espace. Les agrégations peuvent présenter des distributions inégales et une modification alternée du paysage, augmentant ainsi l'hétérogénéité spatiale. Elles peuvent également être éphémères, et disparaître lors de moments de stress environnemental élevé, comme en hiver. Bien que des recherches antérieures aient grandement contribué à notre compréhension de la façon dont cet organisme modifie les sédiments marins, plusieurs lacunes dans ce domaine ont été abordées dans cette thèse. Ces lacunes sont résumées ultérieurement, et leur description détaillée peut être trouvée dans le **chapitre 1**, ainsi que la description des lieux et de l'organisme d'étude. **Notre objectif principal était d'élucider le rôle des dynamiques de la population sur les effets d'ingénierie ainsi que sur la formation et la décomposition des agrégations de *L. conchilega* en zone intertidale.** Nous nous sommes concentrés sur une population intertidale de *L. conchilega* comme cas d'étude, située sur la plage de sable de Boulogne-sur-Mer (Nord Pas-de-Calais, France). Nous avons effectué des expériences à court terme, un suivi à moyen terme (c-à-d. 1.5 ans), de la télédétection ainsi que de la modélisation écologique afin de répondre à notre question. Ce qui suit est un résumé du travail exécuté pour cette thèse.

Plusieurs études utilisant des modèles de simulation suggèrent que l'atténuation du débit par les récifs de *L. conchilega* est un processus dépendant de la densité dans lequel les agrégations de haute densité réduisent le flux de façon plus importante que les agrégations moins denses. Cette relation est probablement non linéaire, c'est-à-dire que la réduction du débit devrait cesser d'intensifier après un seuil défini de densité. Néanmoins, un mécanisme hypothétique d'expansion verticale de *L. conchilega* a également été proposé par l'étude mentionnée ci-dessus. Les dépôts de sédiments fins élevés générés par l'ingénierie autogénique peuvent déclencher l'accrétion de tube, causant alors l'expansion verticale d'une agrégation et ainsi une d'autres dépôts de sédiments fins en hauteur. Cette hypothèse est testée dans le **chapitre 2**, où nous avons étudié les effets d'ingénierie autogénique des agrégations de *Lanice conchilega* à travers des expériences à court terme. Les estimations hebdomadaires *in-situ* des propriétés sédimentaires ont révélé que les récifs de *L. conchilega* ayant une densité comprise entre 3 200 et 16 318 ind·m⁻² ont des propriétés de sédimentation significativement différentes de celles des zones de sable nu. Cependant, ces propriétés ne varient pas dans cet intervalle de densité,

xviii

indiquant donc une relation non-linéaire entre l'atténuation du débit et la densité des agrégations.

L'analyse *in-situ* de la densité en *L. conchilega* et d'une variété de facteurs environnementaux pendant 3 semaines a relevé des tendances temporelles marginalement différentes entre le centre et les bords des agrégations suite à une perturbation naturelle (c-à-d. tempête). Cela indique la présence possible de gradients au sein des agrégations pouvant contribuer à la formation de distributions inégales. Enfin, une expérience de laboratoire a révélé des taux de mortalité significativement plus élevés et une activité de construction de tubes en présence de dépôts de sédiments entre 5 et 12 cm de hauteur de colonne. Ces résultats sont en accord avec l'hypothèse d'accrétion verticale présentée précédemment, ce qui suggère qu'un retour positif entre la sédimentation et l'activité de construction de tubes peut entraîner une expansion verticale. Cependant, cette dernière peut être limitée par la mortalité induite par le dépôt.

Les dimensions ainsi que la hauteur en saillie du tube au-dessus du sédiment déterminent l'impact des agrégations de tube de polychètes en tant qu'ingénieur d'écosystème en changeant l'aire totale obturant le flux d'eau. Au cours de leur développement, les individus de *L. conchilega* peuvent croître de <1mm à environ 5-6 mm dans le diamètre du tube intérieur. À mesure que la domination de la population passe d'une majorité de juvéniles à une majorité d'adultes, on peut s'attendre à ce que l'aire d'obstruction de flux par l'agrégation change. En tant que tel, les dynamique et structure démographiques peuvent avoir un impact sur les effets de l'ingénierie autogénique. Des études précédentes ont abordé la relation entre les effets d'ingénierie et les caractéristiques physiques des tubes, lors d'expériences utilisant des tubes de simulation et des modélisations écologiques. Cependant, un manque de connaissance persistait concernant le rôle du changement de dimension des tubes, et les fluctuations saisonnières de densité, car les populations *in-situ* n'avaient pas été prises en compte. Ceci a été abordé dans le **chapitre 3**, dans lequel nous avons étudié l'évolution saisonnière de la dynamique de population ainsi que des effets d'ingénierie de la population intertidale de notre cas d'étude. Le suivi *in-situ* de 1.5 ans a révélé deux périodes de recrutement de larves: l'une au printemps (en avril) et l'autre en automne (pendant Septembre-Octobre). Le recrutement de printemps était plus important (environ 30 000 ind.m⁻²) que celui d'automne (environ 4 000 ind.m⁻²), et la densité élevée était due à des

conditions environnementales précises. Cela indique que les processus démographiques peuvent être responsables, selon les périodes, d'effets d'ingénierie écosystémique plus prononcés. Néanmoins, une mortalité massive a considérablement réduit la densité de la population pendant l'hiver. Cette dernière a cependant persisté, probablement en raison du recrutement d'individus appartenant à d'autres populations, associés aux dynamiques de court et long-terme.

Lanice conchilega présente souvent une distribution inégale ou fragmentée sur une petite échelle, augmentant ainsi l'hétérogénéité spatiale de l'environnement constituant une partie de leur valeur écologique. Leurs massifs de tubes multiplient les possibilités d'habitat aux espèces associées, permettant alors une richesse et abondance d'espèces plus élevée, comme indiqué auparavant. Des études ultérieures se sont concentrées sur les aspects de dynamique des populations et les effets d'ingénierie de l'écosystème, mais n'ont pas su considérer les dynamiques à la petite échelle. En conséquence, la distribution à petite échelle des agrégations de *L. conchilega* est mal connue malgré son importance. Ceci est certainement dû en partie aux difficultés de méthode d'échantillonnage traditionnel pour un échantillonnage adéquat de ces écosystèmes hétérogènes aux résolutions requises (<1m). A ce jour et à notre connaissance, la caractérisation spatiale des distributions de *L. conchilega* sur une petite échelle n'a pas été étudiée ailleurs que lors de cette étude. Cette lacune est abordée dans le **chapitre 4**: notre population d'étude a été contrôlée pendant 1.5 ans à l'aide de photographie aérienne par un cerf-volant (KAP), ainsi que de photogrammétrie numérique à basse altitude pour cartographier leur distribution à petite échelle à une résolution spatiale <0.5 m. Ces nouvelles méthodologies ont permis la caractérisation à petite échelle des distributions spatiales de *L. conchilega* à une résolution sans précédent. La performance de cette méthode est analysée dans le chapitre 4. Nous avons observé trois modèles de distribution lors de notre étude: taches (patches), bancs (beds) et bancs interrompus. Leurs différentes morphologies indiquent des mécanismes distincts de formation. Les types de distribution ont été formés suite à des périodes de recrutement, ce qui suggère que les motifs observés sont une conséquence des interactions entre la colonisation larvaire et les conditions hydrodynamiques pendant cette période. Ces interactions sont ainsi probablement responsables de la variation entre types de distribution à l'échelle locale.

Les schémas de distribution sont souvent le résultat de plusieurs mécanismes

fonctionnant en tandem. Pour cette raison, des processus supplémentaires de formation de modèles de distribution ont été considérés lors du développement de cette thèse. Ces processus comprennent notamment des interactions consommateur - ressource, dans le sens où la distribution d'un organisme est dictée par la présence de la ressource nécessaire à sa survie. *Lanice conchilega* est un organisme filtreur mais également détritivore, et consomme surtout des microorganismes présents dans la colonne d'eau ainsi qu'en surface sédimentaire. Des expériences avec flume suggèrent que l'alimentation par filtration de *L. conchilega* peut causer l'épuisement local de nutriments de la colonne d'eau, créant ainsi des gradients de concentration en nutriments pouvant avoir un impact sur les vers polychète en aval. De plus, l'alimentation par filtration peut être affectée par la compétition pour les ressources, comme cela a été démontré dans le cas de *L. conchilega* et l'huitre du Pacifique *Crossostera gigas* dans la Baie de Veys (France). A ce titre, nous avons exploré l'impact des interactions consommateur - ressource sur la dynamique de la population grâce à un modèle dans le **chapitre 5**. Un cadre de modélisation a été utilisé dû à la complexité de l'écologie alimentaire de *L. conchilega*, afin d'analyser les effets possibles de la limitation ainsi que de l'assimilation en nutriments sur la population. Des résultats préliminaires des simulations du modèle de population suggèrent une importance moindre des interactions consommateur - ressource sur la dynamique de densité de la population adulte de *L. conchilega*. Au cours de notre étude, la dynamique de la densité totale a été principalement influencée par l'intensité du recrutement et la mortalité subséquente. Ainsi, nos résultats préliminaires ont souligné l'importance du recrutement et de l'établissement de cohortes juvéniles pour la dynamique de la densité de population totale.

Les connaissances acquises au cours de cette thèse sur la dynamique de population de *L. conchilega* et l'ingénierie autogénique dans le temps et l'espace ont été résumées et intégrées dans le **chapitre 6**. Ce dernier démontre l'importance des différentes échelles spatio-temporelles dans l'ingénierie de l'écosystème et explore leur rôle dans la distribution locale de *L. conchilega*. Ce chapitre aborde également les liens entre dynamique de population et ingénierie autogénique, ainsi que les mécanismes potentiels de distribution spatiale. Finalement, il discute comment nos résultats peuvent soutenir les approches de conservation de l'écosystème et présente des perspectives d'avenir pour ce sujet de recherche.

En conclusion, nos résultats soutiennent une relation d'ingénierie non-linéaire entre

la densité en tubes et l'atténuation de flux d'eau, ce dernier cessant d'augmenter au-delà d'une densité limite de 3 200 ind·m⁻². La sédimentation peut effectivement contribuer à l'expansion verticale des agrégations de *L. conchilega*, mais une sédimentation excessive (catastrophique) peut également limiter cette expansion en provoquant des taux de mortalité élevée. Des gradients de densité au sein des récifs de *L. conchilega* peuvent contribuer à la formation de distributions inégales en modulant l'expansion verticale en plus de créer des effets d'ingénierie hétérogènes de l'environnement. Cependant, de plus amples recherches sont nécessaires afin de déterminer si des densités significativement distinctes se produisent entre portions d'une agrégation. La dynamique de la population influence l'intensité de l'ingénierie autogénique, créant des cycles saisonniers d'effets en modulant probablement la zone d'obstruction du flux. Cela peut également contribuer à la formation de distributions inégales en plus des gradients en densité entre les parties d'une agrégation. Cependant, il semble plus probable que les processus liés à l'établissement et au recrutement des larves aient une importance accrue dans la formation de schémas spatiaux à petite échelle dans des environnements peuplés de *L. conchilega*. Nous supposons que ces processus peuvent engendrer des gradients de densité en raison des influences du forçage hydrodynamique et / ou les améliorer en raison de la facilitation de la présence d'adultes par atténuation du forçage hydrodynamique. Ces mécanismes hypothétiques peuvent fournir d'orientation à des recherches futures.



CHAPTER

1

General Introduction

*The present chapter establishes the framework of this thesis by exploring the concept of ecosystem engineering, its manifestations across temporal and spatial scales, and presenting the study-case organism. Henceforth, the concept of organisms as ecosystem engineers is introduced as modulators of ecosystem biodiversity and functioning; two types of ecosystem engineers are differentiated by their mechanisms of action, i.e. autogenic and allogenic engineers. Examples are given that explore various engineering effects throughout different temporal and spatial scales. The study-case subject is introduced, the tube-building polychaete *Lanice conchilega* (Pallas, 1766). An extensive review of the available knowledge on *L. conchilega* temporal and spatial dynamics is produced, followed by a discussion on its ecological importance and conservation status under the current European policy framework. Lastly, the study site is introduced, followed by a summary of the research framework, including specific objectives and an outline of each chapter.*

1.1. Ecosystem engineering

Living organisms can influence ecosystem processes and properties by performing habitat modification through what is known as 'ecosystem engineering' (Romero *et al.*, 2015). Ecosystem engineers are organisms that cause physical state changes in biotic and/or abiotic materials, modulating resource supply to other species (Jones *et al.*, 1994). Although the term could be used to describe most living organisms, its use generally refers to those that substantially reduce environmental constraints to other species, enabling their survival (Crain and Bertness, 2006). For example, the beaver (*i.e. Castor sp*) (Wright *et al.*, 2002). Beaver dams interrupt and/or hinder water flow in riverine systems, causing flooding of river banks and changing the hydrological regime of surrounding areas (Andersen and Shafroth, 2010). These hydrological changes may also modulate sediment biogeochemistry, affecting oxygenation, nutrient cycling, and microbial activity (*e.g.* Briggs *et al.*, 2013). They may also affect sedimentary processes such as erosion and deposition, influencing landscape geomorphology (*e.g.* Butler and Malanson, 2005). Consequently, dam construction by beavers modulates natural resource supply to co-occurring species across the landscape, enabling and/or hindering the survival of several organisms, and changing species composition landscape-wide (*e.g.* Wright *et al.*, 2002). The effect is of such intensity that the presence of beaver dams can convert entire ecosystems from river banks into wetlands, hence completely altering ecosystem functioning (*e.g.* Andersen and Shafroth, 2010; Wright *et al.*, 2002).

Habitat modification through resource modulation can be achieved in various ways, as such ecosystem engineers can be differentiated into two groups according to how they cause change (Jones *et al.*, 1994). Beavers are allogenic engineers, that is, they cause change through their activities (*i.e.* dam building) (*sensu* Jones *et al.*, 1994). Other organisms may cause change through mere presence, comprising the group of autogenic engineers (*sensu* Jones *et al.*, 1994). Such is the case, for instance, of scleractinian corals and the reefs they build (Wild *et al.*, 2011) (Fig 1.1A). Corals build complex calcareous structures (Kaiser *et al.*, 2005), increasing spatial complexity at the sea bottom by providing a myriad of micro-habitats with different environmental conditions, expanding niche and habitat availability (Wild *et al.*, 2011). Reef concretions affect sediment biogeochemistry by acting as substrate for a plethora of microbiota that enhances nitrogen-fixing and nutrient cycling (Fiore *et al.*, 2010). Coral reefs also provide shelter to fish (Kerry and Bellwood, 2012) and serve as

substrate for larval settlement (Price, 2010), among other functions. As such, their presence indirectly enables the formation of biodiversity hotspots in shallow waters (Wild *et al.*, 2011) with distinct biological communities from the surrounding environment (Rogers *et al.*, 2014).

The marine environment possesses a plethora of engineering examples from both allogenic and autogenic groups. Sting rays act as allogenic engineers by creating feeding pits in soft substrates that provide shelter for nearby organisms (O'Shea *et al.*, 2012) (Fig 1.1B). Farmerfishes also behave as allogenic engineers by actively maintaining algae tufts on coral reefs (White and O'Donnell, 2010). This behaviour indirectly influences coral mortality rates and overall coral status by providing physical protection to the farmed areas (White and O'Donnell, 2010). Mangrove crabs allogenicly engineer microbial communities in intertidal bottoms by modulating sediment biogeochemistry through burrow construction and maintenance (Kristensen, 2008) (Fig 1.1C). Lugworms, such as *Arenicola marina* (Volkenborn *et al.*, 2007) allogenicly modulate nutrients to benthic microbial communities by creating burrows that influence nutrient flow in the sediment. Deep-sea corals autogenicly engineer soft bottoms in a similar fashion to shallow water corals, resulting in hotspots of biodiversity (Maynou and Cartes, 2012). Saltmarsh tussocks autogenicly engineer benthic communities by modulating hydrodynamic flow (Balke *et al.*, 2012), resulting in distinct micro-habitats within their canopies for other species (Bouma *et al.*, 2008) (Fig 1.1D).

Autogenic modulation of hydrodynamic conditions has been observed near and within several marine biogenic concretions in addition to the aforementioned. Similar engineering has also been observed for polychaete aggregations (Friedrichs *et al.*, 2000) and mussel beds (Drost, 2013), resulting in significant changes to benthic communities (*e.g.* Ataide *et al.*, 2014; Borthagaray and Carranza, 2007). However, the effects of autogenic and allogenic engineers on the marine environment can be very distinct (Bouma *et al.*, 2009b) (*e.g.* Pillay *et al.*, 2011). Extensive biogenic structures built by benthic autogenic engineers often stimulate the development of epibenthic communities while hindering the growth of endobenthic organisms (Bouma *et al.*, 2009b) (*e.g.* Pillay *et al.*, 2011) (Fig 1.2A). As seen through the previous examples, autogenic concretions hinder sediment mixing, oxygenation and benthic nutrient cycling via flow attenuation, ameliorating hydrodynamic conditions at the epibenthic environment and stimulating these communities. Saltmarsh and

seagrass tussocks modulate water flow passing through shoots, creating varying hydrodynamic conditions within the canopies (e.g. *Spartina sp* - Balke *et al.*, 2012, *Zostera sp* - Wilkie *et al.*, 2012). These are associated to distinct benthic community assemblages (e.g. Bouma *et al.*, 2008; Widdows *et al.*, 2008b). Aggregations of tube-building polychaetes entrap organic matter particles which stimulate the development of benthic meiofauna and microbial communities (Passarelli *et al.*, 2012). They also attenuate water flow as it passes through tube arrays (Friedrichs *et al.*, 2000), increasing fine particle deposition and enhancing local sediment stability (e.g. Ataide *et al.*, 2014; Passarelli *et al.*, 2012).

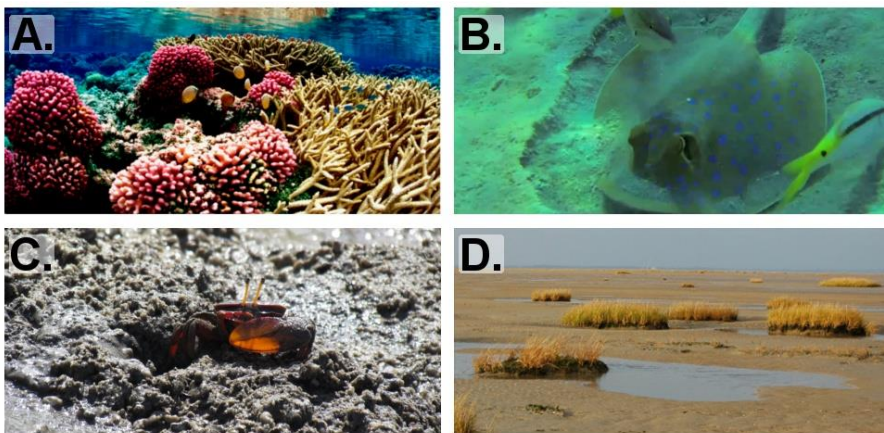


Fig 1.1. Examples of marine ecosystem engineers. Scleractinian corals autogenically engineer the environment by building extensive and complex reefs that harbour high species richness and abundance (A) (photo by Jim Maragos/USFWS). The bluespotted ribbontail ray *Taeniura lymma* allogenicly engineers soft bottoms by making feeding pits (B) (still extracted from footage by Chris Kidd). The Brazilian fiddler crab *Uca maracoani* allogenicly engineers mangrove sediments through burrow construction and maintenance (C) (photo by Thays Emerenciano/GEEFAA). Saltmarsh tussocks autogenically engineer marsh ecosystems by forming tussocks which provide micro-habitats of various sedimentary and hydrodynamic conditions to other species (D) (photo adapted from Balke *et al.*, 2012).

The presence of allogenic engineers conversely enables the development of endobenthic organisms while inhibiting epibenthic proliferation (Bouma *et al.*, 2009b) (e.g. Pillay *et al.*, 2011) (Fig 1.2B). Their activities commonly rework soft sediments,

increasing oxygenation and improving nutrient cycling (Bouma *et al.*, 2009b), which positively impacts endobenthic species. Burrowing engineers, such as the lugworm *Arenicola marina*, destabilize marine sediments during burrow construction and maintenance, inhibiting fine-particle accumulation and influencing the distribution of nutrients, organic matter and water content (Volkenborn *et al.*, 2007). This bioturbation induces decreases of surficial microphytobenthos abundance (Volkenborn *et al.*, 2007). In addition, burrow flushing by *A. marina* may also affect sediment biogeochemistry and pore water content (Volkenborn *et al.*, 2010, 2007), creating micro-habitats with distinct benthic communities (Volkenborn *et al.*, 2007). Similarly, burrow construction by mangrove crabs impacts sediment biogeochemistry through sediment reworking, causing increases in organic matter content through litter burial and changing nutrient profiles as well as sediment oxygenation (Kristensen, 2008). The pink ghost shrimp *Callichirus kraussi* – formerly known as *Callianassa kraussi* (Poore, 2010) – also allogenicly engineers sandy sediments through burrow flushing (Pillay *et al.*, 2007). This bioturbation loosens soft sediments (Pillay *et al.*, 2011) and modulate microbial biofilm development at the surface (Pillay *et al.*, 2007). Through its effect on microbial biofilms, *C. kraussi* indirectly influences macrofauna community assemblages which consume it (Pillay *et al.*, 2008), as well as growth and abundance of grazing fishes (Pillay *et al.*, 2012).

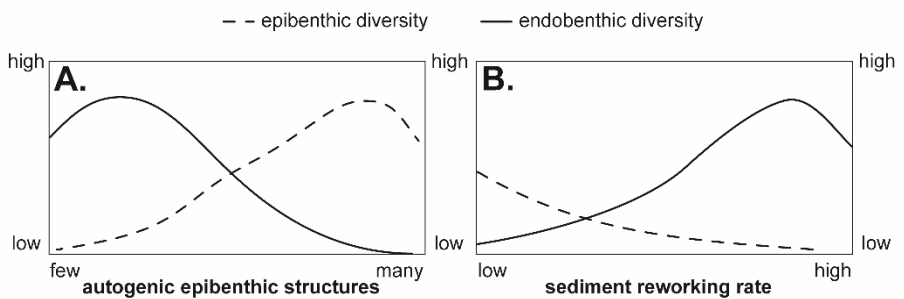


Fig 1.2. Illustration of the epi–endo-exclusion hypothesis adapted from Bouma *et al.* (2009b). The presence of autogenic constructs on soft sediments stimulates epibenthic diversity while hindering the development of endobenthic communities (A). Conversely, increased sediment reworking by allogenic ecosystem engineers strongly hinders epibenthic establishment while stimulating endobenthic diversity (B).

The aforementioned examples show how the effects of autogenic and allogenic engineers on local environmental properties modulate biodiversity. It is worth noting that outcomes may vary to differences in effects on structural and functional biodiversity. Nevertheless, effects may also scale from the local to the landscape level, as initially seen with the beaver transforming riverine systems into wetlands or ponds through flooding (e.g. Andersen and Shafroth, 2010; Wright *et al.*, 2002). In those cases, the presence of an ecosystem engineer determines geomorphology, biodiversity, and ecosystem functioning across the landscape (*sensu* Braeckman *et al.*, 2014). These cases may constitute key species (*sensu* Paine, 1969) and their removal or addition may drastically change ecosystems. The term here refers to the definition of 'keystone species' first mentioned by Paine (1969) to describe the effect of predation by the starfish *Pisaster ochraceus* on its associated intertidal community structure. Keystone species are those with disproportionately large effects on the structure of associated communities relative to their abundance. Some ecosystem engineers may be considered keystone species due to the disproportionately large repercussions of their engineering – e.g. the presence of beavers in riparian zones altering plant communities (Wright *et al.*, 2002). However, the two terms are not synonymous. Ecosystem engineering involves modulation of resources as means to cause change and affect associated species (*sensu* Jones *et al.*, 1994). Conversely, keystone species may have crucial roles in structuring communities due to effects that do not stem from resource modulation via ecosystem engineering – e.g. sea otters top-down control of urchin populations, indirectly affecting kelp forests (Estes *et al.*, 1998). Nevertheless, differentiating between previously considered keystone species that are also ecosystem engineers and ones that are not remains difficult since the two terms are often entwined.

For example, the introduction of beavers into arid ecosystems can improve water retention across large portions of the landscape, affecting the surrounding flora composition (e.g. Andersen and Shafroth, 2010). In addition, the increased sedimentation caused by beaver damming upstream can completely alter landscape geomorphology (e.g. Andersen and Shafroth, 2010). In the marine realm, flow modulation by saltmarsh tussocks can significantly impact erosion/deposition processes (Balke *et al.*, 2012), improving sediment retention and countering erosion in the coastal zone while shaping its geomorphology (e.g. Wang *et al.*, 2008; Widdows *et al.*, 2008b). Thus, the presence of seagrass or saltmarsh tussocks can contribute to coastal protection (e.g. Bouma *et al.*, 2005; Widdows *et al.*, 2008a,

2008b). Due to these and other substantial effects on ecosystem functioning, ecosystem engineers are considered important conservation targets (Braeckman *et al.*, 2014).

One major goal in conservation research is to predict the consequences of biotic and/or abiotic changes on ecosystem health and functioning. In order to achieve that goal we must understand how organisms interact with the ecosystem and be able to predict how those interactions influence landscapes (Crain and Bertness, 2006). Despite general trends, ecosystem engineering effects are situational and hard to predict. For example, marsh tussocks affect hydrodynamic flow as it passes through the canopy (Balke *et al.*, 2012), often resulting on sediment stabilisation (*e.g.* Wang *et al.*, 2008; Widdows *et al.*, 2008b). However, the final outcome of flow modulation may vary, depending on other factors than just presence – *i.e.* tussock density (Bouma *et al.*, 2009a), granulometry and coastal slope (Balke *et al.*, 2012). Engineering effects may vary according to physical properties of the engineered structure as well as baseline environmental characteristics, that is, environmental properties in the absence of the engineer (*sensu* Gutiérrez *et al.*, 2011). Engineering effects in the marine environment may depend on the local environmental context (*e.g.* sediment characteristics and hydrodynamic conditions) as well as density and distribution of the engineering species (Gutiérrez *et al.*, 2011). Autogenic engineering by organisms such as the aforementioned saltmarsh grasses (Balke *et al.*, 2012) and tube-building polychaetes (Borsje *et al.*, 2014) modulate water currents, producing varying effects depending on protrusion height as well as surface area (Eckman *et al.*, 1981). Furthermore, characteristics such as organism size and/or population composition can also influence the outcome of engineering. For example, body size and density in polychaete aggregations determine the area of flow obstruction, dictating the autogenic engineering effect (*e.g.* Eckman *et al.*, 1981; Friedrichs *et al.*, 2000; Luckenbach, 1986). Although the role of these features is yet to be explored for allogenic engineering, it can be hypothesised that it affects its outcomes also.

Predicting engineering outcomes may also be encumbered by scaling through time and space (Hastings *et al.*, 2007). Time scales must be considered when evaluating engineering outcomes as effects may occupy distinct time scales. For example, autogenic engineering from coral reefs (*e.g.* Wild *et al.*, 2011) generally operates at much longer time scales than that from polychaete aggregations (*e.g.* Friedrichs *et al.*, 2000) or saltmarsh grasses (*e.g.* Bouma *et al.*, 2009a). Additionally, effects may

also change over time, such as that of decaying beaver dams which result in different levels of flooding and geomorphological effects over time (e.g. Butler and Malanson, 2005). Nevertheless, engineering outcomes also often encompass the repercussions of localised effects that scale through space (Hastings *et al.*, 2007). For example, although saltmarsh tussocks engineers sediments in a local scale by modulating hydrodynamic flow between its stalks (Bouma *et al.*, 2009a), its effects are realised at larger scales than the aggregation through its indirect influence on erosion/deposition in surrounding areas (Balke *et al.*, 2012). Furthermore, when visualised at the landscape scale, its engineering effects on erosion/sedimentation regimes may dictate coastal geomorphology (e.g. Wang *et al.*, 2008). Thus, predicting the outcome of ecosystem engineering requires its investigation under varying conditions, across both spatial and temporal scales (Hastings *et al.*, 2007).

1.2. Ecosystem engineering and time scales

Modifications by ecosystem engineers can persist through varying scales of time, potentially outliving the ecosystem engineer (Hastings *et al.*, 2007). Part of the ecological value of some ecosystem engineers lies on the longevity of their modifications (*i.e.* effect persistence through time) (*sensu* Hastings *et al.*, 2007). For example, calcareous reefs built by scleractinian corals have a very high conservation value in part because of the long persistence of their effects on landscape biodiversity. These calcareous concretions remain long after the corals are dead (Kaiser *et al.*, 2005), contributing to ecosystem health by sustaining high habitat complexity, species richness and abundance for centuries if undisturbed (Rogers *et al.*, 2014). Similarly, beaver dams can continue to alter the landscape through the modulation of hydrological processes long after the beaver has abandoned it (e.g. Andersen and Shafroth, 2010). Empty shells from marine organisms will continue to introduce complexity into benthic environments for hundreds of years after organismal death (Gutiérrez *et al.*, 2003). However, although effect longevity is considered a crucial feature when evaluating ecological value, it is not the only one to be considered (Hastings *et al.*, 2007).

Engineering effects may also change over time due to variation in environmental properties and/or decay of the engineering effect. Intact beaver dams cause more flooding and higher sediment retention than decaying structures, causing a different set of changes to the environment (Butler and Malanson, 2005). Feeding pits made by sting rays only last for a few days (e.g. O'Shea *et al.*, 2012), resulting in

ephemeral landscape geomorphological changes. Additionally, engineering effects may also vary with population processes, such as density fluctuations and demographic evolution, at short temporal scales (*i.e.* months) (Hastings *et al.*, 2007). Naturally, the growth of marine autogenic engineers impacts their effects on marine environments by causing variations in aggregation/concretion size and porosity as populations undergo phases of development, ultimately dictating the area of flow obstruction (Eckman *et al.*, 1981). For example, species composition and community structure inside reefs of the tube-building polychaete *Sabellaria* sp differ among reef development phases (*e.g.* Dubois *et al.*, 2002; Polgar *et al.*, 2015) likely due to fluctuations in *Sabellaria* sp presence and density influencing their autogenic engineering effects (*e.g.* Eckman *et al.*, 1981; Friedrichs *et al.*, 2000; Luckenbach, 1986). As previously mentioned, density fluctuations in marsh tussocks influence their engineering effect on local hydrodynamic conditions, and consequently sedimentary conditions (Balke *et al.*, 2012). Density fluctuations in freshwater mussel beds can induce substrate erosion, affecting its engineering effect on landscape topography (*e.g.* Allen and Vaughn, 2011). Conversely, it may be expected that as marine allogenic engineers grow, they may impact larger areas, or deeper layers of sediment. Thus, research into marine ecosystem engineers should explicitly consider temporal scales to investigate engineering effects.

1.3. Ecosystem engineering and spatial scales

One of the main challenges in ecological research is to clarify how small-scale processes relate to landscape-level processes and ecosystem functioning (Dittmann, 1999). Organisms can be seen as discrete entities interacting with biotic and abiotic factors of the surrounding environment. These interactions may result in intricate spatial patterns that delineate the landscape (Levin, 1992). Attempting to discover the mechanisms driving spatial pattern formation, thus, is of paramount importance (Levin, 1992). The environment plays a crucial role in the latter, and this is especially true in coastal environments wherein environmental gradients are steep and often result in zonation patterns (Kaiser *et al.*, 2005). Zonation patterns form due to limitations imposed on species-specific physiological tolerance ranges to abiotic factors and/or biotic interactions (Kaiser *et al.*, 2005). For example, air exposure gradients limit the distribution of macro algae and filter-feeding invertebrates with low resistance to desiccation (*e.g.* Christofolletti *et al.*, 2011). Thermal stress from air exposure can also influence the distribution of the barnacle *Semibalanus balanoides*

(e.g. Leonard *et al.*, 1999). Biotic interactions may also limit species distributions (Kaiser *et al.*, 2005). Competition for space between the barnacles *Chthamalus stellatus* and *Balanus balanoides* (e.g. Connell, 1961), and between mussels and macroalgae (e.g. Reichert *et al.*, 2008) limits these species to distinct bands on the intertidal. Preying of the snail formerly named *Thais lapillus* on the barnacle *Chthamalus stellatus* (e.g. Connell, 1961) and of the green crab *Carcinus maenus* on the barnacle *Semibalanus balanoides* (e.g. Leonard *et al.*, 1999) may restrict the distributions of both prey species, contributing to patterning. Nevertheless, pattern formation is frequently context- and/or scale-dependent and combinations of various drivers can result in spatial patterns (Crain and Bertness, 2006) (e.g. Christofolletti *et al.*, 2011; Connell, 1961; Leonard *et al.*, 1999; Reichert *et al.*, 2008).

Spatial patterns in the marine and coastal environments are most often determined by multiple drivers through various mechanisms (Levin, 1992). Presently, we restrict ourselves to examples on distributions of ecosystem engineers, as these are most closely related to the scope of this thesis. Ecosystem engineering can create and/or exacerbate environmental gradients (Crain and Bertness, 2006). In turn, fluctuations in environmental conditions may cause fluctuations of engineering effects across space (Hastings *et al.*, 2007) in addition to creating physiological stress (see aforementioned examples). This interplay between ecosystem engineering and environmental gradients is very apparent when considering autogenic engineers, such as scleractinian corals, marsh grasses, mussels, and tube-building polychaetes. As previously mentioned, scleractinian corals create complex calcareous reefs providing various micro-habitats (e.g. Wild *et al.*, 2011), while mussels (e.g. Borthagaray and Carranza, 2007), saltmarsh grasses (e.g. Bouma *et al.*, 2008) and polychaetes (e.g. Polgar *et al.*, 2015) form aggregations that provide various environmental conditions, enabling the survival of several benthic species. Due to the often patchy distribution of their aggregations and/or concretions, their presence also generates spatial patterns of biodiversity in patchwork landscapes and increasing spatial heterogeneity (Archambault and Bourget, 1996). Spatial heterogeneity is commonly positively associated to landscape biodiversity, species richness, abundance and biomass (e.g. Archambault and Bourget, 1996; de Souza Júnior *et al.*, 2014; Godet *et al.*, 2011; Liu *et al.*, 2014), all of which affect ecosystem functioning (Buhl-Mortensen *et al.*, 2010). As such, understanding the interactions between ecosystem engineers and spatial gradients is crucial to realising the

outcomes of ecosystem engineering effects across a landscape (Crain and Bertness, 2006).

The species distribution of many sessile autogenic engineers is largely determined by larval settlement (Bhaud, 2000) – e.g. recruitment delimits early spatial patterns of the barnacle *Semibalanus balanoides* (Leonard *et al.*, 1999). As such, settlement success is susceptible to influences from any environmental process and/or anthropogenic activity that may heterogeneously affect larval transport, supply in the water column, and mortality in the landscape (Bhaud, 2000). This is the case for several spawning organisms, such as the barnacle *S. balanoides* (e.g. Leonard *et al.*, 1999), corals (e.g. Price, 2010; Thomson *et al.*, 2012) and tube-building worms (e.g. Dodd *et al.*, 2009). Local flow dynamics can significantly influence larval supply and settlement of *S. balanoides*, influencing its distribution (e.g. Leonard *et al.*, 1999). Settlement also depends on the ability of larvae to find suitable habitat within a limited period of time (e.g. Baird *et al.*, 2003; Dodd *et al.*, 2009). Oceanographic processes and changes in settlement cues affect recruitment and distribution (e.g. Baird *et al.*, 2003; Dodd *et al.*, 2009; Van Colen *et al.*, 2009). Changes in light conditions may delay or promote early settlement of coral larvae as well as affect settlement density (e.g. Mundy and Babcock, 1998; Thomson *et al.*, 2012); on the other hand, hard substrata availability limits the distribution of the tube-building polychaete *Serpula vermicularis* (Dodd *et al.*, 2009), known to settle onto that type of substrate (Chapman *et al.*, 2007). However, the majority of studies assessing drivers of distribution are executed at continental to regional scales (*i.e.* > 1km) and very little information is available on drivers of small-scale spatial pattern formation (*i.e.* few centimetres to 10m) for sessile marine organisms, one of the themes addressed by the current work.

Known common mechanisms driving small-scale spatial pattern formation may include but are not restricted to consumer-resource interactions, disturbance-recovery processes, and scale-dependent feedbacks (*sensu* Rietkerk and van de Koppel, 2008). The first encompasses distributions that are a result of fluctuations in resource availability (*sensu* Rietkerk and van de Koppel, 2008), such as the distribution of marsh plants (e.g. van de Koppel *et al.*, 2006). The small-scale distribution of few marsh plants is associated to light availability, which is influenced by the presence and abundance of other plants and their canopy size (van de Koppel *et al.*, 2006). These physiological needs result in inter-specific competition that

determines small-scale distributional patterns (van de Koppel *et al.*, 2006). The second mechanism incorporates disturbance-recovery processes (*sensu* Guichard *et al.*, 2003). Disturbances such as bottom trawling (*e.g.* benthic community - Olsgard *et al.*, 2008), iceberg scouring (*e.g.* benthic community - Teixidó *et al.*, 2007), oyster fishing (*e.g.* polychaetes - Dubois *et al.*, 2002), or wave action (*e.g.* the California mussel *Mytilus californianus* - Guichard *et al.*, 2003) can create fragmentation in the distribution of marine organisms by physically removing individuals. Sedimentary processes, such as erosion and sedimentation (*e.g.* saltmarsh grasses - Balke *et al.*, 2012; polychaetes - Polgar *et al.*, 2015) may limit or stimulate proliferation across the environment, creating patchy landscapes. Recolonization processes may further change spatial patterns of species distribution. For example, gaps created by wave action in the small-scale distribution of *M. californianus* may be colonised by neighbouring conspecifics which move laterally to occupy the empty substrate (Guichard *et al.*, 2003).

The third mechanism encompasses feedback relationships that may stem from combinations of various processes and/or interactions (*sensu* Rietkerk and van de Koppel, 2008). As previously mentioned, while marine ecosystem engineers influence environmental properties and processes through resource modulation, these same properties and processes may influence their survival and distribution. Benthic communities are often modulated by feedback relationships between ecosystem engineers and the environmental conditions that they create (*e.g.* Bouma *et al.*, 2009a; White and O'Donnell, 2010). Saltmarsh tussock formation is affected by feedback processes in addition to consumer-resource interactions (Balke *et al.*, 2012). Flow modulation during tussock formation is highly dependent on stalk density (Bouma *et al.*, 2009a), influencing erosion and sedimentation in and around the tussock (Balke *et al.*, 2012). These processes may limit and/or enable horizontal expansion depending on sheer stress (Balke *et al.*, 2012). Mussel bed patterning comprises another example (Liu *et al.*, 2014). Individual mussels gather and/or disperse as a function of animal density (van de Koppel *et al.*, 2008) and food availability (Dolmer, 2000). At short spatial scales (*i.e.* <10cm), mussels group together likely due to gains in survival from predation and/or removal by currents (van de Koppel *et al.*, 2005). Dispersal occurs when densities become large enough to deplete food in the water column above the cluster (van de Koppel *et al.*, 2005). At larger scales (*i.e.* approx. 25m), gradients in food availability in the water column may develop between the areas above and adjacent to mussel aggregations due to

filtration pressure, creating long-range competition that results in banded patterns of distribution (van de Koppel *et al.*, 2005).

Mussel bed patterning is a self-organised process (van de Koppel *et al.*, 2012), that is scale-dependent feedbacks result in regular spatial patterns (*sensu* Rietkerk and van de Koppel, 2008). Mussel density has short-range positive effects on mussel activity (van de Koppel *et al.*, 2008), but as density increases, its effect on activity becomes negative (van de Koppel *et al.*, 2008). Recent research suggests that many small-scale patterns may be formed through self-organized processes – *e.g.* Bouma *et al.*, 2009a; Rietkerk and van de Koppel, 2008; van de Koppel *et al.*, 2008; Weerman *et al.*, 2010. The small-scale distribution of diatoms on the benthic-boundary layer is one such example in which scale-dependent interactions between sedimentation, diatom growth, and water flow redistribution result in regular distribution patterns (Weerman *et al.*, 2010). Irregularities in coastal relief may create slightly elevated mounds where diatoms grow and produce extracellular polymeric substances (EPS) (Weerman *et al.*, 2010). These substances increase sediment cohesion and decrease roughness (Lubarsky *et al.*, 2010), enabling higher fine-particle deposition and ameliorating conditions for diatom growth in a positive feedback (Weerman *et al.*, 2010). Conversely, water may flow from higher elevation areas and accumulate in lower parts of the relief, hindering EPS accumulation as it is water soluble (Hubas *et al.*, 2010) and limiting biofilm development as a negative feedback (Weerman *et al.*, 2010). Lastly, the patchy distribution of the autogenic engineer *Spartina sp* may also be considered a self-organized process (van de Koppel *et al.*, 2012). Flow modulation by tussocks, create areas of heterogeneous erosion and deposition across the landscape which limit and/or hinder further establishment, dotting the landscape with tussocks (*e.g.* Balke *et al.*, 2012; van de Koppel *et al.*, 2012).

1.4. Introducing the sandmason, *Lanice conchilega*

The present work focuses on a particular coastal ecosystem engineer, the tube-building worm *Lanice conchilega* (Pallas, 1766) (Fig 1.3A). *Lanice conchilega* is a polychaete belonging to the *Terebellidae* family (Read and Bellan, 2012). It is popularly known as the sandmason worm and is widely distributed along the coastal zones of the northern hemisphere, mainly the coasts of the North Atlantic and Pacific oceans (Hartmann-Schröder, 1996), as well as Europe (Godet *et al.*, 2008; Holthe,

1977). *Lanice conchilega* occurs in sandy and muddy marine sediments (Willems *et al.*, 2008), in depths ranging between the intertidal zone and the bathypelagic area (approx. 1 900m deep) (Hartmann-Schröder, 1996). This sessile terebellid builds biogenic tubes consisting of fine-coarse sand grains and fragments of foraminifera, sea urchin spines, shells, amongst other available materials (Hartmann-Schröder, 1996; Ziegelmeir, 1952) (Fig 1.3B). Each tube is normally topped by sand fringes maintained by the worm (Fig 1.3C) (Van Hoey *et al.*, 2006a). *Lanice conchilega* may group into biogenic aggregations consisting of trapped material between arrays of sand tubes (Ziegelmeir, 1952) (Fig 1.3D and E) (see definition of aggregations in table 1.1). These clusters have several functions within the ecosystem, such as providing food (*e.g.* De Smet *et al.*, 2013; Petersen and Exo, 1999) and shelter (*e.g.* Rabaut *et al.*, 2010) to associated species. They may reach densities up to 20 000 ind·m⁻² during recruitment (Buhr and Winter, 1976), protrude up to 16cm above the substrate (Rabaut *et al.*, 2009), and cover areas ranging from few centimetres to a max observed coverage of 15m² (Degraer *et al.*,

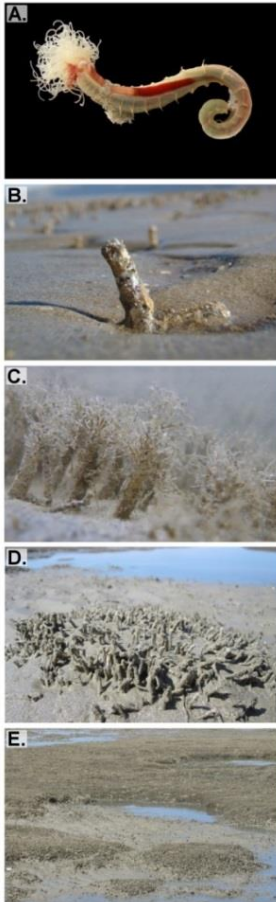


Fig 1.3. The terebellid worm *Lanice conchilega* (A, photo by Matthias Buschmann) is a sessile tube-builder. Its tube is a mosaic of fine-coarse sand grains, fragments of shells, urchin spines, and foraminifera skeletons glued together by mucus (B and C, photos by Renata M. S. Alves). In addition, tubes may be topped by a fringe (C). *Lanice conchilega* forms sand tube aggregations (D and E, photos by Renata M. S. Alves) on intertidal and subtidal soft sediment environments.

2008).

Similarly to other tube-building polychaetes, *L. conchilega* aggregations autogenically engineer the environment (Borsje *et al.*, 2014), modulating water flow as it passes through tube arrays (Friedrichs *et al.*, 2000). Additionally, *L. conchilega* allogenerically engineers the environment through tube irrigation (Braeckman *et al.*, 2014). Water movement induced by piston-pumping oxygenates sediments, modulating nutrient concentrations (*e.g.* Braeckman *et al.*, 2010; Forster and Graf, 1995) and affecting the vertical distribution of benthic fauna (Braeckman *et al.*, 2011). The changes imposed by this polychaete affect both biotic and abiotic ecosystem properties, warranting its consideration as a conservation target (Godet *et al.*, 2008). Its autogenic engineering enables the formation of 'skimming flow', a type of attenuated flow at the benthic-boundary layer (Friedrichs *et al.*, 2000). This influences sedimentary processes, such as sedimentation and erosion, causing higher fine-particle deposition (Rabaut *et al.*, 2007) and modulating surficial sediment composition (Rabaut *et al.*, 2007). It also leads to higher sediment stability (Rabaut *et al.*, 2009), thus contributing to coastal protection. The attenuated flow may also facilitate larval retention as less larvae are physically removed by currents (Rabaut *et al.*, 2009), positively affecting benthic abundance and species richness (*e.g.* Callaway, 2006; De Smet *et al.*, 2015; Rabaut *et al.*, 2007). Nevertheless, akin to other autogenic engineers, this effect is density dependent (Borsje *et al.*, 2014).

Model simulations predict a minimum density threshold, past which tube aggregations strongly attenuate water flow at the benthic-boundary layer (Borsje *et al.*, 2014) (Fig 1.4). Flow attenuation should intensify with tube density, generating increasingly higher sediment deposition up to another density threshold past which the effect ceases to significantly increase (Borsje *et al.*, 2014) (Fig 1.4). Results from these simulations suggest that the increment in sedimentation should be able to sustain the vertical expansion of aggregations through a positive feedback (Borsje *et al.*, 2014). Sediment deposition would trigger tube-building (Hartmann-Schröder, 1996) (Fig 1.5A-C), which in turn would generate more sedimentation through autogenic engineering (Borsje *et al.*, 2014) (Fig 1.5D). However, the existence of such process and its role in driving the vertical growth of *L. conchilega* aggregations remains hypothesised only, as there is no empirical evidence supporting this mechanism. This research gap is addressed in **chapter 2** of this thesis, wherein three experiments explore the autogenic engineering effects of live *L. conchilega* on

sedimentary processes and the role of feedbacks in the vertical expansion of tube aggregations.

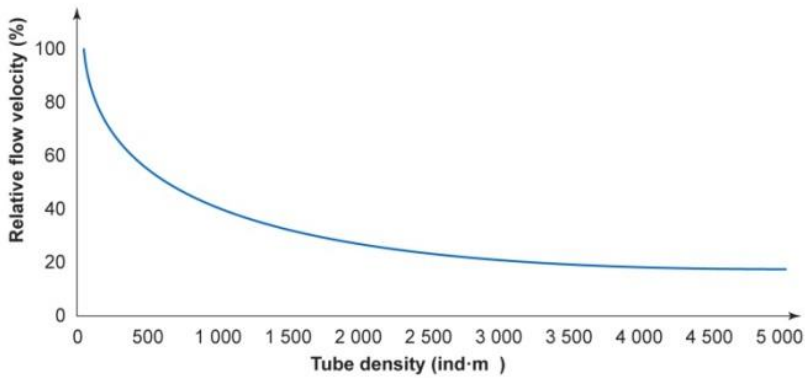


Fig 1.4. Approximate relative flow velocity as assessed at 1cm above the sediment surface passing through a simulated *L. conchilega* bed 3.5cm in height (from the sediment surface). Flow velocity is attenuated non-linearly as it passes through aggregations of increasing tube densities (adapted from Fig 2 in Borsje *et al.*, 2014).

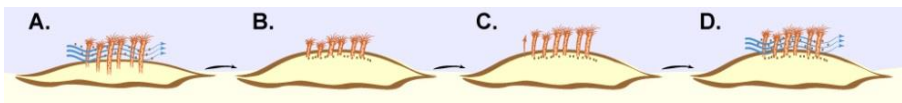


Fig 1.5. Illustration of the process for aggregation vertical expansion (as suggested by Borsje *et al.*, 2014): (A) Water flow passing through *L. conchilega* tube aggregations is attenuated, increasing fine-sediment deposition; (B) *L. conchilega* aggregation may become partially/fully covered in sediment; (C) individuals increase tube accretion rate to escape burial; (D) expanded tubes attenuate water flow further, enabling additional sedimentation.

Table 1.1. Key depicting different types of *L. conchilega* biogenic mounds referred to in this thesis.

Aggregation:	Refers to any <i>L. conchilega</i> conglomerate regardless of size, tube density, and effect on local biotic and abiotic environmental properties.
Patch:	Aggregation morphotype that refers to sparse, compact, mound-shaped, small (<i>i.e.</i> approx. < 1m ² area) <i>L. conchilega</i> conglomerates, regardless of tube density and effect on local biotic and abiotic environmental properties.
Bed/mat:	Aggregation morphotype that refers to continuous <i>L. conchilega</i> conglomerates, covering extensive areas (<i>i.e.</i> approx. > 1m ²), regardless of tube density and effect on local biotic and abiotic environmental properties.
Interrupted bed/mat:	Aggregation morphotype that refers to <i>L. conchilega</i> beds/mats (see above) with discontinuities in coverage and/or spread over the sediment surface, regardless of tube density and effect on local biotic and abiotic environmental properties.
Reef:	Refers to <i>L. conchilega</i> conglomerates shown to possess medium-high value reef-like characteristics as suggested by Rabaut <i>et al.</i> (2009), and/or determined as a reef by peer-reviewed studies.

1.5. Temporal aspects of *L. conchilega* ecosystem engineering

Ecosystem engineering effects, as previously mentioned, often depend on the life-span of the engineer, as well as the nature of the modifications and baseline environmental conditions (Gutiérrez *et al.*, 2011). *Lanice conchilega* is a relatively short-lived ecosystem engineer. Its life span can range from 1 to 3 years (e.g. Beukema *et al.*, 1978; Ropert and Dauvin, 2000; Van Hoey *et al.*, 2006b). During that time, it goes through seven life phases (Kessler, 1963) - for further details on the life cycle of *Lanice conchilega*, the reader is referred to addendum I. Ecosystem engineering by *L. conchilega* is restricted to two of those, the sessile phases encompassed by the juvenile and adult stages (Borsje *et al.*, 2014). Although this period comprises the majority of its life-span (*i.e.* approx. 1-3 years), it also comprises a relatively short amount of time. Little is known about the role of short population dynamics on ecosystem engineering effects. Previous studies present conflicting observations for *L. conchilega*. In some cases engineering effects from *L. conchilega* aggregations persisted for a short span of time after the tube-dweller was gone (e.g. Callaway *et al.*, 2010). In other cases, modifications such as mounds formed due to increased fine-sediment accumulation in *L. conchilega* aggregations persisted through paleontological scales of time (e.g. Carey, 1987). It is unclear why differences such as these occur, but previous research indicates that they likely result from fluctuations in population dynamics and their effect on autogenic engineering. *Lanice conchilega* density fluctuates seasonally with the majority of individuals dying off during moments of lower temperatures and limited primary production, that is winter (e.g. Buhr and Winter, 1976; Callaway *et al.*, 2010; Carey, 1987; Ropert and Dauvin, 2000; Van Hoey *et al.*, 2006b). Previous modelling studies show that the autogenic engineering by *L. conchilega* is very likely density-dependent (Borsje *et al.*, 2014) (illustrated in Fig 1.4 at sub-section 1.4). Thus fluctuations in density, such as the ones observed during population growth and disappearance, are expected to influence engineering effects (e.g. Borsje *et al.*, 2014; Eckman *et al.*, 1981; Friedrichs *et al.*, 2000; Luckenbach, 1986), and probably account for differences in persistence amongst different populations.

Another aspect of population dynamics that may impact autogenic engineering effects is the demographic structure of the population. During development, individuals grow from < 1mm to approx. 5-6mm in diameter (e.g. Bergman and Hup, 1992; Kessler, 1963; Ropert and Dauvin, 2000; Van Hoey *et al.*, 2006b). As

population dominance shifts from a majority of juveniles to adults, the area of obstruction per aggregation changes (*sensu* Eckman *et al.*, 1981; Friedrichs *et al.*, 2000; Luckenbach, 1986). That is, population demographic structure changes within aggregations as *L. conchilega* individuals grow. That change in demographic composition implies that the population changes from a majority of small tubes to larger sand tubes which protrude further from the sediment surface. This should influence the intensity with which *L. conchilega* modulates hydrodynamic flow, as well as its allogenic effects on soft sediments. Previous research has addressed the relationship between engineering effects and physical characteristics of the tubes within the aggregation with experiments using mimic tubes (*e.g.* Passarelli *et al.*, 2012; Rabaut *et al.*, 2009) and ecological modelling (Borsje *et al.*, 2014). However, there is still a knowledge gap on the role of changing tube dimensions and seasonal density fluctuations as *in-situ* populations have not been considered. This is the gap addressed in **chapter 3** of this thesis. In it, we explore temporal fluctuations of population demographic structure and secondary production of intertidal *L. conchilega* aggregations, as well as their effect on local environmental conditions.

1.6. Spatial aspects of *L. conchilega* ecosystem engineering

Lanice conchilega frequently displays a patchy or fragmented distribution, building biogenic concretions that can be structured as beds (Godet *et al.*, 2009b) or patches (Degraer *et al.*, 2008) (Fig 1.6) (see definitions in table 1.1). These may present reef-like characteristics, having a significant effect on local biotic and abiotic properties (Rabaut *et al.*, 2009) (see definition of reefs in table 1.1). The increased spatial heterogeneity produced by the presence of *L. conchilega* aggregations in the landscape is part of their ecological value as they expand habitat availability to associated species (Godet *et al.*, 2008). Although previous research explored processes of formation and decay of *L. conchilega* populations in both intertidal (*e.g.* Callaway, 2003; Callaway *et al.*, 2010; Ropert and Dauvin, 2000; Strasser and Pieloth, 2001) and subtidal conditions (*e.g.* Buhr and Winter, 1976; Van Hoey *et al.*, 2006b), very little is known about how this relates to their small-scale spatial patterns or how the latter form or decay. As sessile organisms, it is to be expected that a large portion of *L. conchilega* distribution results from larval settlement, recruitment, and factors modulating both (Bhaud, 2000). These population processes may largely explain regional- (*e.g.* Ayata *et al.*, 2009; Strasser and Pieloth, 2001) and global-scale distribution patterns (*e.g.* Benedetti-Cecchi *et al.*, 2010) (Bhaud, 2000).

However, it is unclear whether they influence small-scale spatial pattern formation as well.

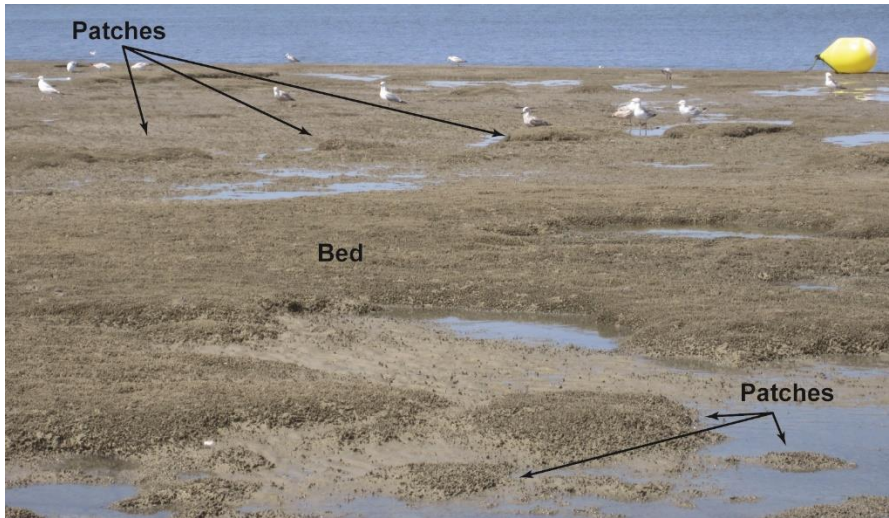


Fig 1.6. *Lanice conchilega* patches and beds at the intertidal zone of the sandy beach in Boulogne-sur-mer, Nord-Pas-de-Calais - France (photo by Renata M. S. Alves).

Previous modelling simulations attempting to clarify the role of larval settlement and recruitment on distribution indicates that patterning of intertidal *L. conchilega* beds is likely determined by local hydrodynamic conditions during settlement and recruitment (Heuers *et al.*, 1998). Lower current speeds should enable higher settlement and recruitment, whereas stronger currents should hinder these processes through animal removal and/or dislodgement (Heuers *et al.*, 1998). Additionally, local hydrodynamic conditions are influenced by tube presence and/or other protruding structures (e.g. Callaway, 2003; Carey, 1987; Heuers *et al.*, 1998; Rabaut *et al.*, 2009). Reduced hydrodynamic stress within tube arrays (Friedrichs *et al.*, 2000) facilitates settlement locally (Callaway, 2003; Heuers *et al.*, 1998; Rabaut *et al.*, 2009). This can constitute a feedback relationship between *L. conchilega* density and hydrodynamic stress, resulting in bed patterning. Nevertheless, other processes may also affect settlement in a spatially-explicit manner. Settlement may also be enhanced by substrate selection by larvae (e.g. red tube worm *Serpula vermicularis*, Chapman *et al.*, 2007). Previously existing *L. conchilega* tube aggregations may

22

provide extra substrate for larval attachment (e.g. Callaway, 2003). Conspecifics in an aggregation may exude settlement cues (e.g. blue tube worm *Spirobranchus cariniferus*, Gosselin and Sewell, 2013). Local modulation of larval settlement and recruitment can also generate density gradients across the landscape (Heuers *et al.*, 1998), and consequently, heterogeneous ecosystem engineering (Borsje *et al.*, 2014). Thus, processes modulating larval settlement and recruitment may give rise to patches and/or fragmented beds (Heuers *et al.*, 1998).

The presence of protruding structures is not a requirement for settlement (e.g. Callaway *et al.*, 2010; Strasser and Pieloth, 2001). In the absence of protruding structures, variation in coastal relief should produce similar effects (Heuers *et al.*, 1998). A modelling endeavour by Heuers *et al.* (1998) predicts that *L. conchilega* will accumulate in topographical depressions likely due to local hydrodynamic conditions. Animals in a depression would be subjected to tidal flushing during flooding and ebbing tides which homogenize food supply in the water column (Heuers *et al.*, 1998) and stimulate filter-feeding (Denis *et al.*, 2007). *In-situ* observations by Ropert and Dauvin (2000) corroborate a preference for topographical depressions likely due to interspersed moments of flushing and stagnation-induced retention, enabling population establishment. Nevertheless, these studies fail to characterize the evolution of *L. conchilega* small-scale spatial patterns, which may aid in the identification of potential mechanisms (pers. comm. van de Koppel). To the best of our knowledge, there are no studies investigating this topic. We address this gap in **chapter 4**, wherein an intertidal population is monitored for 1.5 years using kite aerial photography (KAP) and low-altitude digital photogrammetry to map their small-scale distribution (*i.e.* at a spatial resolution < 0.5m).

Consumer-resource interactions (*sensu* Rietkerk and van de Koppel, 2008) may comprise another mechanism contributing to small-scale spatial patterns development in *L. conchilega* aggregations other than feedback relationships (*sensu* Rietkerk and van de Koppel, 2008). *Lanice conchilega* consumes microorganisms from the water column and/or surficial microphytobenthos, constituting a diet of mainly bacteria and microalgae, but also fragments of macroalgae (e.g. Braeckman *et al.*, 2012; Lefebvre *et al.*, 2009). As both a filter- (Buhr, 1976) and deposit-feeder (Ropert and Gouilletquer, 2000), seasonal fluctuations of microbial community composition have been shown to affect the dietary constitution of *L. conchilega* (e.g. Braeckman *et al.*, 2012; Lefebvre *et al.*, 2009). Namely, the latter fluctuates in

synchrony with the aforementioned seasonal variations (e.g. Braeckman *et al.*, 2012; Lefebvre *et al.*, 2009). Dittmann (1999) suggests that *L. conchilega* is associated to areas of high productivity in regional scales (e.g. Dittmann, 1999; Van Hoey *et al.*, 2008), which suggests that primary production in the water column and sediment surface may influence mortality in that scale (Dittmann, 1999). As such, population disappearance during winter may be attributed to low primary production in addition to low temperature stress in both intertidal (e.g. Beukema, 1992; Callaway *et al.*, 2010; Carey, 1987; Günther and Niesel, 1999; Ropert and Dauvin, 2000; Strasser and Pieloth, 2001) and subtidal zones (e.g. Buhr and Winter, 1976; Van Hoey *et al.*, 2006b). It is likely that *L. conchilega* populations become limited by lack of food during these periods as the abundance of photosynthetic microorganisms declines in both the water column (Lefebvre *et al.*, 2011) and sediment surface (Passarelli *et al.*, 2015). However, it is unclear whether food availability influences distribution patterning despite the important role it plays on population dynamics.

Food limitation has the potential to drive spatially heterogeneous *L. conchilega* distributions by modulating mortality explicitly across the landscape, and augmenting the effect of pre-existing productivity gradients. Previous research provides indications on the potential mechanisms through which consumer-resource interactions may affect spatial pattern formation. Flume experiments suggest that filter-feeding by *L. conchilega* worms can cause local water column depletion, creating gradients in food concentration that may impact individual worms downstream (Denis *et al.*, 2007). *In-situ* observations revealed interspecific competition for food between *L. conchilega* and the filter-feeding Pacific cupped oyster *Crassostrea gigas* in the Bay of Veys (Ropert and Gouletquer, 2000). Aquarium experiments revealed that deposit-feeding may be inhibited within dense tube aggregations since the mass of sand tubes can restrict access to the sediment surface (Buhr, 1976), potentially forcing animals to switch to filtration and stimulating intraspecific competition. Nevertheless, it is still difficult to assess the role of food availability and the two feeding modes on *L. conchilega* population dynamics. This remains a major research challenge as population dynamics may influence spatial pattern formation in *L. conchilega* beds. Unsurprisingly, evaluating such relationships empirically is highly complex. As such, we explore the impact of food availability on population dynamics through a modelling framework in **chapter 5**. An individual-based model was employed to assess the role of both filter- and deposit-feeding behaviours on density dynamics of juvenile and adult *L. conchilega*.

Finally, *L. conchilega* small-scale distribution may also be affected by disturbance-recovery processes as these are known to generate heterogeneity in the landscape level (*sensu* Rietkerk and van de Koppel, 2008). *Lanice conchilega* populations are susceptible to many impacts, such as fishing activities (Bergman and Hup, 1992), tourism (Godet *et al.*, 2008), and aquaculture (Ropert and Gouletquer, 2000). These can have varying effects, influencing small-scale distribution. Previous research has shown that individuals can be removed and/or dislodged by beam-trawling activities that penetrate at least approx. 6-10cm into the sediment (Bergman and Hup, 1992). Significant reduction in population density has been observed as a result despite individual worms being able to retreat into their tubes to avoid physical damage (Bergman and Hup, 1992). If dislodged, worms may be able to re-establish elsewhere (Kessler, 1963). However, human impact is not included in the scope of the present work due to time and logistic limitations, but may be considered during the discussion of results.

1.7. Conservation framework and the status of polychaete aggregations

The legal framework for conservation efforts within the European Union is determined by two official documents, the Birds Directive (2009/147/EC) and the Habitats Directive (92/43/EEC) (Evans, 2006). Both documents list priority cases for conservation, and while the Birds Directive dictates the guidelines for conservation of European avifauna (The Council of The European Communities, 2009), the Habitats Directive lists European habitat types (also known as biotopes) prioritised for protection (The Council of The European Communities, 2007). Selected habitat types are protected by designating management and/or conservation status with the creation of special areas of conservation (SACs) and/ or sites of community interest (SCIs) (The Council of The European Communities, 2007). Priority habitat types and/or species are selected by member states (The Council of The European Communities, 2007) through identification using provided guidelines (Evans, 2006). Conservation of polychaete aggregations falls under the scope of the Habitats Directive as polychaete aggregations may be considered biogenic reefs (*i.e.* habitat type 1170) (Holt *et al.*, 1998). The reef habitat type is defined within the Interpretation Manual of European Union Habitats (EUR28) as follows:

“Reefs can be either biogenic concretions or of geogenic origin. They are hard compact substrata on solid and soft bottoms, which arise from the sea floor in the sublittoral and littoral zone. Reefs may support a zonation of benthic communities of algae and animal species as well as concretions and corallogenic concretions.”

(European Commission DG Environment, 2013)

Polychaete aggregations must meet these requirements to be considered reefs (European Commission DG Environment, 2013). Many polychaete species produce concretions that fit the reef habitat type – e.g. *Sabellaria alveolata*, *Sabellaria spinulosa*, and *Serpula vermicularis* (Holt *et al.*, 1998). These species were evaluated in a study from 1998 and considered reef-builders, as such they are eligible for protection (Holt *et al.*, 1998). The study by Holt *et al.* (1998) defined reef-builders as species that create structures through organism aggregation, rising significantly from the substrate (*i.e.* 20-75cm height), and/or clearly form distinct communities and/or habitats from their surroundings (Holt *et al.*, 1998). Although *L. conchilega* aggregations height range is lower than the aforementioned (*i.e.* ~5cm to ~16cm in height), the aggregations can have significant effects on local environmental properties and biodiversity, gaining reef-like characteristics (Rabaut *et al.*, 2009). Subtidal aggregations have been recognised as reef-habitat (associated to habitat type 1110) for SCI delineation (in the Belgian SAC Vlaamse Banken BEMNZ0001).

Recent research has shown that *L. conchilega* is able to form very large aggregations with significant effects on local biodiversity and habitat characterisation (e.g. De Smet *et al.*, 2015; Rabaut *et al.*, 2009, 2007; Van Hoey *et al.*, 2008). One famous example is the reef bed at the Bay of Mont-Saint-Michel (France) (Godet *et al.*, 2008). However, intertidal aggregations may be ephemeral likely due to strong effects of environmental conditions and recruitment on their ability to establish and maintain reef-level populations (Callaway *et al.*, 2010). Analysing the temporal stability of intertidal *L. conchilega* aggregations and engineering effects is a crucial component of the current work. As such, we discuss the repercussions of our assessments on *L. conchilega* conservation status in light of European conservation frameworks in **chapter 6**. In it, the results of all experiments and observations are juxtaposed and further discussed.

1.8. Study site

All *in-situ* work in the present study took place on a portion of the intertidal zone of a sandy beach in Boulogne-sur-mer (Nord-Pas-De-Calais, France) (400309.649152E, 5621211.02256N) (Fig 1.7) between June 2013 and August 2015. This stretch of coast consists of a sheltered pocket-beach delimited by a harbour wall from the port of Boulogne to the south, and a stone pier to the north (Fig 1.7) (Rabaut *et al.*, 2008). The beach is subjected to a semi-diurnal tidal regime with sea level ranging between 4m and 9m (Jouanneau *et al.*, 2013). The site stretched across an area of approx. 700m² (Fig 1.7), with an exposure time of approximately 4h during each LWST (determined from tidal gauge data) (Service Hydrographique et Océanographique de la Marine - SHOM, 2015). The site was selected due to the presence of a thriving *L. conchilega* population as well as accessibility for sampling/experimentation. Intertidal *L. conchilega* aggregations were spread into two zones at the beginning of the study: The low intertidal area was located approx. 250m north of the harbour wall, as near as possible to the low water spring tide (LWST) limit (Fig 1.7). The high intertidal area comprised the uppermost limit of *L. conchilega* distribution at the site and was distanced by approx. 230m from the high water spring tide mark (HWST) (Fig 1.7) The area is also known for extensive subtidal aggregations (Rabaut *et al.*, 2008), however, these were not included in the present research due to its low accessibility.

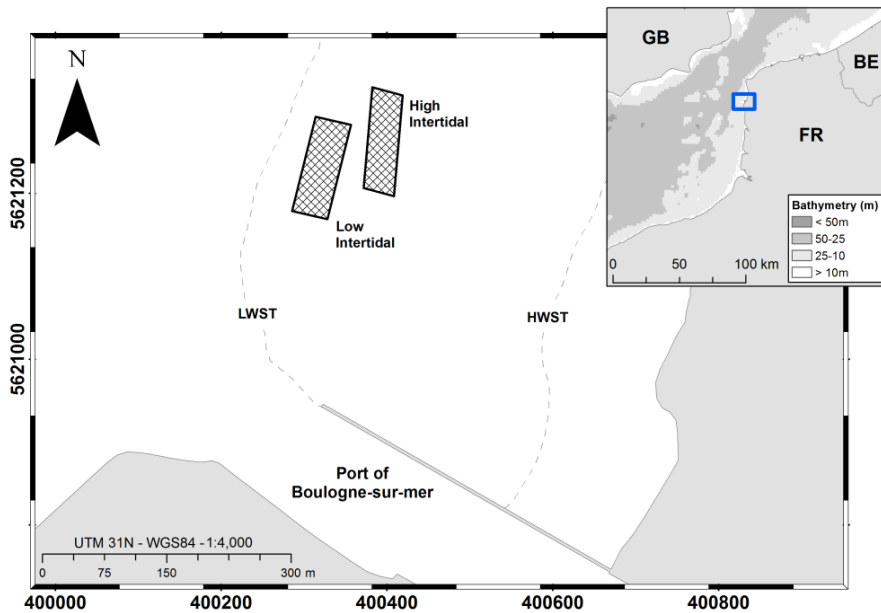


Fig 1.7. The study site (hashed rectangles) was located on the intertidal zone of the sandy beach in Boulogne-sur-mer (Nord-Pas-Des-Calais, France) (blue square). The low intertidal area was distanced approx. 250m from the Boulogne harbour wall and set as close as possible to the low water spring tide (LWST) mark. The high intertidal area was located at the uppermost limit of *L. conchilega* distribution at the site.

1.9. Research framework and thesis outline

Research on the ecology of *Lanice conchilega* is extensive since this tube-worm displays significant functional value, affecting multiple ecosystem compartments. Past research focused on investigating population ecology and the engineering effects of its tube aggregations on biotic and abiotic environmental properties, as well as consequences for associated communities. However, it remains unclear how *L. conchilega* reefs form, decay, and/or become patterned. The present study investigated potential mechanisms related to the aforementioned by focusing on small-scale processes influencing the population dynamics of this tube-dweller, and potentially affecting its distribution. In order to do so, the work was divided into several objectives, assessed specifically for the *L. conchilega* population on the intertidal sandy beach of Boulogne-sur-mer as our study-case.

These objectives are:

1. Analyse the effects of population density variability on the autogenic ecosystem engineering of *L. conchilega*, its modulation of local sediment properties, and feedback effects on population dynamics at very short temporal scales.
2. Evaluate the seasonal fluctuation of intertidal *L. conchilega* population dynamics and its modulation of autogenic ecosystem engineering effects through *in-situ* monitoring of the study-case intertidal aggregations and local sediment properties.
3. Investigate the seasonal fluctuation of small-scale distribution patterns for the study-case intertidal *L. conchilega* aggregations through remote sensing surveys.
4. Explore potential mechanisms influencing spatial pattern formation in the intertidal through population dynamics using a modelling approach.

The combined objectives comprise an effort focused on population dynamics interactions with the environment and potential feedbacks. Each objective was addressed in a distinct chapter with specific methods and targeted discussion.

Lanice conchilega is both an allogenic and autogenic ecosystem engineer. It allogenicly engineers marine sediments through tube irrigation (Braeckman *et al.*, 2014), wherein piston-pumping increases sediment oxygenation and modulates nutrient concentrations (e.g. Braeckman *et al.*, 2014; Forster and Graf, 1995). It also autogenicly engineers marine sediments by attenuating water flow as it passes through its tube aggregations (Borsje *et al.*, 2014), causing increased sedimentation of fine particles (e.g. De Smet *et al.*, 2015; Rabaut *et al.*, 2009). Model simulations indicate that the latter effect occurs as a function of aggregation tube density and likely has a nonlinear relationship to it, ceasing to intensify past a density threshold (Borsje *et al.*, 2014). The aforementioned simulations also indicate that the vertical expansion of *L. conchilega* aggregations may occur via feedbacks between sediment deposition (from autogenic engineering) and tube accretion rates (Borsje *et al.*, 2014). In summary, the aforementioned study hypothesises that sedimentation from autogenic engineering, partially/fully buries *L. conchilega* tubes, triggering higher tube accretion rates and vertical expansion, which in turn cause further increases in sedimentation (Borsje *et al.*, 2014). This hypothetical mechanism was explored in **chapter 2**, wherein we analysed the autogenic ecosystem engineering effects of *L. conchilega* on sedimentary processes and their feedback on population maintenance

and growth. This was investigated through experimental methods within a short temporal scale (*i.e.* 1 week). Objectives comprised: (1) to assess the effects of *L. conchilega* presence and density on erosion and deposition processes, (2) evaluate the influence of these processes on individual survival and tube-maintenance, and (3) assess whether population density displays small-scale spatially explicitly heterogeneity. Results have been published as: Alves RMS, Van Colen C, Vincx M, Vanaverbeke J, De Smet B, Guarini JM, Rabaut M, Bouma TJ. 2017. A case study on the growth of *Lanice conchilega* (Pallas, 1766) aggregations and their ecosystem engineering impact on sedimentary processes. *Journal of Experimental Marine Biology and Ecology*: 489, 15-23. DOI 10.1016/j.jembe.2017.01.005.

Autogenic engineering by polychaete aggregations often depends on their tube density since it affects the area of flow obstruction in aggregations (Eckman *et al.*, 1981). Other features that impact the area of flow obstruction per aggregation include tube dimensions as well as protruding height above the sediment surface (Eckman *et al.*, 1981). As such, individual tube sizes can affect the autogenic engineering effects of an aggregation. *Lanice conchilega* ranges in inner tube diameter from <1mm to 5-6mm as it grows from juvenile to adult, varying in protruding height above the sediment as well (*e.g.* Callaway, 2003; Kessler, 1963; Ropert and Dauvin, 2000; Van Hoey *et al.*, 2006b). As such, we expected that population dynamics and evolution of demographic structure would affect autogenic engineering effects by modulating the area of flow obstruction as populations develop and their demographic composition shifts from predominantly juvenile to predominantly adult. This was explored in **chapter 3**. The work involved *in-situ* monitoring of density and several indicators of autogenic engineering effects in 12 intertidal aggregations from June 2013 until November 2014 of intertidal aggregations. For each sampling event, we evaluated density, population structure, as well as local environmental properties to (1) investigate temporal patterns of *L. conchilega* population dynamics, and (2) assess how these patterns influence *L. conchilega* autogenic engineering of soft sediments. Results have been published as: Alves RMS, Vanaverbeke J, Bouma TJ, Guarini JM, Vincx M, Van Colen C. 2017. Effects of temporal fluctuation in population processes of intertidal *Lanice conchilega* (Pallas, 1766) aggregations on its ecosystem engineering. *Estuarine, Coastal and Shelf Science*: 188, 88-98. DOI 10.1016/j.ecss.2017.02.012.

Mechanisms determining *L. conchilega* distribution and how its autogenic engineering may influence pattern formation were also unclear. Previous studies indicate that *L. conchilega* distribution may be influenced by hydrodynamic conditions at least at the spatial scale of 100-10m – e.g. Callaway, 2003; Heuers *et al.*, 1998; Ropert and Dauvin, 2000). Hydrodynamic flow can influence settlement (Bhaud, 2000) and establishment (e.g. Callaway, 2003; Heuers *et al.*, 1998; Ropert and Dauvin, 2000) by dislodging or removing individuals. Additionally, settlement may be influenced by the presence of protruding structures and/or adult tube presence (Callaway, 2003) as these attenuate hydrodynamic flow (e.g. Callaway, 2003; Heuers *et al.*, 1998; Rabaut *et al.*, 2009). This implies that uneven relief and/or adult distribution should impact settlement variably across space by modulating flow. Although there have been several studies investigating population dynamics (see section 1.4 and 1.5), to the best of our knowledge there were no studies exploring the small-scale patterns of *L. conchilega* aggregations. Small-scale spatial patterns in *L. conchilega* aggregations and their temporal evolution are analysed through remote sensing in **chapter 4**. Intertidal *L. conchilega* aggregations were monitored during the aforementioned campaigns using kite aerial photography (KAP) and low altitude digital photogrammetry. The resulting imagery was used to assemble distribution maps and digital elevation models (*i.e.* 3D relief maps) for (1) assessment of the suitability of KAP and low-altitude digital photogrammetry methods to monitor the small-scale distribution of *L. conchilega* aggregations, (2) develop a detection protocol for remote identification of *L. conchilega* reefs, and (3) analyse the temporal evolution and persistence of small-scale spatial patterns in *L. conchilega* aggregations.

Alternative mechanisms influencing distribution also include consumer-resource interactions (*sensu* Rietkerk and van de Koppel, 2008). *Lanice conchilega* is both a filter- (Buhr, 1976) and deposit-feeder (Ropert and Gouletquer, 2000), consuming mainly microorganisms from the water column and sediment surface (e.g. Braeckman *et al.*, 2012; Lefebvre *et al.*, 2009). Its filter-feeding behaviour is influenced by water flow speed, food availability and particle size (Denis *et al.*, 2007); whereas its deposit-feeding may be hindered by high *L. conchilega* density impeding access to the sediment surface (Buhr, 1976). As such, fluctuations in density and/or hydrodynamic flow conditions can be expected to influence *L. conchilega* feeding through one or both of its feeding modes. Furthermore, *L. conchilega* is often present in areas of high productivity (e.g. Dittmann, 1999; Van Hoey *et al.*, 2006b), and

during periods of low primary production and high thermal stress, such as winter, intertidal (e.g. Beukema, 1992; Callaway *et al.*, 2010; Carey, 1987; Günther and Niesel, 1999; Ropert and Dauvin, 2000; Strasser and Pieloth, 2001) and subtidal populations decline (e.g. Buhr and Winter, 1976; Van Hoey *et al.*, 2006b). This suggests that sustained high food availability may be necessary for establishment and/or population continuity. Thus, food availability fluctuations due to heterogeneous water flow can also be expected to influence population establishment unevenly across space, swaying its distribution. However, assessing the role of feeding and population dynamics on *L. conchilega* distribution is a complex task, and to the best of our knowledge it has not been investigated. This is likely because the task involves complex relationships between several ecosystem compartments in the benthic-pelagic boundary. A population model simulation of a simplified intertidal system comprising nutrients, pelagic algae, microphytobenthos, juvenile, and adult *L. conchilega* was employed in **chapter 5** to investigate the potential effects of (1) food availability and (2) varying food assimilation rates on cohort density dynamics.

Chapter 6 comprises a general discussion, encompassing all obtained results and combining their discussions and conclusions so far. The chapter integrates existing knowledge and the new insights from this thesis to address the role of population dynamics on the temporal evolution of autogenic ecosystem engineering effects, and hypothesises on potential mechanisms for spatial pattern formation in *Lanice conchilega* aggregations based on previous and present findings. Lastly, we discuss how the insights obtained during the making of this thesis can aid and complement ecosystem-based management approaches for conservation efforts, and present prospects for future research.

A monochromatic, blue-tinted underwater photograph showing several dense, branching aggregations of the amphipod *Lanice conchilega* on a sandy seabed. The aggregations are complex, interconnected structures of small organisms. The background is a soft-focus view of the water column.

CHAPTER

2

A case study on the growth of *Lanice conchilega* (Pallas, 1766) aggregations and their ecosystem engineering impact on sedimentary processes

Modified from the publication: Alves RMS, Van Colen C, Vincx M, Vanaverbeke J, De Smet B, Guarini J, Rabaut M, Bouma TJ (2017). A case study on the growth of *Lanice conchilega* (Pallas, 1766) aggregations and their ecosystem engineering impact on sedimentary processes. *Journal of Experimental Marine Biology and Ecology*, 489: 15-23. DOI 10.1016/j.jembe.2017.01.005.

2.1. Abstract

*Ecosystem engineers are organisms that modulate natural resources enabling the survival of other species. They drive environmental change and contribute to several coastal functional attributes such as landscape heterogeneity, sedimentary processes, and coastal protection. Our study focuses on the case of *Lanice conchilega*, a tube-building ecosystem engineer whose aggregations impact sedimentary processes. This polychaete forms biogenic tube aggregations distributed on the coasts of the northern hemisphere from the shallow intertidal to depths of 1 900m. The aggregations engineer sedimentary processes autogenically by altering water flow at the benthic-boundary layer, and harbor highly diverse infaunal communities as a consequence. This study evaluates the relationships between intertidal *L. conchilega* aggregations and sedimentary processes at the intertidal zone of a sandy beach in northern France. Three experiments were executed to investigate (1) the effects of *L. conchilega* presence on sedimentary processes, as well as (2) the impacts of sedimentation on *L. conchilega* survival and aggregation growth, and (3) assess small-scale spatial heterogeneity in density and ecosystem engineering in *L. conchilega* aggregations. Weekly estimations of sedimentary properties in-situ showed that net deposition is significantly higher inside *L. conchilega* aggregations than in bare sand; whereas sediment mixing depth is noticeably reduced in comparison and regardless of tidal height. Variations in tube density above 3 200 ind·m² did not significantly impact sedimentary properties suggesting that the relationship between flow attenuation and tube density is nonlinear. In-situ monitoring of *L. conchilega* aggregations revealed different temporal trends for tube density and EPS content at the sediment surface between the center and edges of aggregations. This hints at the presence of environmental gradients within aggregations that may cause small-scale spatial heterogeneity. Finally, laboratory experiments showed significantly higher mortality rates and tube building activity in the presence of sediment deposition between 5cm and 12cm in column height. Results are in agreement with previous research suggesting that a positive feedback between sedimentation and tube-building activity drives the vertical expansion of tube aggregations. However, vertical expansion may be limited by deposition-induced mortality, thereby controlling population abundance.*

2.2. Introduction

Ecosystem engineers are organisms that modify the environment, modulating natural resource availability directly or indirectly to other species (Jones *et al.*, 1994). Although the term could be used to describe most living organisms, its use generally refers to those that substantially reduce environmental constraints to other species, enabling their survival (Crain and Bertness, 2006). A wide range of organisms engineer coastal environments and affect benthic, pelagic, terrestrial, and intertidal habitats (Gutiérrez *et al.*, 2011). Reef-forming organisms (*e.g.* Dubois *et al.*, 2002), seagrasses (*e.g.* Balke *et al.*, 2012), and bivalves (*e.g.* Drost, 2013) are all examples of autogenic engineers (*i.e.* cause change through presence, Jones *et al.*, 1997). Allogenic engineers include organisms whose activities are the source of change (Jones *et al.*, 1997) (*e.g.* burrowing fauna, Volkenborn *et al.*, 2007; and diatoms, Brouwer *et al.*, 2005). Both types of engineers modulate key functional coastal attributes and processes, such as erosion/accretion (*e.g.* Friedrichs *et al.*, 2000), sediment biogeochemistry (*e.g.* Volkenborn *et al.*, 2007), habitat availability (*e.g.* Dubois *et al.*, 2002) and complexity (*e.g.* Godet *et al.*, 2011), as well as coastal protection (Gutiérrez *et al.*, 2011), thus contributing to ecosystem maintenance (Crain and Bertness, 2006).

This study focuses on the ecosystem engineering by tube aggregations of the terebellid polychaete *Janice conchilega* (Pallas, 1766). This sessile tube-building worm is widely distributed along coastal zones of the northern hemisphere (OBIS, 2015), particularly in Europe (Van Hoey *et al.*, 2008). It occurs in sandy and muddy sediments (Willems *et al.*, 2008) from the shallow intertidal to depths of 1 900m (Hartmann-Schröder, 1996) in biogenic tube aggregations (Godet *et al.*, 2008). These consist of sand tube aggregations that protrude several centimeters above the substrate forming small mounds up to 16cm in height (Godet *et al.*, 2008). Similarly to other tube aggregations, *L. conchilega* aggregations impact water currents locally and modulate sedimentary processes above certain tube density thresholds (Borsje *et al.*, 2014). Furthermore, *L. conchilega* modulates sediment biogeochemistry through tube irrigation (Braeckman *et al.*, 2014). A wealth of associated organisms and high local species richness can be found in *L. conchilega* aggregations (*e.g.* Callaway, 2006; De Smet *et al.*, 2015; Rabaut *et al.*, 2007). These have been attributed to its autogenic and allogenic engineering which positively affect

macrobenthic abundance and species richness as well as epi- and hyperbenthic abundances (De Smet *et al.*, 2015).

The presence of dense tube aggregations enables the formation of 'skimming flow', an attenuated laminar flow formed at the benthic-boundary layer as water passes through the sand tube arrays (Friedrichs *et al.*, 2000). It facilitates fine sediment deposition (Rabaut *et al.*, 2007) that triggers tube-building activity (Borsje *et al.*, 2014). Previous research predicts that flow attenuation intensifies with tube density and sustains the vertical expansion of tube aggregations through a positive feedback process (Borsje *et al.*, 2014). Sediment deposition triggers tube-building activity, which in turn generates more sedimentation and contributes to the vertical expansion of tube aggregations (Borsje *et al.*, 2014). This mechanism has been described through modeling (Borsje *et al.*, 2014) and observed within several biogenic aggregations, such as seagrass beds (Widdows *et al.*, 2008b), mussel mats (Wildish *et al.*, 2008), and marsh vegetation (Bouma *et al.*, 2009a). However, to date, its existence and role in driving *L. conchilega* aggregation growth is not supported by empirical evidence.

Flow attenuation from autogenic engineering also contributes to coastal protection against erosion (Friedrichs *et al.*, 2000) and facilitates larval retention as less larvae are physically removed from the aggregation (Rabaut *et al.*, 2009). Wave attenuation inside polychaete tube aggregations is determined by aggregation size (Eckman *et al.*, 1981), density (Friedrichs *et al.*, 2000), distribution (Koch *et al.*, 2009), and tube protruding height (Eckman *et al.*, 1981). Common drivers of fragmentation include consumer-resource interactions, disturbance-recovery processes, and scale-dependent feedbacks (Rietkerk and van de Koppel, 2008). Our study investigates spatial differences in aggregation properties as a consequence of susceptibility to wave action. In the case of *L. conchilega* aggregations, fragmentation may result from variation in microphytobenthos (MPB) abundance as it is one of its main food sources (Braeckman *et al.*, 2012; Buhr, 1976). Tube density impacts the growth of MPB by modulating particulate organic matter and nutrient entrapment inside aggregations (Passarelli *et al.*, 2012). Consequently, environmental gradients inside tube aggregations can impact polychaete populations leading to variations in MPB abundance and aggregation properties (e.g. Lejeune *et al.*, 2002; Liu *et al.*, 2014). This interaction should influence sediment stability and generate spatial heterogeneity by determining the concentration of extracellular polymeric substances

(EPS) in the sediment surface. EPS is produced by surficial microalgae in the MPB as a motility medium (Lind *et al.*, 1997) and contribute to sediment cohesion and stability of marine sediments (Van Colen *et al.*, 2014).

The aforementioned mechanisms determine the effects of tube aggregations on sediment properties at the benthic-boundary layer, thereby generating spatial heterogeneity in habitat availability and complexity (Godet *et al.*, 2011), and species richness for coastal landscapes (Godet *et al.*, 2008). The current work investigates how intertidal *Lanice conchilega* aggregations affect sedimentary processes at a small scale and the potential feedbacks from these processes onto *L. conchilega* populations. Therefore, we investigate (1) the effects of *L. conchilega* presence on sedimentary processes, as well as (2) the impacts of sedimentation on *L. conchilega* survival and aggregation expansion, and (3) assess small-scale spatial heterogeneity in density and ecosystem engineering in *L. conchilega* aggregations.

2.3. Methods

2.3.1. Study site

Two *in-situ* experiments and one laboratory experiment were executed to investigate the relationship between tube density and local sedimentary processes. The experiments were performed immediately after larval settlement (June 2013 and July 2014) (Ropert and Dauvin, 2000) to increase the probability of finding aggregations that are distinct from its surroundings (Rabaut *et al.*, 2009). The investigated populations were located on an intertidal sandy beach at Boulogne-sur-Mer (Nord Pas-de-Calais, France: 50.7345 N; 1.5881 E) (Fig 2.1). The study site is characterized by an average median grain size of 223.2 μm (SD: 10.6 μm) (see section 2.3.3 for more information), a slope of 0.063 (0.019 SD), and a tidal range of 8.08m (SD: 0.21m) during the summer months (Service Hydrographique et Océanographique de la Marine, SHOM, 2015).

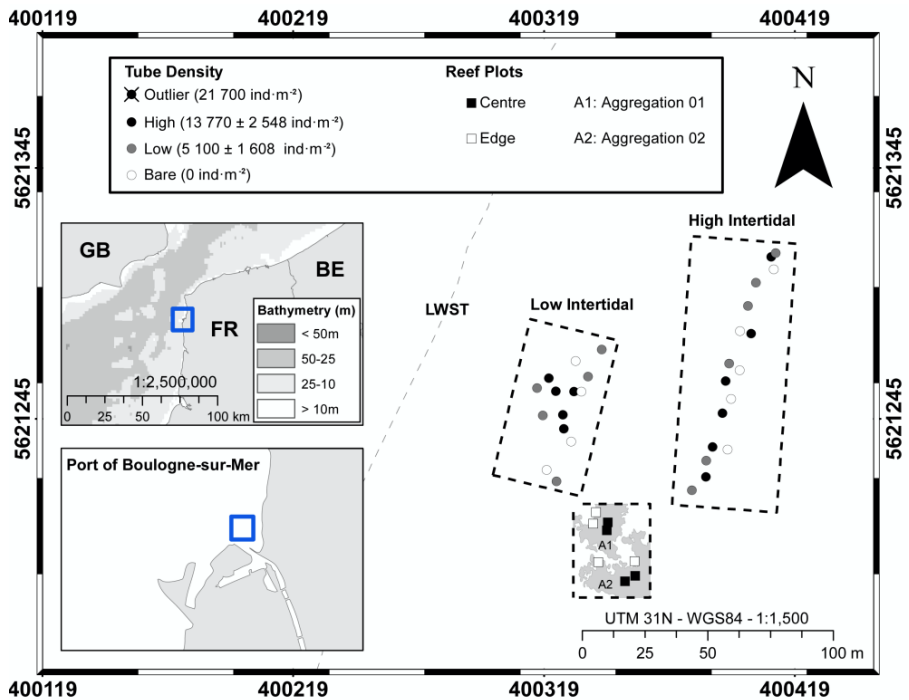


Fig 2.1. Map of the study site on the sandy beach of Boulogne-sur-Mer (France) depicting the experimental units for experiments in sections 2.3.2 and 2.3.3. Aggregations studied in section 2.3.2 were distributed in two portions of the intertidal zone (higher and lower intertidal) and included *L. conchilega* aggregations of high and low densities as well as bare sand (Mean±SD). One aggregation of extreme density was excluded from statistical analyses (outlier). The plots studied in section 2.3.3 can be seen in the figure near the center and edges of two large aggregations (A1 and A2).

2.3.2. Effects of *L. conchilega* presence on sedimentary processes

This experiment investigated the *in-situ* effect of tube density and aggregation tidal height on sedimentary processes for 5 days during June 2013. Two parameters were measured from 31 aggregations distributed on the intertidal zone of the study site: net deposition (ND) and sediment mixing depth (SMD) (adapted from Marion and Orth, 2012). Sediment mixing depth was measured as the distance in centimeters between the sediment surface and the depth at which there is no reworking due to wave action. Net deposition was defined as the difference between the sediment

column height inside cores at the start and the end of the experiment (*i.e.* the net amount of sediment (cm) deposited during the experiment).

Estimations of ND and SMD were made using marked sediment cores distributed *in-situ* between two portions of the intertidal with different tidal heights (lower and higher intertidal in Fig 2.1). The lower intertidal site was delineated as close to the mean low water spring tide as possible while still enabling sampling during the emersion period, whereas the higher intertidal site comprised the upper limit of the distribution of *L. conchilega* aggregations (Fig 2.1). The two areas were separated horizontally by approximately 50m, and vertically by approximately 0.5m (difference in inundation time of approx. 1h).

Thirty one cores (Φ : 3.6cm x 33.0cm height) containing 30 layers of sediment with 0.5cm thickness alternating between clean sand from the site (d_{50} : 192 μ m) and white tracer sand (d_{50} : 191 μ m) (Fig 2.2A) were prepared in laboratory. Subsequently, the cores were transported frozen to the study site and inserted into the center of 31 randomly chosen aggregations: 17 cores in the higher intertidal and 14 cores in the lower intertidal (Fig 2.1). Tube density was estimated for these aggregations through quadrat counts (0.5m x 0.5m) of which 3 subdivisions (0.1m x 0.1m) were assessed. Only fringed tubes were counted since *L. conchilega* maintains a healthy fringe at the top of its tube which is quickly removed by wave action once the animal dies (Van Hoey *et al.*, 2006a). Three density classes were delineated according to the densities found *in-situ* at the time of the study: high (H, average: 13 770, SD: 2 548 ind·m⁻²), low (L, average: 5 100, SD: 1 608 ind·m⁻²), and bare sediment (N, 0 ind·m⁻²) (Fig 2.1). Once the marked cores were deployed, the difference between the surface of each core and the sediment surface of their surroundings was measured with a ruler and called “initial offset” (cm) (Fig 2.2A). The cores were left buried for 5 days, *i.e.* 4 tidal cycles (Service Hydrographique et Océanographique de la Marine, SHOM, 2015) (Fig 2.2B), and extracted with the aid of an extraction core. Subsequently, they were transported to the lab and re-frozen until further analysis. In the lab, the frozen sediment was pushed out of the extraction core, and sectioned longitudinally with a knife. The number of missing layers from each core was counted and used to estimate sediment mixing depth (SMD, eq2.1) per core. The thickness of the layer between the surface of each core and the first observable marked layer was recorded as the “sampled offset” (Fig 2.2C) and used to calculate net deposition (ND, eq2.2) per core.

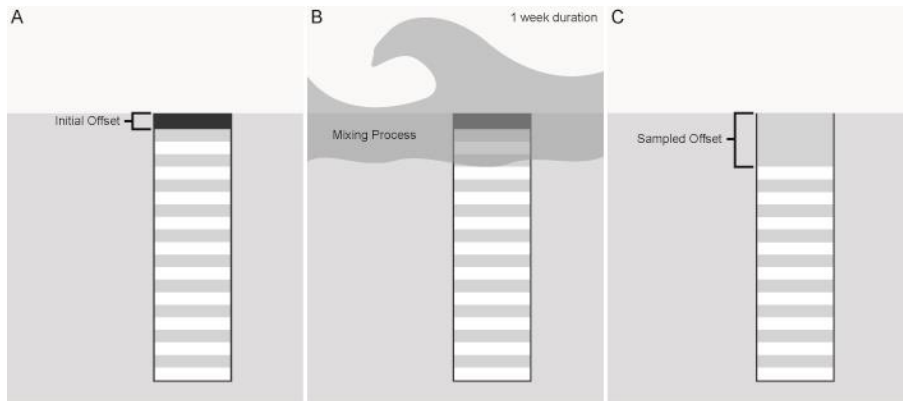


Fig 2.2. In-situ phases of the assessment of *L. conchilega* effects on sedimentary processes: Thirty one marked frozen cores were deployed in the center of aggregations at the study site and the initial offset between the core surface and the surface of the surrounding sediment was registered (A); the cores were exposed to the local tidal regime for 1 week (*i.e.* 8 semidiurnal tidal cycles) (B); cores were retrieved from the field with the aid of an extraction core (C) and transported to the lab for analyses. During analyses, the distance between the first observable layer of marked sediment and the surface of the core was estimated as “sampled offset” (C).

$$\text{Eq 2.1: SMD (cm) = Number of missing layers} * 0.5$$

$$\text{Eq 2.2: ND (cm) = Initial offset + Sampled offset} - \text{SMD}$$

The effects of *L. conchilega* presence on net deposition and sediment mixing depth were tested using 2-way ANOVAs type II each including the effects of aggregation tidal height. The effects of tube density on ND and SMD were also analyzed with 2-way ANOVAs type I including tidal height. Assumptions of case independence, normality in the distribution of residuals, and homoscedasticity were confirmed in all tests. Tube density in core #05 (*i.e.* 21 700 ind·m⁻²) deployed in the lower intertidal deviated markedly from the average density of aggregations in the high density class (*i.e.* 13 770 ± 2 548 ind·m⁻²). As such data from core #05 was excluded from statistical analysis (Fig 2.1).

2.3.3. Spatially-dependent effects of temporal variability in *L. conchilega* density

This experiment compared the temporal evolution of tube density and environmental properties between the center and edges of *L. conchilega* aggregations to evaluate small-scale spatial heterogeneity. It took place *in-situ* for 14 days during July 2014 involving the weekly monitoring of two large aggregations – *i.e.* 3 sampling moments. Tube density was estimated through quadrat counts (0.5m x 0.5m) of which 2 subdivisions (0.1m x 0.1m) were assessed for fringed tubes (Van Hoey *et al.*, 2006a) for plots near the center and edges of two large *L. conchilega* aggregations (A1 and A2 in Fig 2.1). To ensure that each count only included living animals, the fringes of all sand tubes in the experimental plots were removed after each count. Sediment samples (0-1cm in depth) were taken with a core (Φ : 3.6cm) next to the quadrats to assess biotic and abiotic environmental properties. Biotic conditions of the microphytobenthos were assessed through chlorophyll-*a* content (μg of chl-*a* per grams of sediment) as a proxy of microalgae biomass, the relative amount of extracellular polymeric substances (EPS: milligrams of glucose equivalents per milligrams of sediment¹) as an indication of microalgae activity (Lind *et al.*, 1997), and total organic matter content (TOM: grams of organic matter per grams of sediment). Abiotic conditions were assessed using granulometry including the estimation of median (d50: μm), maximum frequency grain size (MFGS) (mode: μm), sediment sorting (dimensionless), mud content (% < 63 μm), and fine-medium sand content (%: 125-500 μm) as well as water content (grams of water per grams of sediment).

Chl-*a* content was estimated using a modification of the methods described in Wright and Jeffrey (1997) for high performance liquid chromatography (HPLC). Samples were extracted in 90% acetone, sonicated and filtered at 0.2 μm , then analyzed using a high resolution HPLC Gilson system with a C18 column. EPS content was estimated for water-extractable carbohydrates fraction using a modification of methods from Hubas *et al.* (2010). Samples were diluted in 400 μL of distilled water, homogenized with a tube roller, put in a warm water bath for 60mins at 30°C, and centrifuged (4 000g for 5mins at 21°C). Subsequently, 200 μL of supernatant was sub-sampled, 200 μL phenol (5%) and 1mL sulfuric acid (100%) were added to it, and the sample was again homogenized. The mixture was incubated for 30 minutes at room temperature and the amount of d-glucose equivalents was measured with a spectrophotometer at 486nm wavelength (Victor3 1420 Multilabel Counter from 42

¹ EPS is composed of several fractions, not only glucose equivalents. We recommend that future work assess its other fractions and refrain from using glucose equivalents as a proxy for EPS alone.

Perkin Elmer). Total organic matter was estimated through the difference between the dry weight of each sample (48h in 60°C) and its weight after burning (2h at 500°C). Median grain size, MFGS, and mud content were obtained through granulometry analysis using a Malvern Mastersizer 2000 particle analyzer (size range: 0.020µm to 2000.000µm). Sediment sorting was calculated according to Inman (1952) using parameters of the granulometry analysis. Water content was estimated per sample as the difference between wet and dry weight following lyophilisation and converted into a ratio of grams of water per grams of sediment.

Repeated measures analyses of variance (rANOVA) were used to compare temporal trends in tube density and environmental conditions between the center and edges of *L. conchilega* aggregations. Mauchly's test was performed to check the sphericity assumption and Greenhouse-Geisser correction was applied in cases under which the assumption was unfulfilled (Greenhouse and Geisser, 1959), *i.e.* tube density, (p : 0.032), chl-*a* (p : 0.006), and water content (p : 0.001). Tukey HSD tests were performed to determine spatial (*i.e.* edge vs center) differences between properties at each sampling date and temporal differences within locations. Finally, a storm occurred prior to t_1 which has impacted results. The occurrence was identified visually by the amount of sediment reworking in the *L. conchilega* aggregations at the moment of sampling and subsequently confirmed from the change in sediment fractions over the course of the experiment (see results).

2.3.4. Effects of abrupt sedimentation on *L. conchilega*

This experiment assessed how sediment deposition affects mortality and tube-building rates of *L. conchilega*. It was executed in the laboratory for 1 week during July 2014. Sediment was collected from the intertidal zone with shovels, transported to the lab in 20L buckets, sieved through 1mm mesh, and homogenized in clean sea water (32 psu) prior to the beginning of the experiment. Specimens were collected from Boulogne after recruitment using 18 cores (Ø: 5.6cm, height: 100cm) containing 10 ± 5 individuals. Cores were incubated in sea water tanks (10°C, 32psu) in the laboratory for 3 days prior to the beginning of the experiment for acclimation purposes. To avoid accumulation of bodily secretions within cores, each core received individual oxygenation and the water in the tanks was constantly recirculated between experimental and reserve tanks. A count of living animals (identified by the status of their fringe, Van Hoey *et al.*, 2006a) was performed at the

start of the experiment, and the tube lengths of three randomly chosen polychaetes per core were measured with a ruler from the sediment surface to the tip of their fringe. Subsequently, each core received a single amount of clean sediment from the study site. The height of the sediment column in each core was increased by one of the following: 0, 3, 5, 7, 9, or 12cm, and replicated using 3 separate cores. The experiment ran for 7 days, mortality was assessed at the end of the experiment, normalized to the proportion of the total number of individuals. In addition, the tube length of the same 3 individuals measured at the start of the experiment was estimated at the end and used to calculate tube accretion rates (TAR, cm·week⁻¹) (eq 2.3). Tube-accretion rates were calculated using tube length at the start (TL₀) and at the end (TL_f) of the experiment, as well as the amount of added sediment (AS) to each core according to equation 3.

$$\text{Eq 2.3: } \text{TAR (cm}\cdot\text{week}^{-1}\text{)} = (\text{AS} - \text{TL}_0) + \text{TL}_f$$

The effect of sediment deposition on arcsine transformed mortality (McDonald, 2014) and tube-accretion rates was tested separately using two Permutational Multivariate Analyses of Variance (PERMANOVAs) type-III based on Euclidean distances between samples with 9999 permutations, and Monte Carlo testing due to the low level of replication per treatment level (3x). PERMDISP was executed in both cases to test the assumption of homogeneity of dispersion. The method was chosen because the data failed the normality assumption for parametric testing. The statistical analyses were executed using PRIMER v6 (Clarke and Gorley, 2006) and the PERMANOVA+ add-on (Anderson *et al.*, 2008).

2.4. Results

2.4.1. Effects of *L. conchilega* presence on sedimentary processes

The analysis revealed noticeable effects from *L. conchilega* presence on net deposition ($F_{1,26}$: 4.862, p : 0.037) and sediment mixing depth ($F_{1,26}$: 6.617, p : 0.016). Aggregations at different tidal heights had similar ND ($F_{1,26}$: 0.545, p : 0.467) and SMD ($F_{1,26}$: 0.297, p : 0.591). Tube density did not significantly affect ND ($F_{1,24}$: 2.445, p : 0.108) or SMD ($F_{1,24}$: 3.372, p : 0.051). Net deposition of 0.14cm (SE: 0.42cm) and 0.14cm (SE: 0.57cm) were observed inside high and low density aggregations respectively, whereas bare sand eroded with average ND of -0.95cm (SE: 0.34cm)

(data pooled from both intertidal areas) (Fig 2.3A). Average SMD was 1.25cm (SE: 0.39cm) and 1.25cm (SE: 0.36cm) in high and low density aggregations respectively, and 2.31cm (SE: 0.43cm) in bare sand (data pooled from both intertidal areas) (Fig 2.3B).

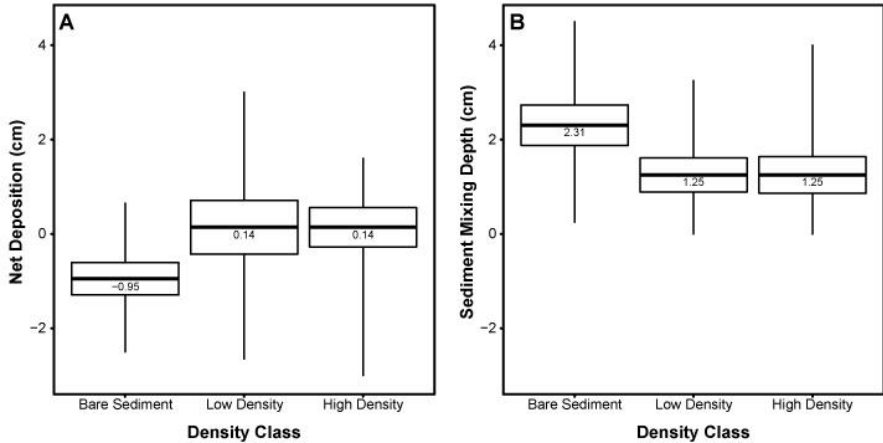


Fig 2.3. Net deposition (A) and sediment mixing depth (B) per tube density class. No significant effects of tube density were found on either sedimentary parameter. Boxplots: Min., Mean \pm SE, Max.

2.4.2. Spatially-dependent effects of temporal variability in *L. conchilega* density

Analyses revealed that tube density was significantly affected by time and the “time x location” interaction (Table 2.1). Significant temporal variation was found for chl-a, EPS, TOM, mud and fine-medium sand content (Table 2.1). Tukey tests revealed that conditions were not significantly different between the center and edges of *L. conchilega* aggregations at t_0 , though tube densities were, on average, higher in the center (12 400 ind·m⁻², SE: 547 ind·m⁻²) than at the edges (8 113 ind·m⁻², SE: 758 ind·m⁻²) (Fig 2.4). From t_0 to t_1 , tube density declined significantly at both locations (p_{center} : 0.000; p_{edge} : 0.003) (Fig 2.4A), as well as chl-a (p_{center} : 0.002; p_{edge} : 0.020) and TOM (p_{center} : 0.012; p_{edge} : 0.025). All measured environmental properties were similar at t_1 at both locations (Fig 2.4). Tube density was at its minimum value and so were concentrations of chl-a, EPS, TOM, and mud content (Fig 2.4A-E). Fine-medium sand content peaked at t_1 (Fig 2.4F) reflecting the occurrence of a storm-

driven sediment deposition/reworking. Subsequently, EPS content significantly increased at the edges between t_1 and t_2 (p : 0.026) with a similar trend observed for tube densities (p : 0.002) (Fig 2.4). At t_2 , tube density (p : 0.000), chl-a (p : 0.008), and TOM (p : 0.017) were significantly lower at the center than at the start of the experiment (t_0) (Fig 2.4A and B).

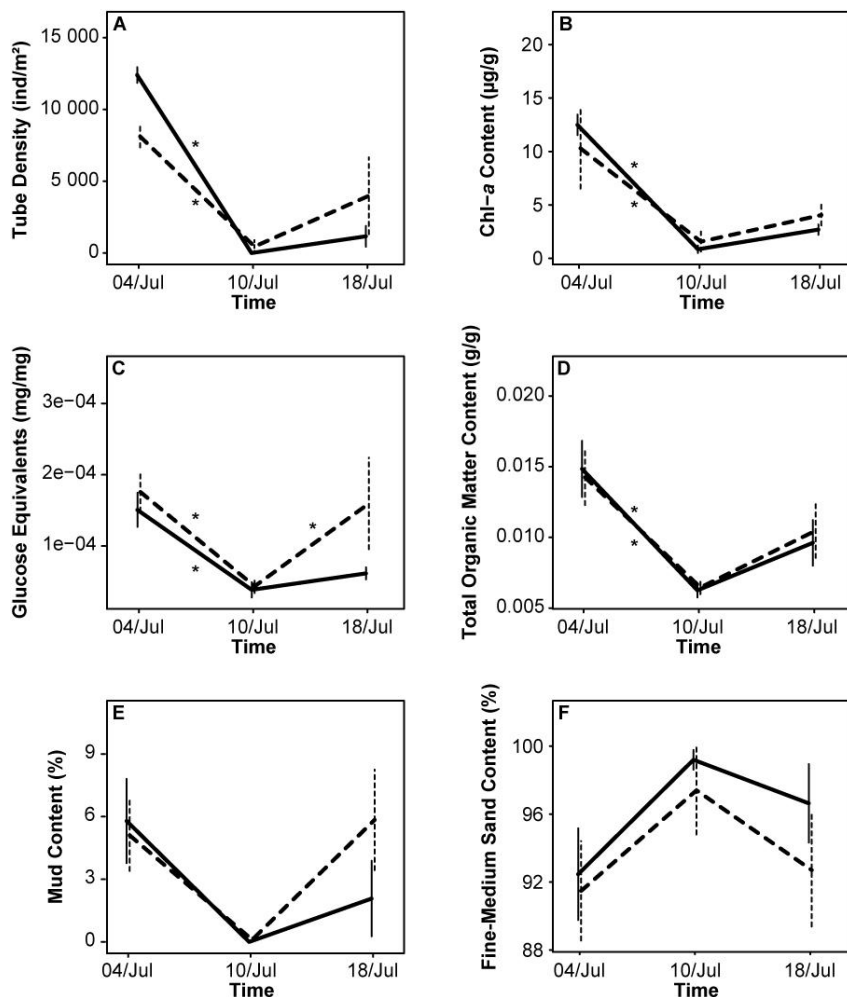


Fig 2.4. Variations of tube density (A), Chl-a content (B), EPS content (C), total organic matter content (D), mud content (E), and fine-medium sand content (F) in the center of reefs (continuous lines) and at reef edges (interrupted lines) through the length of the experiment. Significant results from the rANOVAs are marked with an asterisk (*). Mean \pm SE.

Table 2.1. Results of the repeated measures ANOVA evaluating the effects of within-reef location, time, and their interaction on all variables. Significant results are marked with an asterisk. Greenhouse-Geisser corrected statistics display the adjusted degrees of freedom.

	Factors		
	Reef Location	Time	Location x Time
Tube density (ind m ⁻²)		F _{2,12} : 55.398; p: 0.000 *	F _{2,12} : 6.598; p: 0.035 *
Chl-a (µg g ⁻¹ sediment)		F _{2,12} : 31.702; p: 0.001 *	F _{2,12} : 0.988; p: 0.363
EPS (mg g ⁻¹ sediment)	F _{1,18} : 1.436; p: 0.276	F _{2,18} : 15.690; p: 0.001 *	F _{2,18} : 2.495; p: 0.124
TOM (g g ⁻¹ sediment)	F _{1,18} : 0.007; p: 0.937	F _{2,18} : 39.213; p: 0.000 *	F _{2,18} : 0.312; p: 0.738
Median grain size (µm)	F _{1,18} : 0.470; p: 0.520	F _{2,18} : 0.420; p: 0.669	F _{2,18} : 1.390; p: 0.286
MFGS (µg)	F _{1,18} : 0.820; p: 0.400	F _{2,18} : 0.160; p: 0.856	F _{2,18} : 2.390; p: 0.134
Sediment sorting index	F _{1,18} : 0.372; p: 0.564	F _{2,18} : 3.835; p: 0.052	F _{2,18} : 0.305; p: 0.743
Mud content (%)	F _{1,18} : 0.379; p: 0.561	F _{2,18} : 8.715; p: 0.005 *	F _{2,18} : 1.586; p: 0.245
Sand content (%)	F _{1,18} : 0.499; p: 0.506	F _{2,18} : 8.749; p: 0.005 *	F _{2,18} : 0.506; p: 0.615
Water content (g g ⁻¹ sediment)		F _{2,12} : 1.719; p: 0.238	F _{2,12} : 0.653; p: 0.453

2.4.3. Effects of abrupt sedimentation on *L. conchilega*

The assumption of homogeneity of (univariate) dispersion was tested using PERMDISP and successfully fulfilled for arcsine mortality ($F_{5,12}$: 0.831, p : 0.808) and tube-accretion rate ($F_{5,30}$: 0.097, p : 0.998). Sediment deposition generated significant increases in mortality ($F_{5,12}$: 4.347, p : 0.014). Pairwise comparisons and Monte Carlo testing (MC) revealed that mortality was significantly lower in the absence of sedimentation (0cm) than in its presence - 5cm (p_{MC} : 0.020), 7cm (p_{MC} : 0.009), 9cm (p_{MC} : 0.015), and 12cm (p_{MC} : 0.017) (Fig 2.5). At the end of the experiment 100% mortality was observed in 2 out of 18 cores (5cm and 7cm). *Janice conchilega* tube-building rates ranged from 0.05 to 1.60cm·day⁻¹ with higher rates in the presence of sediment deposition ($F_{5,30}$: 118.76, p_{MC} : 0.000). Post-hoc comparisons show that TAR were significantly lower in control cores (0cm) than in cores with 3cm (p_{MC} : 0.000), 5cm (p_{MC} : 0.000), 7cm (p_{MC} : 0.000), 9cm (p_{MC} : 0.000), and 12cm (p_{MC} : 0.000) of deposited sediment.

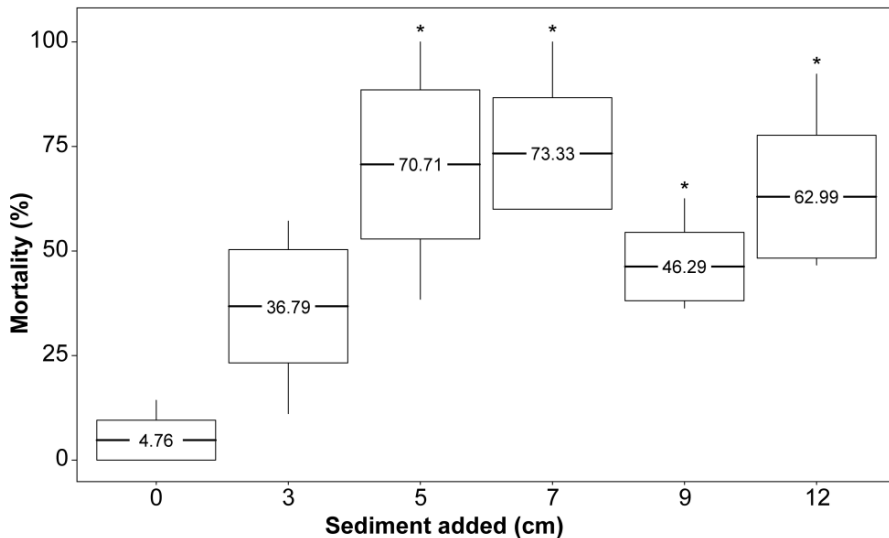


Fig 2.5. Fluctuations in *L. conchilega* mortality relative to sediment added (AS, eq3). Statistical analyses revealed that arcsine mortality in the presence of sediment deposition events from 5cm to 12cm in column height are significantly different (*) than that estimated for the control (0cm). Boxplots: Min., Mean \pm SE, Max.

2.5. Discussion

This study investigated the relationship between *L. conchilega* aggregation properties and small-scale coastal sedimentary properties at the intertidal zone of a sandy beach in Boulogne-sur-Mer (France). Results revealed that (1) net deposition is significantly higher in *L. conchilega* aggregations when compared to bare sand; (2) sediment mixing depth is noticeably shallower inside aggregations than out; (3) net deposition and sediment mixing depth are not affected by tube density for aggregations above 3 200 ind·m⁻²; (4) temporal fluctuations in tube density are noticeably different between the center and edges of aggregations; and (6) sediment deposition from 3cm in column height cause significant increases in tube-building rate, while (7) deposition from 5 to 12cm in column height result in significantly higher *L. conchilega* mortality.

2.5.1. Effects of *L. conchilega* presence on sedimentary processes

Tube aggregations influence two key attributes of the coastal environment, sedimentary processes and coastal protection (Gutiérrez *et al.*, 2011) by changing water flow as a function of tube density (Friedrichs *et al.*, 2000). Water moving through denser aggregations has lower velocity than currents passing through sparser tube arrays (Friedrichs *et al.*, 2000). The changed hydrodynamic conditions create heterogeneity in sedimentary processes at different intensities (*e.g.* Borsje *et al.*, 2014; Passarelli *et al.*, 2012). This study investigated how *L. conchilega* tube aggregations impact small-scale sedimentary processes by comparing net deposition and sediment mixing depth between *L. conchilega* aggregations and bare sand.

Previous *in-situ* observations using mimic tubes revealed significant effects of tube presence with densities as low as 637 ind·m⁻² (Passarelli *et al.*, 2012) and 1 000 ind·m⁻² (Rabaut *et al.*, 2009). A modelling study (Borsje *et al.*, 2014) predicted that the relationship between tube density and water flow deceleration is nonlinear, that is, the effect intensifies sharply as density grows from 0 to 1 000 ind·m⁻² but weakens past that threshold. Our study found noticeable effects of *L. conchilega* presence on sedimentary processes with higher net deposition and shallower sediment mixing depth inside aggregations than in bare sand. This is in accordance with previous observations suggesting that these aggregations affect both erosion/accretion processes and therefore coastal resilience to hydrodynamic impacts. Average ND and SMD were similar between density classes, which was expected as the range of

tube densities in this study was above 1 000ind·m⁻² (Borsje *et al.*, 2014). However it is worth noting that results for SMD were close to the significance threshold of 0.05. Thus the effect of high tube density on sediment mixing depth requires further investigation as results are marginally insignificant (Goodman, 2008).

2.5.2. Spatially-dependent effects of temporal variability in *L. conchilega* density

The functional importance of biogenic concretions in coastal environments includes the physical protection from hydrodynamic impacts such as wave action (Koch *et al.*, 2009). In the case of tube-building organisms, wave attenuation is a function of aggregation size and tube density (Eckman *et al.*, 1981), and is related to patchy distributions and environmental gradients inside the aggregation (*e.g.* Lejeune *et al.*, 2002; Liu *et al.*, 2014). This experiment investigated temporal variations of tube density and environmental properties between the center and edges of *L. conchilega* aggregations to evaluate potential drivers of small-scale spatial heterogeneity.

Animals at the center of aggregations are surrounded by other tubes, and thus less exposed to wave action, while at the edges they are partially encircled and thus more susceptible to hydrodynamic impact. Mortality should be affected by this configuration as it imposes a gradient of susceptibility to wave action within the biogenic aggregation (*e.g.* van Wesenbeeck *et al.*, 2008). Thus environmental gradients can create spatial heterogeneity by inducing spatially-explicit fluctuations in population density (*e.g.* Lejeune *et al.*, 2002; van Wesenbeeck *et al.*, 2008). In this study, tube density varied differently between aggregation edges and center plots as a significant effect was found for “time x location”. This confirms small-scale spatial heterogeneity in fluctuations of population abundance.

Variations in abundance of ecosystem engineers can lead to heterogeneity in environmental properties through autogenic engineering (*e.g.* Bouma *et al.*, 2009a; van Wesenbeeck *et al.*, 2008). Polychaete tubes modulate microalgal abundance as a function of density with denser aggregations facilitating particle entrapment and stimulating the development of the surficial microalgae (Passarelli *et al.*, 2012). Thus, variation in tube density should impact chl-*a*, EPS, TOM, mud and fine-medium sand content through autogenic engineering, creating different environmental conditions between the center and edges of tube aggregations. Temporal trends revealed significant declines in tube density, chl-*a*, EPS, and TOM from t_0 to t_1 at center and

edges suggesting that the storm impacted fluctuations in population abundance and environmental properties from that time onwards. At t_1 , center and edges had lower mud content and higher fine-medium sand content, which is consistent with storm effects reworking surficial sediment and removing and/or burying fauna (e.g. Dobbs and Vozarik, 1983; Regnauld *et al.*, 2004; Yeo and Risk, 1979). No noticeable differences were found between the center and edges of aggregations from t_1 onwards. From t_1 to t_2 , EPS content increased at the edges of aggregations only, suggesting that processes of aggregation maintenance and/or recovery from disturbance vary spatially at a small scale. However, recovery processes could not be fully evaluated with the current setting. Additional research is required to investigate the response of population abundance and structure over time to this type of storm impact. Additionally, fluctuations in EPS should be considered alongside chl-*a* as both are commonly associated to the microphytobenthos and as such are expected to fluctuate in tandem.

Surficial chl-*a* relates to benthic microalgae biomass, whereas EPS content is associated to microalgae activity as it is produced as a motility medium (Lind *et al.*, 1997). Small variations in local conditions, such as hydrodynamic pressure (Tolhurst *et al.*, 2003), light regimes (Cartaxana *et al.*, 2006), and biofilm age and species composition (Smith and Underwood, 2000) can result in varying physiological states of microalgal communities, influencing EPS production and leading to diverging patterns (e.g. Perkins *et al.*, 2003; Ubertini *et al.*, 2015; Underwood *et al.*, 2004). Due to the complexity of MPB dynamics it is not possible to determine which factors caused the observed fluctuations. Therefore, further research on biofilm dynamics is necessary to clarify our observations. Tube density and concentrations of chl-*a* and TOM at center plots were significantly lower at the end of the experiment than at the start, while at the edges no significant differences were found between those dates. This likely reflects the start of population recovery from the storm and substantiates the previously mentioned differences in recovery between the center and edges.

Finally, a storm clearly impacted population dynamics and local environmental characteristics to an unknown extent during the experiment reported in section 2.4.2. Acknowledging the potential effects of storms, a hypothesis can be put forward that such periodic disturbance events are likely to modulate aggregation-related processes contributing to episodes of vertical growth, thus modulating coastal sedimentary processes, maintaining habitat complexity and species richness.

However, the role of population structure in attenuating hydrodynamic flow and modulating microalgae abundance and activity remains unclear. Further study is required to determine whether autogenic engineering can drive small-scale spatial heterogeneity inside polychaete aggregations.

2.5.3. Effects of abrupt sedimentation on *L. conchilega*

The effect of sedimentation on *L. conchilega* mortality rates was investigated. Different levels of deposition were tested since sedimentation can originate from extreme conditions such as storms (Dobbs and Vozarik, 1983), long-term increased deposition from autogenic engineering (e.g. Godet *et al.*, 2011; Rabaut *et al.*, 2009), and/or as a consequence of anthropogenic activities in the coastal zone (Kaiser *et al.*, 2001). Sediment deposition resulted in complete mortality in 2 out of the 18 cores in the study and increased tube-building activity in the surviving individuals. This suggests that *L. conchilega* is able to survive deposition events from 3 to 12cm albeit in limited numbers. Tube-building rates ranged from 0.01 to 1.60 cm-day⁻¹ which is in accordance with what has been observed in previous research (e.g. Borsje *et al.*, 2014; Rabaut *et al.*, 2009). Higher TARs can contribute to individual survival, as well as the vertical expansion of tube aggregations (Borsje *et al.*, 2014). Thus, results corroborate previous work predicting a positive feedback between sediment deposition and tube-building activity which drives aggregation growth (Borsje *et al.*, 2014).

It is worth noting that a control core (*i.e.* devoid of sediment deposition) presented an increase in numbers from 9 to 11 individuals during the experiment, thus adding variance to the control level. This is most likely due to the initial presence of small juveniles that were not detected at the first count. Although this could be the case for other units, it does not undermine the results of the experiment.

2.6. Conclusions

The current study corroborates previous predictions on the influence of polychaete tube aggregations on sedimentary processes using *L. conchilega* aggregations as a case-study. Modelling predictions on the vertical expansion of tube aggregations base the process on positive feedbacks between sediment deposition and tube-building rates. In the current case, significant deposition was created inside tube aggregations *in-situ* and tube-building activity increased under sediment deposition as small as 3cm in height under controlled conditions. The feedback between

increased sedimentation and tube-building can contribute to the vertical expansion of polychaete aggregations. However, deposition between 5 and 12 cm in column height caused higher mortality, which could limit the growth of tube aggregations at least temporarily. The level of net deposition within the studied aggregations at Boulogne-sur-mer was below 5cm in height, and thus it is unlikely that the engineering-mediated deposition regime at the site could lead to increased mortality inside *L. conchilega* aggregations. An alternative hypothetical mechanism should be considered and remains to be tested wherein periodic storm events, such as the one noted during this study, generate enough sedimentation to trigger episodic aggregation development while limiting population density through mortality. Furthermore, population-related processes differed between the center and edges of aggregations impacting the temporal fluctuation of microalgae activity (*i.e.* EPS content). These findings suggest that sedimentary changes imposed by *L. conchilega* may substantially affect benthic communities, as observed by previous research. In addition, small-scale benthic biodiversity gradients may form within aggregations due to fluctuations in the ecosystem engineering effect of *L. conchilega* induced by population development, increasing landscape heterogeneity under conditions that are yet to be clarified.



CHAPTER

3

Effects of temporal fluctuation in population processes of intertidal *Lanice conchilega* (Pallas, 1766) aggregations on its ecosystem engineering

Modified from the publication: Alves RMS, Vanaverbeke J, Bouma TJ, Guarini JM, Vincx M, Van Colen C (2017). Effects of temporal fluctuation in population processes of intertidal *Lanice conchilega* (Pallas, 1766) aggregations on its ecosystem engineering. *Estuarine, coastal and shelf science*, 188: 88-98. DOI 10.1016/j.ecss.2017.02.012.

3.1. Abstract

*Ecosystem engineers contribute to ecosystem functioning by regulating key environmental attributes, such as habitat availability and sediment biogeochemistry. While autogenic engineers can increase habitat complexity passively and provide physical protection to other species, allogenic engineers can regulate sediment oxygenation and biogeochemistry through bioturbation and/or bioirrigation. Their effects rely on the physical attributes of the engineer and/or its biogenic constructs, such as abundance and/or size. The present study focused on tube aggregations of a sessile, tube-building polychaete that engineers marine sediments, *Lanice conchilega*. Its tube aggregations modulate water flow by dissipating energy, influencing sedimentary processes and increasing particle retention. These effects can be influenced by temporal fluctuations in population demographic processes. Presently, we investigated the relationship between population processes and ecosystem engineering through an in-situ survey (1.5 years) of *L. conchilega* aggregations at the sandy beach of Boulogne-sur-Mer (France). We (1) evaluated temporal patterns in population structure, and (2) investigated how these are related to the ecosystem engineering of *L. conchilega* on marine sediments. During our survey, we assessed tube density, demographic structure, and sediment properties (surficial chl-a, EPS, TOM, median and mode grain size, sorting, and mud and water content) on a monthly basis for 12 intertidal aggregations. We found that the population was mainly composed by short-lived (6-10 months), small-medium individuals. Mass mortality severely reduced population density during winter. However the population persisted, likely due to recruits from other populations, which are associated to short- and long-term population dynamics. Two periods of recruitment were identified: spring/summer and autumn. Population density was highest during the spring recruitment and significantly affected several environmental properties (i.e. EPS, TOM, mode grain size, mud and water content), suggesting that demographic processes may be responsible for periods of pronounced ecosystem engineering with densities of approx. 30 000 ind·m⁻².*

3.2. Introduction

Living organisms interact with each other and with the environment in various ways, modifying biotic and abiotic properties of their habitats, and modulating the availability of resources to other species. Through these modifications, organisms engineer ecosystems and condition the survival of other species in otherwise unfavourable environments, earning the title of ecosystem engineers (Jones *et al.*, 1994). Although most living organisms could be described as ecosystem engineers, the term generally refers to those that substantially reduce environmental constraints to other species, enabling their survival (Crain and Bertness, 2006). Jones *et al.* (1994) distinguished two classes of ecosystem engineers: (1) autogenic engineers, consisting of organisms that cause change through physical presence (e.g. coral reefs whose presence increases habitat complexity - Wild *et al.*, 2011), and (2) allogenic engineers, which include organisms that modulate resources through their activities (e.g. fiddler crabs whose burrow construction and maintenance impact sediment biogeochemistry - Kristensen, 2008). The changes imposed by engineering organisms may have extensive consequences to the environment. Their presence and activities impact community species richness (Romero *et al.*, 2015) and functional biodiversity (Gutiérrez and Jones, 2006), as well as matter transport (Kristensen, 2008), sediment accretion/erosion patterns (Bouma *et al.*, 2009a), and sediment composition (De Smet *et al.*, 2015; Monserrat *et al.*, 2009).

Ecosystem engineers can be short-lived (see Jones *et al.*, 1994), but little is known about how a short population dynamics cycle can affect the consequences of ecosystem engineering in the surrounding habitat. The present work addresses this question focusing on a marine species as a case study: the terebellid tubeworm *Lanice conchilega* (Pallas, 1766). This sessile polychaete is a particularly interesting model species as it is both an autogenic and an allogenic ecosystem engineer (Braeckman *et al.*, 2014) with a relatively short life-span from 1 to 3 years (e.g. Beukema *et al.*, 1978; Ropert and Dauvin, 2000; Van Hoey *et al.*, 2006a). It is ubiquitous along European coasts (Van Hoey *et al.*, 2008) and can inhabit an extensive range of depths, from shallow intertidal down to bathypelagic areas (1 900m) (Hartmann-Schröder, 1996). *Lanice conchilega* forms biogenic tube aggregations that can be considered reefs when densities are high and sand tubes are large (Rabaut *et al.*, 2009). These aggregates can occur in densities as high as 20 000 ind·m⁻² during recruitment (Buhr and Winter, 1976) and protrude up to 16cm

above the sediment surface (Rabaut *et al.*, 2009). Their presence can have extensive impacts on the ecosystem (De Smet *et al.*, 2015), and this feature has led to the consideration of *L. conchilega* as a conservation target (Godet *et al.*, 2008).

Reef-like aggregations break water flow and cause deceleration of currents at the benthic-boundary layer (Friedrichs *et al.*, 2000), impacting sedimentary processes (Borsje *et al.*, 2014). The attenuated flow facilitates larval settlement (Rabaut *et al.*, 2009; Volkenborn *et al.*, 2008) and increases fine-particle deposition (De Smet *et al.*, 2015), modulating local sediment composition (Rabaut *et al.*, 2007; Volkenborn *et al.*, 2008). *Lanice conchilega* also affects sediment biogeochemistry through tube flushing (Braeckman *et al.*, 2010) as part of its allogenic engineering. The autogenic engineering effect of *L. conchilega* is related to the size, elevation and density of their biogenic concretions (Borsje *et al.*, 2014), distinguishing denser and taller aggregations composed of adult tubeworms (which cause greater flow deceleration) from small, sparse aggregations containing mainly juveniles. Thus, fluctuations in population demographic composition may influence the autogenic engineering effects of this tube dweller.

The life cycle of *L. conchilega* comprises two types of living, planktonic and sessile (Kessler, 1963) (see addendum I for further details on the life cycle of *L. conchilega*). Individuals spend the first few months of life as planktonic larvae, but the majority of the cycle is spent as a sessile organism on the benthic-boundary layer. Larvae development occurs in the pelagic realm and may last approx. 2-3 months (Kessler, 1963), while the sessile stages – *i.e.* juvenile and adult - vary from 1 to 3 years (*e.g.* Buhr and Winter, 1976; Callaway *et al.*, 2010; Ropert and Dauvin, 2000; Van Hoey *et al.*, 2006b). Initially, individuals go through 3 planktonic stages of development lasting approx. 5 days – prototrochophora, trochophora, and metatrochophora-I (Kessler, 1963). This period culminates on the appearance of metatrochophora-II larvae, a bipartite pelagic larvae that settles for 1 day while building a rudimentary tube (Kessler, 1963). Following this period metatrochophora-II larvae metamorphose into aulophora larvae, the final planktonic life stage of *L. conchilega* (Kessler, 1963). Aulophora larvae remain in the water column for 2 months, and then settle as juveniles that are morphologically similar to adults (Kessler, 1963). Subsequently, the juveniles mature into adults with tube size increasing as individuals mature (*e.g.* Van Hoey *et al.*, 2006b). Previous research using mimic tubes and modelling show that changes in tube dimensions as well as animal density can substantially impact the

outcome of autogenic engineering from polychaete aggregations (e.g. Borsje *et al.*, 2014; Eckman *et al.*, 1981; Friedrichs *et al.*, 2000; Luckenbach, 1986). However, there is a lack of information on the role of changing tube dimensions and density *in-situ* due to population dynamics.

In this study we investigated the relationship between *Lanice conchilega* engineering effects and ontogenetic and demographic population processes related to the (dis)appearance and growth of cohorts in a sandy beach habitat. We therefore evaluated (1) the temporal variation of population demographic structure and secondary production, and (2) spatial-temporal variations of *L. conchilega* aggregation density and its relationship with local sediment properties (e.g. mean and median grain size) at the benthic-boundary layer.

3.3. Methods

3.3.1. Study site

The study area was located in the intertidal zone of a sandy beach adjacent to the harbour of Boulogne-sur-mer in northern France (henceforth referred to as Boulogne) (50.7345 N; 1.5881 E) (Fig 3.1). The area is characterized by soft sediment, predominantly composed by fine and medium sand (Rabaut *et al.*, 2008), with a semi-diurnal tidal regime ranging from 4 to 9m (Jouanneau *et al.*, 2013) and an average sea level of 5.03m (0.17m SD). Two portions of the sandy beach were selected for monitoring due to their well-developed *L. conchilega* aggregations. The “low intertidal” was located north of the harbour wall by 250m, and as near as possible to the low water level at spring tide (LWST) while enabling sampling during emersion periods (centroid: 400309.649152E, 5621211.02256N). The “high intertidal” was approximately 0.5m higher in elevation, located 50m northeast from the “low intertidal”, and included the upper limit of *L. conchilega* distribution at the site (Fig 3.1) (centroid: 400393.019426E, 5621273.01656N). The approximate difference in exposure time between the two sites is 1h. Both zones were sampled with the same frequencies during LWST in order to evaluate possible differences in population structure across the intertidal gradient.

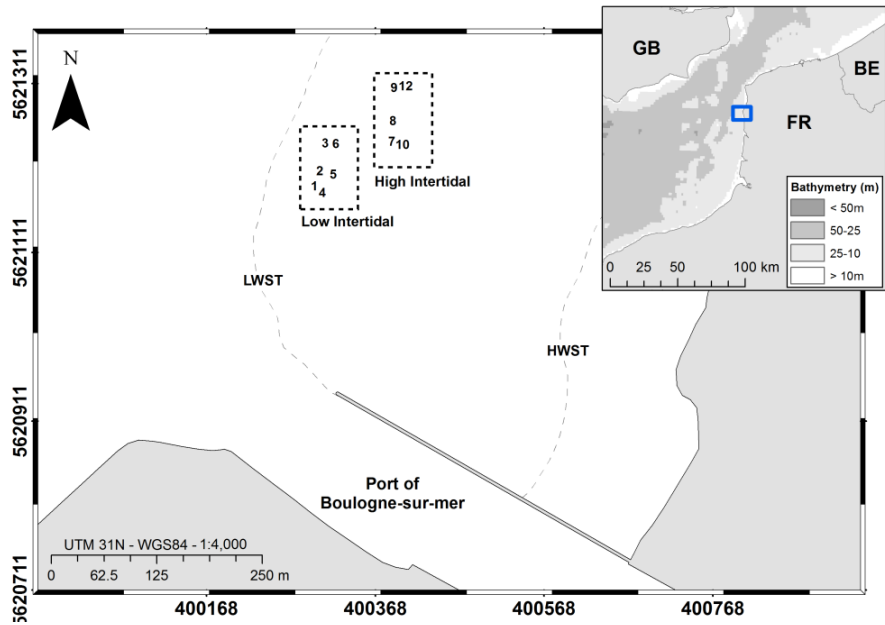


Fig 3.1. Map of the sandy beach in Boulogne depicting the low intertidal and the high intertidal at the study site, the port of Boulogne-sur-mer to the south, and the limits (dashed lines) for low and high water spring tides (LWST and HWST respectively) approximated using satellite imagery. The present study surveyed twelve *L. conchilega* aggregations on the intertidal zone, marked by numbers from 1 to 12.

3.3.2. *In-situ* surveys

Monthly surveys were carried out from June 2013 until November 2014 on twelve *L. conchilega* aggregations distributed equally between two areas of the intertidal zone (Fig 3.1). The location of each aggregation was recorded using a dGPS system, and used to estimate their distance to the LWST (meters) as a representation of existing intertidal gradients, such as dryness/wetness and exposure to wave action (Kaiser *et al.*, 2005). Animal density (ind·m⁻²) was estimated with quadrat counts (0.1m x 0.1m) of fringed sand tubes according to Van Hoey *et al.* (2006a). Counts could not be performed in the high zone during April 2014 due the speed of the rising tide. Sediment samples (0-1cm) were taken with acrylic cores (3.6cm Φ) to investigate dynamics in sediment properties. Properties related to local biotic conditions included chlorophyll-a content (µg·g⁻¹ sediment), extracellular polymeric substances (EPS¹:

¹ EPS is composed of several fractions, not only glucose equivalents. We recommend that future work assess its other fractions and refrain from using glucose equivalents as a proxy for EPS alone.

mg glucose equivalents·mg⁻¹ sediment), and total organic matter content (TOM: %). Whereas properties related to local abiotic processes included water content (%), and granulometry analysis - median grain size (d₅₀: μm), mode grain size (μm), sediment sorting (dimensionless), and mud content (% < 63 μm).

Sediment samples were homogenized prior to the analyses. Chl-a content (μg·g⁻¹) was measured as a proxy for microphytobenthos (MPB) biomass through high performance liquid chromatography (HPLC) (Wright and Jeffrey, 1997). Samples were extracted using acetone (90%), sonicated, filtered at 0.2μm, and analysed on a high resolution HPLC Gilson system with a C18 column. The water-extractable fraction of EPS (mg·mg⁻¹) was measured as an indicator of MPB activity (Lind *et al.*, 1997) using a modification of the methods from Hubas *et al.* (2010). Samples were diluted in 400μL of distilled water, homogenized using a tube roller, and placed in a warm water bath at 30°C for 60mins. The solution was centrifuged (4 000g at 21°C for 5mins), and sub-sampled for 200μL of the supernatant. The sub-samples were homogenized with 200μL phenol (5%) and 1mL sulfuric acid (100%), and incubated for 30min at room temperature. The amount of d-glucose equivalents was measured with a spectrophotometer at 486nm (Victor3 1420 Multilabel Counter from Perkin Elmer). Total organic matter (%) was estimated per sample as the difference between dry weight (48h in 60°C) and ash weight (2h at 500°C).

Median grain size (μm), mode grain size (μm), and mud content (% < 63 μm) were obtained as a result of granulometry analysis using a Malvern Mastersizer 2000 particle analyser (size range: 0.020μm to 2000.000μm), and sediment sorting was calculated using parameters of the granulometry analysis according to Inman (1952). Water content (%) was estimated per sample as the difference between wet and dry weight following lyophilization. Additional monthly records were obtained for average air temperature (Infoclimat.fr, 2016) and net primary production (NPP) in the water column (O'Malley, 2015). These were used to complement the environmental dataset and to determine seasonal fluctuations. NPP was interpolated for November 2013 using a natural spline as data for this month was missing.

Finally, one large sample was taken per aggregation using an inox core (12cm Φ by 38cm in height) to investigate the spatial-temporal evolution of population demographic structure and secondary production (*i.e.* the rate of production of *L. conchilega* biomass). These samples were sieved *in-situ* through a 1mm mesh, transported to the laboratory, and stored in 4% formaldehyde in sea water solution

buffered with lithium carbonate (Li_2CO_3) until analysis. *Lanice conchilega* sand tubes were sorted manually after staining with Rose Bengal from samples belonging to three aggregations in the low intertidal area (1-3 in Fig 3.1). Tubes with intact animals were counted, the polychaete worms were removed from their tubes, the inner tube diameter (ITD) was measured with a conic shaped tool graded from 0mm to 6mm (steps of 0.01mm), and used to assess secondary production and population cohorts.

3.3.3. Analyses of temporal variation in population density, structure, and secondary production

Temporal fluctuations in population density and each of the environmental properties were evaluated through statistical modelling using non-parametric Wilcoxon signed-rank tests with Bonferroni adjustment of p-values between pairs of successive dates. Univariate distance-based linear models (DistLM) were implemented using the PERMANOVA+ add-on (Anderson *et al.*, 2008) for Primer v6 (Clarke and Gorley, 2006) to investigate the relationship between tube density dynamics and a reduced set of environmental properties. The set of sampled properties was reduced through pairwise collinearity, only properties with Pearson's correlation < 0.70 and VIF < 3 were kept for further analyses. The analysis was carried out using the base package in the R statistical language (R Core Team, 2015) inside the RStudio environment (Allaire *et al.*, 2015). The final set of environmental properties contained EPS, TOM, mud content, mode grain size, water content, air temperature, and distance to LWST. In addition, time and distance to the LWST were included as covariates to assess the role of temporal and spatial auto-correlations. EPS and TOM content were fourth-root transformed to correct for skewness prior to modelling. The models explain each of the environmental variables as a function of tube density, distance to the LWST, and time. Model selection was by minimization using the Akaike Information Criterion through the 'Best' method (*i.e.* models using every possible combination of covariates are evaluated) (Anderson *et al.*, 2008).

Population demographic structure was analysed by detecting distinct cohorts - *i.e.* group of individuals originated from a well outlined recruitment moment (*sensu* Van Hoey *et al.*, 2006b). Inner tube diameter (ITD) data was pooled from samples of three *L. conchilega* aggregations in the low intertidal area (1, 2, and 3 in Fig 3.1) and allocated to 0.5mm size classes ranging from 0 to 5mm. The frequency of sizes distribution was estimated per class using Statistica 5.5 (StatSoft.Inc, 2004), and

used for cohort detection in FiSAT II (Food and Agriculture Organization of the United Nations - FAO, 2005). Detection was done through modal progression analysis using Bhattacharya's method. It consisted on the decomposition of tube diameter distributions per date into a sum of modes each corresponding to a Gaussian distribution (Bhattacharya, 1967). Cohorts were consolidated using NORMSEP (Pauly and Caddy, 1985) and cohort-specific growth rates (*i.e.* rate of change in ITD in millimetres per day) were estimated as the difference between the means of ITD between consecutive dates for each cohort.

Secondary production and total biomass were estimated for 2014 as it constituted a full year, and for the whole survey (*i.e.* 1.5 years). Ten undamaged worms were randomly selected from each ITD size class from samples of aggregations 1, 2, and 3 (Fig 3.1). Individual biomass was assessed as wet weight (grams), subsequently converted to ash-free dry weight (AFDW, grams) using a rate for sessile *Terebellidae* according to Brey (2012), and used to build a regression curve relating the natural log of individual AFDW (grams) and ITD (milimeters) (Buhr, 1976) (Fig 3.2). The regression was used to calculate individual biomass (grams AFDW) for all measured specimens and monthly averages of individual biomass per cohort (b_t : grams AFDW·m⁻²). Production increments (P_t) at each time (t) were calculated according to (Brey, 1986) using monthly tube densities per cohort (n_t : ind·m⁻²) and monthly averages of individual biomass per cohort (b_t : grams AFDW·m⁻²) (Eq 3.1).

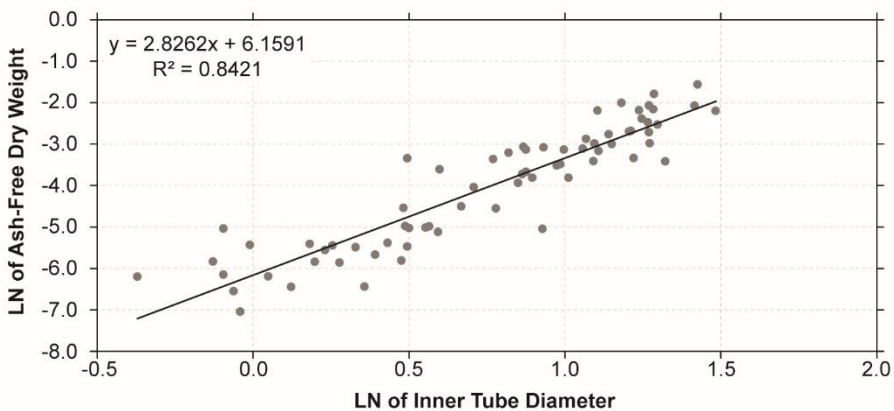


Fig 3.2. Relationship between the natural log of *Lanice conchilega* inner tube diameter (ITD) and the natural log of individual ash-free dry weight (AFDW).

$$\text{Eq 3.1. } P_t = ((n_{t-1} + n_t)/2) \cdot (b_t - b_{t-1})$$

Secondary production (grams AFDW·m⁻²·year⁻¹) was then estimated using the increment-summation method (Brey, 1986), hence the sum of monthly production increments (P_t). Total biomass was estimated as the sum of monthly cohort biomass (grams AFDW·m⁻²).

All statistical estimates were performed with a significance level of $p < 0.05$.

3.4. Results

3.4.1. Temporal patterns in tube density and demographic structure

Five cohorts were identified during the monitoring period (June 2013 – November 2014) (Fig 3.3A). Cohort 1 and 2 were observed at the start of survey (*i.e.* June 2013). Cohort 1 was characterized by large inner tube diameters (average: 3.32mm; SD: 0.40mm), low abundance (725 ind·m⁻²; SD: 780 ind·m⁻²), and was only present for 3 months. Cohort 2 was present from June 2013 until January 2014 (8 months), growing in size throughout that period from an average ITD of 1.37mm (SD: 0.25mm) to 3.43mm (SD: 0.55mm) (Fig 3.3A). Its average density at the start of monitoring was 10 196 ind·m⁻² (SD: 1 557 ind·m⁻²) and subsequently declined until disappearance (Fig 3.3B). Cohort 3 settled during October 2013 with an average ITD of 1.68mm (SD: 0.25mm) and density around 3 469 ind·m⁻² (SD: 1 798 ind·m⁻²) (Fig 3.3). The cohort inhabited the intertidal zone for 10 months until July 2014 when it was last recorded with average ITD of 3.46mm (SD: 0.37) (Fig 3.3A). Cohort 4 was present from April 2014 (30 022 ind·m⁻²; SD: 26 831 ind·m⁻²) until September 2014 (*i.e.* 6 months) (Fig 3.3). Throughout its existence, cohort 4 grew in ITD from 0.67mm (SD: 0.25mm) in April 2014 to 2.50mm (SD: 0.65mm) in September 2014 (Fig 3.3A). Cohort 5 was present from September 2014 (4 713 ind·m⁻²; SD: 2 337 ind·m⁻²) until November 2014 (Fig 3.3). During this period, it grew in ITD from 1.60mm (SD: 0.28mm) to 2.19mm (SD: 0.45mm) (Fig 3.3A). Two out of the 5 detected cohorts had their life cycle fully monitored - cohorts 3 and 4 with life-spans of 10 and 6 months respectively (Fig 3.3). Growth rates for these cohorts ranged from 0.0007 to 0.0357mm in ITD·day⁻¹. The highest growth rates were observed during August 2013 for cohort 1 (0.0227), November 2013 for cohort 2 (0.0277), April 2014 for cohort 3 (0.0133), September 2014 for cohort 4 (0.0357), and October 2014 for cohort 5

(0.0157). Overall, the demographic composition of *L. conchilega* aggregations during 1.5 years of surveys was dominated by individuals smaller than 3.00mm in ITD (average ITD of $2.12 \pm 0.79\text{mm}$) (Fig 3.4).

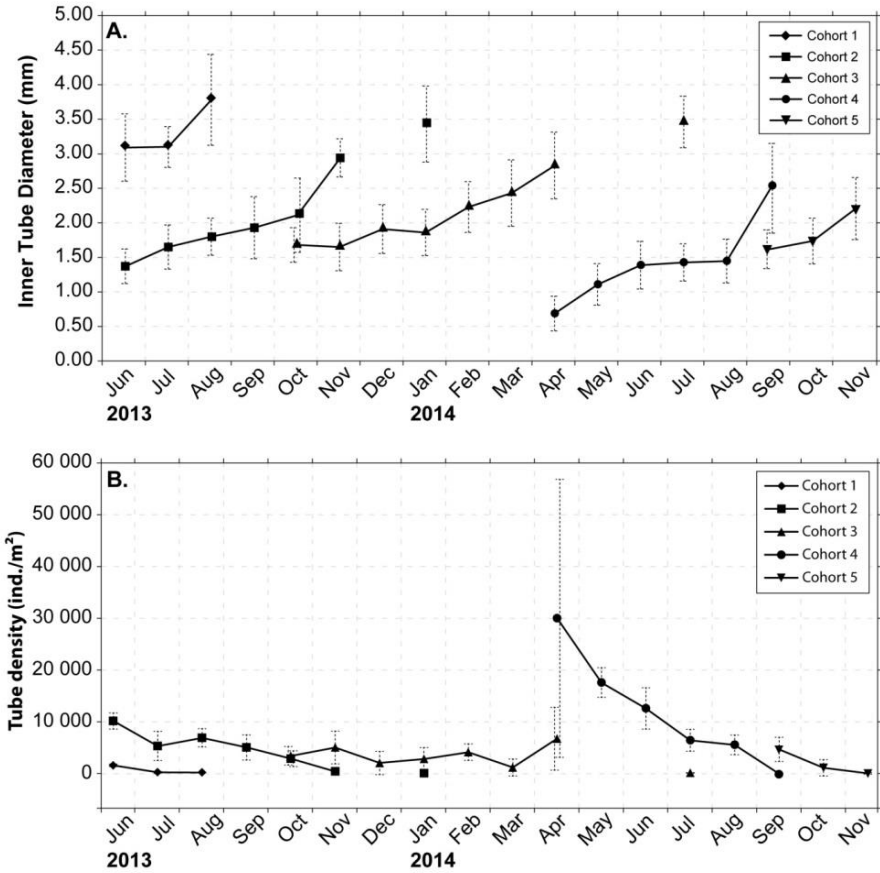


Fig 3.3. Temporal evolution of detected cohorts located on the intertidal zone of the sandy beach in Boulogne-s/m (France, Noord-Pas-Des-Calais). A: temporal evolution of tube diameter per cohort. B: temporal evolution of estimated reef density per cohort. Data is displayed as Mean \pm SD.

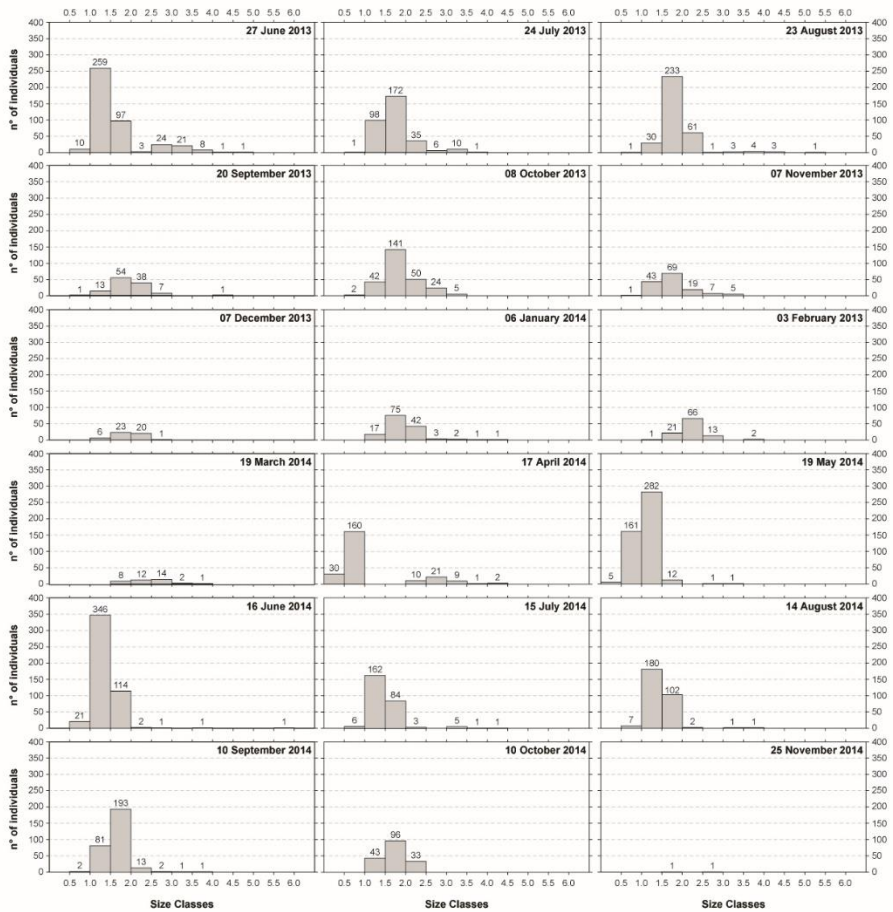


Fig 3.4. Size frequency distribution change of the *L. conchilega* populations in the intertidal zone of the sandy beach in Boulogne-sur-mer (France) between June 2013 and November 2014.

Total secondary production was estimated at $633.96\text{g AFDW}\cdot\text{m}^{-2}$ for a period of 1.5 years (i.e. the equivalent of $422.64\text{ AFDW}\cdot\text{m}^{-2}\cdot\text{year}^{-1}$), whereas total biomass amounted to $1\,340.54\text{g AFDW}\cdot\text{m}^{-2}$. Annual secondary production for the year 2014 was $466.98\text{g AFDW}\cdot\text{m}^{-2}\cdot\text{year}^{-1}$ and annual biomass was $759.84\text{g AFDW}\cdot\text{m}^{-2}$. Total P/B ratio was 0.47, whereas the annual P/B ratio for 2014 was 0.61. The highest production increment was recorded in September 2014, when cohort 4 increased its biomass by $143.41\text{g AFDW}\cdot\text{m}^{-2}$. At that moment its average ITD increased from

1.43mm in August to 2.50mm in September, while estimated cohort density decreased from approximately 5 593 ind·m⁻² to 47 ind·m⁻². In addition, among the two complete cohorts, cohort 4 had the highest P/B ratio (*i.e.* 1.11 vs. 0.39 estimated for cohort 3).

3.4.2. Demographic structure and its consequences to ecosystem engineering

Tube density pooled from both intertidal areas fluctuated around 3 887 ind·m⁻² (SE: 246 ind·m⁻²) during the study (June 2013 - November 2014). The lowest values were recorded in aggregations at the high intertidal area between December 2013 and February 2014 (Fig 3.5A). Tube density was below 100 ind·m⁻² (average: 73 ind·m⁻²; SE: 15 ind·m⁻²) during that period which is considered low for *L. conchilega* (*e.g.* Passarelli *et al.*, 2012; Rabaut *et al.*, 2009). The highest densities were observed at the low intertidal area in April 2014 (27 250 ind·m⁻²; SE: 5 584 ind·m⁻²), May 2014 (18 025 ind·m⁻²; SE: 1 911 ind·m⁻²), and June 2014 (12 503 ind·m⁻²; SE: 669 ind·m⁻²) (Fig 3.5A). Overall, aggregations in the low intertidal area presented higher mean density (4 528 ind·m⁻², SE: 240 ind·m⁻², excl. April 2014 as data for the high intertidal area was lacking for that month; see material and methods) (Fig 3.5A) than those in the high intertidal area (1 911 ind·m⁻², SE: 160 ind·m⁻²).

Wilcoxon signed-rank tests with Bonferroni adjusted p-values revealed significant fluctuations in EPS, TOM, mud and water content, but not tube density nor mode grain size (Fig 3.5). EPS, TOM, mud and water content peaked during May 2014 (Fig 3.5B-D, F), whereas mode grain size showed no discernible maximum (Fig 3.5E). Furthermore, aggregations closest to the LWST presented higher surficial sediment concentrations of chl-a, EPS, total organic matter, mud and water content as well as lower median and mode grain sizes and higher sorting index in comparison to the furthest aggregations (Table 3.1).

DistLMs investigating the effects of tube density, distance to the LWST, and time on the reduced set of environmental properties revealed that tube density and distance to the LWST mark significantly affected all of the evaluated environmental properties (Table 3.2). Furthermore, model selection results show that tube density significantly contributed to the temporal fluctuations of EPS, TOM, mud content, and water content, but not mode grain size (Table 3.3).

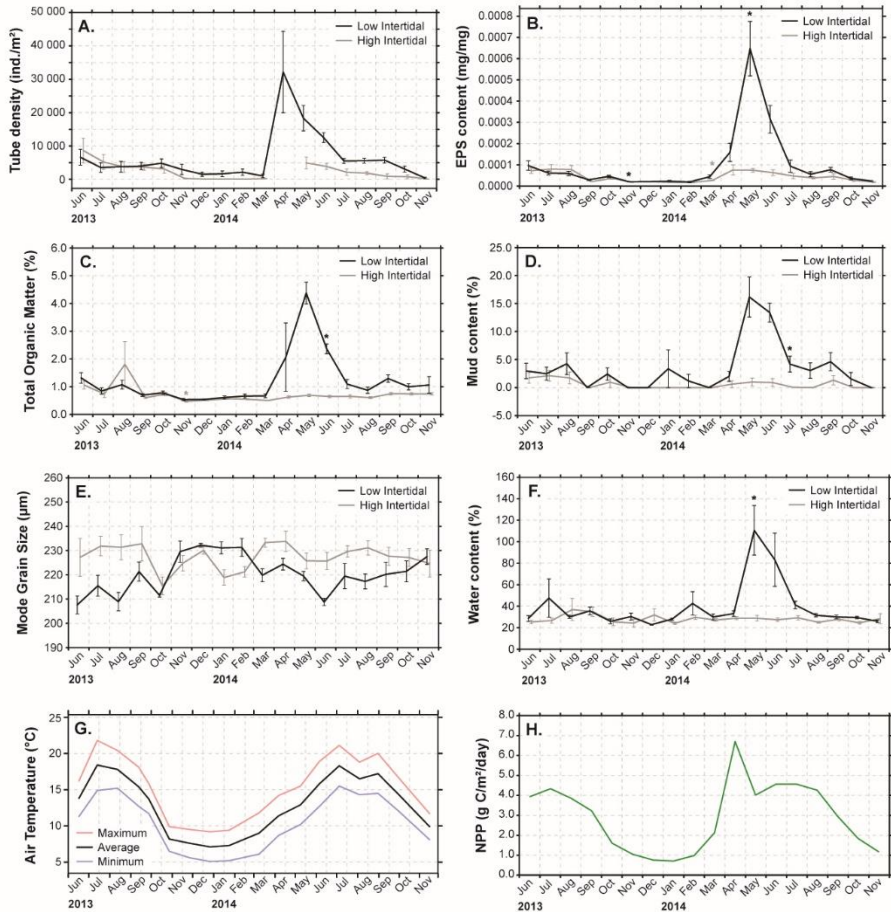


Fig 3.5. Temporal evolution of tube density (A) surficial EPS (B), TOM (C), mud content (D), mode grain size (E), water content (F), air temperature (G), and net primary production in the water column (H) at Boulogne (France). * significant change in dynamics from previous date detected by the Wilcoxon signed-rank tests with Bonferroni adjusted p-values comparing consecutive dates. Data is displayed as Mean \pm SE.

Table 3.1. Mean and standard error for the environmental data per location.

Environmental Variables	Low Intertidal			High Intertidal		
	Mean	St. Deviation	St. Error	Mean	St. Deviation	St. Error
Distance to LWST	59.74 ±	8.05 ,	0.78	111.48 ±	9.52 ,	1.00
Chl-a ($\mu\text{g}\cdot\text{g}^{-1}$)	3.66 ±	6.89 ,	0.67	1.47 ±	1.57 ,	0.16
EPS ($\text{mg}\cdot\text{mg}^{-1}$)	1.02e-4 ±	1.73e-4 ,	1.68e-5	3.91e-5 ±	3.00e-5 ,	3.14e-6
TOM (%)	1.23 ±	1.18 ,	0.12	0.71 ±	0.50 ,	0.05
Mud Content (%)	3.44 ±	5.65 ,	0.55	0.51 ±	1.38 ,	0.14
Median GS (μm)	216.96 ±	17.13 ,	1.66	228.11 ±	10.74 ,	1.13
Mode GS (μm)	220.32 ±	10.89 ,	1.06	226.77 ±	9.52 ,	1.00
Sorting Index	118.88 ±	36.61 ,	3.56	105.46 ±	20.32 ,	2.13
Water content	39.50 ±	30.91 ,	3.00	27.74 ±	8.39 ,	0.88

Table 3.2. Marginal results of DistLM selection for models explaining the temporal fluctuations of environmental properties as a function of *L. conchilega* tube density, time, and distance to the LWST.

Environmental Properties	Density		Distance to LWST		Time	
	<i>pseudo-F</i>	<i>p-value</i>	<i>pseudo-F</i>	<i>p-value</i>	<i>pseudo-F</i>	<i>p-value</i>
EPS	356.97	0.000	14.18	0.000	0.30	0.587
TOM	180.61	0.000	25.00	0.000	2.11	0.151
Mud content	155.43	0.000	19.45	0.000	0.12	0.734
Mode GS	5.69	0.017	12.82	0.000	2.55	0.108
Water content	89.67	0.000	17.88	0.000	0.474	0.505

Table 3.3. Overall best solutions from distance-based model selection per environmental property. Variables: 1. Tube density; 2. Distance to the LWST; 3. Time.

Environmental Properties	AIC	R²	RSS	No. Variables	Selected Variables
EPS	-1679	0.66086	0.028167	2	1, 3
TOM	-892.8	0.52615	1.7092	3	All
Mud content	-237.14	0.46138	53.48	2	1, 2
Mode GS	901.54	0.075569	20763	2	2, 3
Water content	-578.83	0.33687	8.938	2	1, 2

3.5. Discussion

The present study investigated the autogenic engineering of marine soft-sediments by intertidal *Lanice conchilega* aggregations through time. We assessed (1) the temporal evolution of population demographic structure and secondary production, as well as (2) the effect of varying tube density and size on sediment properties. Our findings corroborate previous research, showing that the outcome of autogenic engineering *in-situ* is substantially affected by changing tube density as well as tube size, two consequences of the temporal evolution of population structure within aggregations.

3.5.1. Temporal patterns in tube density and demographic structure

Five cohorts emerging at various moments of the year were detected in this study. Cohort 1 was less abundant than the other detected cohorts and was characterized by large individuals (average ITD > 3.00mm) that must have recruited before the start of the survey. Cohort 2 was more abundant and had much smaller average ITDs during June 2013 in comparison to cohort 1 indicating that this cohort recruited later, most likely during the spring preceding the start of the survey (*i.e.* April - May 2013). Moreover, the cohort data enabled the identification of two annual recruitment periods at Boulogne: one at spring (April 2014), and one in autumn (October 2013 and September 2014).

The spring recruitment was characterized by high abundance (average: 30 022 ind·m⁻²) of small individuals (average ITD: 0.67mm) in extensive and dense reef-like tube aggregations. It was likely a result of the settlement of cohort 4 during April 2014. The autumn recruitment was related to cohorts 3 and 5, which settled during October 2013 and September 2014 respectively. It was characterized by less abundant, larger individuals with the average inner tube diameter approximately 3 times larger than that of the spring recruits (*i.e.* cohort 4) at the time of settlement and tube densities approximately 7.5 times lower. It is worth noting that the temporal resolution of our data limits comparisons between the two recruitment events because short-term processes are unaccounted for. Nevertheless, the occurrence of multiple recruitments per year is common amongst some species of benthic invertebrates – *e.g.* mussels (Frantzen, 2007), barnacles (Cruz *et al.*, 2010), polychaetes (Dubois *et al.*, 2007). Animal density tends to differ between these two periods due to a combination of effects associated to their residence time in the water

column (Bhaud, 2000). During our study, pelagic food availability was less abundant during autumn (see NPP), thus we hypothesize that low food availability and starvation during autumn may have limited the abundance of pelagic individuals (Kessler, 1963), resulting in a less dense recruitment than that observed in spring. The presence of two recruitment events per year is in accordance with previous research showing *L. conchilega* recruitment during spring, summer, and autumn in various locations (e.g. Buhr and Winter, 1976; Callaway, 2003; Ropert and Dauvin, 2000; Smith, 1989; Strasser and Pieloth, 2001; Van Hoey *et al.*, 2006b).

The demographic composition of the studied aggregations was largely dominated by small-medium individuals. Animals larger than 3.0mm in ITD - the recorded size for adult stages of *L. conchilega* (Van Hoey *et al.*, 2006b) - were present in very low densities for much of the survey period, leading to questions as to how the population is sustained through time. It is possible that recruits at the intertidal zone originated from subtidal and/or offshore populations (Ropert and Dauvin, 2000) since *L. conchilega* larvae can last up to 2 months in the water column (Kessler, 1963) and are found all year-round in the North Sea (Van Hoey *et al.*, 2006b). Alternatively, it is possible that these tube worms reach sexual maturity at smaller body sizes than estimated by previous research, successfully supplying new recruits to the intertidal population. The identification of the adult stage of *L. conchilega* has been traditionally based on measurements of inner tube or animal diameter with the threshold between juvenile and adult ranging from 1.5mm to 3.0mm throughout scientific literature (e.g. Buhr and Winter, 1976; Callaway, 2003; Ropert and Dauvin, 2000; Strasser and Pieloth, 2001; Van Hoey *et al.*, 2006b; Zühlke, 2001). However, there is no evidence of a relationship between sexual maturity and animal body size. The status of gametogenesis in *L. conchilega* is driven mainly by seasonality (Kessler, 1963) as is the case with most seasonally reproducing polychaetes (Smart, 2008). In order to determine the level of sexual maturity of individuals in Boulogne further study on the development of their sexual organs and its relationship to seasonal variation is required. Furthermore, the recorded cohort life-spans (*i.e.* 10 and 6 months respectively for cohorts 3 and 4) were noticeably short in comparison to that found by previous research (*i.e.* 1-3 years) (e.g. Beukema *et al.*, 1978; Ropert and Dauvin, 2000; Van Hoey *et al.*, 2006b).

Total production is expected to be lower for intertidal polychaete populations than for subtidal ones where aggregations have higher food availability and longer feeding

times. Nevertheless P/B ratios from this study (0.47 - 0.61) were in accordance with previous estimations for subtidal *Lanice conchilega* populations in the Belgian Part of the North Sea BPNS (0.29-0.55) (Van Hoey *et al.*, 2006b) and the Bay of Veys (0.23 – 0.80) (Ropert, 1999). Total secondary production at Boulogne was approximately ten times higher than that observed for subtidal aggregations in the (BPNS) (*i.e.* 633.96g AFDW·m⁻²·1.5 years⁻¹ versus 10.3 to 64.8g AFDW·m⁻²·1.5 years⁻¹ – Van Hoey *et al.*, 2006b). Total biomass was also larger than the recorded at the BPNS by approximately one order of magnitude. Aggregations at Boulogne amounted to 759.84g AFDW·m⁻², whereas aggregations at the BPNS range from 13.54 to 85.59g AFDW·m⁻² (Van Hoey *et al.*, 2006b). In addition, annual secondary production of the Boulogne population was approximately double of that recorded for subtidal aggregations at the Bay of Veys (France) - 466.98g AFDW·m⁻²·year⁻¹ versus 60.05 - 248.40g AFDW· m⁻²·year⁻¹ (converted from Ropert, 1999, using sessile *Terebellidae* rates from Brey, 2012).

Differences in growth rates were also found between our study and previous research. Growth rates at Boulogne (0.0007-0.0357 mm·day⁻¹) were more variable than the observed for intertidal populations at the Bay of Veys (0.0039-0.0053 mm·day⁻¹) (Ropert and Dauvin, 2000). These differences, as well as discrepancies in total secondary production, are commonly attributed to variation in food type and availability between locations that are related to seasonal patterns (*e.g.* Marsh *et al.*, 1989; Qian, 1994; Taghon and Greene, 1990). In our study the highest growth rates do not concur with peaks in food availability in neither the sediment surface nor the water column. The highest growth rates were observed 7 months following recruitment for cohorts 3 and 4, suggesting that food availability is not the sole driver of variation in growth rates. Rather, the observed growth rates were likely related to the developmental stage of *L. conchilega* as the highest cohort-specific growth rates were observed at later stages of development. This is in accordance with previous research detecting the highest growth rates for juveniles maturing into the adult population and thus at further stages of development than recently settled individuals (*i.e.* Ropert and Dauvin, 2000; Van Hoey *et al.*, 2006b). Finally the temporal evolution of cohort 4 suggests that the high secondary production is maintained by the relatively few juveniles that survive the months following recruitment. This seems to be characteristic of *L. conchilega* populations and has been observed in the English

Channel (Ropert and Dauvin, 2000), the BPNS (Van Hoey *et al.*, 2006b), and the German Bight (Callaway, 2003; Zühlke, 2001).

3.5.2. *Demographic structure and its consequences to ecosystem engineering*

The ecosystem engineering effects of *Lanice conchilega* on the environment are related to physical features of tube aggregations (Borsje *et al.*, 2014; Eckman *et al.*, 1981). Autogenic effects such as particle entrapment (Passarelli *et al.*, 2012) and flow attenuation (Borsje *et al.*, 2014) are positively associated to tube density, as well as aggregation area and height. These affect total organic matter content at the sediment surface and finer fractions of the sediment (*i.e.* mud content) (*e.g.* De Smet *et al.*, 2015; Passarelli *et al.*, 2012; Rabaut *et al.*, 2007). In addition, the changes induced by polychaete aggregations influence surficial microalgae, modulating chlorophyll-*a* and EPS content at the benthic-boundary layer (Passarelli *et al.*, 2012). Our results revealed that tube density significantly affected the temporal variations of EPS, TOM, and mud content, whereas the temporal fluctuation of tube density was significantly affected by distance to the LWST. The latter represents several coastal gradients - *e.g.* food availability, wetness/dryness and exposure to wave action (Kaiser *et al.*, 2005). Consequently, our findings show that coastal gradients can impact local environmental properties indirectly by modulating the temporal evolution of tube density. This results in distinct environmental properties for aggregations at different distances to the LWST. Indeed, aggregations in the lowest zone were among the most dense during the survey and contained higher concentrations of surficial chl-*a*, EPS, total organic matter, and mud content than aggregations at the high intertidal area.

The spring recruitment during April 2014 in aggregations closest to the LWST was followed by concurrent peaks in EPS, TOM, mud and water content. These are likely consequences of autogenic engineering by *L. conchilega* (Borsje *et al.*, 2014; Passarelli *et al.*, 2012). Following this period, tube density declined probably due to mass mortality as a consequence of competition for space and/or food between recently settled juveniles (Eckman, 1996) and/or predation by marine fauna such as birds (De Smet *et al.*, 2013) and fish (Amara *et al.*, 2001). This is not uncommon and has also been recorded for populations along the northern French coast (Ropert and Dauvin, 2000) and the southern English coast (Callaway, 2003). The decline in tube

density was followed by decreases in EPS, TOM, mud and water content. It is possible that as tube aggregations became sparser, they caused less deceleration of water flow at the benthic-boundary layer, resulting in relatively less sedimentation of fine particles (Borsje *et al.*, 2014), as well as lower EPS and TOM content (Passarelli *et al.*, 2012). Thus, decreases in median/mode grain size and organic enrichment of the sediment associated with *L. conchilega* aggregations seems particularly pronounced during spring recruitment with tube densities of approximately 30 000 inds.m⁻². It seems likely that high densities of species typically associated with the engineering effects of *L. conchilega* during the late spring-summer recruitment (De Smet *et al.*, 2015) can contribute to the destabilisation of the surficial sediment via burrowing and grazing activities (e.g. Volkenborn *et al.*, 2008), thus impacting erosion/deposition processes (Gutiérrez *et al.*, 2011).

The lowest tube densities were observed during winter months which were characterized by low air temperatures, surficial EPS, and TOM. Declines in tube density following winter periods are common (e.g. Beukema, 1992; Günther and Niesel, 1999; Strasser and Pieloth, 2001), suggesting a high susceptibility to lower temperatures. This may be related to seasonal decreases in primary producers, both in the water column and the sediment surface, that supply the short- and long-term energy storages for the species (Braeckman *et al.*, 2012). In the present study, we observed lower concentrations of EPS and TOM at the sediment surface, as well as lower net primary production in the water column during the winter period of 2013-2014. This suggests that scarce food sources during winter can be responsible for mass mortality through starvation. Remarkably, several of the aggregations farthest from the sea (*i.e.* from the low water spring tide, LWST) disappeared during winter (*i.e.* 0 ind·m⁻²), likely due to the harsher environmental conditions in comparison to conditions closer to the LWST. Hence aggregation persistence can be threatened for populations consisting of cohorts with short life-spans if animals do not survive until the next moment of reproduction. Although periods of mass mortality were detected during winter, the population at Boulogne seems able to sustain its temporal presence either through reproduction of the surviving fraction of the population and/or via the supply of new recruits from subtidal and/or offshore populations that are more stable (Ropert and Dauvin, 2000). As pointed out by Dittmann, (1999), the long-term population dynamics of *L. conchilega* may be determined by conditions during winter and the availability of new recruits. Thus, further work should attempt to discover the

source of *L. conchilega* recruits for Boulogne, and more importantly, the level of connectivity between *L. conchilega* populations in the North Sea to clarify short- and long-term population dynamics.

An aerial photograph of an intertidal reef. The reef surface is covered with various textures and colors, indicating different biogenic structures. A white grid is laid out on the reef, and a scale bar with the number '1' is visible in the upper right corner. The water is visible in the lower left corner, showing ripples and a darker color.

CHAPTER

4

The use of kite aerial photography and low-altitude digital photogrammetry for studying small-scale spatial patterns in intertidal biogenic reefs

Authored by:

Alves RMS, Stal C, De Wulf A, Rabaut M, Van Colen C, Bouma TJ, Vincx M.

4.1. Abstract

*Biogenic reefs are important conservation targets within the European Union, covered by the legal framework of the Habitats Directive. Remote reef identification is challenging because of the wide set of criteria that potential methods need to abide by for coastal deployment in addition to covering appropriate resolutions for small-scale mapping (< 0.5m). Recent alternatives combine low-cost, technically simple platforms coupled with non-metric digital cameras. One such alternative is evaluated in the first half of this chapter: the use of kite aerial photography (KAP) and low-altitude digital photogrammetry for identification and change detection of intertidal polychaete aggregations. Monthly surveys were performed, resulting in 12 pairs of orthomosaics and digital elevation models (DEMs). A semi-automated protocol was developed to detect intertidal aggregations of the polychaete worm *Lanice conchilega*. Maximum likelihood classification (MLC) was applied to orthomosaics to differentiate *L. conchilega* from marine sediments. DEMs were de-trended to assess structures with positive elevation and identify aggregation edges. *Lanice conchilega* was distinguished from marine sediments by MLC with varying accuracy. Edge identification was also highly variable and displayed systematic biases. Nevertheless, KAP and low-altitude digital photogrammetry are suitable methods for mapping and monitoring intertidal biogenic aggregations, providing abundant materials for protocol development. The observations made of intertidal *L. conchilega* aggregations at Boulogne-sur-mer (France) are addressed in the second half of this chapter. Large global scale errors in the material hindered analytical change detection, thus the material was visually interpreted. *Lanice conchilega* formed three distinct types of small-scale distribution patterns during recruitment seasons, hinting at multiple mechanisms of pattern formation: patches, continuous beds, and interrupted beds. Patterns remained similar in the months following their formation, indicating that removal and/or dislodgement by water currents did not play significant roles in modifying small-scale distribution during our survey. Therefore, we hypothesize that small-scale spatial pattern formation in intertidal *L. conchilega* aggregations is mostly determined by conditions during larval settlement, and post-settlement survival.*

4.2. Background on remote sensing and the Habitats Directive

Legal conservation frameworks in the European Union are formed by the Bird Directive (2009/147/EC) and the Habitats Directive (92/43/EEC) (Evans, 2006). The latter constitutes an integral part of European conservation policy (Evans, 2006), listing habitat types that are prioritised for protection through the designation of management and/or conservation status (The Council of The European Communities, 2007). The Habitats Directive (hereafter referred to as the Directive) provides guidelines for creating special areas of conservation (SACs) and/or sites of community interest (SCIs) based on the identification of priority habitats and/or species per member state (The Council of The European Communities, 2007). Conservation status may be granted to coastal polychaete aggregations in this framework under habitat type 1170, also known as “biogenic reefs” (Hendrick and Foster-Smith, 2006). The interpretation manual for the Directive defines the reef habitat type as hard compact substrata of biogenic or geogenic origin, set on solid and soft bottoms, and arising from the sea floor in the sublittoral and littoral zone (European Commission DG Environment, 2013). The document makes allowances for biological zonation within reefs (European Commission DG Environment, 2013), as such the definition may include concretions like corals reefs (European Commission DG Environment, 2013), and natural formations such as iceberg scoured bottoms (Irvin, 2009), hydrothermal vents and submerged rock walls (Evans, 2006). This broad set of habitats is a result of a vague definition, characterising several marine features which adds uncertainty to habitat identification and differentiation, and may hinder implementation of the Directive (Evans, 2006).

Efforts to improve habitat identification and differentiation focus on landscape classification based on key characteristics related to biodiversity and ecosystem maintenance (Holt *et al.*, 1998). Conventional methods in biogeography and spatial ecology are generally point-based, often failing to encompass the required spatial resolution (*e.g.* transect and core-sampling) (Zajac, 2007). They are also time-consuming and require experienced taxonomists to sort through samples (Godet *et al.*, 2009a). Unsurprisingly, recent studies in habitat identification often employ remote sensing methods to detect and differentiate organisms from their surroundings (*e.g.* Dekker *et al.*, 2005; Mumby *et al.*, 1997; Sanchez-Hernandez *et al.*, 2007) as these methods are capable of covering extensive areas at high resolution, yielding substantial amounts of information (Godet *et al.*, 2009a).

However, remote reef identification remains a challenging endeavour since potential methods must abide by a wide set of criteria for coastal deployment (Goodman *et al.*, 2013). They must resist severe climatic conditions such as high humidity, salt exposure, and frequent powerful wind forces (Goodman *et al.*, 2013); cover large areas with high (*i.e.* 0.5m-10m - Wang *et al.*, 2010) or very high spatial resolutions (*i.e.* <0.5m) (*e.g.* Degraer *et al.*, 2008; Hendrick and Foster-Smith, 2006; Rabaut *et al.*, 2009); and be cost-efficient and technically simple (Turner, 2014) while enabling sampling and comparison of species distribution, abundance, and coverage (Evans, 2006). Common practices often employ cost-intensive methods (Gillespie *et al.*, 2008) with very coarse resolutions, unsuitable for small-scale mapping (Godet *et al.*, 2009a) (*e.g.* satellite-tethered sensors, manned or unmanned aircrafts).

Recent viable alternatives combine low-cost, technically simple platforms coupled with non-metric digital cameras – *e.g.* Bryson *et al.*, 2013; Paneque-Gálvez *et al.*, 2014; Smith *et al.*, 2009. Low-altitude photography is a very promising group of methods for environmental mapping and monitoring due to the ultra-high spatial resolutions attainable with it. Recent applications include assessing vegetation distribution (*e.g.* Paneque-Gálvez *et al.*, 2014) and landscape geomorphology (*e.g.* Marzloff and Poesen, 2009; Wundram and Löffler, 2008). Whereas coastal applications involve, for example, assessing beach litter (*e.g.* Nakashima *et al.*, 2011), and/or, more commonly, spatial patterns in species distribution on- (*e.g.* Bryson *et al.*, 2013; Guichard *et al.*, 2000; Mumby *et al.*, 2004) and offshore (*e.g.* Magome *et al.*, 2007). However, low-altitude remote sensing methods often yield case-specific results, requiring case-by-case analysis so that it can be considered 'fit-for-purpose'. To the best of our knowledge the use of low-altitude methods to assess the distribution of polychaete aggregations on sandy coasts has not been done before. As such, the first objective of our study is to evaluate the use of kite aerial photography (KAP) and low-altitude digital photogrammetry for identification and change detection of reef-like intertidal polychaete aggregations. Presently, we perform a case-study focused on intertidal aggregations of the sessile tube-building polychaete *Lanice conchilega* (Pallas, 1766).

Lanice conchilega forms tube aggregations in temperate regions of the northern hemisphere (Hartmann-Schröder, 1996), and is abundant on European coasts (Godet *et al.*, 2008). The aggregations consist of trapped material between arrays of sand tubes (Ziegelmeir, 1952) that can reach up to 30 000 ind·m⁻² (Alves *et al.*,

2017b), protrude up to 16cm in height (Rabaut *et al.*, 2009), and spread across approximately 15m² in area (Degraer *et al.*, 2008). They are found as patches (Degraer *et al.*, 2008) or beds (Godet *et al.*, 2009b), which are detectable using remote sensing methods – *e.g.* Degraer *et al.*, 2008. Recent efforts to improve identification and monitoring have evaluated tube aggregations in light of the reef definition provided by the interpretation manual (*i.e.* Hendrick and Foster-Smith, 2006; Rabaut *et al.*, 2009). However, application of those recently developed protocols remains restricted due to difficulties in assessing large areas for long-term monitoring (Godet *et al.*, 2008). Thus, our second objective was to develop a protocol for remote detection of intertidal *L. conchilega* aggregations and evaluation of their physical characteristics to ascertain the likeness of intertidal aggregations to biogenic reefs, as well as assess their longevity, which has been an important source of uncertainty in past research.

This chapter is divided into two parts. This first half (*i.e.* sections 4.2-6) aims to (1) evaluate the use of kite aerial photography (KAP) and low-altitude digital photogrammetry to map and monitor intertidal *L. conchilega* aggregations; and (2) develop a protocol for remote identification and quantitative scoring of reef-like tube aggregations following recommendations from previous research. The second half presents observations of intertidal *L. conchilega* aggregations made via our remote methods, and discusses the temporal evolution of its small-scale distribution patterns (sections 4.7-10).

4.3. Study site

An intertidal *L. conchilega* population was selected as a case-study at a sandy beach in Boulogne-sur-mer (Nord-Pas-de-Calais, France) (Fig 4.1). The beach is subjected to a semi-diurnal tidal regime, with sea level ranging from 4 to 9m (Jouanneau *et al.*, 2013). Exposure time for the monitored area was approx. 4h during low water spring tide (LWST) (determined from tidal gauge data) (Service Hydrographique et Océanographique de la Marine - SHOM, 2015). The study site was located north of the harbour wall by 250m (centroid: 400309.649152E, 5621211.02256N) and covered an area of approximately 3 700m² (Fig 4.1), predominantly composed by fine and medium sand (Rabaut *et al.*, 2008). This area was selected due to the presence of well-developed *Lanice conchilega* aggregations and accessibility during LWST for acquisition and sampling.

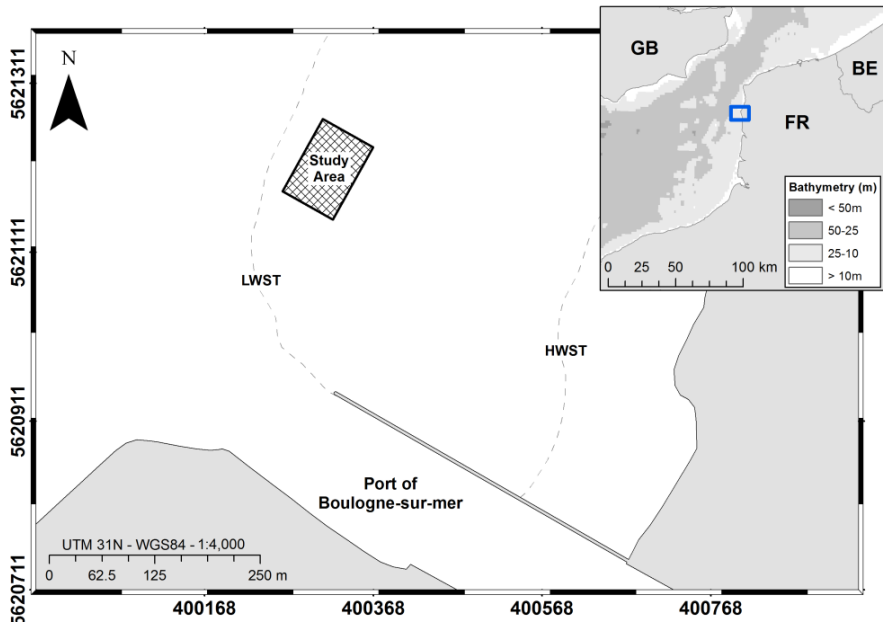


Fig 4.1. Map of the sandy beach in Boulogne depicting the monitored area in the study area (hashed rectangle), the port of Boulogne-sur-mer to the south, and the limits for low and high water spring tides (LWST and HWST respectively) approximated using satellite imagery.

4.4. Mapping and monitoring methods

4.4.1. Aerial image acquisition

The area was sampled on a monthly basis during LWST from June 2013 until November 2014, and again in April and August 2015, totalling 20 campaigns. Image acquisition (Fig 4.2) was performed using a compact digital camera attached to a FlowForm kite (Fig 4.2A and B) through a mechanical picavet suspension (Fig 4.2C). The camera was flown between 7m and 20m in height from ground level, acquiring images with a 3 seconds interval as the kite pilot walked the study site. Aerial photographs were taken using a Canon PowerShot D20 (lens: 28-140mm, sensor size: 6.2mm x 4.6mm, effective pixels: 4000 x 3000) (Fig 4.2C). The Canon Hack Development Kit (CHDK, 2013) was used for image acquisition with controlled parameters: an exposure value of 1/500 seconds, focal length of 28mm, and a fixed ISO determined by light conditions at the beginning of each campaign as either 100 or 200 ISO.

Georeferencing was performed using thirty ground control points (GCPs), equally distributed as a rectangular grid of approx. 80m by 45m. Each GCP consisted of A3 laminated cards (29.7cm x 42.0cm) with a simple black and white target design (Fig 4.3A). Coordinates were registered using two techniques according to equipment availability. The first was a differential georeferencing system based on real-time kinematic (RTK) satellite navigation using global navigation satellite systems (GNSS). It relies on the use of two receivers working in tandem to estimate coordinates within a limited area in space at the resolution of few centimetres (Shuanggen *et al.*, 2013). In summary, one receiver works as a base station, repeatedly receiving carrier phase signals from GNSS satellites, calculating atmospheric-related deviation in coordinate estimation, and transmitting correction signals to the second receiver (Shuanggen *et al.*, 2013). The second receiver (henceforth known as rover) kinematically registers GCP coordinates using phase signals from GNSS satellites and correction signals from the base station (Shuanggen *et al.*, 2013). Presently, we employed a pair of Trimble R6 RTK GNSS receivers (Fig 4.3). The rover was deployed using a 2m pole (Fig 4.3A), while the base station was set on a tripod on a stone pier approx. 400m inland (Fig 4.3B). The coordinates of the base station were determined at the start of the project. The Trimble R6s were deployed when available – *i.e.* in April 2014, October 2014, April 2015, and August 2015 - and a handheld Garmin eTrex 10 GPS receiver was used for all other campaigns with an expected accuracy of approx. 3.5m (Garmin Ltd., 2011).



Fig 4.2. Kite pilot mapping the study site (A) with the Flowform kite (detail in B) mounted with a mechanical picavet suspension carrying a Canon PowerShot D20 digital camera (detail in C).

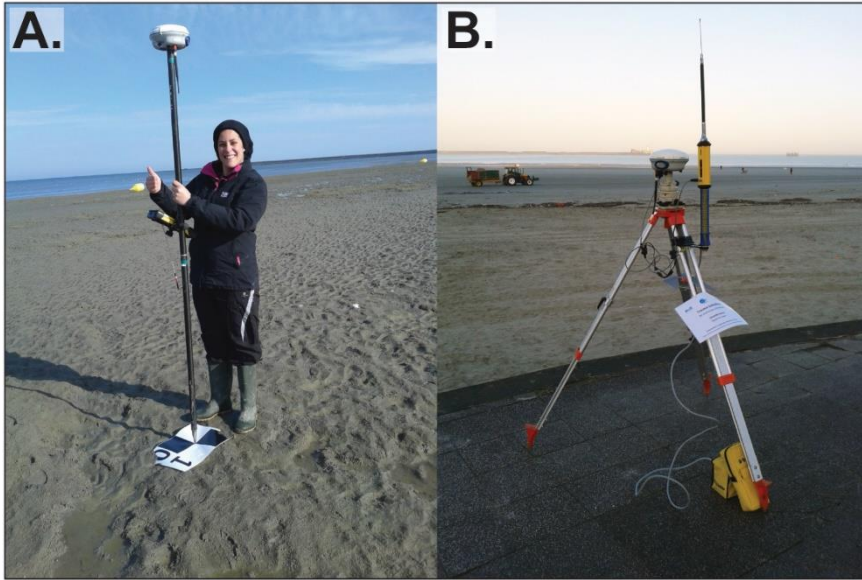


Fig 4.3. A differential system was employed using two Trimble R6 real-time kinematic global navigation satellite system (RTK GNSS) receivers when available. The coordinates of 30 ground control points were registered using one of the RTK GNSS receivers as a rover (A) while the other receiver was set as a base station on a stone pier approx. 400m away (B). The base station received carrier phase signals and sent correction signals to the rover, increasing measurement accuracy.

4.4.2. Image processing, photogrammetric reconstruction, and L. conchilega detection

A virtual 3D reconstruction of the ground relief was built from the sampled aerial photographs per campaign using low-altitude digital photogrammetry. Structure from motion (SfM) algorithms were applied for image alignment, identifying feature points that constitute geometrical similarities between photo pairs and estimating their location in space (see Verhoeven, 2011). Subsequently, a point cloud was generated using the oriented images and the projection of pixels in space (Verhoeven, 2011). The resulting point cloud was interpolated as a height field, resulting in a 2.5D landscape model known as a digital elevation model (DEM) wherein each xy-position has one elevation value (Verhoeven, 2011). The reconstruction was attempted per campaign to create one DEM per month from which digital terrain models (DTMs)

and rectified image mosaics (orthomosaics) were extracted with an aimed resolution of 1cm. Accuracy was assessed by estimating two types of errors per model. Global scale error (*i.e.* position error or root-mean square error, RMSE) was calculated as the difference in meters between the positions of ground control points as estimated by the 2.5D model and their real position (*sensu* Bryson *et al.*, 2013). Local scale error (*i.e.* precision) was estimated as the difference between the dimensions of ground control points as estimated by the 2.5D model and their real dimensions (*i.e.* 29.7cm x 42.0cm) (*sensu* Bryson *et al.*, 2013). This data processing was executed in Agisoft PhotoScan v1.2.3 (Agisoft LLC, 2016).

Lanice conchilega aggregations were evaluated according to Rabaut *et al.* (2009), who developed a system to score aggregations by their level of 'reefiness' (*i.e.* similarity to expected reef-like characteristics). The system evaluates noticeably distinct aggregations (*i.e.* different from their surroundings) and scores nine characteristics related to *L. conchilega* autogenic engineering: average tube density, aggregation relative elevation, aggregation size/area, total extent, sediment consolidation, fragmentation, species richness, Margalef's index, and longevity (Rabaut *et al.*, 2009). We attempted to distinguish *L. conchilega* aggregations from their surroundings by evaluating the characteristics that can be remotely derived – *i.e.* individual area/size, individual relative elevation, total extent, fragmentation, and longevity. Orthomosaics and DTMs were used to develop a semi-automated detection protocol for *L. conchilega* aggregations in ArcGIS Desktop v10.3 (ESRI, 2014). Development consisted of four phases: (1) image classification, (2) reduction of classification noise, (3) conversion of absolute elevation to local differences, and (4) automated edge delineation (AED) (Fig 4.4).

The first phase distinguished *L. conchilega* presence from bare sediment using pixel-based supervised maximum likelihood classification (MLC) (Lillesand *et al.*, 2014). In summary, MLC evaluates the statistical characteristics of pre-determined classes generating class signatures (Fig 4.4B), and subsequently estimates the probability that a given unknown pixel is a member of a particular class via maximum likelihood (Fig 4.4B) (Lillesand *et al.*, 2014). Finally, the algorithm assigns the evaluated pixel to a class based on the estimated probabilities (Lillesand *et al.*, 2014). We defined four classes based on *L. conchilega* presence and the expected ecosystem engineering effects of *L. conchilega* tubes on sediment composition (see De Smet *et al.*, 2015; Rabaut *et al.*, 2007): (1) *Lanice conchilega*, (2) muddy sediment, (3) dry sand, and

(4) intermediate sediment. Each class was visually characterized (Table 4.1) and the MLC algorithm (ESRI, 2016) was executed using manually delineated training samples to produce image classification rasters per campaign (ICR) (Fig 4.4B). Accuracy was assessed by verifying agreement between automated and manual pixel assignments (*i.e.* inter-rater agreement). The produced rasters were reclassified into presence/absence rasters by pooling together all sediment classes (Fig 4.4C); one hundred points were randomly generated, and used to sample the classification rasters. These samples were classified using visual identification, and compared to the ML outputs to estimate true/false pixel assignments between *L. conchilega* presence and absence classes. Subsequently, Cohen's Kappa was calculated per campaign to statistically assess agreement between visual identification and the MLC algorithm pixel assignments.

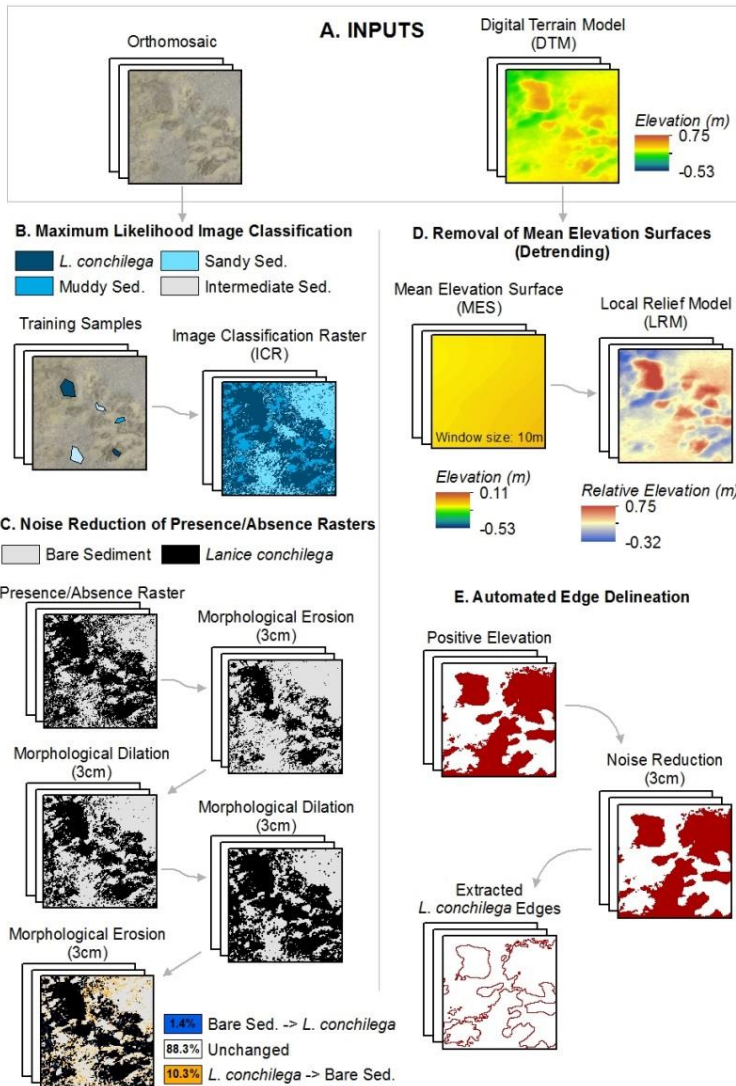

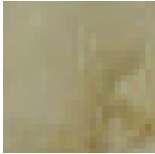

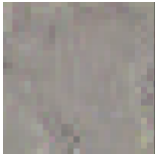


Fig 4.4. Semi-automated reef detection protocol illustrated using inputs from June 2014 (A): Initially, image elements are classified using supervised maximum likelihood image classification (B). Subsequently, the outputs are reclassified into presence/absence rasters and noise reduction is applied using morphological erosion/dilatation (C). Following this phase, mean elevation surfaces are removed from their respective digital terrain models by arithmetic subtraction (*i.e.* de-trending) to obtain relative elevation surfaces known as local relief models (LRMs) (D). Lastly, edges are delineated by extracting the 0m contour line from structures of positive elevation in the LRMs (E).

Table 4.1. Characterization of landscape features used to generate class signatures for supervised maximum likelihood image classification with example samples (each sample corresponds to 25cm x 25cm).

Class	Description
<i>Lanice conchilega</i>	
	Biogenic structures composed by <i>L. conchilega</i> sand tubes characterized by shades of brown with high variability in colour intensity.
Muddy sediment	
	Sediment characterized by light brown colours with moderate variability in colour intensity.
Dry sand	
	Sediment characterized by grey colour of low variability in colour intensity.
Intermediate sediment	
	Sediment characterized by grey colours displaying marks of reworking (<i>i.e.</i> wet sand, resurfaced anoxic sediment, visible grey sediment in shallow water pools).

During phase 2, classification noise in the presence/absence rasters was reduced by removing small features (*i.e.* $\leq 3\text{cm}$ length/diameter) according to Gonzales and Woods (2001) (Fig 4.4C). This was achieved through successive applications of two morphological tools: morphological erosion and dilation. Morphological erosion was applied first, retracting the boundaries of all *L. conchilega* pixel groupings by 3 pixels (*i.e.* 3cm) (Gonzales and Woods, 2001) (Fig 4.4C). This was followed by morphological dilation, expanding the same boundaries by 3 pixels (*i.e.* 3cm) (Gonzales and Woods, 2001) (Fig 4.4C). The process reclassified pixel groupings smaller or equal to 3cm in length/diameter, thus removing noise from the data (Gonzales and Woods, 2001) (Fig 4.4C). Phase 3 encompassed the conversion of absolute elevation to local relief models (LRM) using local de-trending (Gallant and Wilson, 2000) – *i.e.* removal of the overall slope of a neighbourhood and normalisation of the resulting elevation values (Gallant and Wilson, 2000). Mean elevation surfaces (MES) were produced per campaign as estimates of global trends by averaging absolute elevation within moving windows of fixed size (Gallant and Wilson, 2000) (Fig 4.4D). Subsequently, each MES was subtracted from its respective DTM resulting in surfaces of relative elevation per campaign known as local relief models (LRMs) (Gallant and Wilson, 2000) (Fig 4.4D).

Automated edge delineation was performed during the fourth phase. For our study, aggregation edges were defined as the pixels between *L. conchilega* aggregations and bare sediment, constituting a slope (*e.g.* Borsje *et al.*, 2014). We assessed relative elevation to detect the change in conditions between the two environments and selected the values at the base of the slope (*i.e.* closest to the bare sediment). Selection was performed by isolating elements of positive elevation from LRMs, applying noise reduction through morphological erosion/dilation of 3 cm, and extracting the 0m contour line (Fig 4.4E) which reflects deviations from the mean elevation (*i.e.* neighbourhood trend). During this process it became clear that the window size used in MES construction impacted the vertical resolution of LRMs (Gallant and Wilson, 2000), and consequently, edge delineation. Thus, we evaluated several sets of edges delineated using MESs made with different window sizes to assess the impact of MES window size on edge delineation. Tested window sizes ranged from 1m x 1m to 10m x 10m in steps of 1m. The lower limit was selected based on preliminary tests showing that window sizes smaller than 1m x 1m were ineffective at discerning physical structures larger than approximately 1m². This value

coincides with the minimum area for which a score can be attributed to (Rabaut *et al.*, 2009). Conversely, the upper limit was restricted by processing power. Accuracy was evaluated by assessing concordance between automatically and manually delineated edges on data subsets from April 2014, October 2014, April 2015, and August 2015. Edge controls were produced manually (*e.g.* Fig 4.5A), and LRMs were generated for each subset using varying window sizes during MES construction (*e.g.* Fig 4.5B). Subsequently, automated edges were produced from elements of positive elevations, and both automated and manually delineated edges were aligned for comparison (*e.g.* Fig 4.5C). We evaluated the predicted image segmentation from automated edges against manual delineation/segmentation by estimating inter-rater agreement of pixel assignments (*e.g.* Fig 4.5D). Inter-rater agreement was quantified according to the level of concordance between manual and automatic pixel assignment using Cohen's kappa coefficient (Foody, 2002).

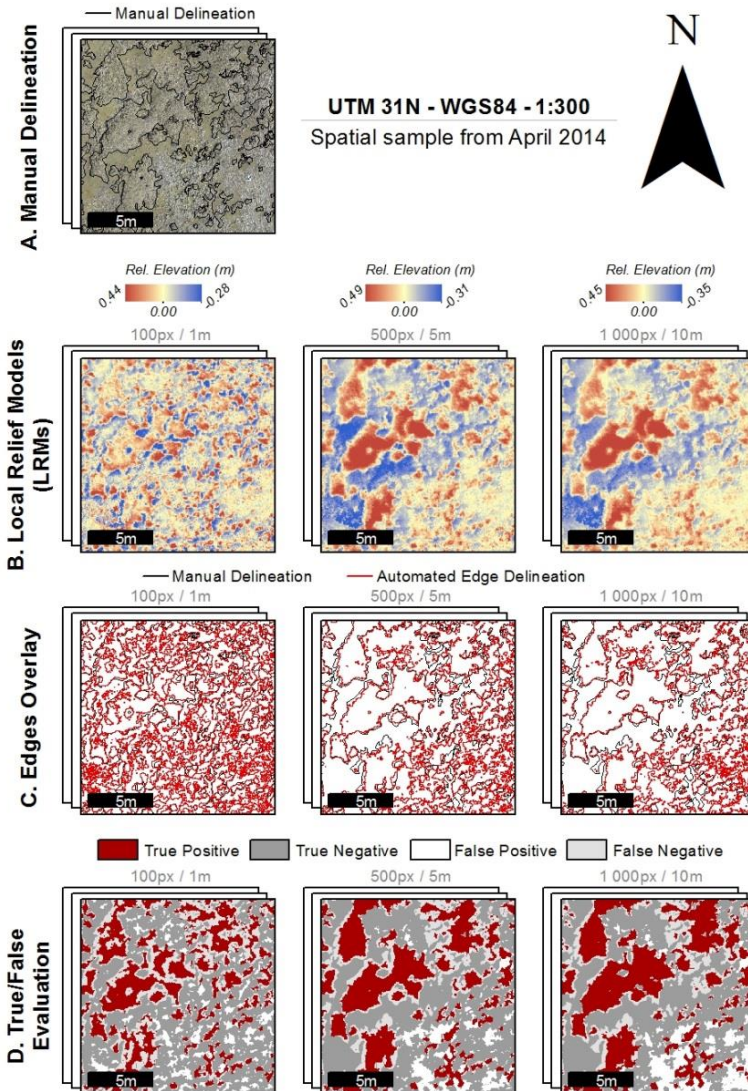


Fig 4.5. Evaluation example of automated edge delineation using a spatial sample from April 2014. The procedure involved (A) producing several control edges via manual delineation; (B) producing local relief models (LRMs) with mean elevation surfaces built using a range of window sizes; (C) extracting elements of positive elevation in the LRMs; performing noise reduction via erosion/dilation of 3 cm, and extracting the 0m contour line. Lastly, (D) concordance between automated and manually delineated edges was assessed with Cohen's kappa.

4.5. Outputs from mapping and monitoring

4.5.1. Acquisition, processing, and reconstruction

Mapping, processing, and photogrammetric reconstruction was successful for 12 data sets out of 20 campaigns that were executed (Table 4.2). Average coverage was 2 488m² (SD: 759m²) from an approximate total area of 3 700m² (*i.e.* 67% coverage) (Table 4.2). Relief reconstruction through digital photogrammetry produced 12 pairs of digital terrain models (Addendum II.A-L) and orthomosaics (Addendum III.A-L): June, July, October, and December 2013; March, April, June, July, August, and October 2014; April and August 2015. The average final spatial resolution per pair was 2.98mm-pixel⁻¹ (SD: 0.74mm-pixel⁻¹), with global scale error of 0.89m (SD: 0.66m) and local scale error of 0.01m (SD: 0.02m) (Table 4.2). Unsurprisingly, global scale errors were higher for reconstructions georeferenced using the Garmin eTrex 10 GPS receiver (average global scale error of 1.30m; SD: 0.35m) in comparison to reconstructions georeferenced using the RTK GNSS system (average of 0.09m; SD: 0.04m) (Table 4.2). Furthermore, although reconstruction was successful, the DTM from December 2013 comprised an unrealistic surface (see Addendum II.D). Reconstruction artefacts were also found in five other DTMs: October 2013, March 2014, October 2014, April 2015, and August 2015 (Fig 4.6). Artefacts were detected visually and defined as features contrasting from expectation once surrounding relief and orthomosaic have been analysed. Linear slopes that contrast with expected relief were detected in portions of two DTMs (4.6A and B), while unusually abrupt changes in the interpolated height field were observed in three others (4.6C-E). In addition, artefacts associated to water presence as well as marked differences in light conditions (*i.e.* brightness and contrast) were identified on four orthomosaics – October 2013, June 2014, August 2014, and August 2015 (Fig 4.7).

Table 4.2. Accuracy assessment of 3D multi-view reconstruction of the sandy beach relief per date. Campaign dates marked by an asterisk and italicized font were georeferenced with the RTK GNSS system. All others were georeferenced using a handheld Garmin eTrex 10 GPS receiver.

Campaign Date	Mapped Area (m²)	Final Pixel Size (mm)	Global Scale Error (m)	Local Scale Error (m)
Jun 2013	3570	4.64	1.655	0.006
Jul 2013	1140	3.17	1.043	0.004
Oct 2013	1690	2.31	1.650	0.003
Dec 2013	2850	2.86	1.738	0.075
Mar 2014	1660	2.33	1.298	0.004
<i>Apr 2014 *</i>	2350	3.30	0.044	0.008
Jun 2014	2570	2.69	1.083	0.005
Jul 2014	2260	3.36	0.754	0.005
Aug 2014	2440	2.04	1.152	0.005
<i>Oct 2014 *</i>	2580	2.97	0.126	0.006
<i>Apr 2015 *</i>	3720	3.76	0.068	0.008
<i>Aug 2015 *</i>	3020	2.29	0.116	0.004
Average	2488	2.98	0.894	0.011
Std. Deviation	759	0.74	0.659	0.020

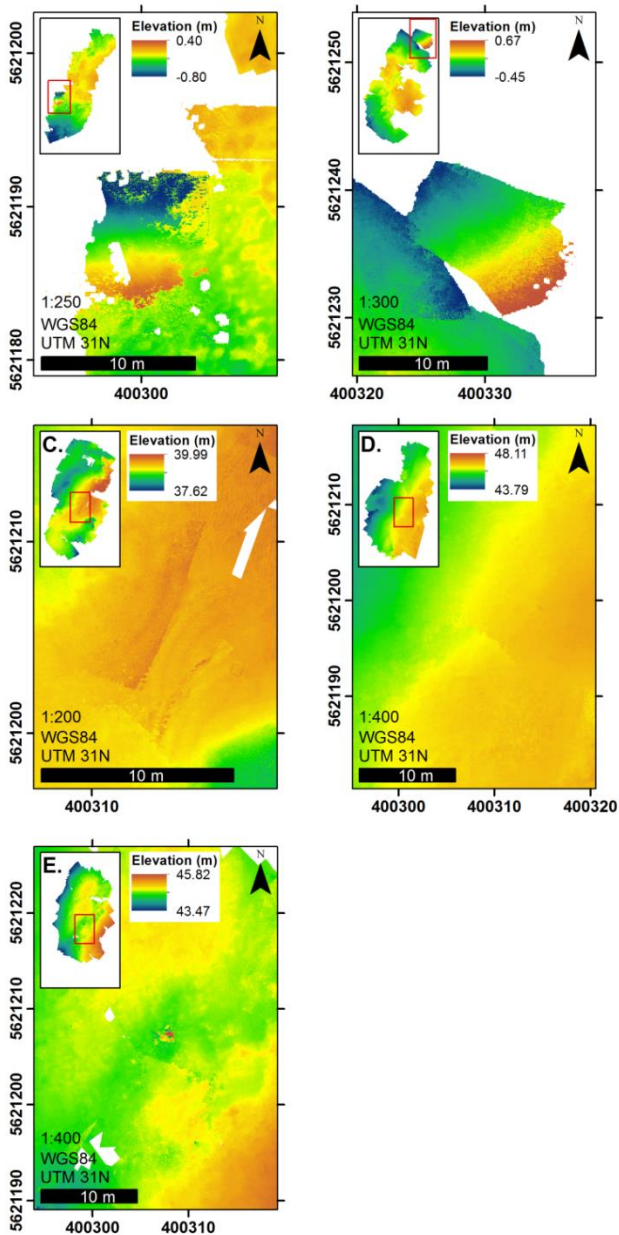


Fig 4.6. Visually identified artefacts (red squares) on local relief models from (A) October 2013, (B) March 2014, (C) October 2014, (D) April 2015, and (E) August 2015. Linear slopes that contrast with expected relief were detected in portions of two DTMs (A and B), while unusually abrupt changes in the interpolated height field were observed in three others (C-E).

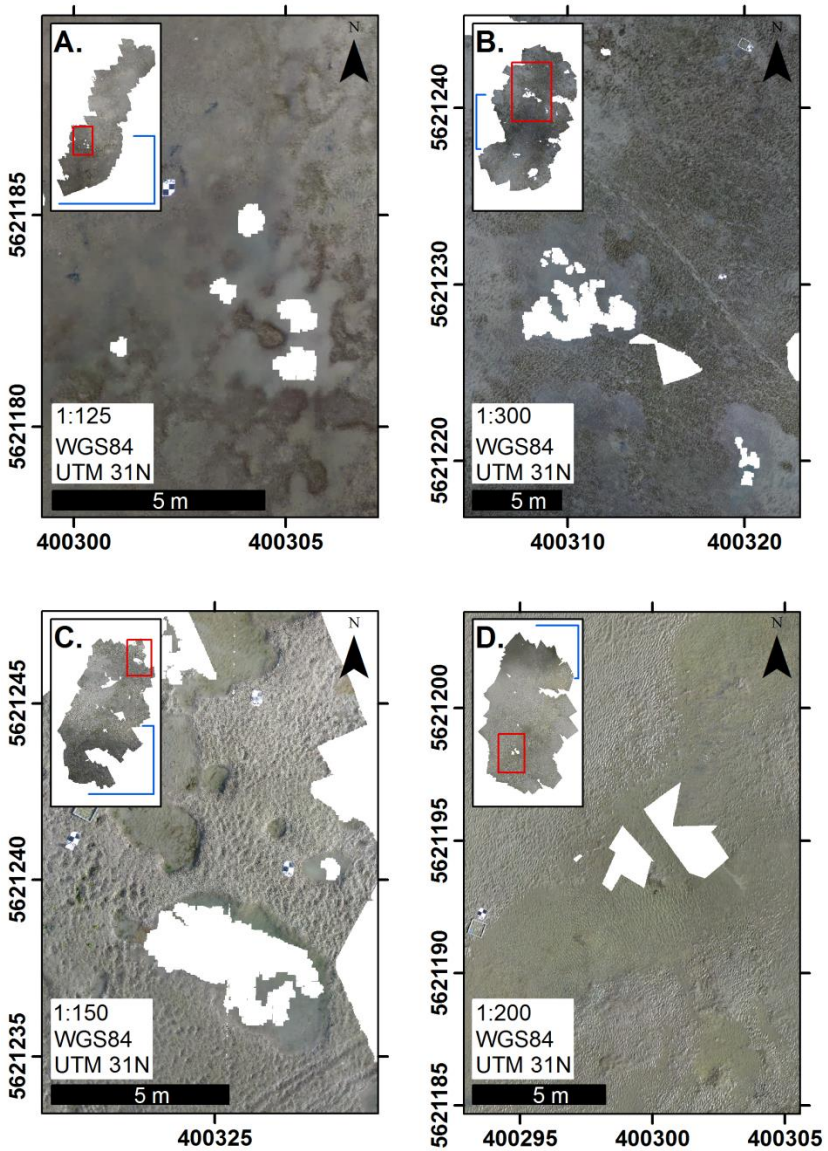


Fig 4.7. Visual inspection of orthomosaics revealed noticeable variation in brightness/contrast (delimited by blue brackets) as well as water-related artefacts due to water accumulation into puddles (red squares and zoom view) in campaigns during (A) October 2013, (B) June 2014, (C) August 2014, and (D) August 2015.

4.5.2. Semi-automated detection protocol

The accuracy of supervised maximum likelihood classification in correctly identifying *L. conchilega* presence was on average 69.95% (SD: 23.17%) per orthomosaic, whereas its ability to correctly identify its absence was 83.55% (SD: 9.94%) (Table 4.3). Agreement between visual identification and MLC was very low with Cohen's Kappa ranging from -0.21 to 0.12. The classification procedure detected *L. conchilega* presence during all campaigns with highest true presence percentage during June and July of each year (Table 4.3). The lowest estimate was found on April 2015 (Table 4.3) for which visual inspection of orthomosaics revealed high interspersed of sand within *L. conchilega* aggregations (Fig 4.8).

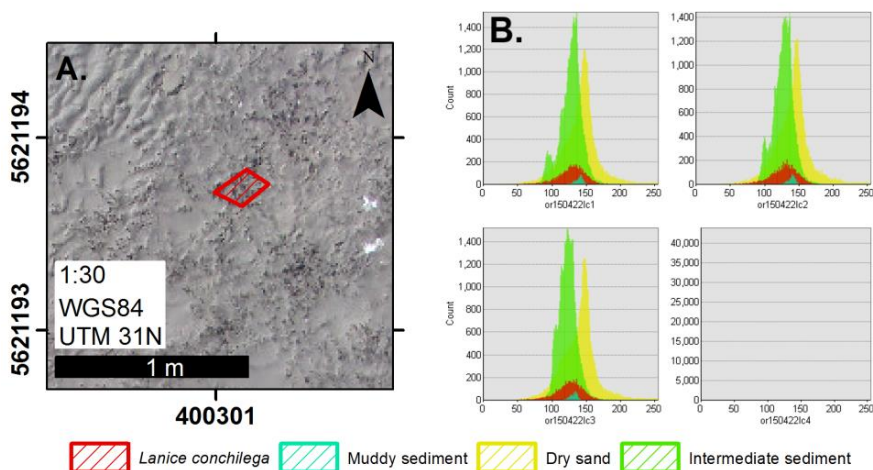


Fig 4.8. Training sample for the *Lanice conchilega* class (red polygon) on the orthomosaic from April 2015 (A). The lowest classification accuracy was observed during this date, likely due to interspersed of sand pixels between *L. conchilega* pixels in the training samples causing overlap between signatures (B). Histograms show count of pixels (vertical axis) per value (horizontal axis) in each band of the orthomosaic for April 2015 (B). Extreme overlapping of class samples (represented by colour) due to similar pixel values can be noted (B).

Table 4.3. Accuracy assessment of supervised MLC per *L. conchilega* presence/absence. Campaigns dates marked by an asterisk and italicized font were georeferenced with the RTK GNSS system. All others were georeferenced using a handheld Garmin eTrex 10 GPS receiver.

Survey Date	Total Area (m ²)	Bare Sediment Coverage (%)	L. conchilega Coverage (%)	True		False		True		False	
				Presence (%)	Absence (%)	Presence (%)	Absence (%)	Presence (%)	Absence (%)	Presence (%)	Absence (%)
June 2013	2 305.1	61.28	38.72	94.44	5.56	68.29	31.71				
Jul 2013	680.4	84.21	15.79	85.71	14.29	93.67	6.33				
Oct 2013	936.0	77.51	22.49	91.30	8.70	89.61	10.39				
Dec 2013	1 458.7	86.62	13.38	78.57	21.43	90.70	9.30				
Mar 2014	900.7	82.68	17.32	69.23	30.77	85.06	14.94				
<i>Apr 2014*</i>	2 368.6	56.14	43.86	77.27	22.73	73.08	26.92				
Jun 2014	1 547.1	59.47	40.53	97.62	2.38	96.55	3.45				
Jul 2014	1 255.9	77.03	22.97	72.41	27.59	83.10	16.90				
Aug 2014	1 462.8	65.08	34.92	46.15	53.85	66.67	33.33				
<i>Oct 2014*</i>	2 596.1	80.17	19.83	46.67	53.33	84.71	15.29				
<i>Apr 2015*</i>	3 731.6	81.31	18.69	20.00	80.00	78.95	21.05				
<i>Aug 2015*</i>	3 036.9	86.23	13.77	60.00	40.00	92.22	7.78				
Average	1 856.7	74.81	25.19	69.95	16.45	83.55	30.05				
Std. Dev.	945.5	11.14	11.14	23.17	9.94	9.94	23.17				
Std. Error	272.9	3.22	3.22	6.69	2.87	2.87	6.69				

Noise reduction resulted in the reclassification of 13.7% (SD: 6.1%) of pixels in the presence/absence rasters. Reclassification was highest for pixels initially assigned to the *L. conchilega* class with 13.0% (SD: 6.1%) being reclassified as bare sediment after noise reduction. Conversely, only 0.6% (SD: 0.6%) of bare sediment pixels were reclassified as *L. conchilega* after noise reduction. The percentage of unchanged pixels fluctuated around 86.3% (SD: 6.1%).

Concordance between automated edge delineation (AED) and manually delineated samples was low with Cohen's kappa ranging from 0.04 to 0.63. In addition, the window sizes used to average elevation influenced delineation accuracy by impacting the final position of automated edges on aggregations edge slope creating spatial trends (e.g. Fig 4.9). The use of small averaging windows (i.e. < 500px/5m) resulted in lower accuracy (i.e. higher false absence) in areas with well-developed *L. conchilega* aggregations than larger windows (e.g. Fig 4.9B). Conversely, employing smaller window sizes resulted in higher accuracy (i.e. lower false absence) for areas with small and sparse aggregations (e.g. Fig 4.9C). Consequently, we were unable to successfully apply the scoring system developed by Rabaut *et al.* (2009) as only aggregations of obviously high value could be reliably identified. This has impacted assessments of *L. conchilega* small-scale distribution patterns as analyses became restricted to visual interpretation of the orthomosaics, digital terrain models, and presence/absence rasters (see sections 4.7-10).

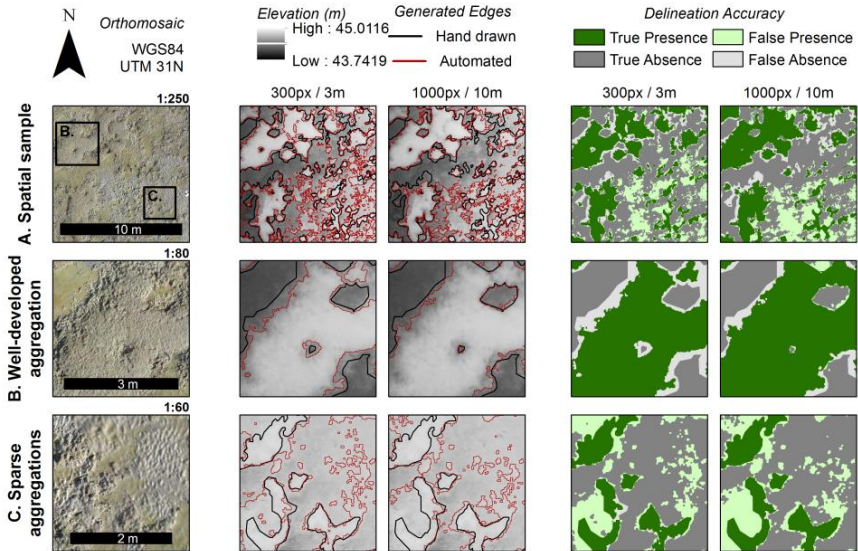


Fig 4.9. The window size used to average elevation during MES construction affected delineation accuracy by impacting the final position of automated edges on elevation slopes, creating spatial patterns (A). (B) The use of smaller window sizes (e.g. 300px/3m) resulted in lower accuracy in areas with well-developed aggregations than employing larger MES window sizes (e.g. 1000px/10m). Conversely, accuracy was higher if small windows were used in areas of sparse distribution (C) than larger averaging windows.

4.6. Evaluating mapping and monitoring methods

The first half of this chapter focused on (1) evaluating the use of kite aerial photography and digital photogrammetry to map intertidal *L. conchilega* aggregations; and (2) developing a protocol for remote detection of these aggregations.

4.6.1. Acquisition, processing, and reconstruction

The success of KAP and digital photogrammetry was assessed by evaluating the image acquisition process (*i.e.* mapping), the accuracy of photogrammetric reconstruction, and the validity of local relief models (Smith *et al.*, 2009). Kite aerial photography fulfilled the environmental requirements for coastal deployment, being

successfully used under a vast array of weather conditions (e.g. high humidity, variable winds, salt exposure, and light rain) (*sensu* Goodman *et al.*, 2013). It is worth noting that KAP deployment in soft sediments may be more difficult than in consolidated or hard substrata, which facilitates the execution of a scanning path with the kite. Nevertheless, deployment in the sandy beach of Boulogne was not hindered by its soft-sediments. Twelve DEMs were produced out of twenty attempts (1 per field campaign) (*i.e.* 60% success rate) with an average coverage of 67% of the total area. Deployment was dependent on climate conditions, namely the tidal cycle and wind conditions (*i.e.* speed and turbulence). Optimal wind speed was between approx. 12km/h (enabling lift-off with rig and camera, pers. obs.) and 38km/h (maximum recommended for the kite by its manufacturer, Didakites at Beeusaert-Braet BVBA, 2010). Wind turbulence during acquisition hindered photo selection and matching in some instances, as it often resulted in blurred photographs (pers. obs.). Therefore, KAP should be deployed frequently when performing environmental monitoring. Alternative platforms such as drones and remote-controlled helicopters may be considered to improve coverage as they are able to maintain fixed courses in windy conditions, but are susceptible to high humidity and/or rain which may restrict sampling frequency. Blimps and/or weather balloons may also display better control during acquisition and improve coverage, but are unstable in high wind speeds and/or turbulence. In addition, these platforms are less cost-efficient than a kite (e.g. Chirayath and Earle, 2016) and require specialized training, hindering their use in long-term monitoring (Godet *et al.*, 2009a). Nevertheless, they may be useful compliments to KAP if available. Thus, we consider the kite a suitable platform for low-cost coastal remote sensing, and suggest a conservative acquisition frequency to overcome weather-related challenges.

The average resolution of local relief models (*i.e.* real pixel size) was within the spatial scale required to monitor small fragmented biogenic tube aggregations (*i.e.* <0.5m) – see Degraer *et al.*, 2008; Hendrick and Foster-Smith, 2006; Rabaut *et al.*, 2009. Our global scale errors were associated to georeferencing with models georeferenced by the RTK GNSSs displaying smaller errors ($0.09 \pm 0.04\text{m}$) than those georeferenced with the handheld GPS ($1.30 \pm 0.35\text{m}$). The latter was similar to previous research using handheld GPS receivers – *i.e.* 1.02m using KAP (Bryson *et al.*, 2013). However, other studies found generally lower errors using survey-grade equipment – e.g. 0.13m using KAP and ground-based trigonometric measurements

(Wundram and Löffler, 2008); approx. 0.08m using blimp/kite aerial photography and a total station (Marzloff and Poesen, 2009); approx. 0.03m using a blimp and unspecified survey-grade equipment (Guichard *et al.*, 2000); and approx. 0.02m using KAP and a total station (Smith *et al.*, 2009). Thus, survey-grade equipment is preferred as it may increase global scale accuracy (Bryson *et al.*, 2013), but will also likely increase costs and technical requirements. Alternatively, significant reduction of global scale errors can be achieved via camera calibration (*e.g.* Bryson *et al.*, 2013; Chandler *et al.*, 2005; Smith *et al.*, 2009). This consists on the estimation of key parameters of the internal geometry of the camera sensor (*e.g.* focal length, ISO, exposure, lens distortions) to remove camera-related distortions (Aber *et al.*, 2010). Presently, all key parameters were fixed prior to each campaign and camera calibration was performed using the self-calibrating bundle in the photogrammetry software (Verhoeven, 2011).

Average local scale errors were very low during our study with the estimate of 0.01m smaller than that recorded by previous studies using similar equipment (*i.e.* 0.04m by Bryson *et al.*, 2013, with KAP and handheld GPS). This enabled accurate distance measuring from individual LRMs (Smith *et al.*, 2009). However, the relatively large global scale errors obtained during the survey hindered automated comparison between campaigns due to the presence of systematic positioning errors (Smith *et al.*, 2009). These global scale errors generate displacement between dates at small-spatial scales resulting in false change detection (Hussain *et al.*, 2013) (*e.g.* Dekker *et al.*, 2005; Fensham *et al.*, 2007). Thus, application of the present methods may be restricted when using a handheld GPS due to the resulting large global scale errors. Nevertheless, the magnitudes of both local and global scale errors obtained presently were consistent with expectations for both georeferencing systems (see section 4.4.1), resulting in DTMs with sufficient resolution for basic metrics estimation and visual comparison between LRMs. Lastly, artefacts related to environmental characteristics were found on five DTMs and four orthomosaics, reinforcing the need to regard environmental conditions during acquisition. These were likely associated to light conditions and water accumulation into puddles on the intertidal prior to surveying, resulting in distortion during relief reconstruction (Aber *et al.*, 2010) (*e.g.* Chandler *et al.*, 2005; Marzloff and Poesen, 2009; Smith *et al.*, 2009).

4.6.2. Semi-automated detection protocol

Remote monitoring of specific habitats and/or organisms often involves applying a classification algorithm onto images and/or mosaics of a landscape resulting in its segmentation which is then used in change detection (Hussain *et al.*, 2013). The process of image classification has been applied in terrestrial systems to assess several landscape properties, such as human land-use (*e.g.* Abd El-Kawy *et al.*, 2011; Erbek *et al.*, 2004) and land cover (*e.g.* Aguirre-Gutiérrez *et al.*, 2012). Coastal applications encompass characterising and assessing changes in coastal landscape morphology (*e.g.* Ekeboom and Erkkilä, 2003; Hoonhout *et al.*, 2015; Sanchez-Hernandez *et al.*, 2007), as well as assessing temporal patterns in the distribution of several organisms. For example, coral reef communities (*e.g.* Hernández-Cruz *et al.*, 2006; Mumby *et al.*, 1997) and submersed aquatic vegetation (SAV) such as macroalgae (*e.g.* Dekker *et al.*, 2005; Gullström *et al.*, 2006) and seagrasses (*e.g.* Dekker *et al.*, 2005; Hernández-Cruz *et al.*, 2006). Nevertheless, results for image classification algorithms often vary in a case-specific manner. Therefore, we compared the accuracy attained presently with maximum likelihood classification (MLC) to its previous uses in coastal regions.

Maximum likelihood classification is a widely used algorithm for image classification and its previous uses in coastal studies obtained highly variable accuracy – *e.g.* 62-94% (saltmarsh biome - Sanchez-Hernandez *et al.*, 2007), 21-60% (coral reefs - Mumby *et al.*, 1997), 80-100% (SAV communities - Dekker *et al.*, 2005), 21-23% (forest biome – Sanchez-Hernandez *et al.*, 2007). Similarly, our classification accuracy (*i.e.* true presence percentage) was highly variable and agreement between the automated classification and visual identification was extremely low. This may be due to uncertainties during class signature delineation as similarity between signatures can result in inconsistent classifications (Mumby *et al.*, 1997). Visual interpretation of orthomosaics revealed that the classification raster with the lowest accuracy (*i.e.* April 2015) coincided with the presence of sand and mud sediments inside *L. conchilega* aggregations. This can generate low separability between classes and result in overlap between signatures, biasing pixel assignment (Mumby *et al.*, 1997) (*e.g.* Dekker *et al.*, 2005). Although signature separability was assessed visually prior to MLC, and training samples adjusted accordingly, additional analytical assessment of signature separability may improve results (*e.g.* Dekker *et al.*, 2005), but should increase technical requirements considerably. Lastly, alternative

classification methods may be considered, such as support vector machines and/or support vector data which have shown higher accuracy in coastal landscapes than MLC (e.g. Sanchez-Hernandez *et al.*, 2007).

Edge delineation was attempted by analysing relative elevation (see section 4.4.2), an important feature for reef identification (*sensu* Hendrick and Foster-Smith, 2006; Rabaut *et al.*, 2009). The procedure resulted in low concordance between the automatically generated edges and hand delineation with high variation between dates. This indicates that relative elevation is insufficient to delineate protruding *L. conchilega* aggregations and should be complemented. Furthermore, results revealed a relationship among false absence/presence percentages and relief complexity wherein areas with well-developed *L. conchilega* aggregations displayed lesser mismatch between automatically and manually delineated edges than areas with small and sparse aggregations.

It has also been found that the window size used in MES construction indirectly affected false absence/presence percentages by influencing the position of generated edges during the delineation phase and modifying its placement on the actual edge gradient. Future work should attempt to reduce these two biases as it could greatly improve concordance. Improvements could include a conditional selection of polygons based on the image classification outputs (e.g. by selecting polygons using *L. conchilega* pixel counts from presence/absence rasters). Changing how the reference elevation surface is calculated may also improve detection. Presently, a moving window is used to create mean elevation surfaces (MESs) as references to convert DTMs into LRMs (see section 4.4.2). The process creates reference surfaces that may contain localised biases due to changes in elevation from the presence of *L. conchilega* aggregations. An alternative solution could involve a different interpolation method to create reference elevation surfaces. As such, the bias from *L. conchilega* presence may be avoided by sampling elevation from points in bare sediment, then subsequently interpolating the height field from these values. Unfortunately, this method of interpolation was avoided presently because we are unable to ensure that only points outside of *L. conchilega* aggregations were sampled from the DTMs for interpolation of the reference surface. Further improvement may be achieved by sampling extra information from the environment (see further).

The presence of dense *L. conchilega* aggregations affects sediment properties which may be remotely sensed to improve reef detection. For example, *Lanice conchilega* aggregations attenuate water flow by acting as a physical barrier (Borsje *et al.*, 2014) and microscopic photosynthesizing organisms tend to develop further in these conditions than in bare sediment (Passarelli *et al.*, 2012). As such, *L. conchilega* aggregations indirectly modulate chlorophyll-*a* concentration at the sediment surface (De Smet *et al.*, 2015). Thus, a remote evaluation of surficial chl-*a* content should aid in differentiating *L. conchilega* aggregations from their surroundings since chl-*a* content is expected to be higher within *L. conchilega* aggregations due to its effect on flow (Passarelli *et al.*, 2012). Detection of chl-*a* concentration at the sediment surface can be achieved by sampling the near-infrared part of the spectrum (e.g. Bryson *et al.*, 2013; Pauly and De Clerk, 2011). Adapting the acquisition camera to image this portion of the spectrum can be easily achieved without largely inflating costs but may require further technical expertise in analysing the data (Pauly and De Clerk, 2011). In addition, recent research at Boulogne shows that the effect of *L. conchilega* on surficial chl-*a* content varies seasonally with higher concentrations inside aggregations during spring relative to autumn (De Smet *et al.*, 2015). Thus, although imaging the NIR spectrum may improve detection, it warrants further investigation as the effect of seasonality could influence the outputs.

Employing KAP enabled detection of tube aggregations as small as 4cm in diameter/length (post-noise reduction), but excluded smaller aggregations. This may result in underestimation of total *L. conchilega* coverage and low-value aggregations coverage, but should not impact the identification of high-value concretions which are commonly targeted for conservation monitoring (Rabaut *et al.*, 2009). The relationship among error types, *L. conchilega* aggregation size, and relative elevation may still be employed to distinguish aggregations of low and high value. However, due to the aforementioned challenges in edge detection and time constrains, the scoring system could not be applied. As such, further development is necessary to (semi-) automate the process as well as apply the scoring system by Rabaut *et al.* (2009). Comparatively, previous research successfully detected both intertidal and subtidal *L. conchilega* aggregations at coarser resolutions (*i.e.* larger than 0.8m²) using very-high resolution side-scan sonar (Degraer *et al.*, 2008). Thus, although both methods are suitable for the detection of small-scale patterns, each displays unique characteristics that should be taken into account when designing monitoring

efforts. Side-scan sonar requires higher technical expertise to analyse the data and has higher financial requirements than KAP. However, very-high resolution side-scan sonar may be deployed in subtidal environments (Degraer *et al.*, 2008) where KAP cannot. In addition, the application of KAP may be limited by unfavourable atmospheric conditions, whereas deployment of side-scan sonar depends on sea conditions (Degraer *et al.*, 2008). Nevertheless, both methods can be used to complement each other, since side-scan sonar may be used under conditions that KAP cannot and vice-versa. Despite technical challenges, valuable ecological information was successfully extracted using KAP and low-altitude photogrammetry. The subsequent sections of this chapter address these observations and the case-study of *Lanice conchilega* aggregations.

4.7. Background on the spatial ecology of polychaete aggregations and *Lanice conchilega*

Polychaete tube aggregations generally contribute to ecosystem functioning through ecosystem engineering of local environmental properties (*sensu* Jones *et al.*, 1994), regulating resources to other species in two possible ways: autogenically (*i.e.* via physical presence; *e.g.* seagrasses modulating hydrodynamic flow - Balke *et al.*, 2012) and/or allogenicly (*i.e.* via its activities; *e.g.* burrowing fauna such as mangrove crabs - Kristensen, 2008) (Jones *et al.*, 1994). As autogenic engineers, polychaete aggregations affect water flow as it passes through tube arrays modulating local hydrodynamic regimes (Friedrichs *et al.*, 2000) and influencing related processes – *e.g.* sedimentation rates (Borsje *et al.*, 2014) and larval recruitment (Bhaud, 2000). They also add complexity to micro-scale topography (Crain and Bertness, 2006), increasing habitat availability (*e.g.* Dubois *et al.*, 2002; Godet *et al.*, 2008) and spatial heterogeneity (*e.g.* Godet *et al.*, 2011; Zühlke, 2001). As allogenic engineers, polychaetes alter sediment biogeochemistry via bioturbation and/or bioirrigation (*e.g.* Braeckman *et al.*, 2010; Volkenborn *et al.*, 2007). These changes produce different micro-habitats, expanding overall niche availability (Boogert *et al.*, 2006) and impacting associated communities (*e.g.* microphytobenthos - Passarelli *et al.*, 2012; infaunal diversity - Dubois *et al.*, 2002). Thus, polychaete aggregations should be considered valuable targets for conservation and coastal management (Godet *et al.*, 2008).

As previously mentioned, *Lanice conchilega* builds sand tube aggregations in temperate coastal zones (Hartmann-Schröder, 1996), and is particularly abundant on the North Sea (Godet *et al.*, 2008). Its aggregations can reach up to 30 000 ind·m⁻² (Alves *et al.*, 2017b), 16cm in height (Rabaut *et al.*, 2009), and 15m² in area (Degraer *et al.*, 2008), being structured as patches (Degraer *et al.*, 2008) or beds (Godet *et al.*, 2009b). Similarly to other polychaete aggregations, *L. conchilega* tube aggregations autogenically engineer (*sensu* Jones *et al.*, 1994) water flow at the benthic-boundary layer and adjacent marine sediments by posing as physical barriers to water, attenuating flow as it passes through the sand tubes and reducing its velocity (Borsje *et al.*, 2014). The attenuated flow leads to increases in local sedimentation rates (Borsje *et al.*, 2014), altering surficial sediment composition and larval settlement (Rabaut *et al.*, 2009). In addition, *L. conchilega* tube arrays can also entrap organic matter, supporting the development of microbial communities (Passarelli *et al.*, 2012). The changes imposed by *L. conchilega* are extensive, impacting several ecosystem processes and properties, and positively affecting biodiversity (De Smet *et al.*, 2015).

Autogenic engineering effects from *L. conchilega* aggregations may vary with tube density (Borsje *et al.*, 2014). Past certain thresholds, flow attenuation is such that aggregations develop reef-like characteristics (Rabaut *et al.*, 2009). Tube mounds may achieve significantly different elevation from their surroundings (Borsje *et al.*, 2014) with contrasting sediment properties (*e.g.* cohesion and composition) (Rabaut *et al.*, 2007), and develop a distinct biological community (De Smet *et al.*, 2015). Thus, large aggregations, such as extensive beds may be considered high value reefs under the Habitats Directive framework (Rabaut *et al.*, 2009). Indeed, subtidal aggregations have been recently recognized as part of habitat type 1170 (*i.e.* biogenic reefs) and included in the delineation of a SCI on the Belgian coast (SAC Vlaamse Banken BEMNZ0001). However, some uncertainties remain regarding *L. conchilega* aggregations longevity (*i.e.* ability to maintain reef-like characteristics through time) (Holt *et al.*, 1998).

The temporal stability of engineering effects is an important factor in conservation research (Holt *et al.*, 1998). Long-lasting autogenic concretions are expected to have a higher ecological value than comparable but ephemeral constructs (Callaway *et al.*, 2010), because constantly disappearing effects may result in a reduction of resources, such as shelter or food to other species – *e.g.* coral reefs (Graham, 2014). The temporal stability of autogenic ecosystem engineers depends on the properties

of their concretions determining rates of decay (Hastings *et al.*, 2007). Seasonal fluctuations in *L. conchilega* abundance may result in substantial reduction or complete disappearance of both intertidal (e.g. Alves *et al.*, 2017b; Callaway *et al.*, 2010; Ropert and Dauvin, 2000) and subtidal aggregations (e.g. Buhr and Winter, 1976; Van Hoey *et al.*, 2006b) during periods of harsh conditions. This likely occurs due to strong effects of environmental conditions and recruitment success on the ability of *L. conchilega* to establish and maintain reef-level population densities (Callaway *et al.*, 2010). As such, seasonal cycles can result in highly dynamic populations with ephemeral aggregations as observed by Callaway *et al.* (2010) for an intertidal *L. conchilega* population in Rhossili Bay (South Wales, UK).

Several factors may influence the formation of the commonly observed patchy structure of *L. conchilega* aggregations. As a sessile spawner, the distribution of *L. conchilega* may vary according to processes pertaining to larval recruitment and settlement (Bhaud, 2000), as well as post-settlement survival (Levin, 1992). The presence of adult tubes or similarly protruding structures may facilitate larval settlement locally by providing additional substrate for attachment (Callaway, 2003), and/or ameliorating hydrodynamic conditions through physical attenuation (Rabaut *et al.*, 2009). The presence of living conspecifics may also influence local settlement by exuding chemical cues to settling individuals (Callaway, 2003). Heterogeneous topography may also induce different hydrodynamic conditions in space and facilitate *L. conchilega* occurrence, sustaining spatial patterns at a local scale (*i.e.* 100-1000m) without the need for the presence of tubes and/or other similar structures. Previous research has shown *L. conchilega* larvae settling in the absence of those features (e.g. Dittmann, 1999; Strasser and Pieloth, 2001), potentially constituting a way for aggregations to form in previously bare sediment. Additionally, differential hydrodynamic stress may also result in heterogeneous dislodgement and/or removal of individual worms post-settlement (see Heuers *et al.*, 1998; Ropert and Dauvin, 2000), further contributing to landscape heterogeneity and changing early patterns (*sensu* Levin, 1992). These interactions should modulate tube density, aggregation size and distribution in the coastal environment. Therefore, our last objective was to analyse the temporal evolution and persistence of small-scale *L. conchilega* distribution in the intertidal zone, as well as aggregation longevity.

4.8. Methods to assess the temporal evolution of *L. conchilega* small-scale distribution

Percentage coverage was estimated from presence/absence rasters derived from supervised maximum likelihood image classification (see section 4.4.2). The relationship between topographical features and *L. conchilega* presence was evaluated visually by aligning the presence/absence rasters with their respective DTMs (see section 4.4.2). Longevity was estimated for individual aggregations by counting the number of sequential months in which clearly identifiable concretions were present, whereas persistence was evaluated by estimating the longevity of *L. conchilega* presence in the intertidal from orthomosaics. Lastly, visual interpretation of orthomosaics, digital terrain models, and presence/absence rasters was used to identify *L. conchilega* small-scale distribution patterns and evaluate their temporal evolution.

4.9. Observations on the temporal evolution of *L. conchilega* small-scale distribution

Lanice conchilega was detected at all campaigns during the survey with visual inspection of orthomosaics (Addendum III) confirming detection results (see section 4.5.2). Percentage coverage within the study area ranged between 13.38% and 43.86%. Higher coverage (*i.e.* above 30%) was observed during June 2013, and April, June and August 2014 (see Table 4.3 previously). In addition, although aggregations comprised areas of positive relative elevation within the study area (Fig 4.10A), the total extent of *L. conchilega* distribution was restricted to a depression in the intertidal zone (Fig 4.10B and 4.10C). Maximum individual aggregation longevity was 5 months (*i.e.* June 2013-October 2013) (Fig 4.11). Furthermore, three aggregation types were distinguished during the survey according to their physical characteristics (Fig 4.11). The first type was identified in the period between June 2013 and October 2013, and was observed again during April 2014 (Fig 4.11), and October 2014 (see Addendum III.J). Type 1 distribution consisted of tube aggregations that were visually distinct from bare sediment while being compact and mound-shaped, *i.e.* patches (Fig 4.11). The second type constituted extensive beds occurring in June 2014 (Fig 4.11), while type 3 distribution consisted of regularly interrupted beds, observed from July 2014 until August 2014 (Fig 4.11). The reader is referred to table 1.1 for detailed definitions of small-scale distribution types.

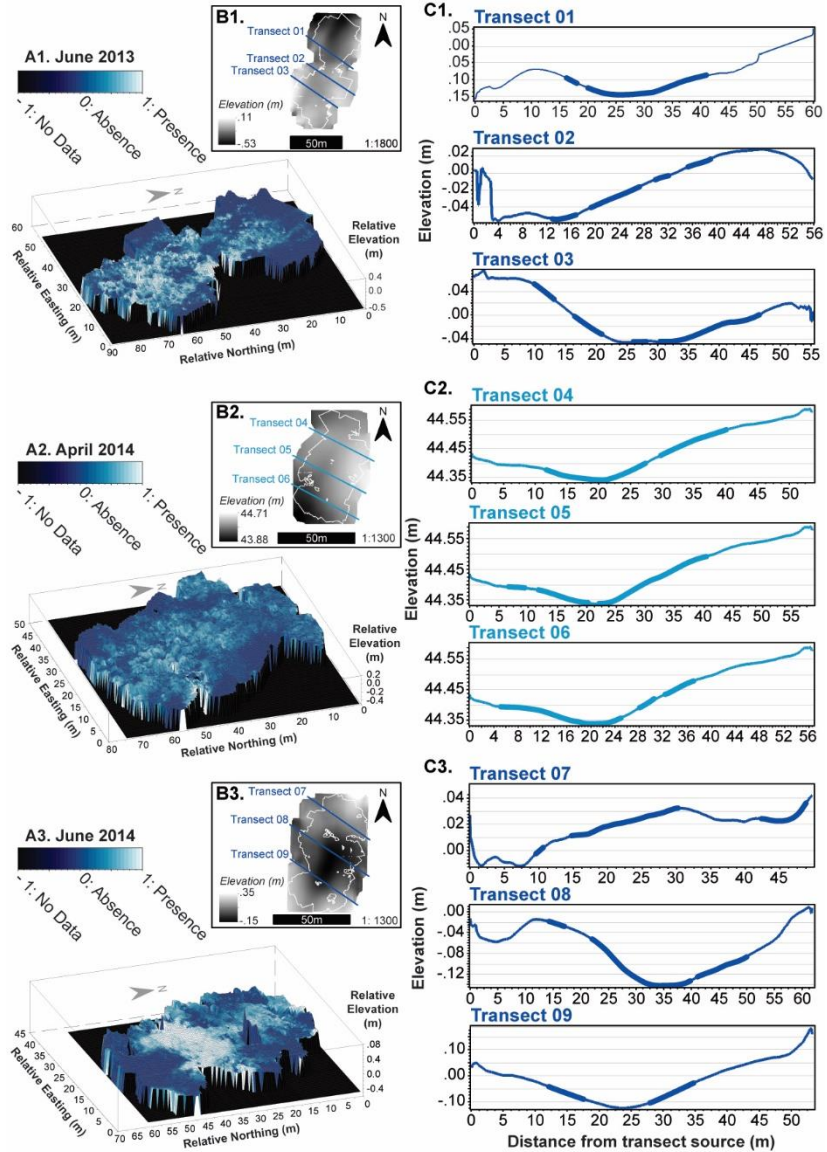
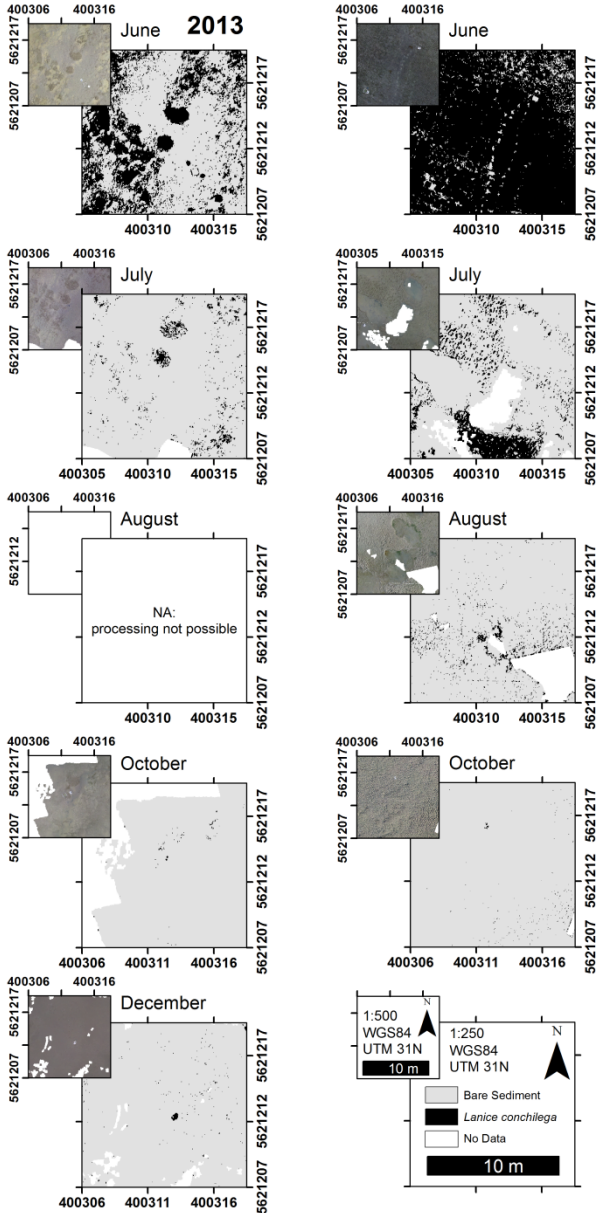


Fig 4.10. Illustration of the relationship between *Lanice conchilega* presence and relative elevation: (A) Individual aggregations (white) were related to positive relative elevation. Note that the surface was rescaled for plotting from a resolution of 0.01m to 0.5m using arithmetic averages. (B, C) Transects of the mean elevation surfaces show overall presence is concentrated on a depression in the intertidal zone (thicker lines in C).

Fig 4.11. Temporal persistence of *L. conchilega* aggregations and evolution of its distributional patterns. Small variations in patch location between dates is a consequence of georeferencing accuracy between campaigns.



4.10. Discussion on the temporal evolution of *L. conchilega* small-scale distribution patterns

Our study focused on intertidal aggregations located near the low water spring tide mark (LWST), an area in which *L. conchilega* occurs in high abundance and seems to prefer (in addition to shallow subtidal waters) (Strasser and Pieloth, 2001). Intertidal aggregations have been considered physically similar to subtidal concretions (Degraer *et al.*, 2008), enabling comparison between the two. However, the different environmental conditions between these two zones may generate divergent processes and/or properties. Therefore, caution is advised when comparing the present findings from an intertidal zone to research with subtidal populations.

Seasonal fluctuations in environmental conditions affect *L. conchilega* abundance and can result in substantial reductions or complete disappearance of aggregations during periods of harsh conditions in both intertidal (e.g. Callaway *et al.*, 2010; Ropert and Dauvin, 2000) and subtidal zones (e.g. Buhr and Winter, 1976; Van Hoey *et al.*, 2006b). However, *L. conchilega* distribution may display 'long-lasting persistence' (Callaway *et al.*, 2010) with individuals being able to re-establish aggregations regardless of the preceding presence of protruding structures and/or adult tubes (e.g. Dittmann, 1999; Strasser and Pieloth, 2001). Our observations on the sandy beach at Boulogne corroborate these trends. Coverage fluctuated seasonally throughout the survey, peaking during known recruitment months (*i.e.* April-June) (e.g. Ropert and Dauvin, 2000; Van Hoey *et al.*, 2006b). *Lanice conchilega* was present during the entire survey while individual aggregations persisted at most for 5 months. In addition, distribution was highly influenced by topography with total extent restricted to a depression on the intertidal zone. At these spatial scales (*i.e.* 100m – 1000m) it is likely that *L. conchilega* distribution is determined by larval recruitment and survival in a similar fashion to other sessile spawners (Bhaud, 2000) – e.g. Callaway *et al.*, 2010; Heuers *et al.*, 1998; Ropert and Dauvin, 2000; Strasser and Pieloth, 2001. These processes are often influenced by larvae availability in the water column (Strasser and Pieloth, 2001), hydrodynamic regime at the benthic-boundary layer (Heuers *et al.*, 1998), and level of wave-action exposure (Callaway *et al.*, 2010). None of these factors has been assessed in the present effort. Nevertheless, previous observations suggest that *L. conchilega* may accumulate in topographical depressions as a function of local hydrodynamic conditions (e.g. Heuers *et al.*, 1998; Ropert and Dauvin, 2000). These areas may display relatively high speed water

currents (Heuers *et al.*, 1998), resulting in high water exchange which effectively flushes topographical depressions (Ropert and Dauvin, 2000). It can be hypothesized that the high exchange rate maintains a uniform chlorophyll concentration in these depressions since water stagnation may lead to chl-*a* depletion by *L. conchilega* through filter-feeding pressure (Denis *et al.*, 2007). Similarly to the aforementioned, the accumulation of *L. conchilega* in an intertidal depression in Boulogne is likely related to local hydrodynamic conditions. However, since the relationship between topography and flow condition is highly complex (Jouanneau *et al.*, 2013), inferences cannot be made regarding current speeds at the study site, requiring further research.

Small-scale spatial pattern formation in *L. conchilega* aggregations may be influenced by interactions between populations and hydrodynamic processes as previously mentioned – *e.g.* animal dislodgement (*e.g.* Ropert and Dauvin, 2000) and/or heterogeneity in larval settlement (Heuers and Jaklin, 1999). Nevertheless, larval processes may also contribute to spatial pattern formation (Levin, 1992). Irregular larval settlement may be caused by the presence of protruding structures facilitating larval recruitment locally (*e.g.* Callaway, 2003; Rabaut *et al.*, 2009), and giving rise to early patterns which can be later modified by post-settlement mortality (Levin, 1992). In addition, water flow may be ameliorated as it passes through and around tube aggregations (Borsje *et al.*, 2014), facilitating larval retention and settlement (Rabaut *et al.*, 2009). Furthermore, large-scale hydrodynamic conditions may also influence small-scale pattern formation in dynamic environments (Callaway *et al.*, 2010), such as intertidal zones. Different patterns may form following different settlement moments due to spatially irregular hydrodynamic conditions (*e.g.* Callaway *et al.*, 2010). *Lanice conchilega* has two settlement moments within its life-cycle (Kessler, 1963). The first occurs during the bipartite pelagic larval phase, while the second marks the beginning of juvenile development (Kessler, 1963). The two settlement moments occur during spring season (approx. May-June) (see Ropert and Dauvin, 2000; Van Hoey *et al.*, 2006b), and are separated by a 1 month interval (Kessler, 1963) (see addendum I for details on the life cycle of *L. conchilega*). As such, multiple small-scale spatial patterns are expected to be observed within the time span of one life-cycle, and particularly within recruitment season.

Three small-scale patterns were observed on the intertidal zone during that time frame: (1) sparse and compact mound-shaped aggregations (*i.e.* patches), (2)

extensive beds, and (3) interrupted beds. The beach of Boulogne has a highly dynamic tidal cycle with flood and ebb tides displaying distinct regimes characterized by eddy formation and localised turbulence (Jouanneau *et al.*, 2013). Therefore, it is likely that different patterns were formed as a function of distinct hydrodynamic conditions during settlement moments, and changed later due to post-settlement mortality (Levin, 1992). Patches were dominant in Boulogne during the first half of the survey (June 2013 – April 2014) with an interruption between December 2013 and March 2014 (*i.e.* during winter). The other two types were observed between June 2014 and August 2014, followed by a patchy distribution again in October 2014. These moments of spatial pattern formation are in agreement with the aforementioned expected settlement moments during spring season (Kessler, 1963). Additionally, animal dislodgement by water currents may have influenced pattern formation. However, results indicate that it is unlikely since spatial patterns remained similar following their formation in recruitment seasons. Heterogeneous larval settlement due to the presence of aggregation remnants (*i.e.* protruding *L. conchilega* tubes) and/or similar structures protruding from the sediment surface is also unlikely. The small-scale spatial patterns observed between 2013 and 2014 were morphologically dissimilar despite concentrating at the same general location. Thus, we hypothesize that small-scale spatial pattern formation may follow a seasonal cycle as a consequence of interacting hydrodynamics and larval settlement.

Finally, our results and aforementioned considerations point to a hypothetical yearly cycle explaining small-scale spatial pattern formation at the site wherein a nearly/completely barren intertidal zone is populated by the first *L. conchilega* settlement, resulting in one distribution type at the beginning of spring season. Following a temporary sessile moment, animals may detach into the water column (Kessler, 1963), dispersing the previous spatial pattern (*e.g.* Callaway, 2003). A second settlement approx. 1 month later should result in another small-scale spatial pattern which would decay during the following months. Taking this hypothetical causal structure into account, the first spring settlement likely occurred between March 2014 and April 2014 during the present study (*e.g.* Callaway, 2003; Ropert and Dauvin, 2000; Van Hoey *et al.*, 2006b), resulting in the formation of a patchy distribution. Findings from chapter 3 corroborate this hypothesis, identifying 3 recruitment moments during our campaigns: October 2013, April 2014, and September 2014.

The spring recruitment in April 2014 was characterised by high density of very small individuals (*i.e.* approx. 30 022 ind·m⁻² with average inner tube diameter of 0.67mm) (see chapter 3 or Alves *et al.*, 2017b). These sizes are similar to the expected size of aulophora larvae (*i.e.* approx. 0.40mm in body diameter – Kessler, 1963) instead of the metatrochophora-II bipartite larval stage (*i.e.* approx. 0.1mm in body diameter – Kessler, 1963) (see also Addendum I). The observed inner tube diameters (see chapter 3) suggest that these settling individuals are in the aulophora stage instead of the metatrochophora-II stage. As such, the patterns that followed those observed in April 2014 (*i.e.* extensive beds), were likely formed by subsequent aulophora recruits, since recruitment may last several months (*e.g.* Callaway, 2003; Van Hoey *et al.*, 2006b). Consequently, we hypothesised that settlement occurred throughout April-June 2014, changing the fragmented distribution observed in April 2014 into extensive beds observed in June 2014. Unsurprisingly, decay of the *L. conchilega* bed observed in June 2014 occurred between that period and October 2014. The beds became interrupted between June and July likely due to physical removal and/or mortality resulting in the interrupted beds observed in July (*i.e.* type 3). Decay continued until October, at which time the distribution became again characterized by patches. It is likely that these patches continued to decay until the following recruitment moment which was not observed.

4.11. Conclusions

4.11.1. Mapping, detecting, and monitoring

Kite aerial photography and digital photogrammetry proved suitable methods to map and monitor intertidal aggregations, enabling the extraction of accurate digital elevation models and orthomosaics. The presence of large global scale errors hindered analytical comparisons for change detection (*e.g.* image differencing), limiting analyses to visual interpretation. Maximum likelihood image classification successfully distinguished *L. conchilega* from its surroundings, but varying accuracy warrants further improvement. Similarly, edge detection was highly variable and displayed systematic biases which hindered scoring of *L. conchilega* aggregations. Further study of these biases in edge detection may improve differentiation between *L. conchilega* and its surroundings, as well as differentiation between aggregations of distinct ecological values. In addition, further characterisation of *L. conchilega* aggregations *in-situ* during acquisition may aid remote identification. We suggest an

analysis of the near infrared spectrum since the species modulates chl-*a* concentration at the sediment surface, increasing its surficial content to a significantly different level than that found in bare sediments.

4.11.2. *Temporal evolution of L. conchilega small-scale distribution patterns*

Despite technical challenges, valuable ecological information was successfully extracted from the aerial photographs. Our surveys revealed *L. conchilega* aggregations forming three distinct types of small-scale distribution patterns during recruitment seasons: patches, continuous beds, and interrupted beds. This suggests multiple mechanisms of pattern formation. No evidence was found of animal dislodgement and/or removal as patterns remained similar in the months following their formation during larval settlement periods. This indicates that these mechanisms do not play significant roles in generating spatial heterogeneity in the intertidal zone at Boulogne. Therefore, we hypothesize that small-scale spatial pattern formation in *L. conchilega* beds in intertidal zones is likely determined by larval settlement which may be influenced by hydrodynamic conditions, as well as post-settlement survival.

An aerial photograph of a coral reef, showing various shades of brown and tan. The reef is composed of numerous small, irregular patches of coral. A small white marker, possibly a survey point, is visible on the ground in the lower-left quadrant of the image. The overall scene is a top-down view of a natural marine ecosystem.

CHAPTER

5

Simulation-based exercise on the effects of consumer-resource interactions on population dynamics of the reef-building ecosystem engineer *Lanice conchilega* (Pallas, 1766)

Authored by: Alves RMS, Van Colen C, Vincx M, Guarini JM.

5.1. Abstract

*The tube-building polychaete *Lanice conchilega* forms aggregations that autogenically engineer marine sediments, hindering water flow at the benthic-boundary layer and creating micro-habitats of distinct hydrodynamic conditions within its tube arrays. Mechanisms underlying formation and decay of *L. conchilega* aggregations are unclear, and may be influenced by related to consumer-resource interactions. The latter may influence spatial pattern formation by modulating population dynamics through mortality across a landscape. The aim of the present exercise was to investigate how consumer-resource interactions may affect *L. conchilega* population dynamics. Due to the complexity of the task, a population based simulation model was employed to investigate (1) how fluctuations in food availability can impact average juvenile and adult *L. conchilega* density during one yearly population cycle, and (2) how variations in food assimilation can influence average juvenile and adult densities. The model was parametrised using information available in literature as well as data collected from an intertidal *L. conchilega* population from Boulogne-sur-mer (France). A sensitivity analysis was performed on parameters related to feeding and maturation, and outputs were analysed visually for preliminary results. Juvenile density dynamics were unaffected by variations in food availability and assimilation, whereas adult density dynamics were highly dependent on these. Total density dynamics was largely dictated by recruitment and juvenile density dynamics, as such, it was generally unaffected by variations in food availability and assimilation. Our preliminary findings indicate that consumer-resource interactions (as studied by our model) likely play a marginal role on *L. conchilega* population dynamics. Differences in density decline rates following recruitment during the simulations suggest that aggregation decay may involve further mechanisms than those analysed presently.*

5.2. Introduction

Ecosystem engineers are organisms that modulate natural resources to other species by imposing changes on biotic and/or abiotic processes and/or properties of the environment (Jones *et al.*, 1994). Although most living organisms can be considered ecosystem engineers, the term is largely used referring to organisms that substantially reduce environmental constraints to other species, enabling their survival (Crain and Bertness, 2006). Resource modulation by these organisms often culminates on the creation of distinct environments within the landscape with the engineering effect enabling the survival of species that would otherwise perish (Jones *et al.*, 1994). Ecosystem engineers can be distinguished into two groups according to how they induce change (Jones *et al.*, 1994). Autogenic engineers cause change through their own presence (Jones *et al.*, 1994) (*e.g.* corals - Wild *et al.*, 2011), whereas allogenic engineers cause change through their activities (Jones *et al.*, 1994) (*e.g.* mangrove crabs - Kristensen, 2008). Engineering effects may be modulated by population dynamics as it dictates organism size and population density (Eckman *et al.*, 1981). In the marine environment, this means that population dynamics may modulate engineering effects by influencing interaction outcomes between engineering populations and hydrodynamic flow. For example, the area of obstruction for an autogenic construct changes as demographic structure of an autogenic engineer population develops through time because the average individual size of its members change (*e.g.* Alves *et al.*, 2017b; Bouma *et al.*, 2005). Thus, population dynamics of ecosystem engineers may indirectly impact species small-scale distribution, creating patchy landscapes (*i.e.* landscape heterogeneity).

Landscape heterogeneity is often associated to ecosystem function due to its effect on biodiversity (Rietkerk *et al.*, 2004), in that it positively affects species richness (Romero *et al.*, 2015), abundance and biomass (Buhl-Mortensen *et al.*, 2010) by providing a myriad of micro-habitats and ecological niches (*e.g.* Wild *et al.*, 2011, Wright *et al.*, 2002). As such, changes in landscape heterogeneity may significantly influence ecosystem functioning through effects on species richness, abundance and/or biomass (*e.g.* Andersen and Shafroth, 2010; Buhl-Mortensen *et al.*, 2010). Unsurprisingly, ecosystem engineers that create patchy landscapes and enhance biodiversity often influence ecosystem functioning (Rietkerk *et al.*, 2004) – *e.g.* Koch *et al.*, 2009; Volkenborn *et al.*, 2007. Identifying the mechanisms through which

spatial patterns develop remains a major challenge in conservation research because spatial pattern formation is a context-specific process (Turner, 2005).

Spatial pattern formation in the marine and coastal environments is influenced by a myriad of factors and processes (Levin, 1992). Environmental gradients and biotic interactions in the coastal zone may dictate distribution limits by imposing physiological stress outside of the tolerance ranges of certain species (Kaiser *et al.*, 2005) – e.g. the effect of air exposure gradients on the distribution of macro algae and filter-feeding invertebrates with low resistance to desiccation (Christofoletti *et al.*, 2011), or the effect of competition for space between the barnacles *Chthamalus stellatus* and *Balanus balanoides* (Connell, 1961). Ecosystem engineering can create and/or exacerbate environmental gradients (Crain and Bertness, 2006), which in turn, may influence engineering effects across space (Hastings *et al.*, 2007) in addition to potentially modulating further physiological stress. This is highly conspicuous for autogenic engineers forming concretions that increase landscape heterogeneity – e.g. scleractinian corals (Wild *et al.*, 2011), mussels (Borthagaray and Carranza, 2007), saltmarsh grasses (Bouma *et al.*, 2008) and polychaetes (Polgar *et al.*, 2015).

Known mechanisms driving small-scale spatial pattern formation may include but are not restricted to consumer-resource interactions, disturbance-recovery processes, and scale-dependent feedbacks (*sensu* Rietkerk and van de Koppel, 2008). The first encompasses distributions that are a result of fluctuations in resource availability (*sensu* Rietkerk and van de Koppel, 2008) – e.g. the small-scale distribution of a few marsh plants associated to light availability (van de Koppel *et al.*, 2006). The second mechanism incorporates disturbance-recovery processes wherein disturbance/recovery regimes create fragmented distributions (*sensu* Guichard *et al.*, 2003) – e.g. oyster fishing affecting polychaete distribution (Dubois *et al.*, 2002), or wave action affecting the distribution of the California mussel *Mytilus californianus* (Guichard *et al.*, 2003). The last mechanism revolves around feedback relationships that may stem from combinations of various processes and/or interactions (*sensu* Rietkerk and van de Koppel, 2008) – e.g. saltmarsh tussock formation (Balke *et al.*, 2012; Bouma *et al.*, 2009a), or the formation of mussel patches (van de Koppel *et al.*, 2008) (see section 1.3 for further details).

Case-studies such as the aforementioned examples comprise a crucial part of the body of work, revealing various scenarios that enable the development of theories in this research field – e.g. Bouma *et al.* (2009a), van de Koppel *et al.* (2008), Weerman

et al. (2010). The present exercise adds to this body of research with the case study of an intertidal ecosystem engineer *Lanice conchilega* (Pallas, 1766). *Lanice conchilega* is a sessile terebellid worm (Hartmann-Schröder, 1996) commonly occurring in European shores (Godet *et al.*, 2008). It forms biogenic tube aggregations between the intertidal zone down to depths of approximately 1 900m (Hartmann-Schröder, 1996). These autogenically modulate water flow at the benthic-boundary layer by physically obstructing its passage (Borsje *et al.*, 2014), influencing sedimentation/erosion processes (Borsje *et al.*, 2014), sediment composition (Rabaut *et al.*, 2009), and particle entrapment (Passarelli *et al.*, 2012). Aggregations also extend micro-habitat availability to benthic communities (Godet *et al.*, 2008), contributing to landscape spatial heterogeneity (Zühlke, 2001). *Lanice conchilega* also allogically engineers the environment by piston-pumping to flush its tube, which modulates sediment biogeochemistry (Braeckman *et al.*, 2014). The changes imposed by *L. conchilega* substantially affect associated benthic communities (De Smet *et al.*, 2015), often resulting in higher macrobenthic species richness and abundance as well as higher epi- and hyperbenthic abundances than its surroundings (De Smet *et al.*, 2015).

Lanice conchilega is both a filter- (Buhr, 1976) and a deposit-feeder (Ropert and Gouletquer, 2000), consuming mainly microorganisms from the water column and sediment surface – namely bacteria and microalgae, but also fragments of macroalgae (e.g. Braeckman *et al.*, 2012; Lefebvre *et al.*, 2009). Its diet is influenced by seasonal fluctuations in primary production (e.g. Braeckman *et al.*, 2012; Lefebvre *et al.*, 2009) which are associated to higher mortality rates (e.g. Buhr and Winter, 1976; Callaway *et al.*, 2010; Ropert and Dauvin, 2000; Strasser and Pieloth, 2001; Van Hoey *et al.*, 2006b). Several factors can affect the feeding activity of this tube-worm and a wide range of individual clearance rates has been observed for *L. conchilega* - from $0.016\text{L}\cdot\text{h}^{-1}$ to $0.171\text{L}\cdot\text{h}^{-1}$ (Buhr, 1976; Denis *et al.*, 2007). These may vary according to animal size (Buhr, 1976), current velocity (Denis *et al.*, 2007), and particle size (Ropert and Gouletquer, 2000). Additionally, *Lanice conchilega* can create gradients in the concentration of primary producers in the water column by filtration-induced depletion (Denis *et al.*, 2007), creating areas of differentiated mortality within the population. Furthermore, deposit-feeding may be hindered in high density aggregations as sand tubes restrict access to the sediment surface (Buhr, 1976), potentially forcing animals to switch to filtration and stimulating intraspecific

competition. Finally, food assimilation may substantially decrease in the presence of potential predators (De Smet *et al.*, 2016a). As such, we hypothesised that consumer-resource interactions could lead to spatial patterning of *L. conchilega* aggregations by modulating mortality and creating intraspecific competition. The present study focuses on consumer-resource interactions because the aforementioned research on *L. conchilega* feeding ecology suggests that these interactions may affect population dynamics unevenly through space, creating spatial patterns. Additionally, the sampled data in the present effort enabled the investigation of these dynamics.

The myriad factors influencing *L. conchilega* feeding hampers a solid experimental/empirical study of its effect on population dynamics and spatial pattern formation within *L. conchilega* aggregations. As such, a modelling approach was employed focusing on examining the effects of varying food availability and food assimilation on population density dynamics of an intertidal *L. conchilega* population. However, due to time constraints, the study is still underway and only a preliminary evaluation of the exercise is performed here. This first half of the modelling framework employed a population based model (PBM) to investigate whether (1) fluctuations in food availability would significantly impact average juvenile and adult *L. conchilega* density throughout one yearly population cycle, and (2) whether variations in assimilation would indirectly impact average juvenile and adult densities by modulating maturation.

5.3. Methods

5.3.1. Case-study intertidal population

The present exercise assesses a population based model simulation of an intertidal *L. conchilega* population from a sandy beach in Boulogne-sur-Mer (Nord Pas-de-Calais, France: 50.7345 N; 1.5881 E) (hereafter referred to as Boulogne) (Fig 5.1). Population based modelling was chosen because it enabled us to simulate the dynamics of distinct population cohorts based on processes related to feeding, maturation, and mortality, while being suitable for transposition to a spatially-explicit environment. The latter enables studying the role of population dynamics and processes on spatial distribution (*e.g.* Dunning *et al.*, 1995). The location was selected due to the presence of a thriving *L. conchilega* population and ease-of-access during low water spring tide (LWST) for sampling. The sandy beach is

predominantly composed by fine and medium sand (Rabaut *et al.*, 2008), subjected to a semi-diurnal tidal regime ranging from 4m to 9m (Jouanneau *et al.*, 2013), a mean sea level of 5.03m (0.17m SD) and exposure time of approx. 4h during LWST (estimated from tidal gauge data) (Service Hydrographique et Océanographique de la Marine - SHOM, 2015). Data for parametrisation was obtained from a monthly survey of three intertidal *L. conchilega* aggregations (1-3 in Fig 5.1) from June 2013 until November 2014 (see Alves *et al.*, 2017b for further information).

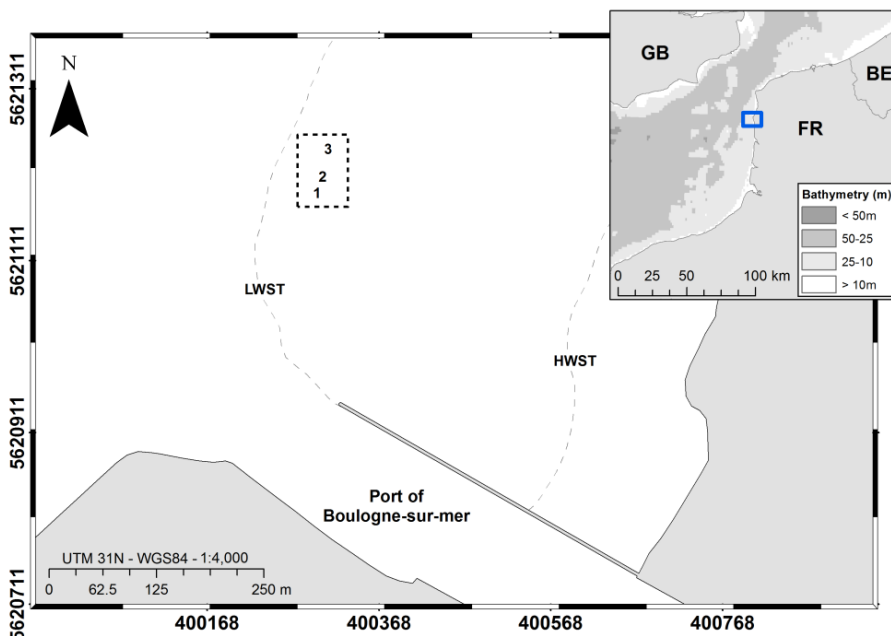


Fig 5.1. Map of the sandy beach in Boulogne-sur-mer depicting the three monitored *L. conchilega* aggregations (1-3) near the low water spring tide limit (grey dashed line, LWST). To the south of the site is the entrance to the port of Boulogne. To the east lies the main land and the high water spring tide mark (dashed line, HWST). Both low and high water spring tides were approximated using satellite imagery.

Localization during surveys was performed using an RTK-GNSS system and hand-held GPS receivers (see chapter 4 for further information). *Lanice conchilega* density was estimated for each aggregation through quadrat counts (0.5m x 0.5m) of fringed tubes according to Van Hoey *et al.* (2006a). Samples were extracted from each

aggregation using a large inox core (12cm Φ , 38cm in height) to assess population demographic structure per month. Juvenile and adult cohorts were assessed using Bhattacharya's method (Bhattacharya, 1967) (see Alves *et al.*, 2017b for further information). In addition, sediment samples were taken from each aggregation using acrylic cores (3.6cm Φ , 0-1cm depth) to assess surficial chlorophyll-*a* content ($\mu\text{g}\cdot\text{g}^{-1}$ sediment) as a proxy for microphytobenthos (MPB) biomass (Jeffrey *et al.*, 1997). Surficial sediment samples were extracted using acetone (90%), sonicated, filtered at 0.2 μm , and analysed on a high resolution, high performance liquid chromatographer (*i.e.* HPLC Gilson system with a C18 column) (Wright and Jeffrey, 1997) (see Alves *et al.*, 2017b for further information).

5.3.2. Modeled ecological dynamics

The population based model system consisted on a set of five ordinary differential equations (ODEs) (Eq 5.1-5.5) simulating three ecological processes: feeding-dependent maturation, feeding-dependent mortality, and density-dependent mortality. The model simulates simplified population processes involving 5 ecosystem compartments: generic nutrients (*N*), pelagic algae (*A*), surficial microphytobenthos (*P*), juvenile (*J*) and adult *L. conchilega* (*L*) (Eq 5.1-5.5). Simulations were developed and executed using the Scilab computing environment v5.5.1. (Scilab Enterprises, 2012), employing a deterministic approach with discrete time intervals (*sensu* Gurney and Nisbet, 1998). One of the main characteristics of the model was stiffness, that is, most integration methods resulted in numerically unstable solutions unless a very small time step was adopted. Stiffness likely emerged due to a large difference in the scale of dynamics between *L. conchilega* compartments and the other model compartments. Therefore, the simulation time step was very small with ODE integration at one-minute steps and simultaneous updates of all variables. The backward differentiation formula (*i.e.* BDF method) (*sensu* Süli and Mayers, 2003) was used for ODE integration through the dedicated solver for stiff equations in Scilab (Scilab Enterprises, 2015). All parameters were scaled to a spatial unit of 1m² (if related to sediment surface dynamics) or 1L (if related to pelagic dynamics), and adjusted to a time step of 1 minute.

$$\text{Eq 5.1.} \quad \frac{dN}{dt} = +r_n - g_a \frac{N}{r_a + N} A - advN$$

$$\text{Eq 5.2.} \quad \frac{dA}{dt} = +g_a \frac{N}{r_a + N} A + \frac{r_p}{h} P - \frac{f}{h} A(J + L) - advA$$

$$\text{Eq 5.3.} \quad \frac{dP}{dt} = +g_p S_{max} - r_p P - zP(J + L)$$

$$\text{Eq 5.4.} \quad \frac{dJ}{dt} = +g_j \left(1 - \frac{J}{k_j} - \frac{L}{k_l}\right) - g_l \frac{asm}{asm + Rc} J - m_j \frac{Rc}{asm + Rc} J$$

$$\text{Eq 5.5.} \quad \frac{dL}{dt} = +g_l \frac{asm}{asm + Rc} J - m_l \frac{k_m}{(k_m + L)} L$$

$$\text{Eq 5.6.} \quad asm = e(fA + zP)$$

The first two equations in the model system describe pelagic processes, which include the temporal dynamics of generic nutrients ($\mu\text{g Chl-a}\cdot\text{L}^{-1}\cdot\text{min}^{-1}$) (Eq 5.1) and pelagic algae ($\mu\text{g Chl-a}\cdot\text{L}^{-1}\cdot\text{min}^{-1}$) (Eq 5.2). Generic nutrient concentration increases through remineralisation (Eq 5.1: first term) according to a dynamic parameter (Eq 5.1: r_n) ($\mu\text{g chl-a}\cdot\text{L}^{-1}\cdot\text{min}^{-1}$) (Fig 5.2A). This parameter represents the total amount of chl-a added to the water column at each time step independently of the concentration on the previous time step. As such, it displays two seasonal peaks, in spring and summer (*i.e.* days 60-151 and 152-243 respectively) which coincide with chl-a blooms observed by Breton *et al.* (2000) for the coastal waters of Boulogne-sur-Mer. The generic nutrient pool is depleted by pelagic algae (Eq 5.1: second term) for cellular multiplication determined by a static growth rate (Eq 5.1 and 5.2: g_a) (proportion $\cdot\text{min}^{-1}$). In turn, cellular multiplication is constrained by nutrient availability through a growth limitation parameter (Eq 5.1 and 5.2: r_a) ($\mu\text{g Chl-a}\cdot\text{L}^{-1}$). The latter determines a threshold nutrient concentration from which point pelagic algal growth becomes impaired due to low food availability. Generic nutrients may also be depleted through advection loss/gain (Eq 5.1: third term) determined by a fixed rate (Eq 5.1: adv) (proportion $\cdot\text{min}^{-1}$). As previously mentioned, pelagic algae growth is

based on generic nutrient consumption (Eq 5.2: first term). In addition the algal pool may grow through microphytobenthos resuspension (Eq 5.2: second term). Resuspension is modulated by a static rate (Eq 5.2 and 5.3: r_p) (proportion·min⁻¹) for a water column height of 2.16m (Eq 5.2: h) – *i.e.* the maximum water column height at Boulogne during high water spring tide (HWST) estimated from the localization data. Pelagic algae is diminished through filter-feeding from both adult (Eq 5.2: L) and juvenile (Eq 5.2: J) *L. conchilega* (Eq 5.2: third term). Filter-feeding is modulated by a static filtration rate (Eq 5.2: f) (L·ind⁻¹·min⁻¹) and water column height (Eq 5.2: h) (*i.e.* 2.16 meters). Lastly, similarly to the generic nutrient compartment, pelagic algae may lose/gain biomass due to current-induced advection (Eq 5.1 and 5.2: last term), modulated by a static rate (Eq 5.2: adv) (proportion·min⁻¹).

The last three equations simulate dynamics at the benthic boundary layer, that is microphytobenthos biomass ($\mu\text{g Chl-}a\cdot\text{m}^{-2}\cdot\text{min}^{-1}$) (Eq 5.3), juvenile density (Eq 5.4) (ind·m⁻²·min⁻²), and adult density (Eq 5.5) (ind·m⁻²·min⁻²). Temporal dynamics of MPB biomass was simulated for a generic biofilm layer previously assessed from the soft-sediments in the study site through chl-*a* concentration (see Alves *et al.*, 2017b). Fluctuations in this compartment are described by the third differential equation (Eq 5.3), which includes a growth term (Eq 5.3: first term) ruled by a dynamic growth rate (g_p) (proportion·min⁻¹) (Fig 5.2B). The latter varies seasonally, peaking during summer (*i.e.* day 152-242, that is June 1st – August 30th), and is modulated by the sediment surface capacity for MPB biomass (S_{max}) ($\mu\text{g Chl-}a\cdot\text{m}^{-2}$) estimated from sediment samples. Microphytobenthos is depleted by the resuspension term (Eq 5.3: second term), and grazing from both *L. conchilega* compartments (Eq 5.3: third term) at a static rate (z) (m²·ind⁻¹·min⁻¹).

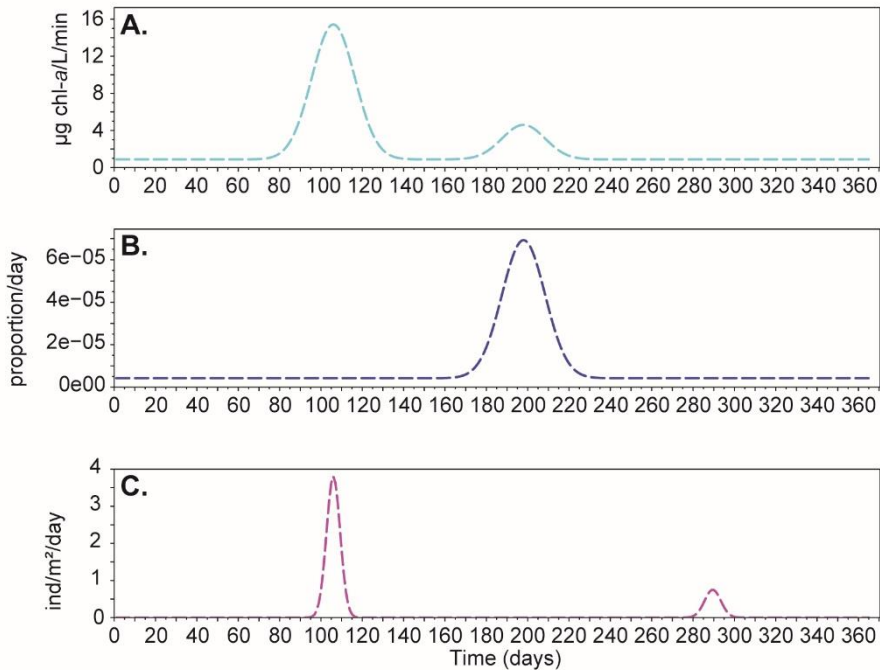


Fig 5.2. All dynamic rates were simulated following Gaussian curves. The remineralisation parameter (A) presented two yearly peaks, in spring (*i.e.* day 60-151) and summer (*i.e.* day 152-243). The dynamic MPB growth rate (B) peaks during summer (*i.e.* day 152-242). The dynamic juvenile *L. conchilega* growth rate (*i.e.* recruitment input) peaks twice per year, spring (*i.e.* 91-120) and autumn (*i.e.* 274-304).

The fourth equation simulates density fluctuations for juvenile *L. conchilega* (Eq 5.4) – *i.e.* dynamics for cohorts within the first 3 months counting from the settlement moment. Simulated juvenile cohorts may increase in numbers through external recruitment (Eq 5.4: first term) based on a dynamic recruitment rate (g_j) ($\text{ind}\cdot\text{m}^{-2}\cdot\text{min}^{-1}$). *Lanice conchilega* recruitment was delineated by two Gaussian curves based on cohort analysis of the aggregations at Boulogne (see Alves *et al.*, 2017b for more information). The first simulated recruitment was in spring from day 91 to 120 (*i.e.* April 1st – 30th) and the second was in autumn, from day 274 to 304 (*i.e.* October 1st – 31st) (Fig 2C). Recruitment is density-limited by a logistic curve with distinct carrying capacities for juveniles (k_j) ($\text{ind}\cdot\text{m}^{-2}$) and adults (k_l) ($\text{ind}\cdot\text{m}^{-2}$) (Eq 5.4: first term). Furthermore, the juvenile cohort is diminished through maturation of individuals into

the adult compartment (Eq 5.4: second term), and through mortality modulated by food-availability (Eq 5.4: third term). Juvenile maturation is determined by a static rate (g_t) (proportion·min⁻¹), food availability represented by an assimilation function (Eq 5.4 and 5.6: asm) (µg Chl-*a*·ind⁻¹·min⁻¹), and a threshold value for food limitation (Eq 5.4: Rc) (µg Chl-*a*·ind⁻¹·min⁻¹). The assimilation function scales chl-*a* dynamics between the microorganisms and macrofauna in the system. It is based on an efficiency rate (Eq 5.6: e) (dimensionless) to estimate the total amount of chl-*a* consumed by individual *L. conchilega* from filtrated (Eq 5.6: fA) and grazed food (Eq 5.6: zP). Juvenile mortality (Eq 5.4: third term) is determined by a static mortality rate (Eq 5.4: m_j) (proportion·min⁻¹) and food-availability in a similar manner to maturation (*i.e.* through assimilation and threshold-based food limitation). The fifth equation describes the dynamics for adult *L. conchilega* – *i.e.* dynamics for cohorts within the last 3 months of existence during the *in-situ* survey. Adult *L. conchilega* density grows via food-dependent maturation (Eq 5.5: first term; Eq 5.4: second term). Adult *L. conchilega* is diminished through density-dependent mortality (Eq 5.5: second term) modulated by a static rate (Eq 5.5: m_t) (proportion·min⁻¹), and a parameter that is half of the adult carrying capacity (Eq 5.5: k_m) (ind·m⁻²). The reader is referred to Fig 5.3 for a graphical summary of the model causal structure illustrating all the aforementioned interactions among variables.

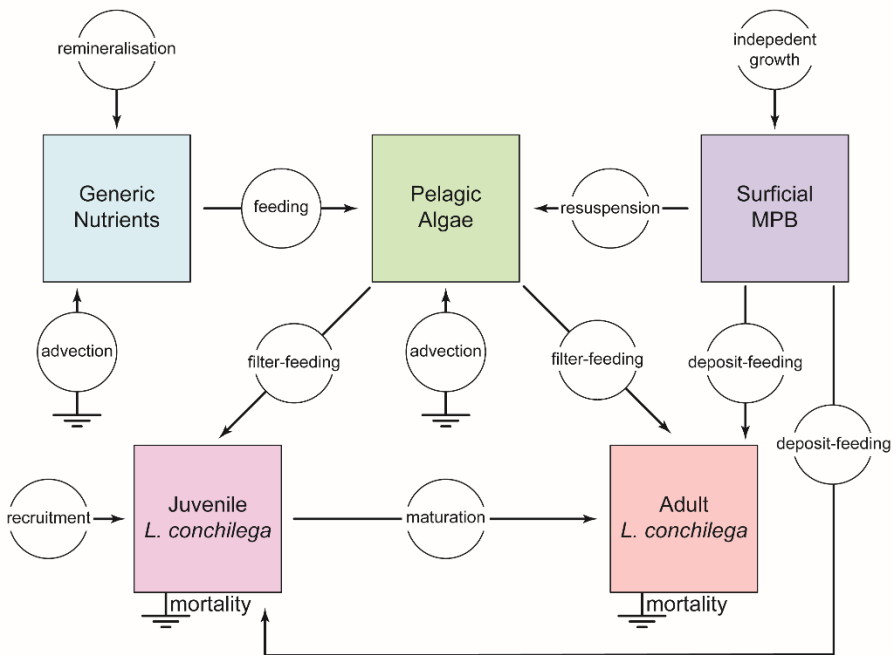


Fig 5.3. Graphical summary of the model causal structure illustrating all relationships among the 5 modelled variables: generic nutrients (light blue box), pelagic algae (green box), surficial microphytobenthos (pale blue box), juvenile *L. conchilega* (pink box), adult *L. conchilega* (red box). Processes are represented in circles, whereas sinks are represented by grounding symbols. Note that advection may act as either a sink or a source of matter within the model.

5.3.3. Parametrisation

Data sampled between 1995 and 1997 from coastal waters off of Boulogne-sur-Mer was adapted from Breton *et al.* (2000) and Hernández-Fariñas *et al.* (2014) to estimate parameters for both generic nutrient and pelagic algae compartments (Table 5.1). It should be noted that the variable named generic nutrients was added to modulate pelagic algae behaviour and should not be interpreted as an ecologically relevant variable, comprising instead a mathematical tool. Future work should focus on replacing this variable by ecologically relevant factors influencing pelagic algal growth – *e.g.* available nitrogen/phosphorus (Hernández-Fariñas *et al.*, 2014). Simulated generic nutrient remineralisation is a dynamic parameter (Fig 5.2A), following a seasonal cycle according to Breton *et al.* (2000) and Hernández-Fariñas

et al. (2014). Remineralisation (r_n) peaks between days 60 and 151 (*i.e.* March 1st – May 31st), and again between days 152 and 243 (*i.e.* June 1st – August 31st) (Breton *et al.*, 2000). Peak values were adapted from observations by Breton *et al.* (2000) of maximum ($14.55\mu\text{g chl-a}\cdot\text{L}^{-1}\cdot\text{min}^{-1}$) and average ($3.72\mu\text{g chl-a}\cdot\text{L}^{-1}\cdot\text{min}^{-1}$) chl-a concentration for near-bottom waters off the Boulogne coast respectively (Table 5.1). A fixed rate of $0.8872\mu\text{g chl-a}\cdot\text{L}^{-1}\cdot\text{min}^{-1}$ (minimum observed by Breton *et al.*, 2000) was used for the rest of the simulated year. The average increase rate for chl-a concentration during spring and summer blooms observed by Breton *et al.* (2000) was employed as the algal growth rate parameter (g_a) (Table 5.1). The limitation rate to algal growth (r_a) was calculated as ratio between average chl-a concentration (Breton *et al.*, 2000) and average phytoplankton abundance (Hernández-Fariñas *et al.*, 2014) (Table 5.1). The advection rate (adv) ($\text{proportion}\cdot\text{min}^{-1}$) was set to zero for the reference scenario because a stagnant water column is known to result in concentration gradients across space due to filtration pressure (Denis *et al.*, 2007).

Parameters for the MPB compartment were estimated based on *in-situ* measurements of surficial chl-a concentration (Alves *et al.*, 2017b). Microphytobenthos growth rate (g_p) consisted of a dynamic rate, peaking during summer (*i.e.* days 152-242, that is June 1st - August 30th) with a maximum of $6.51\cdot 10^{-5}\cdot\text{min}^{-1}$, while a rate of $4.18\cdot 10^{-6}\cdot\text{min}^{-1}$ was fixed for the rest of the simulated year (Fig 5.2B). These peaks were calculated as the maximum and minimum inter-month change rate respectively from the *in-situ* monitoring data (Table 5.1). Sediment surface capacity for MPB biomass (S_{max}) was fixed at the maximum chl-a concentration observed at the sediment surface during *in-situ* monitoring (Table 5.1). The resuspension rate (r_p) was adapted from Denis *et al.* (2007), and constitutes the average rate of change in pelagic chl-a concentration within a flume chamber containing bare, clean and sieved sediment from Boulogne (Table 5.1). Water column height (h) was defined as the height between the sediment surface and the water surface during high water spring tide (HWST) in Boulogne. It constitutes a difference between study site height relative to Earth (assessed using localisation data collected during the *in-situ* survey) and tidal gauge data of sea level height at HWST (Service Hydrographique et Océanographique de la Marine - SHOM, 2015) (Table 5.1).

The adult and juvenile compartments shared 4 parameters (hereafter referred to as “*L. conchilega* global parameters”): assimilation efficiency (e) (dimensionless),

filtration rate (f) ($L \cdot \text{ind}^{-1} \cdot \text{min}^{-1}$), grazing rate (z) ($\text{m}^2 \cdot \text{ind}^{-1} \cdot \text{min}^{-1}$), and threshold for food limitation (R_c). The assimilation efficiency coefficient (e) was adapted from the average assimilation observed by Ropert and Gouletquer (2000) for *L. conchilega* (Table 5.1). A fixed filtration rate (f) was employed during this exercise. It was calculated for water currents between 0.0 and $0.5 \text{m} \cdot \text{s}^{-1}$ (Table 5.1) which are predominant in Boulogne (Jouanneau *et al.*, 2013) using the relationship derived by Denis *et al.* (2007) (Eq 5.7), where “ v ” stands for flow velocity:

$$\text{Eq 5.7. } \textit{clearance rate} = -0.0007v^2 + 0.0221v + 0.0125$$

No estimations for *L. conchilega* grazing rate (z) were found in available scientific literature during model development, thus, the grazing rate was set equal to the filtration rate, assuming equal importance between the two feeding modes (Table 5.1). The threshold for food limitation of *L. conchilega* growth (R_c) was calculated as a ratio between the average surficial chl-*a* concentration sampled during winter in Boulogne (*i.e.* November-February) and the average tube density estimated *in-situ* during the same period (Alves *et al.*, 2017b) (Table 5.1). This period was selected because previous studies suggest that at this time, populations may be limited by food scarcity (*e.g.* Alves *et al.*, 2017b; Buhr, 1976). Juvenile *L. conchilega* growth rate (g_j) was adjusted to produce a spring recruitment of approx. 30 000 individuals (Table 5.1) and an autumn recruitment of approx. 5 000 individuals as observed by Alves *et al.* (2017b) in Boulogne-sur-mer. The simulated spring recruitment occurred between days 91 and 120 (*i.e.* April 1st – 30th), whereas the autumn recruitment lasted from day 274 to 304 (*i.e.* October 1st – 31st) (Alves *et al.*, 2017b). The *in-situ* survey data enabled the estimation of the rate of change for juvenile density over time, but it did not allowed us to assess how this rate is partitioned between maturation (g_l) and natural mortality (m_j). As such, the two aforementioned rates were assumed to contribute equally to the overall rate of change in juvenile density, and each was calculated as one half of it (Table 5.1) (see Alves *et al.*, 2017b for further information on the cohort analysis results). Lastly, the adult mortality rate (m_l) was an average of the rate of decrease in adult density (Table 5.1) (see Alves *et al.*, 2017b for further information on the cohort analysis results). Lastly, all variables and parameters were scaled to minutes, and are summarised in table 5.1 alongside their respective calculation methods.

5.3.4. Model assumptions

The first assumption was that adult *L. conchilega* mortality is density dependant, wherein higher densities result in less mortality. Previous research indicates that a density gradient develops from the centre to the edges of aggregations between approx. 3 500 and 16 000 ind.m⁻² (Alves *et al.*, 2017a), but the nature of the relationship between density and mortality is unknown and could only be hypothesized. We hypothesized that density negatively affects mortality through its positive relationship with flow amelioration, reducing hydrodynamic stress to individuals inside aggregations (see Borsje *et al.*, 2014; Friedrichs *et al.*, 2000). Nevertheless, empirical testing of this part of the causal structure could not be performed due to time constrains. The second assumption was that *L. conchilega* employs both feeding modes all the time and at equal rates because tidal dynamics could not be included in the model which would limit feeding through time, and information on their individual importance and drivers of mode switching was unknown during model development. In third place, we assume that grazing is not affected by tube density in contrast to previous research (Buhr, 1976) because estimates of the effect of density on grazing were not available during model development. The fourth assumption is that filtration rates are static, that is, it is the same for adults and juveniles (*sensu* Buhr, 1976), and it does not vary with either particle size (*sensu* Ropert and Gouletquer, 2000) or current speed (Denis *et al.*, 2007) as suggested by previous research. These mechanics were not included because Boulogne-specific information on those factors was not sampled during *in-situ* surveys and was not available in literature during model development. The fifth assumption is that settlement is homogeneous within a 1m² space, contrasting with previous observations for the population at Boulogne (Alves *et al.*, 2017a). This assumption is a limitation imposed by the spatial resolution of the model of 1m². In sixth place, we assume a static resuspension rate although previous research indicates that it should vary with tube density (e.g. Carey, 1983; Eckman *et al.*, 1981; Friedrichs *et al.*, 2000; Luckenbach, 1986), biofilm conditions (e.g. Lubarsky *et al.*, 2010; Passarelli *et al.*, 2012), and current speed (Denis *et al.*, 2007). This was so because detailed information was unavailable on the relationship between resuspension and the first two factors to model the dynamics at the time of model development. Additionally, since the model does not predict current speeds and time constrains did not allow the coupling of this model to algorithms predicting current

speed, this factor also remains unaccounted for. Lastly, *L. conchilega* mortality varies with food availability and tube density, excluding further causes for animal removal such as predation (e.g. De Smet *et al.*, 2013; Petersen and Exo, 1999), wave force (e.g. Heuers *et al.*, 1998; Ropert and Dauvin, 2000), and/or natural disasters (e.g. Alves *et al.*, 2017b; Strasser and Pieloth, 2001). These factors were implicitly accounted for by assessing removal from *in-situ* data, but further discrimination was not possible due to restricted time for experiments.

5.3.5. Sensitivity analyses

A numerical approach was taken wherein the model was executed under various initial conditions, assuming a stagnant water column (*i.e.* $adv = 0$). Stagnant conditions were selected because previous research indicated that these conditions are more likely to originate food concentration gradients through local column depletion (Denis *et al.*, 2007), enabling comparison. Several parameters were stressed, namely advection (adv), algae growth rate (g_a), filtration rate (f), grazing rate (z), and assimilation efficiency (e). The stress tests were executed on the complete model and repeated on a version of the model without food-dependant maturation (*i.e.* replacing equations 5.4 and 5.5 by 5.8 and 5.9, hereafter referred to as the reduced model). The model could not be stressed with active flow conditions due to time constraints. However, a preliminary stress test of the advection parameter was executed. Outputs for the executed analyses are presented and compared as preliminary results in the next section.

$$\text{Eq 5.8. } \frac{dJ}{dt} = +g_j \left(1 - \frac{J}{k_j} - \frac{L}{k_l}\right) - g_l J - m_j J$$

$$\text{Eq 5.9. } \frac{dL}{dt} = +g_l J - m_l \frac{k_m}{(k_m + L)} L$$

Table 5.1.1. Summary of model variables, parameters, and functions.

Variable	Unit	Description	Parameter Value	Source
N	µg chl-a/L	nutrient biomass		
A	µg chl- a /L	algae biomass		
P	µg chl- a /m ²	microphytobenthos biomass		
J	ind/m ²	juvenile <i>Lanice conchilega</i> biomass		
L	ind/m ²	adult <i>Lanice conchilega</i> biomass		
Parameters	Unit	Description	Parameter Value	Source
h	m	water column height including reef below it	2.16	Estimated from a digital elevation model from Oct 2014 (Chapter 4).
adv	/min	rate of biomass loss/gain from current advection	0.0	Set to zero for reference scenario.
r _n	µg chl- a /L/min	remineralization parameter	3.72-14.55	Average and maximum observed chl-a concentrations for near-bottom coastal waters (Breton <i>et al.</i> , 2000).
g _a	/min	production rate of algae	0.00000894	Average change rate for algal blooms from Breton <i>et al.</i> (2000).
r _a	µg chl- a /L	nutrient limitation threshold	0.0001	Minimum µg chl- a at coastal waters (Breton <i>et al.</i> , 2000) divided by average cell/L (Hernández-Fariñas <i>et al.</i> , 2014) (1995-1997).

f	L/ind/min	filtration rate for <i>Lanice conchilega</i>	0.000766	Denis <i>et al.</i> (2007).
g_p	/min	production rate of microphytobenthos	0.000004-0.000065	Change rates for surficial chl-a calculated from sediment samples.
S_{max}	$\mu\text{g chl-} a /\text{m}^2$	average microphytobenthos biomass at sediment surface	22.983	Max. chl-a content observed during the field survey.
r_p	/min	resuspension rate	0.000117	Denis <i>et al.</i> (2007) (chl-a change rate from control samples, <i>i.e.</i> no <i>L. conchilega</i>).
z	$\text{m}^2/\text{ind}/\text{min}$	grazing rate of <i>Lanice conchilega</i>	0.000766	Unavailable, set equal to filtration.
g_j	$\text{ind}/\text{m}^2/\text{min}$	recruitment of juvenile <i>Lanice conchilega</i> from outside sources	0.116-0.694	Estimated from density increases of cohort 3 and 4 (Alves <i>et al.</i> , 2017b).
k_j	ind/m^2	carrying capacity for juvenile <i>Lanice conchilega</i>	56853	Max. density during the first 3 months per cohort (when available) (Alves <i>et al.</i> , 2017b).
m_j	/min	maximum mortality rate of juvenile <i>Lanice conchilega</i>	0.0000025	Half of the average density decay rate for cohorts within the first 3 months of recruitment (when available) (Alves <i>et al.</i> , 2017b).
asm	$\mu\text{g chl-} a /\text{ind}/\text{min}$	amount of chl-a assimilated per individual per minute	-	Estimated during integration.

e	dimensionless	assimilation efficiency, mass turnover (max=1)	0.17-0.73	Range observed by Ropert and Gouletquer, 2000.
Rc	$\mu\text{g chl-}a$ /ind/min	threshold of food for limitation	0.000000002	Average chl- <i>a</i> concentration during winter (i.e. Nov-Feb) divided by average density during the same period (Alves <i>et al.</i> , 2017b).
gI	/min	maturation rate of juvenile <i>Lanice conchilega</i> (i.e. growth of adult pool)	0.00000025	Half of the average density decay rate for cohorts within the first 3 months of recruitment (when available) (Alves <i>et al.</i> , 2017b).
k _i	ind/m ²	carrying capacity for adult <i>Lanice conchilega</i>	12870	Max. density during the last 3 months per cohort (when available) (Alves <i>et al.</i> , 2017b).
k _m	ind/m ²	half of k _i , parameter for modulation of density-dependence on mortality	0.5 · k _i	Assessed from carrying capacity.
m _i	/min	maximum mortality rate of adult <i>Lanice conchilega</i>	0.00000069	Average density decay rate for the last 3 months per cohort (when available) (Alves <i>et al.</i> , 2017b).

5.4. Preliminary results and discussion

5.4.1. Findings from the sensitivity analyses

Analyses revealed that the model remains in one state under realistic parametrisation and stagnant water conditions (*i.e.* $adv = 0$) regardless of the initial chl-*a* concentration (*e.g.* Fig 5.4A and B). This state (hereafter referred to as “the reference scenario”) was characterised by a chl-*a* depletion in both the water column and surficial sediment. Juvenile density (*e.g.* Fig 5.4C) was unaffected by fluctuations in the initial conditions, while adult *L. conchilega* density was always severely underestimated (*i.e.* simulations predicted densities below 1 adult ind- m^{-2} , whereas our *in-situ* observations show approx. 500 adult ind- m^{-2}) (*e.g.* Fig 5.4D). Total *L. conchilega* density dynamics was mainly dictated by juvenile density dynamics (*e.g.* Fig 5.4C-E). Severe underestimation of adult density likely occurred due to an assimilation cap (*e.g.* Fig 5.5A), forming as a function of food availability. Unsurprisingly, excluding food dependency from the maturation term results in its linear increase dictated by the adult growth rate (Fig 5.5B). In this scenario adult densities increase to approx. adult carrying capacity (*i.e.* 6 665 ind- m^2). However simulated total density dynamics was similar between models running with and without assimilation-dependent maturation (Fig 5.6). Furthermore, both aforementioned simulated total density curves were similar to *in-situ* density counts. However, the rate of density decline between May and July was underestimated in simulations, which could have contributed to the difference in average density between simulations and *in-situ* data from May onwards (Fig 5.6). This indicates that food availability and assimilation may not significantly impact the shape of the yearly population cycle and/or the model likely underestimates or misses a mechanism for animal removal.

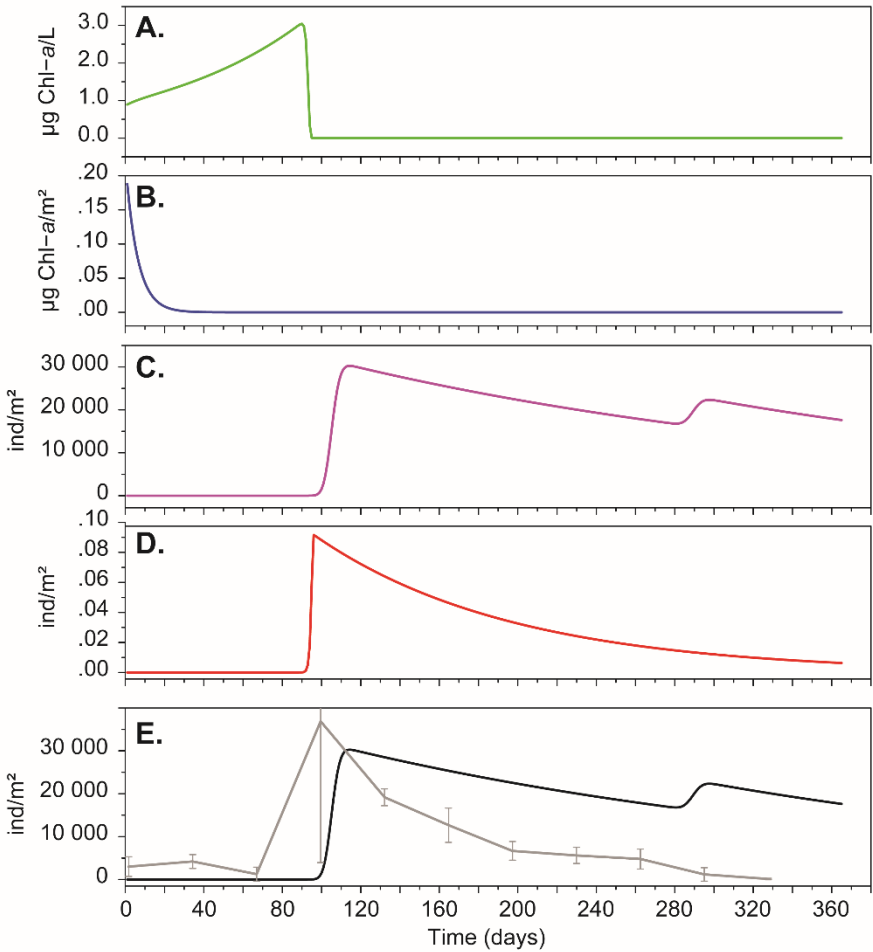


Fig 5.4. Reference scenario of the PBM simulation with advection turned off and predation turned on. In this scenario, chl-a is depleted from both the water column (A) and sediment surface (B), adult density is severely underestimated (D), and total density dynamics (E) is mostly dictated by juvenile density fluctuations (C). Densities assessed *in-situ* during monitoring are juxtaposed for reference in gray (E).

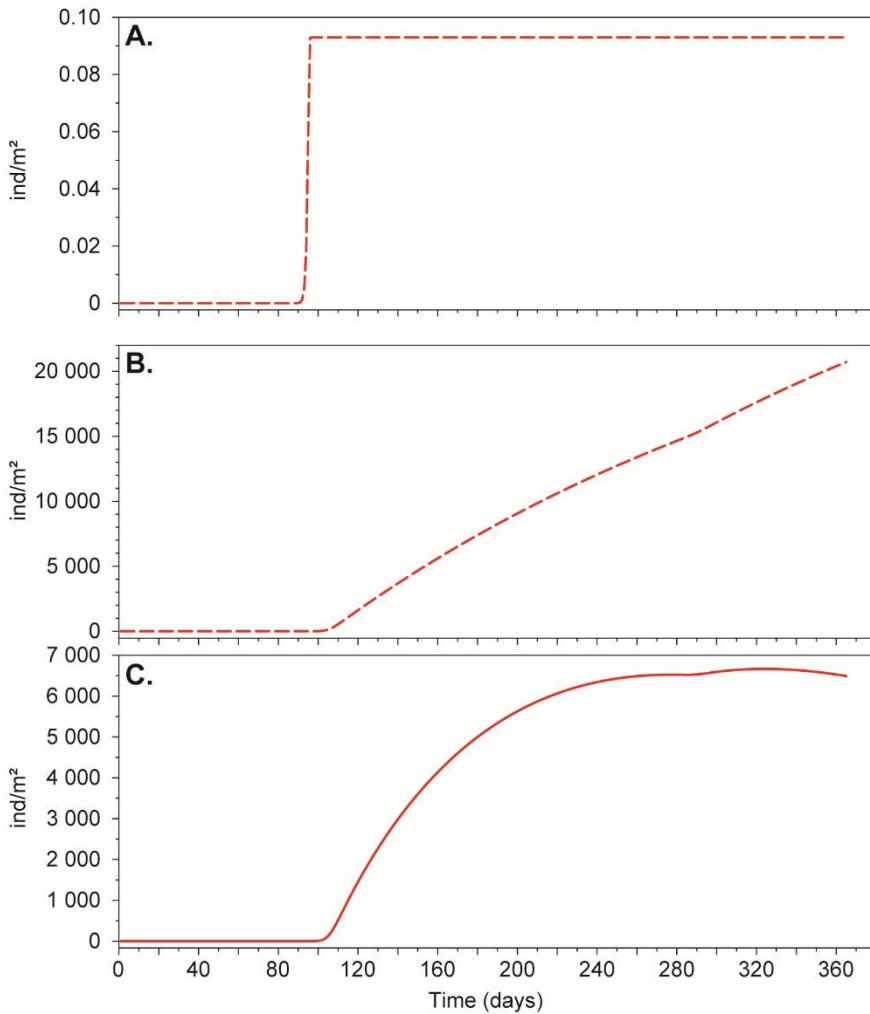


Fig 5.5. Food assimilation significantly impacted adult density dynamics, scaling down and limiting maturation in the complete model (A). Its absence results in a linearly increasing maturation term (B), and higher adult density in the reduced model (C).

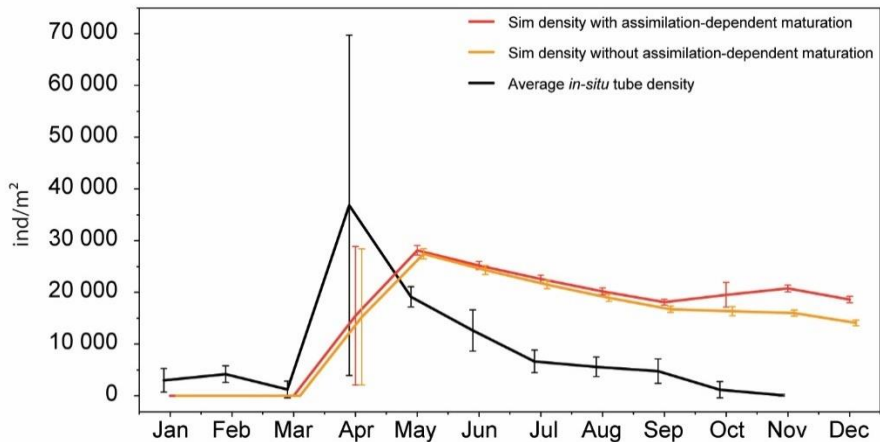


Fig 5.6. Comparison amongst the temporal evolution of the average *in-situ* tube density (black) and simulated total density including assimilation-dependent maturation (red) and excluding assimilation-dependent maturation (orange). Simulation data underestimate the animal removal rate between May and July, indicating that additional mechanisms likely affect population dynamics that were not accounted for.

Stress tests executed on the pelagic algae growth rate (g_a) using the complete model (*i.e.* Eq 5.1-5.6) revealed three conditional responses of the algae compartment. The first occurred with $g_a = 0$ and was characterised by a slight initial increase in chl-*a* concentration – likely due to MPB resuspension – and depletion upon the first *L. conchilega* recruitment (Fig 5.7A). The second occurred for several values of g_a between 0 and .0047 and was characterized by a single chl-*a* concentration peak immediately before the first *L. conchilega* recruitment (*e.g.* Fig 5.7B). It constituted a bug in the model wherein pelagic algae consumed non-existent nutrients, driving generic nutrient concentration to negative values (*e.g.* cyan details in Fig 5.7B). The cause of the bug has not yet been identified and further exploration of the system is required to clarify its source. Nevertheless, a third response scenario was identified for all other values of g_a . It was characterized by a gradual increase in pelagic chl-*a* concentration followed by depletion at the beginning of the spring *L. conchilega* recruitment (*e.g.* Fig 5.7C). Furthermore, fluctuations in the pelagic algae growth rate using the complete model visibly affected maximum adult *L. conchilega* density (*e.g.* red details on Fig 5.7), but it did not visibly affect the juvenile compartment nor total density fluctuations (responses not shown).

Stressing the same parameters in the reduced model (*i.e.* excl. assimilation-dependent maturation) revealed similar results to the tests performed with the complete model. Three response scenarios were found for the pelagic algae compartment when stressing its growth rate (g_a). Similarly to the complete model stress tests results, the first response occurred for $g_a = 0$ in which case chl-*a* concentration rose initially due to resuspension followed by depletion upon *L. conchilega* recruitment (Fig 5.8A). The second response constituted a similar bug to the previously found in the complete model, also occurring for several values of g_a between 0 and .0047 (*e.g.* Fig 5.8B). It was characterized by a single peak of pelagic chl-*a*, which drove the nutrient compartment to negative concentrations (*e.g.* Fig 5.8B) with unknown cause. Values of g_a which did not result in a bug presented the third response instead. The third response was characterized by increasing chl-*a* concentration peaking at approx. 150 000 $\mu\text{g chl-}a\cdot\text{L}^{-1}$ just prior to the first *L. conchilega* recruitment, at which time chl-*a* was depleted from the water column by recruiting juveniles (*e.g.* Fig 5.8C). Furthermore, fluctuations in the pelagic chl-*a* growth rate using the reduced model did not impact *L. conchilega* density dynamics (*e.g.* adults shown in red details of Fig 5.8, juveniles not shown).

Fluctuations on the filtration rate (f : $\text{L}\cdot\text{ind}^{-1}\cdot\text{min}^{-1}$) noticeably impacted average adult *L. conchilega* density and average pelagic algae concentration. Higher rates resulted in lower adult density as well as chl-*a* concentration in the water column (Fig 5.9). The reduction was sharper for $f > .50 \text{ L}\cdot\text{ind}^{-1}\cdot\text{min}^{-1}$ (Fig 5.9) and was likely due to a combination of depleted MPB and quicker water column depletion leading to higher juvenile mortality and lower maturation. Results from the stress test executed on the reduced model revealed a similar trend with both average chl-*a* concentration and adult density declining with increasing filtration rates (Fig 5.10). However, the effect on average chl-*a* concentration in the water column and average adult *L. conchilega* density differed from the aforementioned scenario, being less intense on chl-*a* concentration and more intense on adult density for $f > .50 \text{ L}\cdot\text{ind}^{-1}\cdot\text{min}^{-1}$ (Fig 5.10).

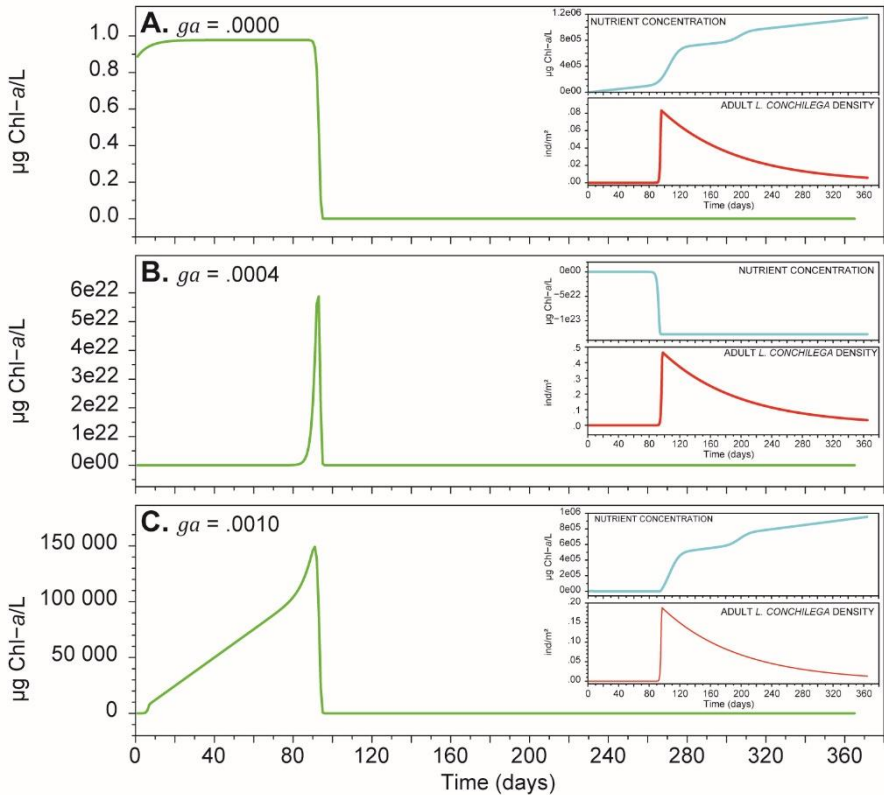


Fig 5.7. Behaviours displayed by the algae compartment during stress test of its growth rate (g_a). The first response (A) occurs when $g_a = 0$, with an initial rise in chl-a concentration due to resuspension, followed by depletion upon the spring *L. conchilega* recruitment. The second response (B) constitutes a bug that may occur when $0 < g_a < .0047$ (i.e. 700% growth per day), at which case the pelagic algae compartment, fuelled by non-existent nutrients (cyan detail) increases past the observed minimum concentration of $2 \times 10^{11} \mu\text{g chl-a-L}^{-1}$ before being depleted by recruiting *L. conchilega* juveniles. This bug occurs for the majority of values between 0 and .001 with few exceptions in which the algae compartment behaves similarly to the third and last response scenario. The third response (C) occurs when $g_a \geq .001$, wherein the pelagic algae compartment gradually grows starting on day 10 to peak at approx. $150\,000 \mu\text{g chl-a-L}^{-1}$ just prior to recruitment and algal depletion by *L. conchilega* juveniles at day 90-100.

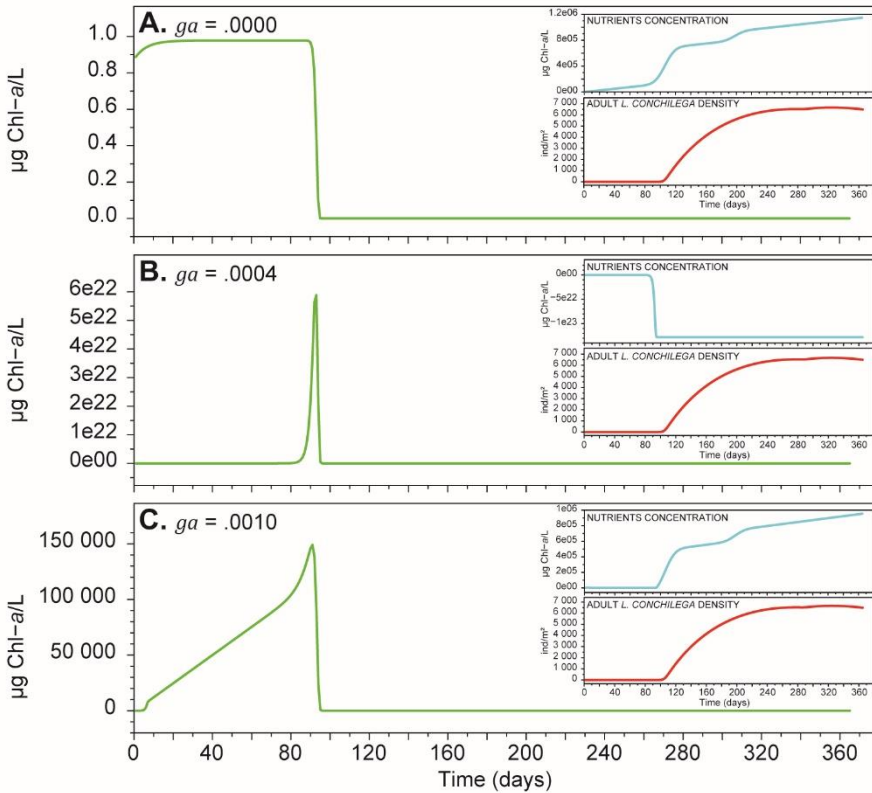


Fig 5.8. Behaviours displayed by the algae compartment during stress test of its growth rate (g_a) using the reduced model. The first response (A) occurs when $g_a = 0$, resulting in slight initial increase of chl-a concentration due to resuspension and subsequent depletion upon the first *L. conchilega* recruitment. Similarly to the stress test results using the complete model, the second response (B) comprises a bug that occurs for values of g_a between 0 and .0047 (*i.e.* approx. 700% growth per day). In this case pelagic algae increases to past the minimum observed concentration of approx. $2 \cdot 10^{11} \mu\text{g chl-a-L}^{-1}$ fuelled by non-existent nutrients (cyan detail) until depletion by spring *L. conchilega* recruits. The cause for the bug is unknown and displays several exceptions for which the algae compartment displays the third response scenario. The third response (C) occurs for all other values of g_a and results in an gradual increase in the pelagic algae compartment until its peak at approx. $150\,000 \mu\text{g chl-a-L}^{-1}$ just prior to the spring *L. conchilega* recruitment, at which time pelagic algal depletion occurs.

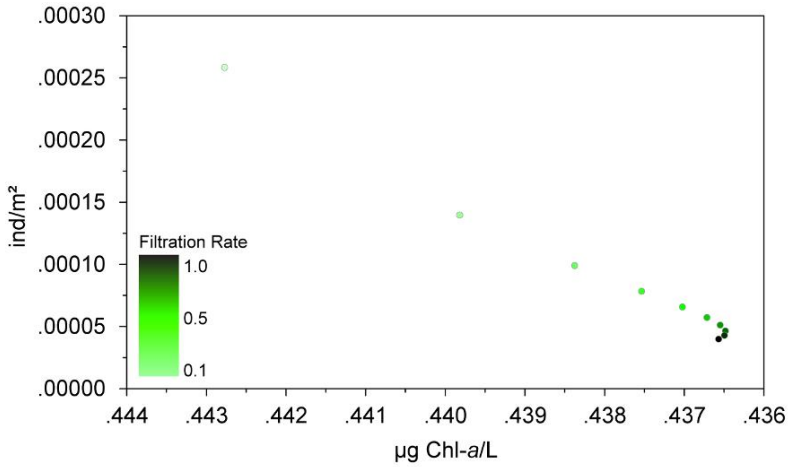


Fig 5.9. Effect of fluctuations in the filtration rate in the complete model on average adult density (ind/m²) and average pelagic algae concentration (µg Chl-a/L). Increasing filtration rates result in nonlinear decreases in both average adult *L. conchilega* density and average pelagic algae concentration. Note that the x axis is inverted to match filtration rates order.

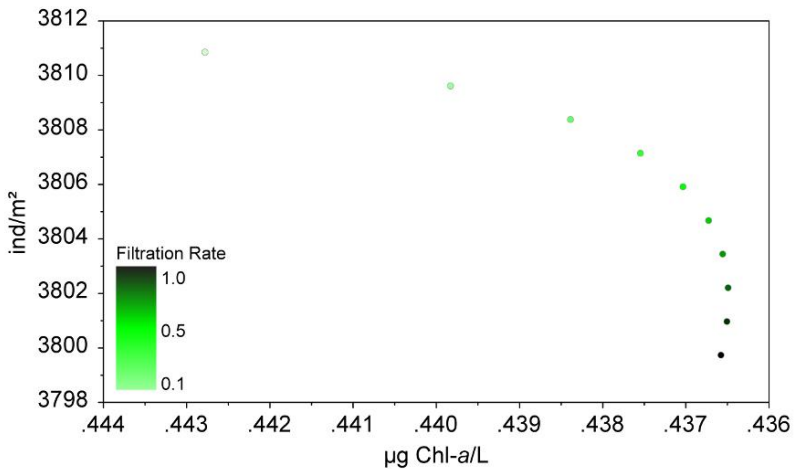


Fig 5.10. Effect of fluctuations in the filtration rate in the reduced model on average adult density (ind/m²) and average pelagic algae concentration (µg Chl-a/L). Increasing filtration rate results in a decline of both average adult *L. conchilega* density and chl-a concentration in the water column in a nonlinear fashion. The effect intensifies with higher filtration rates. Note that the x axis is inverted to match filtration rates order.

The microphytobenthos compartment was depleted during stress tests of the grazing rate (z) ($\text{m}^2\cdot\text{ind}^{-1}\cdot\text{min}^{-1}$) (data not shown) with all tested values including $z = 0$, indicating that MPB depletion is caused by its other sink, the resuspension term. Thus, we stressed the resuspension rate (r_p) ($\text{proportion}\cdot\text{min}^{-1}$) to find a depletion threshold r_p value prior to further stress of the grazing rate. Fluctuation in the resuspension rate (r_p) noticeably affected MPB concentration alone, resulting in four response scenarios: $0 \leq r_p < .0000042$, $r_p = .0000042$, $.0000042 < r_p \leq .000130$, and $r_p > .000130$. Microphytobenthos concentration was depleted during spring recruitment in all response scenarios (Fig 5.11) and responses differed on MPB concentration trends prior to that period. The first response was characterised by increasing MPB concentration until the spring *L. conchilega* recruitment, at which point, MPB is depleted by recruiting juveniles (e.g. Fig 5.11A). MPB concentration remains stable with $r_p = .0000042$ (Fig 5.11B), and declines past this value until the spring recruitment at which time recruiting juveniles deplete the MPB compartment (e.g. Fig 5.11C). The fourth and last response was characterised by MPB depletion prior to the spring recruitment due to resuspension (e.g. Fig 5.11D). Stress test of the resuspension rate using the reduced model resulted in the same response scenarios (results not shown). Further stress tests of the grazing rate (z) were executed using $r_p = .000042$.

Stressing the grazing rate resulted in three response scenarios in which fluctuations of the rate noticeably affected average MPB concentration and adult *L. conchilega* average density. The first response scenario occurred with $z = 0$, and was characterized by MPB remaining in its initial concentration (i.e. $.20 \mu\text{g chl-a}\cdot\text{m}^{-2}$) until day 175, at which time MPB concentration starts to rise sharply due to the seasonal increase in its growth rate, reaching $2.33 \mu\text{g chl-a}\cdot\text{m}^{-2}$ on day 230 and stabilising at that concentration (Fig 5.12A). The second response occurred for $z = 10^{-9}$ and was characterized by an initially stable MPB concentration of $.20 \mu\text{g chl-a}\cdot\text{m}^{-2}$ until the spring *L. conchilega* recruitment (Fig 5.12B). During recruitment surficial MPB concentration declines reaching $.011 \mu\text{g chl-a}\cdot\text{m}^{-2}$ at day 183 due to grazing pressure from recruited juveniles (Fig 5.12B), and subsequently rises due to a seasonal increase in its growth rate, reaching a peak of $.03 \mu\text{g chl-a}\cdot\text{m}^{-2}$ at day 214 (Fig 5.12B). This peak is followed by a decline once MPB growth rate returns to its base

value (i.e. $.00000418 \cdot \text{min}^{-1}$) to near depletion at day 365 (Fig 5.12B). The third scenario occurred for $z > 10^{-9}$ and was characterized by a stable MPB concentration of $.20 \mu\text{g chl-a} \cdot \text{m}^{-2}$ until the spring *L. conchilega* recruitment, at which time, MPB starts to decline until depletion due to grazing pressure from recruiting individuals (e.g. Fig 5.12C). Furthermore, changes in the grazing rate affected adult *L. conchilega* density dynamics (red details in Fig 5.12) as well as MPB concentration with both average density and average concentration declining as grazing rate increases (Fig 5.13). Lastly, the same response scenarios were observed during the stress test using the reduced model, albeit fluctuations in the grazing rate only marginally affected adult *L. conchilega* density (Fig 5.14).

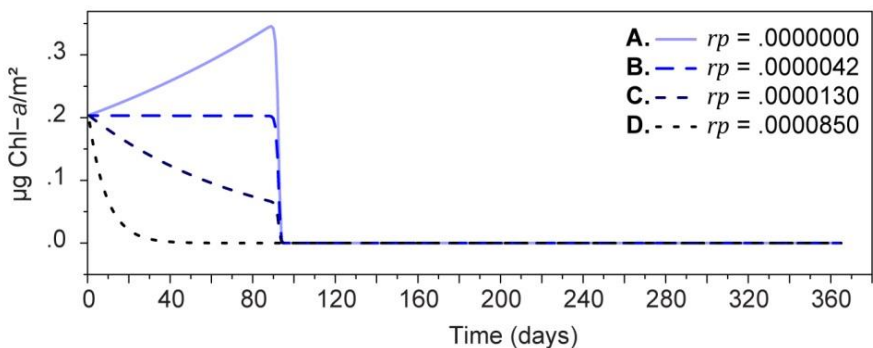


Fig 5.11. Fluctuations on the resuspension rate noticeably affected MPB concentration only. Four response scenarios were observed during the stress test of the resuspension rate. The first response occurred for $0 \leq r_p < .0000042$, wherein MPB concentration increased gradually until the spring *L. conchilega* recruitment, at which time MPB was depleted due to grazing pressure (A). The second response scenario transpires for $r_p = .0000042$, in which case, MPB concentration remains unchanged until *L. conchilega* recruits increase grazing pressure, leading to MPB depletion (B). Resuspensions rates between $.0000042$ and $.0000130$ result in declining MPB concentration without causing depletion prior to *L. conchilega* recruitment (C), whereas resuspension rates higher than $.0000130$ cause MPB depletion prior to *L. conchilega* recruitment (D).

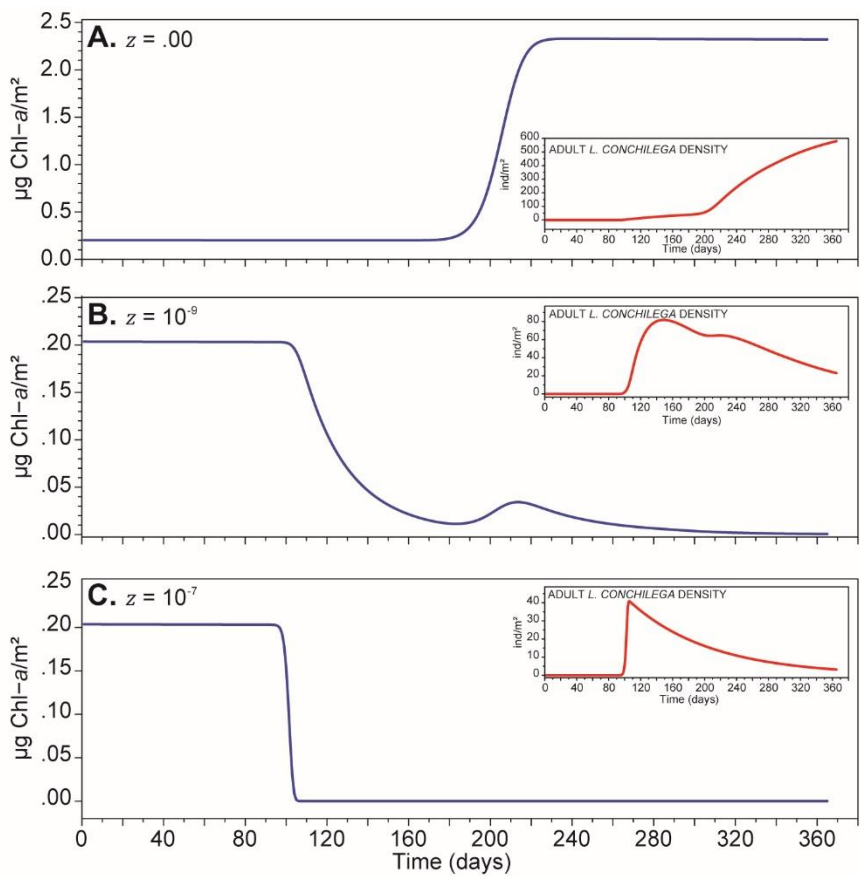


Fig 5.12. Response scenarios observed during the stress tests of the grazing rate (z). In the absence of grazing pressure, MPB remains in its initial concentration and rises during its seasonal growth peak (A). When grazing pressure is employed, MPB concentration declines from the spring recruitment onwards, being slightly replenished by its seasonal growth peak for $z = 10^{-9}$ (B), but being depleted for higher values of z (e.g. C).

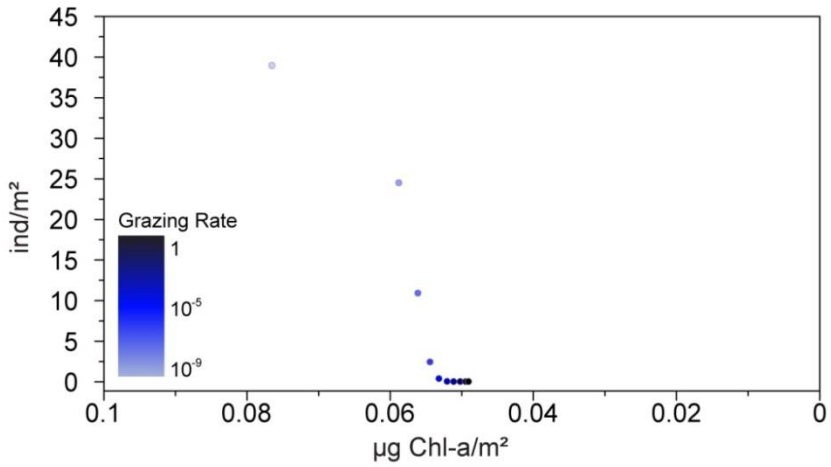


Fig 5.13. Varying the grazing rate (z) noticeably affected MPB concentration ($\mu\text{g Chl-}a/\text{m}^2$) and adult *L. conchilega* density (ind/m^2). Higher grazing rates resulted in decreases in average MPB concentration and average adult density. Furthermore, the effect weakens with increasing grazing rate. Note that the x axis is inverted to match grazing rate stress.

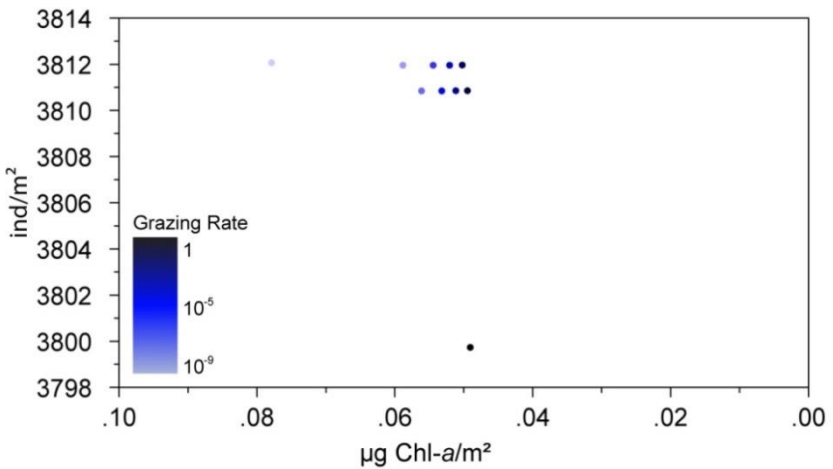


Fig 5.14. Fluctuating the grazing rate (z) in the reduced model noticeably affected MPB concentration ($\mu\text{g Chl-}a/\text{m}^2$) but only had a marginal effect on adult *L. conchilega* density (ind/m^2). Note that the x axis is inverted to match grazing rate stress.

Fluctuations in current advection impacted generic nutrient and pelagic algae concentration in the water column (Fig 5.15A). Unsurprisingly, both average concentrations declined exponentially with higher advection loss while microphytobenthos mean concentration remained unaffected (Fig 5.15A). Juvenile and adult average densities on the benthic-boundary layer were also impacted by fluctuations in advection flow (Fig 5.15B). Juvenile density declined linearly with increasing advection loss, whereas adult density declined exponentially with higher advection loss (Fig 5.15B). The effect on *L. conchilega* density is likely due to pelagic algae removal diminishing food availability. Stress test responses using the complete model can be divided according to their effect on algae dynamics: $0 \leq adv \leq .0000093$; and $adv > .0000093$. While $0 \leq adv \leq .0000093$, pelagic algae concentration increases until the *L. conchilega* spring recruitment, at which time it declines due to filtration pressure from recruiting individuals. For $adv > .0000093$, chl-*a* concentration declines exponentially at higher rates with higher advection loss. Stress tests performed with the reduced model revealed similar results to the tests executed on the complete model. The same response scenarios were found, and increases in advection loss caused reductions in generic nutrients and pelagic algae average concentrations while MPB concentration was unaffected (Fig 5.15C). Variation in advection also affected juvenile and adult mean density in the reduced model, causing linear declines in both (Fig 5.15D). The difference in the shape of decline for adult average density is likely resultant from the lack of scaling in the reduced model which was provided by the assimilation function in the complete model. The observed decline in density ranged between 16 and 40 individuals for juvenile *L. conchilega*, which dictate total density dynamics for this system. These results indicate that strong currents may only marginally affect *L. conchilega* population dynamics through modulation of its food supply.

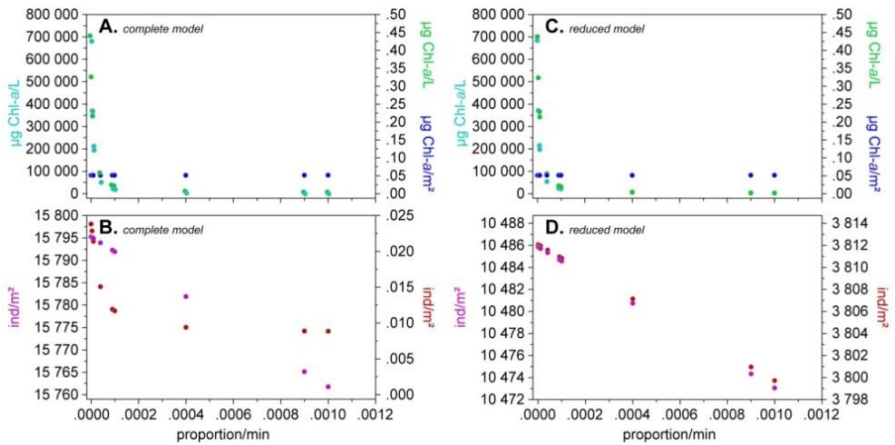


Fig 5.15. Increasing advection loss rates during stress tests noticeably impacted nutrient (cyan) and pelagic algae (green) average concentration in the water column for the complete model (A), while MPB (A, blue) remained unchanged. It indirectly influenced *L. conchilega* density, causing a linear decline in juvenile average density (pink) in the complete model (B) and an exponential decline in average adult density (B, red). Results for the complete model were similar regarding generic nutrient (cyan), pelagic algae (green), and MPB concentration (blue) (C), as well as juvenile average density (D, pink). However, adult average density (red) linearly declined with higher advection loss (D).

5.4.2. Model shortcomings

Modelling ecosystems requires simplifying several processes to evaluate potential causal structures for given scenarios (Shiple, 2000). In the present exercise we explored how different levels of food availability and assimilation can influence *L. conchilega* population dynamics as potential mechanisms for spatial pattern formation. Preliminary findings were presented and discussed regarding their implications for *L. conchilega* population dynamics, but the question remains about the impact of assumptions and simplifications on results. Several assumptions were made regarding *L. conchilega* ecology (see section 5.3.4) highlighting gaps in knowledge requiring further study. The first assumption is that adult mortality is density-dependant. A reformulation of that mechanic to replace it by a fixed mortality rate would influence model outputs by biasing the shape of the curves representing density dynamics towards a more linear response through time. Our second assumption was that *L. conchilega* employs both feeding modes constantly and at

equal rates. Recent research assessing carbon flows in *L. conchilega* aggregations suggest that the two feeding modes may differ in importance. *Lanice conchilega* aggregations seem to mainly depend on external inputs of phytoplankton through filtration, displaying restricted input from microphytobenthos (De Smet *et al.*, 2016b). This information was not available during model development and could not be incorporated due to time constraints. Nevertheless, model outputs would likely be unaffected by different contributions from filtration and grazing because implementing these adjustments would result in lower feeding pressure – *i.e.* the current assumption ensures the maximum amount of feeding pressure on both food sources and adjustment would involve imposing restrictions.

The third assumption is that grazing is unaffected by tube density, that is, high densities do not act as a barrier to the feeding tentacles to reach sediment as hypothesised by Buhr (1976). This assumption refers to triggers of mode switching, which are currently largely unexplored in literature. Buhr (1976) only hypothesised on this mechanic, and to the best of our knowledge there is no data available or study assessing whether this occurs in *L. conchilega* aggregations or how the relationship between tube density and grazing rate/efficiency may be like. As such, we cannot attempt to predict the effect of incorporating this dynamic into the model on its outputs. The fourth assumption revolves around the filtration rate in that it is static and equal between adults and juveniles. Previous research has shown that filtration may vary due to animal size (Buhr, 1976), particle size (Ropert and Gouletquer, 2000), and/or current speed (Denis *et al.*, 2007). In summary, filtration is likely to increase with animal size (Buhr, 1976), and present a bell shape relationship to particle size (Ropert and Gouletquer, 2000) and flow speed (Denis *et al.*, 2007), reflecting the presence of filtration optimum ranges for the latter two. The complexity of integrating all of these relationships hinders us from inferring potential effects on model outcomes. The fifth assumption is that settlement is homogeneous within a 1m² space, a consequence of the spatial resolution of the model. This assumption is expected to restrict future work by limiting the spatial scale at which the model could produce patterns once transposed to a spatial grid. However, the modelling exercise has yet to achieve this phase of development.

The sixth assumption is that the resuspension rate is static, which contrasts with previous research in that it is expected to vary with tube density (*e.g.* Carey, 1983; Eckman *et al.*, 1981; Friedrichs *et al.*, 2000; Luckenbach, 1986) and biofilm

conditions (e.g. Lubarsky et al., 2010; Passarelli et al., 2012). Adjusting the model to account for these dynamics would likely alter the amount of available food from each food source in the model (i.e. pelagic algae in the water column and MPB at sediment surface). However, we are unable to assess the shape and direction that this modification would create in the outputs and/or model behaviour at the present moment due to the presence of complex interactions between the two sources and *L. conchilega*. Our final assumption is that *L. conchilega* mortality depends on feeding dynamics and tube density only, excluding additional causes for mortality such as predation (e.g. De Smet et al., 2013; Petersen and Exo, 1999), physical removal by strong currents (e.g. Heuers et al., 1998; Ropert and Dauvin, 2000), and/or the impact from natural disasters (e.g. Alves et al., 2017; Strasser and Pieloth, 2001). These may impact model outcomes by reducing feeding pressure on food sources at their specific time scales, making it less likely that mortality due to food limitation may occur since fewer individuals would be competing for resources, but increasing stochasticity in model responses.

Our model assumptions highlighted several gaps in knowledge that we attempted to address previously. Nevertheless, further gaps exist that future research of would improve model outputs. Research is necessary to clarify the importance of grazing and filter-feeding for population maintenance, the triggers for mode switching, and conditions enhancing and/or limiting feeding per mode. Gaps regarding the grazing behaviour of *Lanice conchilega* were especially conspicuous during the exercise since no estimation was available of its rate or affecting factors at the time of model development. However, this has been recently addressed by De Smet et al. (2016b) and future work should incorporate this new information. Another assumption is that filter- and deposit-feeding have equal importance. However, recent research suggests that deposit-feeding may play a larger role in population maintenance than filter-feeding (De Smet et al., 2016b). This is another facet of *L. conchilega* feeding ecology that needs to be considered in future work. It is worth noting that a deterministic approach was employed to identify main trends in population dynamics. However, most natural processes and interactions require some level of stochastic behaviour, especially small populations (Gurney and Nisbet, 1998). As such, future work should involve incorporating randomness to the model and evaluate its effect on model outputs, especially on the role of recruitment in population maintenance.

5.5. Preliminary conclusions

The present modelling exercise explored the role of food availability, density-dependent mortality, and recruitment on *L. conchilega* population dynamics as potential mechanisms for spatial pattern formation through ecological modelling. Results suggest that consumer-resource interactions involved in *Lanice conchilega* feeding likely only marginally affect its population dynamics (over its seasonal cycle). However, the mechanisms explored by this exercise revealed several gaps in knowledge regarding *L. conchilega* feeding and recruitment, which require further investigation. To identify whether the hypothesised interactions could lead to spatial heterogeneity within a *L. conchilega* aggregation, the developed model should be evaluated on a spatially-explicit environment. Additionally, further work is necessary to identify equilibrium criteria for the model.

CHAPTER

6

General Discussion

*The present PhD work explored the dynamics of a sessile ecosystem engineer with high conservation value, the reef-building polychaete *Lanice conchilega* (Pallas, 1766) from several innovative perspectives. Previous research has focused on quantifying its autogenic and allogenic ecosystem engineering, and investigating its population dynamics over regional spatial scales. Knowledge gaps on the temporal and spatial dynamics of this tube-building polychaete and how these dynamics influence its ecosystem engineering effects through time and space were addressed in the present work, with the main objective of elucidating the role of population dynamics on engineering effects and the formation and decay of *L. conchilega* aggregations (cf. reef-building). **Section 6.1** addresses the relationship between population dynamics and autogenic ecosystem engineering explored in chapters 2 and 3. **Section 6.2** addresses the small-scale distribution of *L. conchilega* explored in chapter 4 and hypothesises potential mechanisms of spatial pattern formation within that framework. The aforementioned sections also include discussions on alternative mechanisms for spatial pattern formation, such as consumer-resource interactions which were further explored by the work in chapter 5. **Section 6.3** integrates the previous sections to discuss the ramifications of our findings for current conservation efforts and present how our insights can support ecosystem-based approaches to environmental management. Lastly, **section 6.4** summarises main conclusions of this thesis and presents prospects for future research.*

6.1. Habitat modification through autogenic engineering

The autogenic engineering effects of *Lanice conchilega* stem from its tube aggregations as these modulate hydrodynamic flow passing through tube arrays (*sensu* Friedrichs *et al.*, 2000). Similarly to other polychaete aggregations (*e.g.* Eckman *et al.*, 1981; Friedrichs *et al.*, 2000; Luckenbach, 1986), their engineering effect varies with tube density (*i.e.* Fig 1.4 in chapter 1) (Borsje *et al.*, 2014). Polychaete tubes act as barriers to water flow, attenuating its velocity, creating distinct flow conditions within aggregations, and changing sedimentation regimes locally (Friedrichs *et al.*, 2000). Model simulations suggest that the vertical expansion of *L. conchilega* aggregations may be a consequence of a positive feedback between increased sedimentation from autogenic engineering and tube accretion rates triggered by it (Borsje *et al.*, 2014) (*i.e.* Fig 6.1 and 1.5 in chapter 1) (see also chapter 1). Our experimental work (see chapter 2) provides evidence for the predictions made by Borsje *et al.* (2014). Chapter 2 investigated the relationship between *L. conchilega* aggregation properties and small-scale coastal sedimentary properties at the intertidal zone of a sandy beach in Boulogne-sur-Mer (France). Results revealed that (1) net deposition is significantly higher in *L. conchilega* aggregations when compared to bare sand; (2) sediment mixing depth is noticeably shallower inside aggregations than out; (3) net deposition and sediment mixing depth were not affected by tube density for aggregations above 3 200 ind·m⁻²; (4) temporal fluctuations in tube density are noticeably different between the center and edges of aggregations; and (6) sediment deposition from 3cm in column height cause significant increases in tube-building rate, while (7) deposition from 5 to 12cm in column height result in significantly higher *L. conchilega* mortality.

The presence of *L. conchilega* in densities above 3 200 ind·m⁻² significantly affected both net sedimentation and sediment mixing depth locally (*e.g.* Fig 6.1, middle solid arrow leading into sedimentation), in agreement with the findings from previous research (see chapter 1). However, sedimentation/erosion did not differ among aggregations ranging from 3 200 and 16 318 ind·m⁻² during those experiments, suggesting that a nonlinear relationship between density and engineering effect is likely. Additional findings corroborated the existence of a feedback mechanism wherein tube accretion increased under sediment deposition of at least 3cm in height under controlled conditions (*e.g.* Fig 6.1A, left-hand solid arrow leading into protruding height). However, increased mortality was also observed for abrupt

deposition between 5cm and 12cm in height (e.g. Fig 6.1, right-hand solid arrow outside of blue box), hinting at a limitation to vertical expansion speed through mortality. Due to the magnitude of deposition (*i.e.* >3cm in height), alternative sources of sediment deposition other than autogenic engineering are likely triggers to vertical expansion with higher mortality – e.g. storms (see chapter 2), dredge disposal (e.g. De Backer *et al.*, 2014; Katsiaras *et al.*, 2015), and/or beach nourishment (e.g. Colosio *et al.*, 2007; Speybroeck *et al.*, 2006). Nevertheless, our findings hinted at potential mechanisms of aggregation maintenance involving tube accretion triggered by increased deposition from autogenic engineering (e.g. Friedrichs *et al.*, 2000; Passarelli *et al.*, 2012; Rabaut *et al.*, 2009), since treatments with 3cm deposition resulted in significantly higher tube accretion rates than no deposition, while having no significant effect on mortality (see chapter 2). It is worth noting that our study only assessed abrupt deposition, and the effect of gradual sedimentation remains unclear. It can be hypothesised that gradual sedimentation as is observed from autogenic engineering (Friedrichs *et al.*, 2000) may enhance vertical expansion without increasing mortality as predicted by Borsje *et al.* (2013).

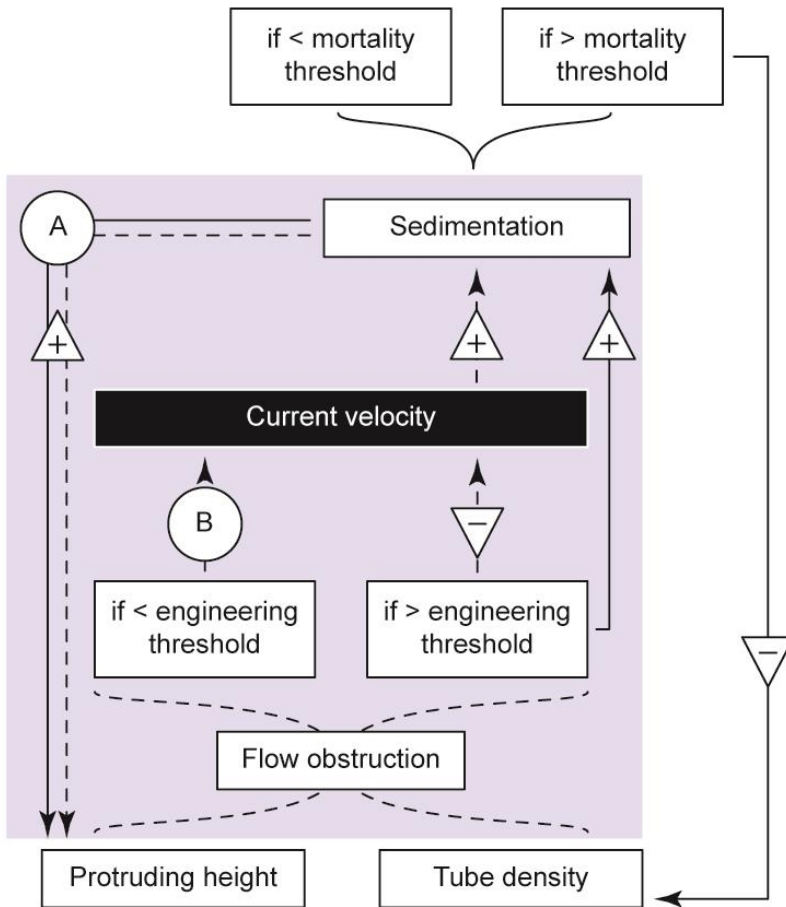


Fig 6.1. Flow chart showing the effects of autogenic engineering and the causal structure hypothesised by Borsje *et al.* (2014) (dashed arrows) for aggregation vertical expansion and findings of current thesis (solid arrows). Triangles pointing upwards with an addition sign represent positive effects, whereas those pointing downwards, encasing a minus sign, represent negative effects. Past certain thresholds, density and protrusion height may negatively affect water current velocity through autogenic engineering, resulting in increased sedimentation (solid arrow: association shown experimentally without assessing current velocity). The latter has a positive impact on protruding height by triggering tube accretion (A). In turn, the latter affects aggregation ability to attenuate flow in a feedback loop. Insignificant engineering effects (B) may be present if density and protrusion height do not surpass the aforementioned engineering thresholds. Additionally, our findings show that abrupt sedimentation equal or above 5cm in column height may trigger significantly higher mortality, negatively affecting tube density (right-hand solid arrow outside of blue box).

Chapter 3 further explored the aforementioned findings and feedbacks by analysing the seasonal dynamics of population density, demographic structure, and ecosystem engineering effects at a larger temporal scale (*i.e.* across seasons). *Lanice conchilega* population dynamics was investigated through *in-situ* monitoring of three intertidal aggregations in a period of 1.5 years (*i.e.* from June 2013 until November 2014) at the sandy beach in Boulogne-sur-mer (Nord-Pas-de-Calais, France) (see chapter 1 for study site details). Furthermore, simultaneous monitoring of additional variables representing local environmental properties for each aggregation enabled the study of the temporal evolution of *L. conchilega* autogenic engineering effects on surficial sediments (*i.e.* 0-1cm layer) and their association to population dynamics. Two distinct recruitment periods per year were identified: one in spring and another in autumn. These periods were marked by steep increases in *L. conchilega* density (see chapter 3) (*e.g.* Fig 6.4, solid arrow from settlement to tube density). The spring recruitment (during April) was characterised by extremely abundant settlement of very small juveniles (*i.e.* approx. 30 000 ind·m⁻² with average inner tube diameter of .67mm). Comparatively, the autumn recruitment (during September-October) was less dense and contained larger juveniles (*i.e.* approx. 4 000 ind·m⁻² with average inner tube diameter of approx. 1.65mm) (see chapter 3). Furthermore, autogenic engineering effects fluctuated in tandem with seasonal population cycles, intensifying during recruitment in comparison to other moments of the year. This is likely due to the steep increases in tube density as recruits establish themselves augmenting the area of flow obstruction per aggregation (*sensu* Eckman *et al.*, 1981). These findings in combination with aforementioned results from chapter 2, suggest that processes pertaining to aggregation maintenance (and perhaps formation and decay) vary seasonally, as aggregation density fluctuates and modulates autogenic engineering as well as vertical expansion.

6.2. Population dynamics and distribution

6.2.1. Interactions with hydrodynamic flow

Population dynamics has the potential to affect the spatial distribution of polychaete aggregations. This is the case with the honeycomb worm *Sabellaria alveolata* (Gruet, 1986). *Sabellaria alveolata* reefs go through several stages of development, growing in size during settlement, but slowly and constantly decaying in the periods in

between as adults die off (Gruet, 1986). Population dynamics may also dictate aggregation formation for *Lanice conchilega*. The mechanisms presented in section 6.1 and density-dependent autogenic engineering effects (Borsje *et al.*, 2014) have a high potential for the latter. That is, fluctuations of density across the landscape can result in gradients of ecosystem engineering effects, influencing aggregation maintenance (see section 6.1). Nevertheless, as a sessile spawner, *L. conchilega* distribution is also likely influenced by larval processes akin to other sessile marine organisms (Bhaud, 2000). For example, adult distribution of corals is associated to settlement success (Baird *et al.*, 2003). Larval settlement can be influenced by a myriad of factors. Local hydrodynamic conditions may sway settlement by facilitating or hindering attachment (Bhaud, 2000). Hydrodynamics, wind conditions, and tidal oscillations influence larval transport, creating spatial gradients of larvae availability and uneven settlement as been observed for the tube builder *Owenia fusiformis* (Thiébaud *et al.*, 1994). Conversely, active substrate selection by larvae may also bias settlement across space, commonly occurring with many polychaete species (*e.g.* red tube worm *Serpula vermicularis*, Chapman *et al.*, 2007; trumpet worm *Lagis koreni*, Olivier *et al.*, 1996; honeycomb worm *Sabellaria alveolata*, Pawlik, 1988). Settlement cues from conspecifics may also influence settlement – *e.g.* blue tube worm *Spirobranchus cariniferus* (Gosselin and Sewell, 2013). Lastly, substrate selection may also enhance settlement at specific locations – *e.g.* *L. koreni* (Olivier *et al.*, 1996).

Lanice conchilega larvae settle preferentially on sandy and muddy marine sediments (Willems *et al.*, 2008). Previous studies on intertidal populations also show that *L. conchilega* larvae have a tendency to settle in locations with previous presence of adult tubes and/or similarly protruding structures (*e.g.* Callaway, 2003; Rabaut *et al.*, 2009). This is similar to observations made for other tube-building polychaetes – *e.g.* *Sabellaria alveolata* (Pawlik, 1988), *Lagis koreni* (Olivier *et al.*, 1996), *Owenia fusiformis* (Thiébaud *et al.*, 1994). The presence of these structures may influence larval settlement and early juvenile distribution (*sensu* Levin, 1992) through several mechanisms. Tube arrays attenuate water currents, facilitates settlement by enhancing larval retention (Rabaut *et al.*, 2009). They may also provide additional substrate for attachment (*e.g.* Callaway, 2003; Heuers *et al.*, 1998; Rabaut *et al.*, 2009) and/or settlement cues (Callaway, 2003) (Fig 6.2, green box). These may constitute a myriad of factors, such as substrate availability (Dodd *et al.*, 2009), chemical cues from microbial communities specific to the environments created by

conspecifics (Qian, 1999), chemical substances exuded by living conspecifics (Callaway, 2003), among others. An example of chemical cues influencing larval settlement of marine tube-building polychaetes includes the settlement of *S. alveolata* wherein conspecifics coat the sediment in specific fatty acids that trigger settlement (Qian, 1999).

Pre-recruitment presence of *L. conchilega* tubes and/or similarly protruding structures may not be necessary for its population establishment, as settlement has been observed in intertidal locations lacking those features (e.g. Dittmann, 1999; Strasser and Pieloth, 2001). As such, additional factors may influence larvae settlement location in addition to previous conspecific presence which may require further research. Sediment granulometry has been shown to comprise one of these factors for *L. conchilega* (Willems *et al.*, 2008) as previously mentioned. Previous research also suggests a role of local hydrodynamic forcing in settlement (Rabaut *et al.*, 2009) and post-settlement permanence/survival (Levin, 1992). The latter has been shown to dictate the stages of reef development for the honeycomb worm *S. alveolata* (Gruet, 1986), and hypothesised for *L. conchilega* (Heuers *et al.*, 1998).

Additional potential factors may also include food availability impacting post-settlement survival (Dittmann, 1999). The temporal evolution of *L. conchilega* small-scale distribution observed during our remote survey (see chapter 4) corroborates previous observations that *L. conchilega* may settle in “bare” sand. In addition, *L. conchilega* post-recruitment presence was dissociated from pre-recruitment presence and/or previously noticeable protruding structures in the intertidal zone (see chapter 4), indicating that the studied population did not require these features for settlement and/or establishment.

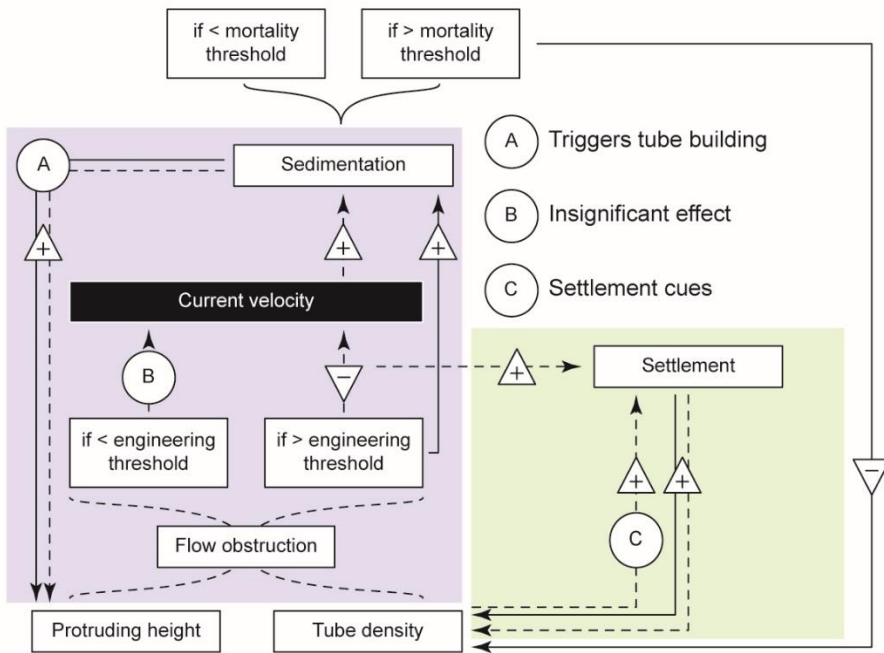


Fig 6.2. Modified flow chart showing the effects of autogenic engineering on water flow, sedimentation, feedback effects for aggregation protruding height (blue box); our findings on the effects of abrupt sedimentation in mortality (right-hand solid pathway outside of coloured boxes); and how settlement, aggregation tube density, and hydrodynamics interact (green box). Solid arrows represent findings from this thesis, whereas dashed arrows represent relationships indicated in literature. Triangles pointing upwards with an addition sign represent positive effects, whereas those pointing downwards, encasing a minus sign, represent negative effects. Blue box (adapted from fig 6.1): Past certain thresholds, density and protrusion height may negatively affect water current velocity, resulting in increased sedimentation (solid arrow: association shown experimentally without assessing current velocity). The latter has a positive impact on protruding height by triggering tube accretion (A). Insignificant engineering effects (B) may be present if density and protrusion height do not surpass the aforementioned engineering thresholds. Green box: flow attenuation within aggregations may have a positive effect on larval settlement through facilitation. Higher settlement has a positive effect on tube density which may positively affect settlement in return through settlement cues (C) in addition to its engineering effect on flow velocity.

Previous research on the distribution of intertidal *Lanice conchilega* has also revealed a tendency for accumulation in large topographical depressions (approx. ~100 000m²), such as channels (e.g. Ropert and Dauvin, 2000). This may be related to hydrodynamic conditions as large depressions and elevated areas may constitute areas of high current velocities during ebb and flood tides (Heuers *et al.*, 1998), creating environments of high water exchange and intermittent mixing. Topographical depressions may also retain water during ebb tide (see orthomosaics in chapter 4), increasing the period in which *L. conchilega* can filter-feed. *Lanice conchilega* has also been found to accumulate in areas of high productivity in both the intertidal (e.g. Dittmann, 1999) and subtidal zones (e.g. Van Hoey *et al.*, 2008), indicating that feeding facilitation due to water accumulation into puddles may have positive effects on survival. However, *L. conchilega* may also deplete the water column under stagnant conditions (Denis *et al.*, 2007). As such, the effect of water puddles on population dynamics is unknown and requires further study. Nevertheless, hydrodynamic flow also impacts intertidal *L. conchilega* filter-feeding by affecting its clearance rates (Denis *et al.*, 2007) – *i.e.* the relationship between flow velocity and clearance rate is dome-shaped (see Fig 4 in Denis *et al.*, 2007). Thus, the aforementioned research comprises indications that hydrodynamic conditions can modulate *L. conchilega* distribution through influence over its filter-feeding behaviour (within a scale of hundreds of meters).

Hydrodynamic flow may also exert influence over distribution through physical forcing. Physical forcing from water currents can remove and/or dislodge individuals (within a scale of hundreds of meters) (Fig 6.3, yellow box), creating density spatial gradients. Change in distribution due to physical forcing by water currents is a common phenomenon (Bradbury and Snelgrove, 2011). This is the case for a few polychaete species – e.g. the trumpet worm *L. koreni* (Thiébaud *et al.*, 1998) and *O. fusiformis* (Thiébaud *et al.*, 1994) – and it has been observed by Ropert and Dauvin (2000) for an intertidal *L. conchilega* population in the Bay of Veys (France). Density gradients across the landscape could result in mounds of varying physical attributes through the mechanisms described in section 6.1, generating patchwork landscapes with ecosystem engineering effects of varying intensity and driving heterogeneity across the landscape. As such, *Lanice conchilega* distribution may be further influenced by events of catastrophic sedimentation driving mortality, which should impact aggregation maintenance (see section 6.1). Deposition events may include

bedload transport from natural disasters such as storms (e.g. Dobbs and Vozarik, 1983) (see chapter 2) and tsunamis (e.g. Lomovasky *et al.*, 2011), beach nourishment (e.g. Colosio *et al.*, 2007; Speybroeck *et al.*, 2006), as well as deposition from human activities such as dredge disposal (e.g. De Backer *et al.*, 2014; Katsiaras *et al.*, 2015). Spatial differences in density may also create gradients in feeding and clearance rates as these depend on local density (Buhr, 1976) – in addition to flow speed, food concentration and particle size (Denis *et al.*, 2007). Variation of food availability in areas adjacent to densely populated areas may create gradients in mortality (e.g. as shown for mussels by van de Koppel *et al.*, 2005), directly affecting distribution.

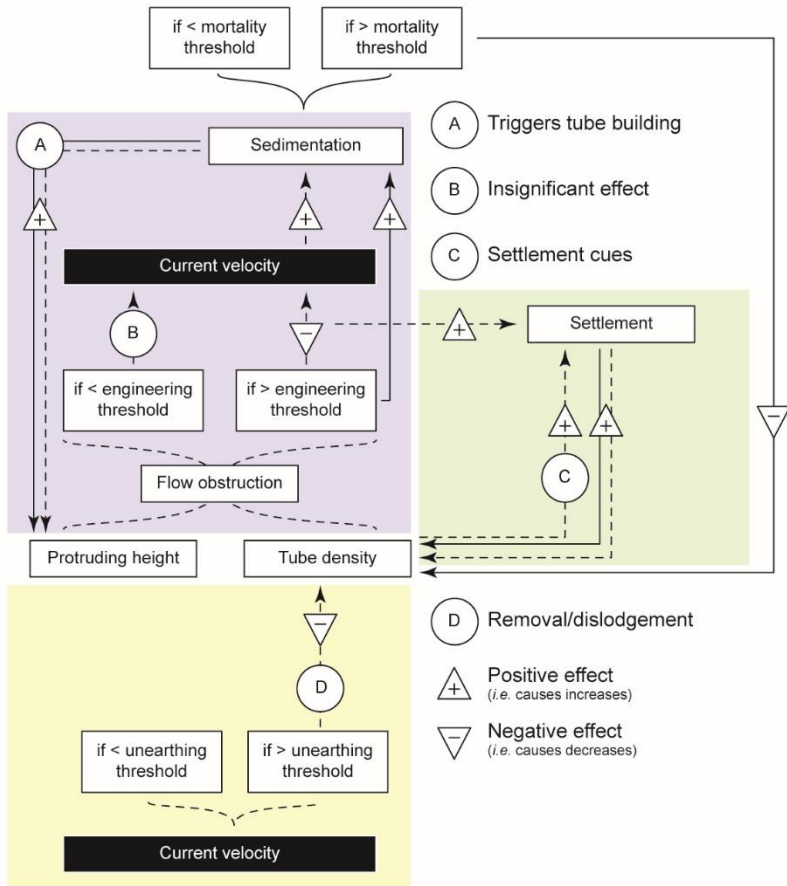


Fig 6.3. Modified flow chart showing the effects of autogenic engineering on water flow (blue box); how settlement, aggregation tube density, and hydrodynamics interact according to previous studies (green box); and the effects of hydrodynamic flow on tube density according to previous studies (yellow box). Blue box (adapted from fig 6.2): Past certain thresholds, density and protrusion height may negatively affect water current velocity, resulting in increased sedimentation (solid arrow: association shown experimentally without assessing current velocity). The latter has a positive impact on protruding height by triggering tube accretion (A). Insignificant engineering effects (B) may be present if density and protrusion height do not surpass the aforementioned engineering thresholds. Green box (adapted from fig 6.2): flow attenuation within aggregations may have a positive effect on larval settlement through facilitation. Higher settlement has a positive effect on tube density which may positively affect settlement in return through settlement cues (C) in addition to its engineering effect on flow velocity. Yellow box: Strong water currents may have a negative effect on tube density by removing and/or dislodging *L. conchilega* from aggregations (D).

6.2.2. Observed patterns and how they may have formed

Lanice conchilega occurrence was restricted to a large depression on the intertidal zone and independent of the presence of protruding structures during our surveys (see chapter 4). This suggests the existence of a relationship between topography and presence at least in intertidal areas. A modelling approach has shown that this may be due to interactions among hydrodynamic flow, topography, and *L. conchilega* aggregations following establishment (Heuers *et al.*, 1998). Under that framework, our results indicate that high water exchange (occurring at a scale of hundreds of meters during ebb and flood tides) may be of high importance for juvenile establishment (at scales <10m) (see Fig 6.3 for a summary). Additionally, submersion/emersion periods may influence intertidal *L. conchilega* by not only determining feeding periods and exposure to air (*i.e.* desiccation stress) (Ager, 2008), but also by limiting the impacts of hydrodynamic flow to a window of time that varies along coastal exposure gradients (Kaiser *et al.*, 2005). Since the hypothesised effect of hydrodynamic regimes occurs at a scale of approx. 100m - 1 000m, it seems likely that other processes may be involved in determining small-scale (*i.e.* < 10m) distribution (*i.e.* the formation of patchy patterns).

Another possibility is that hydrodynamic flow may have yet unexplored effects at smaller scales (Levin, 1992). For example, a modelling study by Guichard *et al.* (2003) illustrates how oceanographic regimes can influence distribution of sessile organisms (*i.e.* intertidal mussel beds) on a small scale through local hydrodynamic disturbance. The study shows a system in which mussel colonisation of available substrate might be hindered by wave-action stress and facilitated by the presence of conspecifics due to physical protection and reduction of mortality (Guichard *et al.*, 2003). Another alternative may be that accumulated water in the intertidal affects filter-feeding, modulating survival/mortality across space (see section 6.2.1). Lastly, hydrodynamic flow may influence larval settlement by hindering or facilitating larval substrate selection and/or attachment (*e.g.* Callaway, 2003; Heuers *et al.*, 1998, Rabaut *et al.*, 2009) (see section 6.2.1).

Small-scale spatial patterns consistently formed soon after recruitment during our remote sensing survey (see chapter 4), indicating that conditions during these periods indeed dictate small-scale *L. conchilega* distribution. Three types of patterning were observed following the different recruitment moments encompassed

by our study: patches (Fig 6.4A), beds (Fig 6.4B), and interrupted beds (Fig 6.4C) (see table 1.1 in chapter 1 for definitions). All patterns were irregular in space (see chapter 4), suggesting that it is unlikely that their formation resulted from self-organized processes as these often create regular patterns (Rietkerk and van de Koppel, 2008). Nevertheless, the different distribution types hinted at distinct processes of formation. *Lanice conchilega* patches were identified from observations during 2013 (Fig 6.4A), and we initially expected them to form in a similar fashion to marsh tussocks (see Balke *et al.*, 2012). We hypothesised that conditions within aggregations positively affected survival by providing protection from hydrodynamic stress and predation. Whereas conditions at the edge would negatively affect survival due to heightened exposure to hydrodynamic stress, erosion created by flow divergence (*sensu* Balke *et al.*, 2012), and predation. However, our findings contrast with that hypothetical mechanism.

During an *in-situ* experiment we witnessed stronger population recovery trends in the edges of *L. conchilega* aggregations in comparison to their central regions following disturbance by a storm (see chapter 2). Additionally, visual inspection of digital elevation models from the remote sensing survey (see chapter 4) showed no evidence of increased hydrodynamic stress around aggregation edges – *i.e.* there were no erosion-related troughs. This suggests that conditions at the edge differ from our original predictions, making it unlikely that spatial pattern formation in *L. conchilega* aggregations is driven by the aforementioned hypothetical causal structure. It may be possible that tubes at the edge of aggregations facilitate larval retention by providing additional surface for attachment (Callaway, 2003), which may not be as readily accessible in an aggregation centre due to crowding. Nevertheless, further study is required to identify mechanisms acting within an aggregation that contribute to spatial pattern formation.

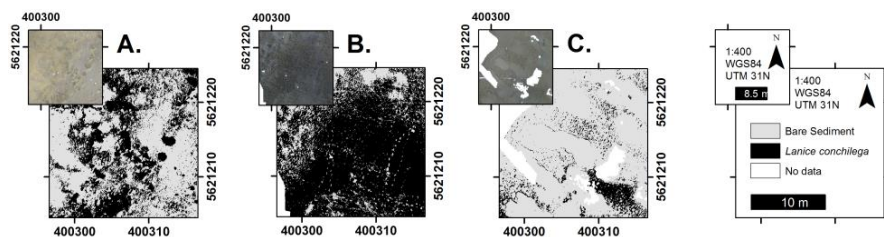


Fig 6.4. Three morphologically distinct small-scale distribution types were observed during our study and presented in chapter 4: patches (A), beds (B), and interrupted beds (C).

Results from chapter 2 and 3 hinted at a strong role of sediment dynamics and hydrodynamic conditions in modulating aggregation development (see section 6.1), enabling the formulation of alternative hypothetical mechanisms for further investigation. Recovery trends observed following a storm event in Boulogne during *in-situ* experiments hinted at a trend for the development of spatial density gradients within *L. conchilega* aggregations (see chapter 2). Recovery in the centre of aggregations was on average lower than on edges, although non-significantly different since recovery at the edges was highly variable (see chapter 2). Nevertheless, if differences in density develop between portions of an aggregation, it can be expected that population dynamics and mound development may also differ, resulting in distinct engineering effects (see chapter 3). As such, different levels of sediment deposition through autogenic engineering may be expected between those portions (see section 6.1) due to an effect dependence on tube density (Borsje *et al.*, 2014). However, our study did not assess differences in fine-sediment deposition between centre and edges, thus we are unable to confirm or refute associations among population dynamics, hydrodynamic stress, and sedimentation on a spatially-explicit framework.

Gradients in mortality can create distinct tube densities between portions of an aggregation. As such, heightened sedimentation of fine particles above *L. conchilega* aggregations (as seen for intertidal aggregations by Passarelli *et al.*, 2012; Rabaut *et al.*, 2009) may happen distinctly across space, leading to varying rates of higher tube accretion (see section 6.1). This may result in uneven vertical expansion across the settled landscape and distinct autogenic attenuation of currents across space (Fig 6.5). Additionally, uneven intertidal relief may generate heterogeneous hydrodynamic conditions across the landscape (*sensu* Borsje *et al.*, 2014) which would affect subsequent settlement during recruitment (Heuers *et al.*, 1998). In turn, this may culminate on the rise of early spatial patterns following recruitment (*sensu* Levin, 1992) which may change as the population develops due to external forcing, such as hydrodynamic driven post-settlement mortality (Levin, 1992) and/or catastrophic deposition driven mortality (e.g. chapter 2). Nevertheless, it is emphasised that this mechanism remains hypothetical, requiring further research for confirmation or refusal since there are many knowledge gaps involved – e.g. whether there are significant differences in population dynamics between different portions of an aggregation, what are effects of deposition of smaller sediment heights than those

presently examined on population dynamics, and the impact of varying hydrodynamic forcing in *L. conchilega* settlement across spatial scales.

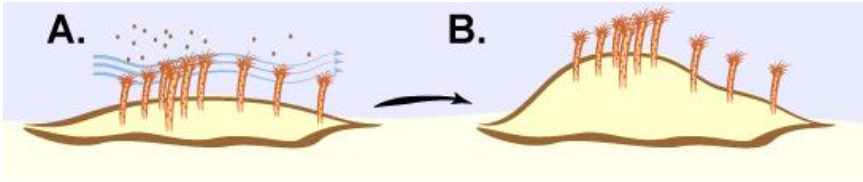


Fig 6.5. Illustration showing how heterogeneous *L. conchilega* tube density across a landscape can drive spatial heterogeneity. Uneven density within aggregations may result in spatially distinct autogenic effects on hydrodynamic flow (A). This results in distinct levels of sedimentation (B) and potentially different micro habitats, driving spatial heterogeneity.

The aforementioned hypothetical mechanism relies on positive feedbacks between *Lanice conchilega* and its autogenic engineering effects, *i.e.* water flow modulation (see section 6.1). As mentioned previously, the effect of *L. conchilega* on hydrodynamic flow is density-dependent (Borsje *et al.*, 2014). As such, *L. conchilega* establishment may rely on density thresholds, wherein a certain number of individuals per unit of space need to be present before flow is significantly modulated (*sensu* Bouma *et al.*, 2009b). This means that new *L. conchilega* populations might need to overcome a density threshold in order to facilitate further settlement through hydrodynamic stress amelioration. Once these thresholds are conquered and population established, vertical growth may ensue through the aforementioned feedback between sedimentation and tube accretion, while being limited by increased mortality during events of catastrophic deposition (see section 6.1). Although it is unclear how a population may reach those thresholds, we hypothesise that intense settlement, such as the one observed in June 2014 (Fig 6.4B previously), may contribute towards initial aggregation establishment through the mechanisms described in section 6.2. Further observations of patch formation at smaller temporal scales than those presently investigated may be required to elucidate its formation since the patch type was formed within the period of 1 month (see chapter 4) and verify our hypothesis.

Multiple mechanisms likely act upon *L. conchilega* populations to generate small-scale spatial patterns. As previously mentioned, the remote sensing survey found three distinct small-scale distribution types (see chapter 4). Potential mechanisms of formation for the patch type were discussed in the last few paragraphs. Two more types remain that were identified from observations during 2014: beds and interrupted beds (Fig 6.4B and C respectively) (see chapter 4). The *L. conchilega* bed type was characterised as a relatively homogeneous and continuous large aggregation (see table 1.1 in chapter 1 for further detail) that was observed in June 2014 (Fig 6.6B) (*sensu* chapter 4). The distribution observed in the following month, July 2014, was characterised as a bed interrupted by large holes (Fig 6.6C) (see interrupted beds/mats in table 1.1 in chapter 1). As such, these observed patterns hint at disturbances as likely drivers of small-scale distribution during that period. Nevertheless, the presence of different patterns following *L. conchilega* settlement moments support the hypothesis of early spatial pattern formation driven by conditions during settlement as suggested by Heuers *et al.* (1998) for *L. conchilega*, and Levin (1992) as a general mechanism. Furthermore, our findings suggest that pattern formation follows distinct mechanistic paths depending on conditions at the time of settlement and/or immediately after it. As such, pattern formation may vary per settlement moment with *L. conchilega* displaying multiple pattern morphologies within one seasonal population cycle (as seen in chapter 4).

Aerial imagery from April and June 2014 show two distinct pattern types, patches (Fig 6.6A and B) and extensive beds (Fig 6.6C and D) respectively (see chapter 4). April marked the beginning of the spring recruitment with the appearance of a cohort composed of extremely small and highly abundant individuals – *i.e.* approx. 30 000ind·m⁻² with .67mm inner tube diameter (see chapter 3). This moment likely comprises individuals nearing the final settlement in the life cycle of *L. conchilega*, as the observed average inner tube diameter approximates the size of individuals during this life stage – *i.e.* approximately 0.40mm in diameter (Kessler, 1963) (see also Addendum I). The small-scale pattern during the following month (*i.e.* June 2014) changed into an extensive bed (Fig 6.6C and D), indicating that the population at that time may have been comprised of not only growing survivors, but also subsequent settlers since recruitment lasts a few months for both intertidal (*e.g.* Callaway, 2003) and subtidal populations (*e.g.* Van Hoey *et al.*, 2006b). However, a comparison between average tube density in the two periods revealed a steep decline (see

chapter 3), contrasting with the latter hypothesis. As such, an alternative mechanism for pattern change between these two months is necessary and may be found in the works of Callaway (2003) on an intertidal population at Rhossili Bay (South Wales, UK). Callaway (2003) found that juvenile *L. conchilega* may settle upon adults, attaching themselves to the large tubes for a brief period of time. After approximately 1 month, these juveniles detach and settle on the available substrate (Callaway, 2003). As such, hydrodynamic conditions near the sediment surface during that time may modify spatial patterns by influencing settlement location through larval removal (Callaway, 2003) and/or larval retention within aggregations (Rabaut *et al.*, 2009) (Fig 6.7, bottom half of green box). Hydrodynamic phenomena such as eddies and/or gyres can substantially increase local larval retention whereas water fronts and currents may decrease it by transporting larvae away, affecting recruitment across space (Bradbury and Snelgrove, 2011). This may drive the creation of density gradients across space – *e.g.* *Owenia fusiformis* (Thiébaud *et al.*, 1994). Nevertheless, our results show that spatial pattern may not only form during settlement, but may also change throughout the 1-2 months following its beginning.

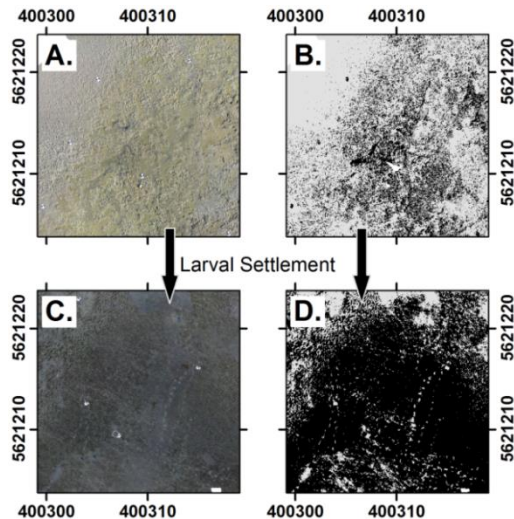


Fig 6.6. Small-scale distribution types presented in chapter 4 changed throughout the recruitment period of 2014. Visual comparison of orthomosaics (on the left) and presence maps (on the right: black indicates presence, while grey indicates absence) from April (A, B) and June 2014 (C, D) revealed that the distribution changed from sparse patches (A, B) to an uninterrupted bed (C, D) during the 2 month period likely due to juvenile resettlement (*sensu* Callaway, 2003).

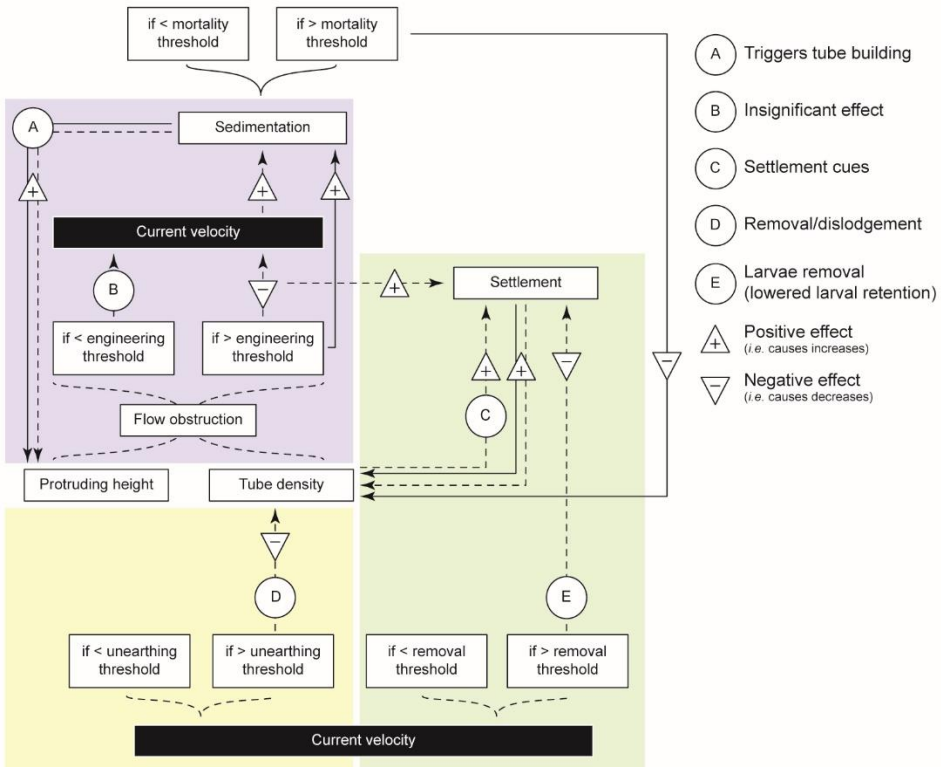


Fig 6.7. Modified flow chart showing the effects of autogenic engineering on water flow (blue box); how settlement, aggregation tube density, and hydrodynamics interact according to previous studies (green box); and the effects of hydrodynamic flow on tube density according to previous studies (yellow box). Blue box (adapted from fig 6.3): Past certain thresholds, density and protrusion height may negatively affect water current velocity, resulting in increased sedimentation (solid arrow: association shown experimentally without assessing current velocity). The latter has a positive impact on protruding height by triggering tube accretion (A). Insignificant engineering effects (B) may be present if density and protrusion height do not surpass the aforementioned engineering thresholds. Green box (adapted from fig 6.3): flow attenuation within aggregations may have a positive effect on larval settlement through facilitation. Higher settlement has a positive effect on tube density which may positively affect settlement in return through settlement cues (C) in addition to its engineering effect on flow velocity. Yellow box (adapted from fig 6.3): Strong water currents may have a negative effect on tube density by removing and/or dislodging *L. conchilega* from aggregations (D). Additionally, previous studies indicate that high hydrodynamic stress (represented here by current velocity) may remove larvae from the vicinity of aggregations and lower larval retention, negatively impacting settlement locally (green box, E).

6.2.3. *The role of consumer-resource interactions*

Common mechanisms for spatial pattern formation include but are not restricted to consumer-resource interactions, disturbance-recovery processes, and scale-dependent feedbacks (*sensu* Rietkerk and van de Koppel, 2008). As previously mentioned in chapter 1, population dynamics may influence pattern formation as it may differ between portions of a landscape due to either pre-established environmental gradients or gradients resulting from ecosystem engineering (Crain and Bertness, 2006). As an autogenic engineer, *L. conchilega* has the potential to create gradients of food availability in areas adjacent to its aggregations through filtration-pressure (Denis *et al.*, 2007) in a similar manner to mussels creating gradients in chlorophyll-a concentration in the water column (van de Koppel *et al.*, 2005). As such, we hypothesised that consumer-resource interactions influence spatial pattern formation in *Lanice conchilega* aggregations. However, this potential mechanism would involve the examination of multiple processes, such as growth, maturation, recruitment survival, among others. Since evaluating the role of consumer-resource interactions on population dynamics comprises a complex task (see chapter 1), we elected to explore it through ecological modelling parameterised using data from our *in-situ* monitoring of the intertidal *L. conchilega* population in Boulogne (see chapter 5).

A population simulation model was constructed with a *Lanice conchilega* population divided into juvenile and adult cohorts, as well as ecosystem compartments for generic nutrients, pelagic algae, and microphytobenthos (see chapter 5). The five equations system simulated *L. conchilega* population growth dependent on the consumption of pelagic algae and microphytobenthos. As such, growth of both cohorts could be limited if concentration of food sources decreased below pre-established thresholds (see chapter 5 for further detail). Several scenarios were examined with varying levels of food availability and food assimilation, and the model was partially stressed (see chapter 5 for further detail). Preliminary results revealed that food-dependent growth would largely influence the temporal dynamics of average adult density by modulating juvenile maturation into that population cohort under the considered causal structure. Juvenile density dynamics were mostly determined by recruitment intensity. Total *L. conchilega* density was not noticeably affected by food limitation during the simulation study as it generally reflected the temporal dynamics of juvenile average density. These preliminary findings suggest

that it is unlikely that consumer-resource interactions as predicted by the hypothesised causal structure could influence population dynamics in a significant manner. Therefore, they also suggest that it is also unlikely that this mechanism would affect spatial pattern formation since very small effects of food limitation were observed on total population density. Nevertheless, the simulation model could not be fully stressed, and further research and a full suite of stress tests are required to establish all equilibrium states as well as confirm or refute current findings. Other mechanisms that were not included in the modelling effort may also influence small-scale distribution, such as variable filtration rates due to current speed and particle size (Denis *et al.*, 2007), or limitation of feeding due to high tube density (Buhr, 1976) and emersion during ebbing tide for intertidal populations.

6.2.4.A note on potential mechanisms for spatial pattern formation

Our preliminary findings for this portion of the work suggest that it is unlikely that food availability influences population dynamics to the intensity necessary for spatial pattern formation (see chapter 5). Instead, the findings discussed so far from previous chapters indicate that spatial pattern formation for *L. conchilega* aggregations seems to be a dynamic seasonal process, resulting in changing patterns throughout the year (see section 6.2.2). We hypothesised several mechanisms through which spatial patterns may form in *L. conchilega* aggregations based on the integration of our findings (see fig 6.7 for a graphical summary). These have in common the potential effects of hydrodynamic flow on larval settlement and establishment, which could not be explored in the present effort. As such, we suggest that future work attempt to explore possible influences of hydrodynamic flow on *L. conchilega* settlement and formation of early patterns at a spatial scale <1m, especially in such unconsolidated and dynamic environments as sandy intertidal zones. Nevertheless, the variability in distribution and presence throughout seasonal cycles grants *Lanice conchilega* aggregations an ephemeral nature that has been previously noted by Callaway *et al.* (2010) and has impacted discussions about its conservation status (*e.g.* Godet *et al.*, 2008; Holt *et al.*, 1998; Rabaut *et al.*, 2009). This topic is discussed in the following section.

6.3. Ecological value and current conservation frameworks

Legal conservation frameworks within the European Union are determined by two documents, the Birds Directive (2009/147/EC) and the Habitats Directive

(92/43/EEC) (Evans, 2006). They list guidelines for the conservation of European avifauna (The Council of The European Communities, 2009) and habitats (The Council of The European Communities, 2007) respectively. Polychaete aggregations may be granted conservation status under the framework of the Habitats Directive as habitat type 1170, *i.e.* “reefs” (European Commission DG Environment, 2013). The reef habitat type is defined within the Interpretation Manual of European Habitats as:

“Reefs can be either biogenic concretions or of geogenic origin. They are hard compact substrata on solid and soft bottoms, which arise from the sea floor in the sublittoral and littoral zone. Reefs may support a zonation of benthic communities of algae and animal species as well as concretions and corallogenic concretions.”

(European Commission DG Environment, 2013)

The provided guideline is unclear, enabling the inclusion of a broad range of marine constructs – *e.g.* hydrothermal vents and submerged rock walls (Evans, 2006). The latest revision of potential reef habitats within the UK has included 3 polychaete species for consideration – *i.e.* *Sabellaria alveolata*, *Sabellaria spinulosa*, and *Serpula vermicularis* (Holt *et al.*, 1998). These species were included because (1) they create structures through conglomeration, (2) their structures rise significantly from the substrate surface (*i.e.* 20-75cm height), and (3) they comprise distinct communities from their surroundings (Holt *et al.*, 1998). Comparatively, *Lanice conchilega* does not rise above the substrate as much as the included polychaete species (*i.e.* its aggregations rise approx. 5-16cm above the sediment surface – Rabaut *et al.*, 2009). However, its aggregations can have significant effects on environmental properties and communities (*e.g.* De Smet *et al.*, 2015), attaining reef-like characteristics at much lower aggregation heights (Rabaut *et al.*, 2009). Nevertheless, *L. conchilega* was not considered a reef habitat due to uncertainties surrounding the level of distinctness between aggregations and their surroundings, as well as the longevity of their effects on the ecosystem (Holt *et al.*, 1998). Novel research has shown that *L. conchilega* aggregations display varying levels of distinctness depending on aggregation density (Rabaut *et al.*, 2009). The autogenic engineering effects from *Lanice conchilega* rely on the capacity of its aggregations to influence environmental properties through hydrodynamic modulation (*e.g.* De Smet *et al.*, 2015; Passarelli *et al.*, 2015; Rabaut *et al.*, 2009, 2007; Van Hoey *et al.*, 2008) (see chapter 1). Flow modulation by *L. conchilega* ameliorates hydrodynamic stress

(Friedrichs *et al.*, 2000), creating conditions that positively affect macrobenthic abundance and species richness as well as epi- and hyperbenthic abundances (De Smet *et al.*, 2015). As such, after certain density thresholds, *L. conchilega* aggregations become distinct entities from their surroundings due to increasingly intense engineering effects (*e.g.* De Smet *et al.*, 2015; Rabaut *et al.*, 2007) and can be considered reefs of high conservation value at least in subtidal areas (Rabaut *et al.*, 2009). Subtidal aggregations have been recognized as 1170 habitat (associated to 1110 habitat) for SCI delineation (SAC Vlaamse Banken BEMNZ0001). Nevertheless, the question of effect longevity as raised by Holt *et al.* (1998) during an evaluation of potential reef-builders in the UK remains.

Part of the ecological value of autogenic engineers lies on the longevity of their concretions (*i.e.* how long concretions persist through time) and sustained engineering effects (Hastings *et al.*, 2007). Temporal stability of engineering effects is a crucial factor in conservation research (Holt *et al.*, 1998), as constantly disappearing effects may result in reduction of resources to other species, such as shelter or food – *e.g.* coral reefs (Graham, 2014), *Sabellaria alveolata* (Dubois *et al.*, 2002). For example, reefs built by the polychaete *S. alveolata* display varying levels of species richness among its different reef stages (Dubois *et al.*, 2002). As previously mentioned, these stages are highly dependant on population dynamics cycles with recruitment periods replenishing the population and causing reef growth (Gruet, 1986), whereas decay takes part in the absence of recruitment (Gruet, 1986). The temporal stability of autogenic ecosystem engineers depends on the properties of their concretions determining rates of decay (Hastings *et al.*, 2007) (see chapter 1). As such, *Lanice conchilega* aggregation longevity may be influenced by population processes as it modulates engineering effects and vertical expansion (see section 6.1). In summary, fluctuations in density (Borsje *et al.*, 2014) and individual tube size modulate the area of flow obstruction (Eckman *et al.*, 1981) and consequently, mound maintenance through sedimentation and tube accretion (see section 6.1) (see fig 6.1 for a graphical summary). As such, seasonal cycles can result in highly dynamic populations with ephemeral aggregations as observed by Callaway *et al.* (2010) for an intertidal population in Rhossili Bay (South Wales, UK) and during our survey of the Boulogne intertidal population (see chapter 4). Presently, the seasonal aspect of *L. conchilega* concretions and consequently their

engineering effect on associated communities is responsible for its uncertain conservation status (Holt *et al.*, 1998).

The longevity of populations in Boulogne during our studies was much lower than that observed at other locations by previous research. Intertidal aggregations were noticeable for a maximum of 5 months in the sandy intertidal zone (see chapter 4). Comparatively, other studies report a persistence of approximately one year for intertidal aggregations (*e.g.* Callaway *et al.*, 2010). Intertidal zones are generally highly dynamic environments with emersion and submersion from tidal regimes often resulting in a wide range of environmental conditions throughout a day, and overall high environmental stress (Kaiser *et al.*, 2005). The highly dynamic and pronounced fluctuations of environmental conditions in the intertidal zone (Kaiser *et al.*, 2005) mean that intertidal *L. conchilega* populations may be susceptible to population declines as they must overcome these conditions. Our findings indicate that population dynamics and temporal stability in intertidal aggregations may be a result of environmental stress such as those imposed by seasonal fluctuations in conditions and/or natural events – *e.g.* water temperature (see chapter 3) and/or intense sedimentation from storms (see chapter 2). Environmental stress in Boulogne may also include anthropogenic impact, since *L. conchilega* aggregations are located near a large harbour (Rabaut *et al.*, 2008), and on a highly visited portion of the coast for tourism (*pers. obs.*) and small-scale fisheries (Martin *et al.*, 2009). The ramifications of anthropogenic impact may account for the lower persistence observed in Boulogne in comparison to other intertidal populations (*e.g.* Callaway *et al.*, 2010)

Seasonal fluctuations in intertidal *L. conchilega* population dynamics likely influence their ability to sustain aggregations and engineering effects (see section 6.1). As such, ecosystem functions performed by intertidal *L. conchilega* should also fluctuate seasonally, impacting several species that are associated to its aggregations. For example, previous research has suggested that several fish species, such as the North Sea plaice *Pleuronectes platessa* actively select for tube aggregations consisting of *Chaetopterus* sp and *L. conchilega* near Boulogne (Rees *et al.*, 2005). Additionally, juvenile *P. platessa* densely occupies *L. conchilega* aggregations in the Belgian Part of the North Sea (BPNS) during spring (Rabaut *et al.*, 2010). This period comprises the spawning period for the North Sea plaice (van der Veer *et al.*, 1990) and recruitment for *L. conchilega* (see chapter 3). Nursery grounds availability and connectivity (*i.e.* easiness to be reached by developing individuals) during that time

strongly influence *P. platessa* population abundances by modulating survival - see Rijnsdorp *et al.* (1995) and van der Veer *et al.* (2000) for further details. Thus, the dense presence of juvenile *P. platessa* in *L. conchilega* aggregations during spring suggests that these biogenic concretions function as nursery grounds (Rabaut *et al.*, 2010), providing structures for juveniles to hide in as an alternative to burying in bare sand (Rabaut *et al.*, 2010). This seasonal relationship between *L. conchilega* and *P. platessa* illustrates how ephemeral aggregations may significantly contribute to maintenance of other species through seasonal demand for its ecological roles. Furthermore, previous research shows that *Lanice conchilega* aggregations in Boulogne entrap large amounts of organic matter, increasing food supply to associated species that maintain larger macrofaunal food webs when compared to bare sand (De Smet *et al.*, 2016b). As such, assessments of *L. conchilega* conservation status in intertidal areas should be complimented with data on the ramifications of its presence, density, and intensity of engineering to the rest of the trophic network it is inserted in, as its functional value may not be readily apparent.

6.4. Conclusions and future prospects

This thesis explored the autogenic engineering effects of the sessile reef-building polychaete *Lanice conchilega* through two temporal scales using short-term experiments and analysing the seasonal evolution of its population dynamics and ecosystem engineering effects as well as small-scale distribution for the first time. *In-situ* monitoring enabled the exploration of population dynamics and engineering effects through seasonal cycles, as well as characterisation of *L. conchilega* small-scale distribution patterns. Additionally, we explored the impact of consumer-resource interactions on population dynamics through population-based modelling. Our experimental findings revealed interactions between sedimentation, tube accretion, and mortality, associating *L. conchilega* autogenic engineering with population dynamics and aggregation maintenance. Remote sensing methods applied during monitoring revealed the temporal evolution of *L. conchilega* small-scale distribution at unprecedented spatial resolution. This enabled the identification of three distribution types (*i.e.* patches, beds, and interrupted beds). Distribution types were formed following recruitment periods, suggesting that pattern formation is a consequence of interactions between larval settlement and hydrodynamic conditions during that period. An analysis of pattern types allowed the construction of hypothetical mechanisms of pattern formation and maintenance for *L. conchilega*

aggregations. As such, we hypothesise that (1) patches may form as a result of hydrodynamic impact on larval settlement and survival until the end of recruitment, as well as (2) heterogeneous density and autogenic engineering across the landscape impacting hydrodynamic stress at a local scale. We also hypothesise that (3) extensive *L. conchilega* beds may be formed during intense settlement events, and that (4) local disturbances may lead to the transformation of *L. conchilega* small scale (*i.e.* <1m) distribution through time (see section 6.1). It is worth noting that these hypotheses remain untested and require further examination. Lastly, preliminary results from the population model simulations suggest only a marginal importance of consumer-resource interactions on adult *L. conchilega* and highlighted the importance of recruitment and establishment of juvenile cohorts for total population density dynamics.

Current conservation frameworks provide broad definitions which increase the difficulty in identifying priority habitat types for conservation. As such, identifying and granting conservation status to reef-like *L. conchilega* populations is difficult. However, the framework does not fully exclude the creation of special areas of conservation (SACs) nor sites of community interest (SCIs) based on *L. conchilega* reef-like aggregations and subtidal high density beds are recognised as habitat 1170 in Belgium. Our work focuses on intertidal high density aggregations and revealed a shorter longevity of intertidal *L. conchilega* in Boulogne in comparison to other intertidal zones. Conservation status may be harder to achieve for intermittent intertidal aggregations such as these. Nevertheless, ephemeral *L. conchilega* aggregations may still play a crucial role on the temporal fluctuations of associated species with seasonal population cycles – *e.g.* North Sea plaice (see section 6.3). As such, it is advised that evaluating the conservation status of *L. conchilega* aggregations should be complimented with studies about the ramifications of its presence, density, and ecosystem engineering effects on its associated trophic network in addition to indicators such as longevity if we want to evaluate the conservation potential in intertidal areas.

The main goal of this thesis was to investigate potential mechanisms for spatial pattern formation while focusing on small-scale processes influencing *L. conchilega* population dynamics. Although considerable headway was achieved during the making of this thesis, several knowledge gaps remain that should be addressed by future research to clarify processes of spatial pattern formation in *L. conchilega*

aggregations. These challenges are discussed subsequently in a suggested order for prioritisation. Our findings point toward critical roles for hydrodynamic forcing and larval settlement, establishment, and survival in pattern formation. As such, examining the role of local hydrodynamic stress on settlement, establishment, and post-settlement survival of juvenile *L. conchilega* is of crucial importance, as it may improve our understanding on the formation of early patterns. Identifying the hydrodynamic conditions under which larvae and adult removal occur is also important since these may trigger fragmentation of *L. conchilega* aggregations. Additionally, the ability of *L. conchilega* to re-establish itself following removal may also be of interest since it may influence small-scale distribution. Furthermore, the interactions among hydrodynamic flow, tube density, and sedimentation should be further explored in a spatial explicit manner. For example, determining a sedimentation threshold and/or range after which mortality becomes significantly higher within an *L. conchilega* aggregation may enable an understanding of how population dynamics and recovery following catastrophic sedimentation events can affect spatial pattern formation. Exploring recovery mechanisms of *L. conchilega* aggregations following catastrophic sedimentation events also require further study and may help clarify how these events affect spatial pattern formation by modulating population dynamics. Our findings also indicated that population dynamics may differ between portions of an aggregation, but this could not be confirmed nor refuted due to the short time frame of the study. Further investigation of spatial dynamics inside *L. conchilega* aggregations may provide clues as to how spatial heterogeneity may be created, initialising fragmentation. Lastly, determining the role of water accumulation into puddles on population dynamics as different facets of *L. conchilega* filter-feeding may result in contrasting outcomes for population survival, with potential cascading effects on its spatial distribution from heterogeneous accumulation across space.

Additional factors may further contribute to spatial pattern formation in *L. conchilega* aggregations which are not immediately apparent during the making of this thesis, but should also be considered for future research. Conservation efforts would profit from research exploring the evolution of *L. conchilega* small-scale distribution alongside the evolution of its associated community structure. Associated fauna may have different functional roles, countering and/or amplifying the effects of *L. conchilega* aggregations on its environment. These complex interactions between *L.*

conchilega and its associated communities may affect spatial pattern formation in *L. conchilega* aggregations. Investigating the role of protection and anthropogenic disturbance may also contribute to our understanding of dynamics in *L. conchilega* aggregations, since human activities, such as port traffic and tourism may have a significant impact on exposed *L. conchilega* populations. In other words, it is possible that non-protection caused the variability observed in our study site which may be subjected to influences from the Port of Boulogne as well as visiting tourists. Lastly, this thesis evaluated intertidal *L. conchilega* aggregations in one location, and future research would benefit from additional, comparable case-studies, enabling the corroboration or rebuttal of underlying processes for spatial pattern formation in *L. conchilega* aggregations. For example, the imbalance between the amount of research investigating intertidal and subtidal dynamics was remarkable during the making of this thesis. As such, we suggest future investigation of more case-studies regarding subtidal *L. conchilega* populations and their connectivity to intertidal populations which seem to heavily depend on larvae from subtidal aggregations.



WGS 84
UTM 31N
1m

Elevation (m)



ADDENDUMS

- I. *L. conchilega* life cycle
- II. Digital elevation models
- III. Orthomosaics

Addendum I: *L. conchilega* life cycle

The life cycle of *Lanice conchilega* can last between 1-3 years (e.g. Beukema *et al.*, 1978; Ropert and Dauvin, 2000; Van Hoey *et al.*, 2006b). During that time, the polychaete worm goes through seven life phases (Fig I.A) - for further details on the life cycle of *Lanice conchilega*, the reader is referred to the works of Bhaud (1988), Bhaud and Cazaux (1990), and Kessler (1963). The cycle starts with spawning and once in the water column, the eggs develop into prototrochophora larvae within the first day (Fig I.A: 1) (Kessler, 1963). These are free living planktonic larvae that remain near the substrate (Kessler, 1963). This larva is characterized by a spherical shape, a band of cilia near its equator, and an apex plate at one of its “extremities” (Kessler, 1963). After the first 24h, prototrochophora larvae develop cilia on the apex plate and a pygidial telotroch as they change into trochophora larvae (Kessler, 1963) (Fig I.A: 2). From day 2 until day 4, trochophora larvae turn into metatrochophora-I larvae (Fig I.A: 2-4), wherein their bodies take on a pear-shape form, and cell groups differentiate into precursors of the intestine, mouth, and anus. During development, metatrochophora-I larvae develop segmentation, and the digestive system connects to the extracorporeal environment (Kessler, 1963). In addition, eye precursors emerge, while several sets of cilia develop for swimming (Kessler, 1963).

The next stage, metatrochophora-II, lasts from the 5th to the 6th day (Fig I.A: 5-6) and is characterized by bipartite living, that is a transitional stage between planktonic and benthic existence as *L. conchilega* settles for the first time (Kessler, 1963). It is unclear how *L. conchilega* settles during the metatrochophora-II phase. However, several physiological adaptations develop that facilitate settling. These include, but are not restricted to, the development of geotaxis (*i.e.* the ability to navigate based on Earth’s gravitational field), and larval bristles with which larvae attach themselves onto substrate (Kessler, 1963). Once settled, metatrochophora-II larvae develop specialized cells for mucus production, employed in building rudimentary detritus tubes (Kessler, 1963). The rudimentary tube and mucus production likely aid positioning (Kessler, 1963) and buoyancy (Bhaud and Cazaux, 1990) during the next planktonic phase. On the 6th day, metatrochophora-II larvae release themselves back into the water column (Kessler, 1963), and develop into the last planktonic phase, the aulophora larvae (Kessler, 1963) (Fig I.A: 30). Once detached, the aulophora larvae move away from the substrate and onto open water for a period of approx. 48 days

(Kessler, 1963). That period is marked by a growth in length through further segmentation and migration of provisional organs to their final positions (Kessler, 1963). Further morphological changes occur that grant *L. conchilega* its adult aspect – e.g. development of feeding tentacles, attachment hooks, gills from larval precursors (Kessler, 1963). After gill development, the aulophora larvae settle (approx. day 60), marking the beginning of the juvenile phase (Fig I.A: 60), in which individuals grow in size while widening their tubes, until adulthood (Fig I.A: 1-3years) (Kessler, 1963).

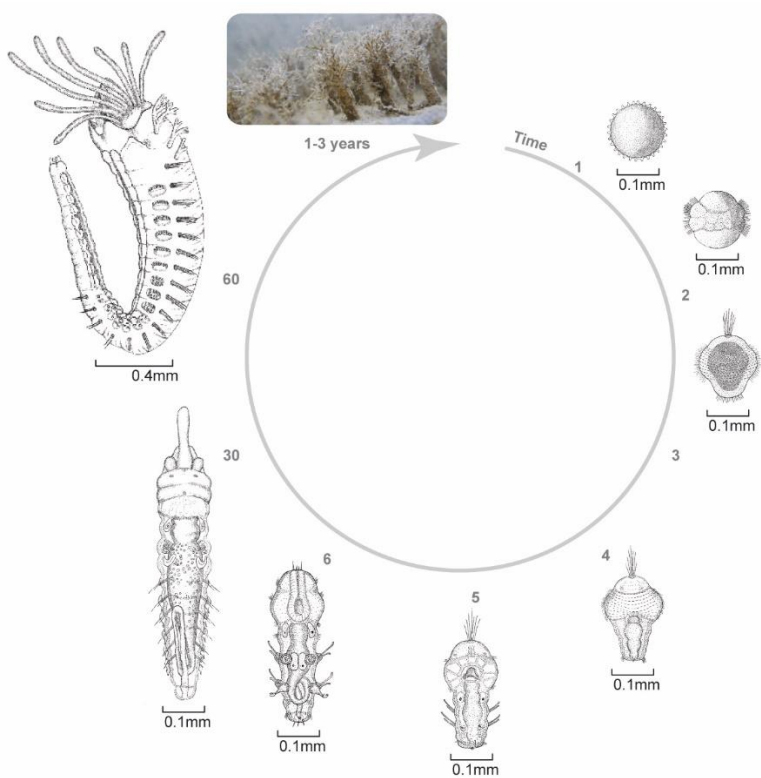
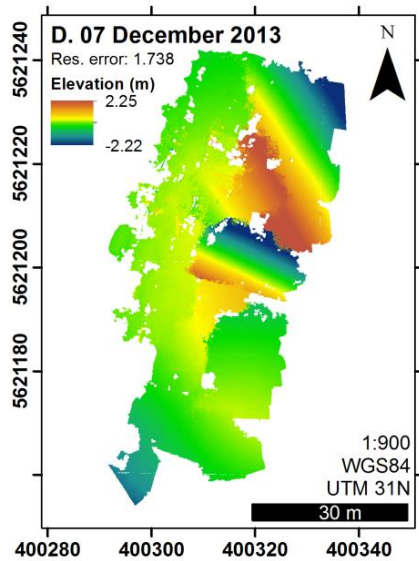
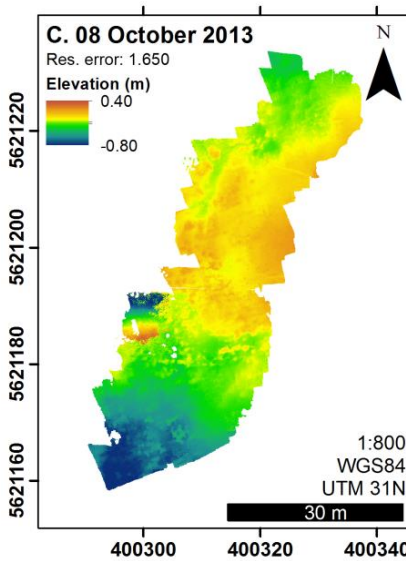
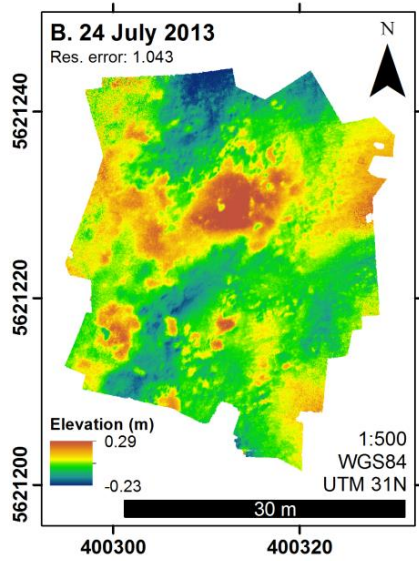
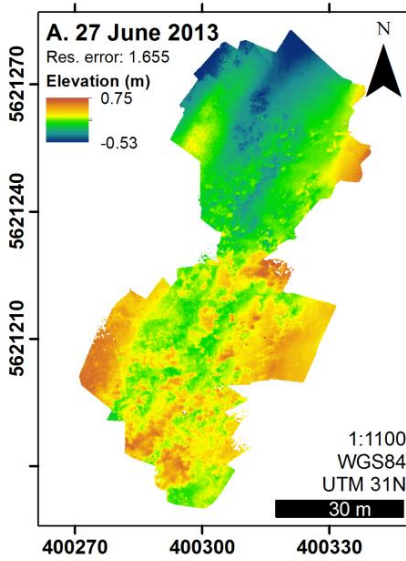
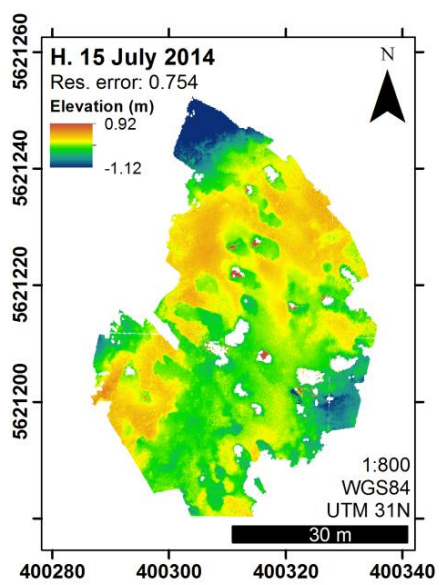
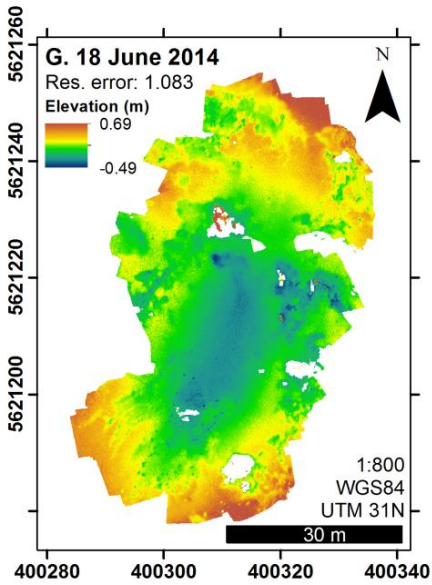
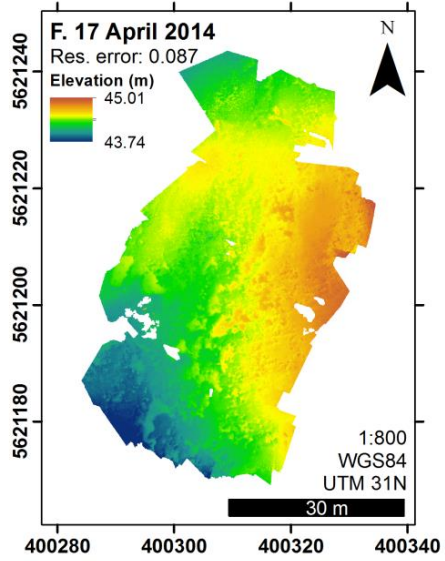
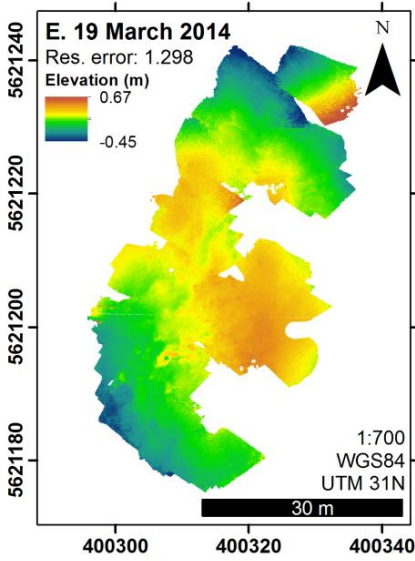
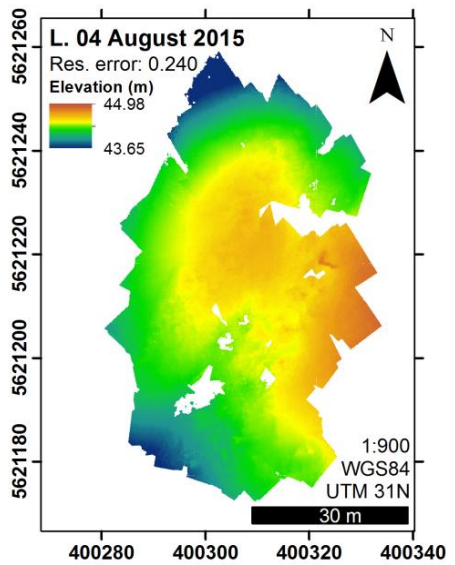
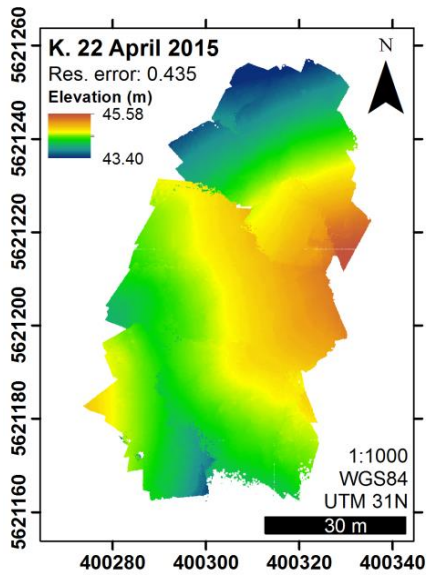
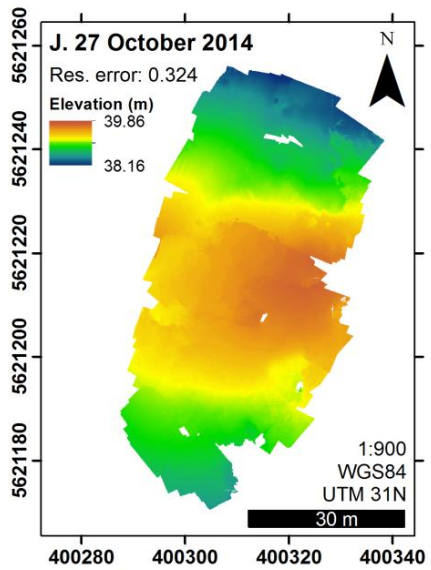
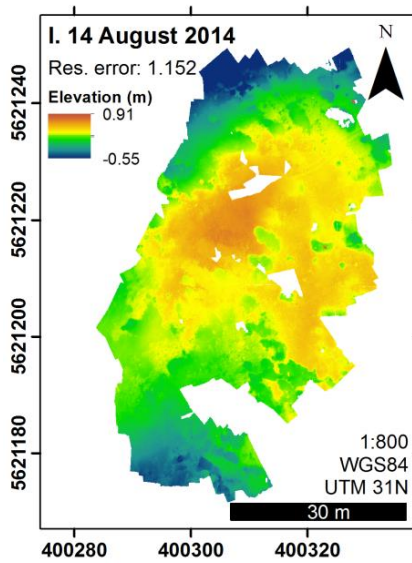


Fig A. Life cycle of *L. conchilega*: Following release, eggs develop into prototrochophora larvae during the first day by developing an apex plate and a band of cilia around its equator (1). Subsequently, prototrochophora larvae turn into trochophora larvae with the appearance of cilia on the apex plate and a pygidial telotroch (2). From day 2 to day 4, trochophora larvae change into metatrochophora-I larvae. The most noticeable changes comprise the body taking on a pear shape, segmentation and cell differentiation begin, the digestive system connects to the outside, and eye precursors emerge (2-4). These metamorphose into metatrochophora-II larvae, characterized by bipartite living (5-6). Changes during this stage include the development of geotaxis, bristles (used to attach the worm to the substrate), and specialized cells for mucus production (5-6). Metatrochophora-II larvae develop into the last larval stage, aulophora larvae (6-30). This planktonic larvae remains on the water column for approximately 30 days and is characterized by a marked growth in length via further body segmentation, migration of provisional organs to their final positions within the body, and gill development (30). Following these changes larvae settle and develop into juveniles (60), building their sand tubes and growing in size. Illustrations adapted from Kessler (1963). Photo by Renata M. S. Alves.

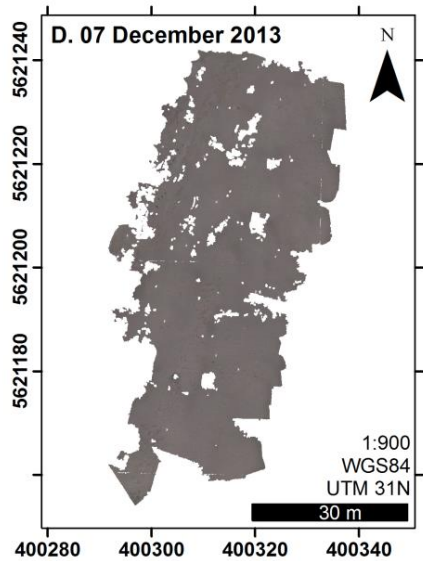
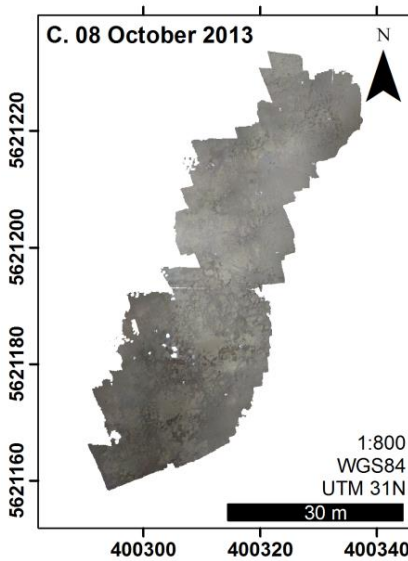
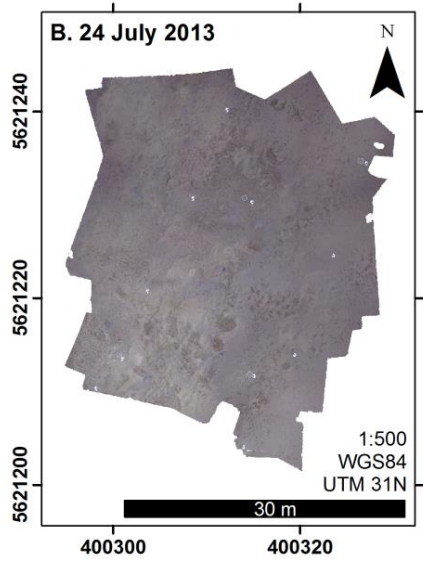
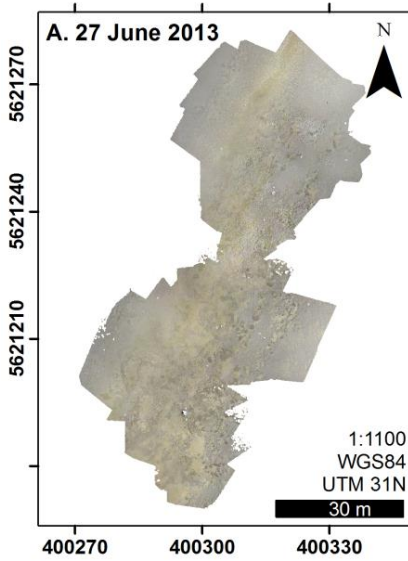
Addendum II: Digital elevation models

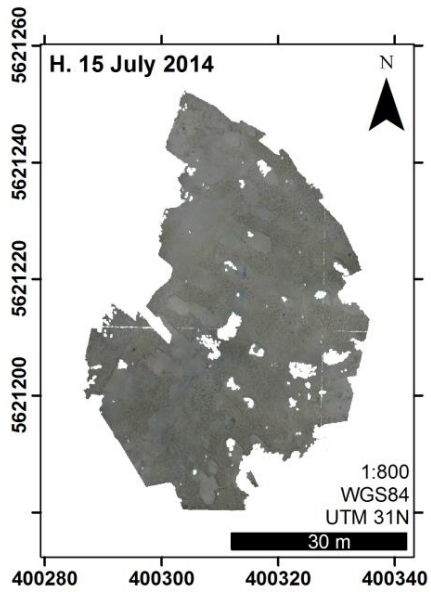
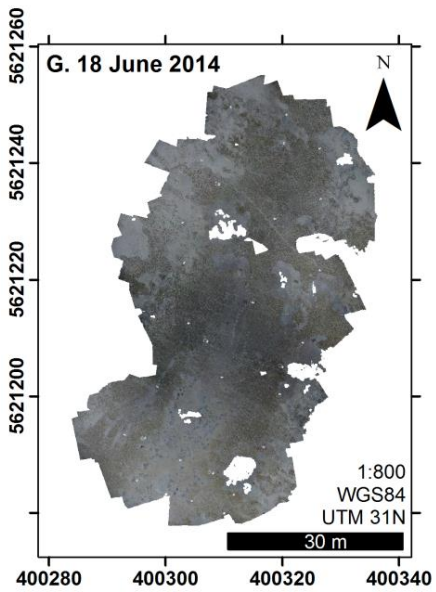
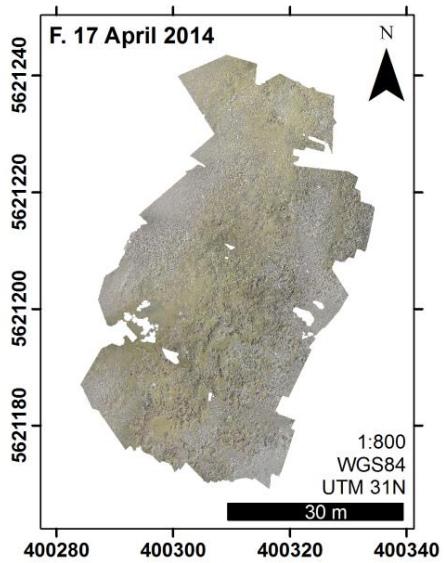
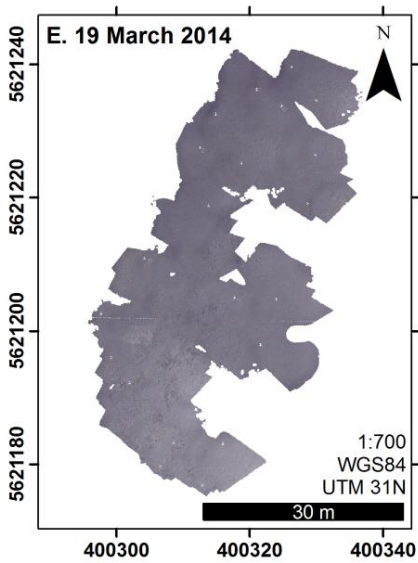


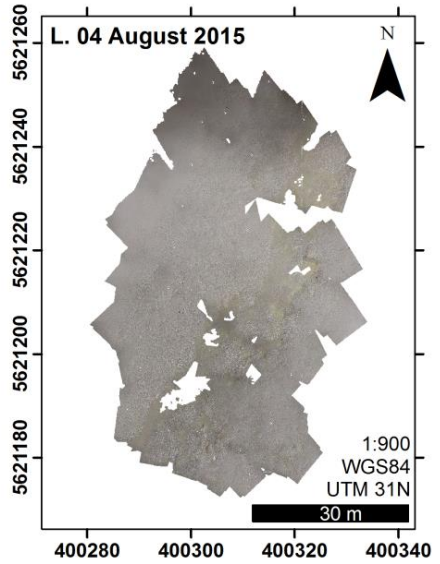
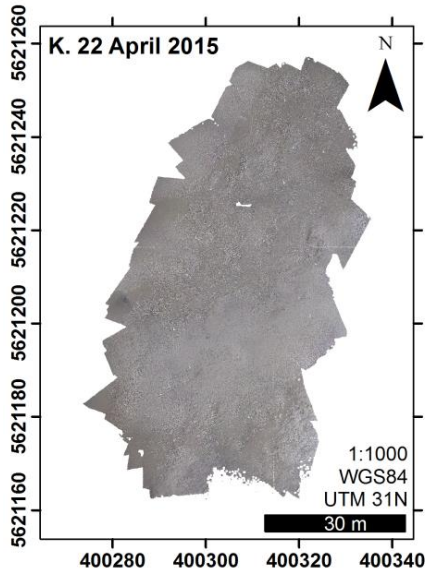
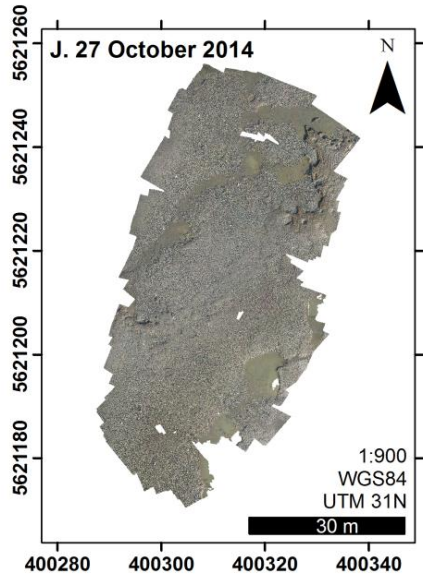
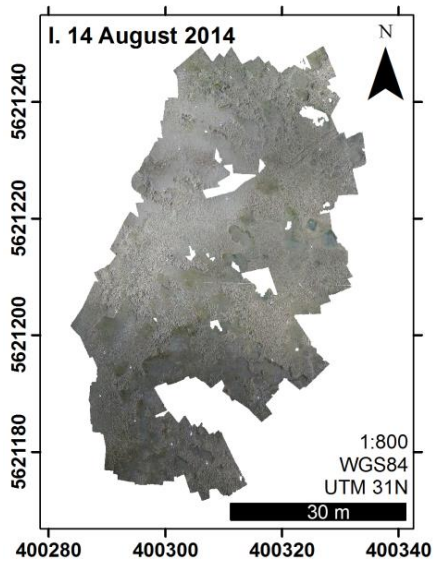




Addendum III: Orthomosaics









Cited Literature

- Abd El-Kawy, O.R., Rød, J.K., Ismail, H.A., Suliman, A.S., 2011. Land use and land cover change detection in the western Nile delta of Egypt using remote sensing data. *Applied Geography* 31, 483–494. DOI: 10.1016/j.apgeog.2010.10.012
- Aber, J.S., Marzloff, I., Ries, J., 2010. *Small-Format Aerial Photography: Principles, techniques and geoscience applications*, 1 edition. ed. Elsevier Science.
- Ager, O., 2008. *Lanice conchilega*. Sand mason. Marine Life Information Network: Biology and Sensitivity Key Information Sub-programme. [WWW Document]. The Marine Life Information Network (MarLIN). URL <http://www.marlin.ac.uk/speciesbenchmarks.php?speciesID=3633> (accessed 1.16.13).
- Agisoft LLC, 2016. Agisoft PhotoScan Professional Edition v1.2.3. Agisoft LLC, St. Petersburg, Russia.
- Aguirre-Gutiérrez, J., Seijmonsbergen, A.C., Duivenvoorden, J.F., 2012. Optimizing land cover classification accuracy for change detection, a combined pixel-based and object-based approach in a mountainous area in Mexico. *Applied Geography* 34, 29–37. DOI: 10.1016/j.apgeog.2011.10.010
- Allaire, J., Allen, J., Atkins, A., Carney, B., Chang, W., Cheng, J., Grolemond, G., Karimeddini, F., Kawaf, T., Kipp, A., Knast, P., McPherson, J., Oberg, R., Peters, S., Pylvainen, I., Ushey, K., Wickham, H., Xie, Y., 2015. RStudio v0.98.945.
- Allen, D.C., Vaughn, C.C., 2011. Density-dependent biodiversity effects on physical habitat modification by freshwater bivalves. *Ecology* 92, 1013–1019. DOI: 10.1890/10-0219.1
- Alves, R.M.S., Van Colen, C., Vincx, M., Vanaverbeke, J., De Smet, B., Guarini, J.-M., Rabaut, M., Bouma, T.J., 2017a. A case study on the growth of *Lanice conchilega* (Pallas, 1766) aggregations and their ecosystem engineering impact on sedimentary processes. *Journal of Experimental Marine Biology and Ecology* 489, 15–23. DOI: 10.1016/j.jembe.2017.01.005
- Alves, R.M.S., Vanaverbeke, J., Bouma, T.J., Guarini, J.-M., Vincx, M., Van Colen, C., 2017b. Effects of temporal fluctuation in population processes of intertidal *Lanice conchilega* (Pallas, 1766) aggregations on its ecosystem

engineering. *Estuarine, Coastal and Shelf Science* 188, 88–98. DOI: 10.1016/j.ecss.2017.02.012

Amara, R., Laffargue, P., Dewarumez, J.M., Maryniak, C., Lagardère, F., Luzac, C., 2001. Feeding ecology and growth of O-group flatfish (sole, dab and plaice) on a nursery ground (Southern Bight of the North Sea). *Journal of Fish Biology* 58, 788–803. DOI: 10.1111/j.1095-8649.2001.tb00531.x

Andersen, D.C., Shafroth, P.B., 2010. Beaver dams, hydrological thresholds, and controlled floods as a management tool in a desert riverine ecosystem, Bill Williams River, Arizona. *Ecohydrol.* 3, 325–338. DOI: 10.1002/eco.113

Anderson, M., Gorley, R., Clarke, K.R., 2008. PERMANOVA+ for PRIMER: Guide to software and statistical methods. PRIMER-E Ltd., Plymouth, UK.

Archambault, P., Bourget, E., 1996. Scales of coastal heterogeneity and benthic intertidal species richness, diversity and abundance. *Mar Ecol Prog Ser* 136, 111–121. DOI: 10.3354/meps136111

Ataide, M.B., Venekey, V., Filho, J.S.R., Santos, P.J.P. dos, 2014. Sandy reefs of *Sabellaria wilsoni* (*Polychaeta: Sabellariidae*) as ecosystem engineers for meiofauna in the Amazon coastal region, Brazil. *Mar Biodiv* 44, 403–413. DOI: 10.1007/s12526-014-0248-x

Ayata, S.-D., Ellien, C., Dumas, F., Dubois, S., Thiébaud, É., 2009. Modelling larval dispersal and settlement of the reef-building polychaete *Sabellaria alveolata*: Role of hydroclimatic processes on the sustainability of biogenic reefs. *Continental Shelf Research* 29, 1605–1623. DOI: 10.1016/j.csr.2009.05.002

Baird, A.H., Babcock, R.C., Mundy, C.P., 2003. Habitat selection by larvae influences the depth distribution of six common coral species. *Mar Ecol Prog Ser* 252, 289–293. DOI: 10.3354/meps252289

Balke, T., Klaassen, P.C., Garbutt, A., van der Wal, D., Herman, P.M.J., Bouma, T.J., 2012. Conditional outcome of ecosystem engineering: A case study on tussocks of the salt marsh pioneer *Spartina anglica*. *Geomorphology* 153–154, 232–238. DOI: 10.1016/j.geomorph.2012.03.002

Benedetti-Cecchi, L., Iken, K., Konar, B., Cruz-Motta, J., Knowlton, A., Pohle, G., Castelli, A., Tamburello, L., Mead, A., Trott, T., Miloslavich, P., Wong, M.,

- Shirayama, Y., Lardicci, C., Palomo, G., Maggi, E., 2010. Spatial Relationships between Polychaete Assemblages and Environmental Variables over Broad Geographical Scales. PLoS ONE 5, e12946. DOI: 10.1371/journal.pone.0012946
- Bergman, M.J.N., Hup, M., 1992. Direct effects of beamtrawling on macrofauna in a sandy sediment in the southern North Sea. ICES J Mar Sci 49, 5–11. DOI: 10.1093/icesjms/49.1.5
- Beukema, J.J., 1992. Expected changes in the Wadden Sea benthos in a warmer world: Lessons from periods with mild winters. Netherlands Journal of Sea Research 30, 73–79. DOI: 10.1016/0077-7579(92)90047-1
- Beukema, J.J., De Bruin, W., Jansen, J.J.M., 1978. Biomass and species richness of the macrobenthic animals living on the tidal flats of the Dutch Wadden Sea: Long-term changes during a period with mild winters. Netherlands Journal of Sea Research 12, 58–77. DOI: 10.1016/0077-7579(78)90025-X
- Bhattacharya, C.G., 1967. A Simple Method of Resolution of a Distribution into Gaussian Components. Biometrics 23, 115–135. DOI: 10.2307/2528285
- Bhaud, M.R., 2000. Two contradictory elements determine invertebrate recruitment: dispersion of larvae and spatial restrictions on adults. Oceanologica Acta 23, 409–422. DOI: 10.1016/S0399-1784(00)00146-8
- Bhaud, M.R., 1988. The two planktonic larval periods of *Lanice conchilega* (Pallas, 1766) *annelida polychaeta*, a peculiar example of the irreversibility of evolution. Ophelia 29, 141–152. DOI: 10.1080/00785326.1988.10430825
- Bhaud, M.R., Cazaux, C.P., 1990. Buoyancy characteristics of *Lanice conchilega* (Pallas) larvae (*Terebellidae*). Implications for settlement. J. Exp. Mar. Biol. Ecol. 141, 31–45. DOI: 10.1016/0022-0981(90)90155-6
- Boogert, N.J., Paterson, D.M., Laland, K.N., 2006. The Implications of Niche Construction and Ecosystem Engineering for Conservation Biology. BioScience 56, 570–578. DOI: 10.1641/0006-3568(2006)56[570:TIONCA]2.0.CO;2
- Borsje, B.W., Bouma, T.J., Rabaut, M., Herman, P.M.J., Hulscher, S.J.M.H., 2014. Formation and erosion of biogeomorphological structures: A model study on

the tube-building polychaete *Lanice conchilega*. *Limnol. Oceanogr.* 59, 1297–1309. DOI: 10.4319/lo.2014.59.4.1297

- Borthagaray, A.I., Carranza, A., 2007. Mussels as ecosystem engineers: Their contribution to species richness in a rocky littoral community. *Acta Oecologica* 31, 243–250. DOI: 10.1016/j.actao.2006.10.008
- Bouma, T.J., Friedrichs, M., van Wesenbeeck, B.K., Temmerman, S., Graf, G., Herman, P.M., 2009a. Density-dependent linkage of scale-dependent feedbacks: a flume study on the intertidal macrophyte *Spartina anglica*. *Oikos* 118, 260–268. DOI: 10.1111/j.1600-0706.2008.16892.x
- Bouma, T.J., Olenin, S., Reise, K., Ysebaert, T., 2009b. Ecosystem engineering and biodiversity in coastal sediments. *Helgol. Mar. Res.* 63, 95–106. DOI: 10.1007/s10152-009-0146-y
- Bouma, T.J., Ortells, V., Ysebaert, T., 2008. Comparing biodiversity effects among ecosystem engineers of contrasting strength: macrofauna diversity in *Zostera noltii* and *Spartina anglica* vegetations. *Helgoland Marine Research* 63, 3. DOI: 10.1007/s10152-008-0133-8
- Bouma, T.J., Vries, M.B.D., Low, E., Kusters, L., Herman, P.M.J., Tánčzos, I.C., Temmerman, S., Hesselink, A., Meire, P., Regenmortel, S. van, 2005. Flow hydrodynamics on a mudflat and in salt marsh vegetation: identifying general relationships for habitat characterisations. *Hydrobiologia* 540, 259–274. DOI: 10.1007/s10750-004-7149-0
- Bradbury, I.R., Snelgrove, P.V.R., 2011. Contrasting larval transport in demersal fish and benthic invertebrates: the roles of behaviour and advective processes in determining spatial pattern. *Canadian Journal of Fisheries and Aquatic Sciences*. DOI: 10.1139/f01-031
- Braeckman, U., Colen, C.V., Soetaert, K., Vincx, M., Vanaverbeke, J., 2011. Contrasting macrobenthic activities differentially affect nematode density and diversity in a shallow subtidal marine sediment. *Marine Ecology Progress Series* 422, 179–191. DOI: 10.3354/meps08910
- Braeckman, U., Provoost, P., Gribsholt, B., Gansbeke, D.V., Middelburg, J.J., Soetaert, K., Vincx, M., Vanaverbeke, J., 2010. Role of macrofauna

- functional traits and density in biogeochemical fluxes and bioturbation. *Mar Ecol Prog Ser* 399, 173–186. DOI: 10.3354/meps08336
- Braeckman, U., Provoost, P., Sabbe, K., Soetaert, K., Middelburg, J.J., Vincx, M., Vanaverbeke, J., 2012. Temporal dynamics in the diet of two marine polychaetes as inferred from fatty acid biomarkers. *Journal of Sea Research* 68, 6–19. DOI: 10.1016/j.seares.2011.11.003
- Braeckman, U., Rabaut, M., Vanaverbeke, J., Degraer, S., Vincx, M., 2014. Protecting the Commons: the use of Subtidal Ecosystem Engineers in Marine Management. *Aquatic Conserv: Mar. Freshw. Ecosyst.* 24, 275–286. DOI: 10.1002/aqc.2448
- Breton, E., Brunet, C., Sautour, B., Brylinski, J.-M., 2000. Annual variations of phytoplankton biomass in the Eastern English Channel: comparison by pigment signatures and microscopic counts. *J. Plankton Res.* 22, 1423–1440. DOI: 10.1093/plankt/22.8.1423
- Brey, T., 2012. Conversion Factors for Aquatic Organisms. In: *The Virtual Handbook on Population Dynamics v01.2*. Alfred Wegener Institute (AWI), Bremerhaven, Germany.
- Brey, T., 1986. Estimation of annual P/B-ratio and production of marine benthic invertebrates from length-frequency data. *Ophelia* 4, 45–54.
- Briggs, M.A., Lautz, L.K., Hare, D.K., González-Pinzón, R., 2013. Relating hyporheic fluxes, residence times, and redox-sensitive biogeochemical processes upstream of beaver dams. *Freshwater Science* 32, 622–641. DOI: 10.1899/12-110.1
- Brouwer, J.F.C. de, Clarke, K., Ruddy, G.K., Jones, T.E.R., Stal, L.J., 2005. Biogenic Stabilization of Intertidal Sediments: The Importance of Extracellular Polymeric Substances Produced by Benthic Diatoms. *Microb. Ecol.* 49, 501–512. DOI: 10.1007/s00248-004-0020-z
- Bryson, M., Johnson-Roberson, M., Murphy, R.J., Bongiorno, D., 2013. Kite Aerial Photography for Low-Cost, Ultra-high Spatial Resolution Multi-Spectral Mapping of Intertidal Landscapes. *PLoS ONE* 8, e73550. DOI: 10.1371/journal.pone.0073550

- Buhl-Mortensen, L., Vanreusel, A., Gooday, A.J., Levin, L.A., Priede, I.G., Buhl-Mortensen, P., Gheerardyn, H., King, N.J., Raes, M., 2010. Biological structures as a source of habitat heterogeneity and biodiversity on the deep ocean margins. *Marine Ecology* 31, 21–50. DOI: 10.1111/j.1439-0485.2010.00359.x
- Buhr, K.-J., 1976. Suspension-feeding and assimilation efficiency in *Lanice conchilega* (Polychaeta). *Mar. Biol.* 38, 373–383. DOI: 10.1007/BF00391377
- Buhr, K.J., Winter, J.E., 1976. Distribution and maintenance of a *Lanice conchilega* association in the Weser estuary (FRG), with special reference to the suspension-feeding behaviour of *Lanice conchilega*, in: Proceedings of the Eleventh European Symposium of Marine Biology, University College, Galway. pp. 5–11.
- Butler, D.R., Malanson, G.P., 2005. The geomorphic influences of beaver dams and failures of beaver dams. *Geomorphology, Dams in Geomorphology* 33rd Annual Binghampton International Geomorphology Symposium 71, 48–60. DOI: 10.1016/j.geomorph.2004.08.016
- Callaway, R., 2006. Tube worms promote community change. *Mar Ecol Prog Ser* 308, 49–60. DOI: 10.3354/meps308049
- Callaway, R., 2003. Juveniles stick to adults: recruitment of the tube-dwelling polychaete *Lanice conchilega* (Pallas, 1766). *Hydrobiologia* 503, 121–130. DOI: 10.1023/B:HYDR.0000008494.20908.87
- Callaway, R., Desroy, N., Dubois, S.F., Fournier, J., Frost, M., Godet, L., Hendrick, V.J., Rabaut, M., 2010. Ephemeral bio-engineers or reef-building polychaetes: how stable are aggregations of the tube worm *Lanice conchilega* (Pallas, 1766)? *Integr. Comp. Biol.* 50, 237–250. DOI: 10.1093/icb/icq060
- Carey, D.A., 1987. Sedimentological effects and palaeoecological implications of the tube-building polychaete *Lanice conchilega* Pallas. *Sedimentology* 34, 49–66. DOI: 10.1111/j.1365-3091.1987.tb00559.x
- Carey, D.A., 1983. Particle Resuspension in the Benthic Boundary Layer Induced by Flow around Polychaete Tubes. *Can. J. Fish. Aquat. Sci.* 40, s301–s308. DOI: 10.1139/f83-291

- Cartaxana, P., Mendes, C.R., van Leeuwe, M.A., Brotas, V., 2006. Comparative study on microphytobenthic pigments of muddy and sandy intertidal sediments of the Tagus estuary - Research database - University of Groningen. *Estuar. Coast. Shelf Sci.* 66, 225–230. DOI: j.ecss.2005.08.011
- Chandler, J.H., Fryer, J.G., Jack, A., 2005. Metric capabilities of low-cost digital cameras for close range surface measurement. *The Photogrammetric Record* 20, 12–26. DOI: 10.1111/j.1477-9730.2005.00302.x
- Chapman, N.D., Moore, C.G., Harries, D.B., Lyndon, A.R., 2007. Recruitment patterns of *Serpula vermicularis* L. (*Polychaeta, Serpulidae*) in Loch Creran, Scotland. *Estuarine, Coastal and Shelf Science* 73, 598–606. DOI: 10.1016/j.ecss.2007.03.001
- CHDK, 2013. Canon Hack Development Kit - PowerShot D20.
- Chirayath, V., Earle, S.A., 2016. Drones that see through waves – preliminary results from airborne fluid lensing for centimetre-scale aquatic conservation. *Aquatic Conserv: Mar. Freshw. Ecosyst.* 26, 237–250. DOI: 10.1002/aqc.2654
- Christofoletti, R.A., Takahashi, C.K., Oliveira, D.N., Flores, A.A.V., 2011. Abundance of sedentary consumers and sessile organisms along the wave exposure gradient of subtropical rocky shores of the south-west Atlantic. *Journal of the Marine Biological Association of the United Kingdom* 91, 961–967. DOI: 10.1017/S0025315410001992
- Clarke, K., Gorley, R., 2006. PRIMER v6: User Manual/Tutorial., PRIMER. PRIMER-E Ltd., Plymouth, UK.
- Colosio, F., Abbiati, M., Aioldi, L., 2007. Effects of beach nourishment on sediments and benthic assemblages. *Marine Pollution Bulletin* 54, 1197–1206. DOI: 10.1016/j.marpolbul.2007.04.007
- Connell, J.H., 1961. The Influence of Interspecific Competition and Other Factors on the Distribution of the Barnacle *Chthamalus stellatus*. *Ecology* 42, 710–723. DOI: 10.2307/1933500

- Crain, C.M., Bertness, M.D., 2006. Ecosystem Engineering across Environmental Gradients: Implications for Conservation and Management. *BioScience* 56, 211–218. DOI: 10.1641/0006-3568(2006)056[0211:EEAEGI]2.0.CO;2
- Cruz, T., Castro, J.J., Hawkins, S.J., 2010. Recruitment, growth and population size structure of *Pollicipes pollicipes* in SW Portugal. *Journal of Experimental Marine Biology and Ecology, The Biology of Barnacles' in honour of Margaret Barnes* 392, 200–209. DOI: 10.1016/j.jembe.2010.04.020
- De Backer, A., Van Hoey, G., Coates, D., Vanaverbeke, J., Hostens, K., 2014. Similar diversity-disturbance responses to different physical impacts: Three cases of small-scale biodiversity increase in the Belgian part of the North Sea. *Marine Pollution Bulletin* 84, 251–262. DOI: 10.1016/j.marpolbul.2014.05.006
- De Smet, B., Braeckman, U., Soetaert, K., Vincx, M., Vanaverbeke, J., 2016a. Predator effects on the feeding and bioirrigation activity of ecosystem-engineered *Lanice conchilega* reefs. *Journal of Experimental Marine Biology and Ecology* 475, 31–37. DOI: 10.1016/j.jembe.2015.11.005
- De Smet, B., D'Hondt, A.-S., Verhelst, P., Fournier, J., Godet, L., Desroy, N., Rabaut, M., Vincx, M., Vanaverbeke, J., 2015. Biogenic reefs affect multiple components of intertidal soft-bottom benthic assemblages: the *Lanice conchilega* case study. *Estuarine, Coastal and Shelf Science* 152, 44–55. DOI: 10.1016/j.ecss.2014.11.002
- De Smet, B., Godet, L., Fournier, J., Desroy, N., Jaffré, M., Vincx, M., Rabaut, M., 2013. Feeding grounds for waders in the Bay of the Mont Saint-Michel (France): the *Lanice conchilega* reef serves as an oasis in the tidal flats. *Mar Biol* 160, 751–761. DOI: 10.1007/s00227-012-2130-3
- De Smet, B., Oevelen, D. van, Vincx, M., Vanaverbeke, J., Soetaert, K., 2016b. *Lanice conchilega* structures carbon flows in soft-bottom intertidal areas. *Mar Ecol Prog Ser* 552, 47–60. DOI: 10.3354/meps11747
- de Souza Júnior, M.B., Ferreira, F.F., de Oliveira, V.M., 2014. Effects of the spatial heterogeneity on the diversity of ecosystems with resource competition. *Physica A: Statistical Mechanics and its Applications* 393, 312–319. DOI: 10.1016/j.physa.2013.08.045

- Degraer, S., Moerkerke, G., Rabaut, M., Van Hoey, G., Du Four, I., Vincx, M., Henriët, J.-P., Van Lancker, V., 2008. Very-high resolution side-scan sonar mapping of biogenic reefs of the tube-worm *Lanice conchilega*. *Remote Sensing of Environment* 112, 3323–3328. DOI: 10.1016/j.rse.2007.12.012
- Dekker, A.G., Brando, V.E., Anstee, J.M., 2005. Retrospective seagrass change detection in a shallow coastal tidal Australian lake. *Remote Sensing of Environment* 97, 415–433. DOI: 10.1016/j.rse.2005.02.017
- Denis, L., Desroy, N., Ropert, M., 2007. Ambient flow velocity and resulting clearance rates of the terebellid polychaete *Lanice conchilega* (Pallas, 1766). *Journal of Sea Research* 58, 209–219. DOI: 10.1016/j.seares.2007.03.005
- Didakites at Beeuzaert-Braet BVBA, 2010. Flow form 4 | Didakites [WWW Document]. Didakites | The most professional kite systems. URL <http://www.didak.com/shop/en/store/kites/one-line-kites/flow-form-4> (accessed 11.6.17).
- Dittmann, S. (Ed.), 1999. *The Wadden Sea ecosystem: stability properties and mechanisms*, 1 edition. ed. Springer, Berlin ; New York.
- Dobbs, F.C., Vozarik, J.M., 1983. Immediate effects of a storm on coastal infauna. *Mar. Ecol. Prog. Ser.* 11, 273–279. DOI: 10.3354/meps011273
- Dodd, J., Baxter, L., Hughes, D.J., 2009. Mapping *Serpula vermicularis* (*Polychaeta: Serpulidae*) aggregations in Loch Teacuis, western Scotland, a new record. *Marine Biology Research* 5, 200–205. DOI: 10.1080/17451000802345858
- Dolmer, P., 2000. Algal concentration profiles above mussel beds. *Journal of Sea Research* 43, 113–119. DOI: 10.1016/S1385-1101(00)00005-8
- Drost, E.J., 2013. *Hydrodynamics over a patch structure on an intertidal mussel bed*. Universiteit Utrecht, Utrecht, Netherlands.
- Dubois, S., Comtet, T., Retière, C., Thiébaud, E., 2007. Distribution and retention of *Sabellaria alveolata* larvae (*Polychaeta: Sabellariidae*) in the Bay of Mont-Saint-Michel, France. *Marine Ecology Progress Series* 346, 243–254. DOI: 10.3354/meps07011
- Dubois, S., Retière, C., Olivier, F., 2002. Biodiversity associated with *Sabellaria alveolata* (*Polychaeta: Sabellariidae*) reefs: effects of human disturbances.

Journal of the Marine Biological Association of the United Kingdom 82, 817–826. DOI: 10.1017/S0025315402006185

Dunning, J.B., Stewart, D.J., Danielson, B.J., Noon, B.R., Root, T.L., Lamberson, R.H., Stevens, E.E., 1995. Spatially Explicit Population Models: Current Forms and Future Uses. *Ecological Applications* 5, 3–11. DOI: 10.2307/1942045

Eckman, J.E., 1996. Closing the larval loop: linking larval ecology to the population dynamics of marine benthic invertebrates. *Journal of Experimental Marine Biology and Ecology* 200, 207–237. DOI: 10.1016/S0022-0981(96)02644-5

Eckman, J.E., Nowell, A.R., Jumars, P.A., 1981. Sediment destabilization by animal tubes. *Journal of Marine Research* 39, 361–374.

Ekeboom, J., Erkkilä, A., 2003. Using aerial photography for identification of marine and coastal habitats under the EU's Habitats Directive. *Aquatic Conserv: Mar. Freshw. Ecosyst.* 13, 287–304. DOI: 10.1002/aqc.553

Erbek, F.S., Özkan, C., Taberner, M., 2004. Comparison of maximum likelihood classification method with supervised artificial neural network algorithms for land use activities. *International Journal of Remote Sensing* 25, 1733–1748. DOI: 10.1080/0143116031000150077

ESRI, 2016. Maximum Likelihood Classification - Help | ArcGIS for Desktop [WWW Document]. URL <http://desktop.arcgis.com/en/arcmap/10.3/tools/spatial-analyst-toolbox/how-maximum-likelihood-classification-works.htm> (accessed 9.12.16).

ESRI, 2014. ArcGIS Desktop v10.3. ESRI, Redlands, United States of America.

Estes, J.A., Tinker, M.T., Williams, T.M., Doak, D.F., 1998. Killer Whale Predation on Sea Otters Linking Oceanic and Nearshore Ecosystems. *Science* 282, 473–476. DOI: 10.1126/science.282.5388.473

European Commission DG Environment, 2013. Interpretation Manual of European Union Habitats (EUR28).

Evans, D., 2006. The Habitats of the European Union Habitats Directive. *Biology and Environment: Proceedings of the Royal Irish Academy* 106B, 167–173.

- Fensham, R.J., Bray, S.G., Fairfax, R.J., 2007. Evaluation of aerial photography for predicting trends in structural attributes of Australian woodland including comparison with ground-based monitoring data. *Journal of Environmental Management* 83, 392–401. DOI: 10.1016/j.jenvman.2006.03.013
- Fiore, C.L., Jarett, J.K., Olson, N.D., Lesser, M.P., 2010. Nitrogen fixation and nitrogen transformations in marine symbioses. *Trends in Microbiology* 18, 455–463. DOI: 10.1016/j.tim.2010.07.001
- Food and Agriculture Organization of the United Nations - FAO, 2005. Fisheries and aquaculture software. FISAT II - FAO-ICLARM Stock Assessment Tools II. FAO Fisheries and Aquaculture Department [online], Rome, Italy.
- Foody, G.M., 2002. Status of land cover classification accuracy assessment. *Remote Sensing of Environment* 80, 185–201. DOI: 10.1016/S0034-4257(01)00295-4
- Forster, S., Graf, G., 1995. Impact of irrigation on oxygen flux into the sediment: intermittent pumping by *Callianassa subterranea* and “piston-pumping” by *Lanice conchilega*. *Marine Biology* 123, 335–346. DOI: 10.1007/BF00353625
- Frantzen, S., 2007. Recruitment of blue mussels, *Mytilus edulis* L., on suspended collectors in Finnmark, North Norway (70–71°N). *Marine Biology Research* 3, 37–48. DOI: 10.1080/17451000601182627
- Friedrichs, M., Graf, G., Springer, B., 2000. Skimming flow induced over a simulated polychaete tube lawn at low population densities. *Mar Ecol Prog Ser* 192, 219–228. DOI: 10.3354/meps192219
- Gallant, J.C., Wilson, J.P., 2000. Chapter 3: Primary Topographic Attributes, in: *Terrain Analysis: Principles and Applications*. John Wiley & Sons, New York, NY (USA), p. 522.
- Garmin Ltd., 2011. eTrex Owner’s Manual for use with models 10, 20, 30. United States of America (USA).
- Gillespie, T.W., Foody, G.M., Rocchini, D., Giorgi, A.P., Saatchi, S., 2008. Measuring and modelling biodiversity from space. *Progress in Physical Geography* 32, 203–221. DOI: 10.1177/0309133308093606

- Godet, L., Fournier, J., Jaffré, M., Desroy, N., 2011. Influence of stability and fragmentation of a worm-reef on benthic macrofauna. *Estuarine, Coastal and Shelf Science* 92, 472–479. DOI: 10.1016/j.ecss.2011.02.003
- Godet, L., Fournier, J., Toupoint, N., Olivier, F., 2009a. Mapping and monitoring intertidal benthic habitats: a review of techniques and a proposal for a new visual methodology for the European coasts. *Progress in Physical Geography* 33, 378–402. DOI: 10.1177/0309133309342650
- Godet, L., Toupoint, N., Fournier, J., Le Mao, P., Retière, C., Olivier, F., 2009b. Clam farmers and Oystercatchers: Effects of the degradation of *Lanice conchilega* beds by shellfish farming on the spatial distribution of shorebirds. *Marine Pollution Bulletin* 58, 589–595. DOI: 10.1016/j.marpolbul.2008.11.001
- Godet, L., Toupoint, N., Olivier, F., Fournier, J., Retière, C., 2008. Considering the Functional Value of Common Marine Species as a Conservation Stake: The Case of Sandmason Worm *Lanice conchilega* (Pallas 1766) (*Annelida, Polychaeta*) Beds. *Ambio* 37, 347–355.
- Gonzales, R.C., Woods, R.E., 2001. Chapter 9: Morphological Image Processing, in: *Digital Image Processing*. Prentice-Hall Inc, New Jersey, USA, pp. 519–566.
- Goodman, J.A., Purkis, S.J., Phinn, S.R., 2013. *Coral Reef Remote Sensing: A Guide for Mapping, Monitoring and Management*. Springer Science & Business Media.
- Goodman, S., 2008. A dirty dozen: twelve p-value misconceptions. *Semin. Hematol.* 45, 135–140. DOI: 10.1053/j.seminhematol.2008.04.003
- Gosselin, L.A., Sewell, M.A., 2013. Reproduction, larval development and settlement of the intertidal serpulid polychaete *Spirobranchus cariniferus*. *Journal of the Marine Biological Association of the United Kingdom* 93, 1249–1256. DOI: 10.1017/S0025315412001701
- Graham, N.A.J., 2014. Habitat Complexity: Coral Structural Loss Leads to Fisheries Declines. *Current Biology* 24, R359–R361. DOI: 10.1016/j.cub.2014.03.069
- Greenhouse, S.W., Geisser, S., 1959. On methods in the analysis of profile data. *Psychometrika* 24, 95–112. DOI: 10.1007/BF02289823

- Gruet, Y., 1986. Spatio-temporal changes of sabellarian reefs built by the sedentary polychaete *Sabellaria alveolata* (Linné). *Marine Ecology* 7, 303–319. DOI: 10.1111/j.1439-0485.1986.tb00166.x
- Guichard, F., Bourget, E., Agnard, J.-P., 2000. High-resolution remote sensing of intertidal ecosystems: A low-cost technique to link scale-dependent patterns and processes. *Limnol. Oceanogr.* 45, 328–338. DOI: 10.4319/lo.2000.45.2.0328
- Guichard, F., Halpin, P.M., Allison, G.W., Lubchenco, J., Menge, B.A., 2003. Mussel disturbance dynamics: signatures of oceanographic forcing from local interactions. *Am. Nat.* 161, 889–904. DOI: 10.1086/375300
- Gullström, M., Lundén, B., Bodin, M., Kangwe, J., Öhman, M.C., Mtolera, M.S.P., Björk, M., 2006. Assessment of changes in the seagrass-dominated submerged vegetation of tropical Chwaka Bay (Zanzibar) using satellite remote sensing. *Estuarine, Coastal and Shelf Science* 67, 399–408. DOI: 10.1016/j.ecss.2005.11.020
- Günther, C.-P., Niesel, V., 1999. Effects of the Ice catastrophe 1995/96, in: Dittmann, D.S. (Ed.), *The Wadden Sea Ecosystem*. Springer Berlin Heidelberg, pp. 193–205.
- Gurney, W.S.C., Nisbet, R.M., 1998. *Ecological Dynamics*, 1 edition. ed. Oxford University Press, New York.
- Gutiérrez, J.L., Jones, C.G., 2006. Physical Ecosystem Engineers as Agents of Biogeochemical Heterogeneity. *BioScience* 56, 227–236. DOI: 10.1641/0006-3568(2006)056[0227:PEEAAO]2.0.CO;2
- Gutiérrez, J.L., Jones, C.G., Byers, J.E., Arkema, K.K., Berkenbusch, K., Commito, J.A., Duarte, C.M., Hacker, S.D., Lambrinos, J.G., Hendriks, J.E., Hogarth, P.J., Palomo, M.G., Wild, C., 2011. 7.04 - Physical Ecosystem Engineers and the Functioning of Estuaries and Coasts, in: *Treatise on Estuarine and Coastal Science*. Academic Press, Waltham, pp. 53–81.
- Gutiérrez, J.L., Jones, C.G., Strayer, D.L., Iribarne, O.O., 2003. Mollusks as ecosystem engineers: the role of shell production in aquatic habitats. *Oikos* 101, 79–90. DOI: 10.1034/j.1600-0706.2003.12322.x

- Hartmann-Schröder, G., 1996. *Annelida*, Borstenwürmer, *Polychaeta*: Die Tierwelt Deutschlands, Teil 58, 2nd ed. ConchBooks.
- Hastings, A., Byers, J.E., Crooks, J.A., Cuddington, K., Jones, C.G., Lambrinos, J.G., Talley, T.S., Wilson, W.G., 2007. Ecosystem engineering in space and time. *Ecology Letters* 10, 153–164. DOI: 10.1111/j.1461-0248.2006.00997.x
- Hendrick, V.J., Foster-Smith, R.L., 2006. *Sabellaria spinulosa* reef: a scoring system for evaluating in the context of the Habitats Directive. *Journal of the Marine Biological Association of the United Kingdom* 86, 665–677. DOI: 10.1017/S0025315406013555
- Hernández-Cruz, L.R., Purkis, S.J., Riegl, B.M., 2006. Documenting decadal spatial changes in seagrass and *Acropora palmata* cover by aerial photography analysis in Vieques, Puerto Rico: 1937–2000. *Bulletin of Marine Science* 79, 401–414.
- Hernández-Fariñas, T., Soudant, D., Barillé, L., Belin, C., Lefebvre, A., Bacher, C., 2014. Temporal changes in the phytoplankton community along the French coast of the eastern English Channel and the southern Bight of the North Sea. *ICES J Mar Sci* 71, 821–833. DOI: 10.1093/icesjms/fst192
- Heuers, J., Jaklin, S., 1999. Initial settlement of *Lanice conchilega*. *Senckenbergiana maritima* 29, 67–69. DOI: 10.1007/BF03043124
- Heuers, J., Jaklin, S., Zühlke, R., Dittmann, S., Günther, C.-P., Hildenbrandt, H., Grimm, V., 1998. A model on the distribution and abundance of the tube building polychaete *Lanice conchilega* (Pallas, 1766) in the intertidal of the Wadden Sea. *Verh. Ges. Ökol.* 28, 207–215.
- Holt, T.J., Rees, E.I., Hawkins, S.J., Seed, R., 1998. Biogenic Reefs (Volume IX): An overview of dynamic and sensitivity characteristics for conservation management of marine SACs, UK Marine SACs Project Report. Scottish Association for Marine Science (SAMS), Liverpool, UK.
- Holthe, T., 1977. The zoogeography of the *Terebellomorpha* (*Polychaeta*) of the northern European waters. *Sarsia* 63, 191–198. DOI: 10.1080/00364827.1978.10411339

- Hoonhout, B.M., Radermacher, M., Baart, F., van der Maaten, L.J.P., 2015. An automated method for semantic classification of regions in coastal images. *Coastal Engineering* 105, 1–12. DOI: 10.1016/j.coastaleng.2015.07.010
- Hubas, C., Sachidhanandam, C., Rybarczyk, H., Lubarsky, H.V., Rigaux, A., Moens, T., Paterson, D.M., 2010. Bacterivorous nematodes stimulate microbial growth and exopolymer production in marine sediment microcosms. *Mar Ecol Prog Ser* 419, 85–94. DOI: 10.3354/meps08851
- Hussain, M., Chen, D., Cheng, A., Wei, H., Stanley, D., 2013. Change detection from remotely sensed images: From pixel-based to object-based approaches. *ISPRS Journal of Photogrammetry and Remote Sensing* 80, 91–106. DOI: 10.1016/j.isprsjprs.2013.03.006
- Infoclimat.fr, 2016. Normales et records des stations météo de France - Infoclimat [WWW Document]. URL <http://www.infoclimat.fr/climatologie-07002-boulogne.html> (accessed 3.16.16).
- Inman, D.L., 1952. Measures for describing the size distribution of sediments. *J. Sediment. Res.* 22, 125–145. DOI: 10.1306/D42694DB-2B26-11D7-8648000102C1865D
- Irvin, R., 2009. The identification of the main characteristics of stony reef habitats under the Habitats Directive (Summary report of an inter-agency workshop 26-27 March 2008 No. 432), JNCC Report Series. Joint Nature Conservation Committee, Peterborough, UK.
- Jeffrey, S.W., Mantoura, R.F.C., Wright, S.W., 1997. *Phytoplankton Pigments in Oceanography: Guidelines to Modern Methods*. UNESCO, Paris.
- Jones, C.G., Lawton, J.H., Shachak, M., 1997. Positive and negative effects of organisms as physical ecosystem engineers. *Ecology* 78, 1946–1957. DOI: 10.1890/0012-9658(1997)078[1946:PANEOO]2.0.CO;2
- Jones, C.G., Lawton, J.H., Shachak, M., 1994. Organisms as ecosystem engineers. *Oikos* 69, 373–386. DOI: 10.2307/3545850
- Jouanneau, N., Sentchev, A., Dumas, F., 2013. Numerical modelling of circulation and dispersion processes in Boulogne-sur-Mer harbour (Eastern English

Channel): sensitivity to physical forcing and harbour design. *Ocean Dyn.* 63, 1321–1340. DOI: 10.1007/s10236-013-0659-4

Kaiser, M.J., Collie, J.S., Hall, S.J., Jennings, S., Poiner, I.R., 2001. Impacts of fishing gear on marine benthic habitats. Presented at the Reykjavik Conference on Responsible Fisheries in the Marine Ecosystem, FAO, Reykjavik, Iceland, p. 19.

Kaiser, M.J., Attrill, M.J., Jennings, S., Thomas, D.N., Barnes, D.K., Brierley, A.S., Polunin, N.V., Raffaelli, D.G., Williams, P.J. le B., 2005. Part 2: Systems, in: *Marine Ecology: Processes, Systems, and Impacts*. Oxford University Press, Oxford, UK, p. 557.

Katsiaras, N., Simboura, N., Tsangaris, C., Hatzianestis, I., Pavlidou, A., Kapsimalis, V., 2015. Impacts of dredged-material disposal on the coastal soft-bottom macrofauna, Saronikos Gulf, Greece. *Science of The Total Environment* 508, 320–330. DOI: 10.1016/j.scitotenv.2014.11.085

Kerry, J.T., Bellwood, D.R., 2012. The effect of coral morphology on shelter selection by coral reef fishes. *Coral Reefs* 31, 415–424. DOI: 10.1007/s00338-011-0859-7

Kessler, M., 1963. Die Entwicklung von *Lanice conchilega* (Pallas) mit besonderer Berücksichtigung der Lebensweise. 1963; 8:425-76. *Helgoland Wiss Meer* 8, 425–76.

Koch, E.W., Barbier, E.B., Silliman, B.R., Reed, D.J., Perillo, G.M., Hacker, S.D., Granek, E.F., Primavera, J.H., Muthiga, N., Polasky, S., Halpern, B.S., Kennedy, C.J., Kappel, C.V., Wolanski, E., 2009. Non-linearity in ecosystem services: temporal and spatial variability in coastal protection. *Front. Ecol. Environ.* 7, 29–37. DOI: 10.1890/080126

Kristensen, E., 2008. Mangrove crabs as ecosystem engineers; with emphasis on sediment processes. *Journal of Sea Research, Mangrove Macrobenθος Special Issue Proceedings of the Mangrove Macrobenθος Meeting II* 59, 30–43. DOI: 10.1016/j.seares.2007.05.004

Lefebvre, A., Guiselin, N., Barbet, F., Artigas, F.L., 2011. Long-term hydrological and phytoplankton monitoring (1992–2007) of three potentially eutrophic

systems in the eastern English Channel and the Southern Bight of the North Sea. *ICES J Mar Sci* 68, 2029–2043. DOI: 10.1093/icesjms/fsr149

- Lefebvre, S., Marín Leal, J.C., Dubois, S., Orvain, F., Blin, J.-L., Bataillé, M.-P., Ourry, A., Galois, R., 2009. Seasonal dynamics of trophic relationships among co-occurring suspension-feeders in two shellfish culture dominated ecosystems. *Estuarine, Coastal and Shelf Science* 82, 415–425. DOI: 10.1016/j.ecss.2009.02.002
- Lejeune, O., Tlidi, M., Couteron, P., 2002. Localized vegetation patches: A self-organized response to resource scarcity. *Phys. Rev. E* 66, 10901. DOI: 10.1103/PhysRevE.66.010901
- Leonard, G.H., Ewanchuk, P.J., Bertness, M.D., 1999. How recruitment, intraspecific interactions, and predation control species borders in a tidal estuary. *Oecologia* 118, 492–502. DOI: 10.1007/s004420050752
- Levin, S.A., 1992. The Problem of Pattern and Scale in Ecology. *Ecology* 73, 1943–1967. DOI: 10.2307/1941447
- Lillesand, T., Kiefer, R.W., Chipman, J., 2014. Chapter 7: Digital Image Analysis, in: *Remote Sensing and Image Interpretation*. John Wiley & Sons, New York, NY (USA), pp. 485–608.
- Lind, J.L., Heimann, K., Miller, E.A., van Vliet, C., Hoogenraad, N.J., Wetherbee, R., 1997. Substratum adhesion and gliding in a diatom are mediated by extracellular proteoglycans. *Planta* 203, 213–221.
- Liu, Q.-X., Herman, P.M.J., Mooij, W.M., Huisman, J., Scheffer, M., Olf, H., van de Koppel, J., 2014. Pattern formation at multiple spatial scales drives the resilience of mussel bed ecosystems. *Nat Commun* 5. DOI: 10.1038/ncomms6234
- Lomovasky, B.J., Firstater, F.N., Salazar, A.G., Mendo, J., Iribarne, O.O., 2011. Macro benthic community assemblage before and after the 2007 tsunami and earthquake at Paracas Bay, Peru. *Journal of Sea Research* 65, 205–212. DOI: 10.1016/j.seares.2010.10.002
- Lubarsky, H.V., Hubas, C., Chocholek, M., Larson, F., Manz, W., Paterson, D.M., Gerbersdorf, S.U., 2010. The Stabilisation Potential of Individual and Mixed

Assemblages of Natural Bacteria and Microalgae. PLoS ONE 5, e13794.
DOI: 10.1371/journal.pone.0013794

Luckenbach, M.W., 1986. Sediment stability around animal tubes: The roles of hydrodynamic processes and biotic activity. *Limnology and Oceanography* 31, 779–787. DOI: 10.4319/lo.1986.31.4.0779

Magome, S., Yamashita, T., Kohama, T., Kaneda, A., Hayami, Y., Takahashi, S., Takeoka, H., 2007. Jellyfish patch formation investigated by aerial photography and drifter experiment. *J Oceanogr* 63, 761–773. DOI: 10.1007/s10872-007-0065-y

Marion, S.R., Orth, R.J., 2012. Seedling establishment in eelgrass: seed burial effects on winter losses of developing seedlings. *Mar. Ecol. Prog. Ser.* 448, 197–207. DOI: 10.3354/meps09612

Marsh, A.G., Gémare, A., Tenore, K.R., 1989. Effect of food type and ration on growth of juvenile *Capitella* sp. I (*Annelida: Polychaeta*): macro- and micronutrients. *Mar. Biol.* 102, 519–527. DOI: 10.1007/BF00438354

Martin, C.S., Carpentier, A., Vaz, S., Coppin, F., Curet, L., Dauvin, J.-C., Delavenne, J., Dewarumez, J.-M., Dupuis, L., Engelhard, G., Ernande, B., Foveau, A., Garcia, C., Gardel, L., Harrop, S., Just, R., Koubbi, P., Lauria, V., Meaden, G.J., Morin, J., Ota, Y., Rostiaux, E., Smith, R., Spilmont, N., Vérin, Y., Villanueva, C., Warembourg, C., 2009. The Channel habitat atlas for marine resource management (CHARM): an aid for planning and decision-making in an area under strong anthropogenic pressure. *Aquatic Living Resources* 22, 499–508. DOI: 10.1051/alr/2009051

Marzloff, I., Poesen, J., 2009. The potential of 3D gully monitoring with GIS using high-resolution aerial photography and a digital photogrammetry system. *Geomorphology* 111, 48–60. DOI: 10.1016/j.geomorph.2008.05.047

Maynou, F., Cartes, J.E., 2012. Effects of trawling on fish and invertebrates from deep-sea coral facies of *Isidella elongata* in the western Mediterranean. *Journal of the Marine Biological Association of the United Kingdom* 92, 1501–1507. DOI: 10.1017/S0025315411001603

McDonald, J.H., 2014. *Handbook of Biological Statistics*, 3rd Edition. ed. Sparky House Publishing, Baltimore, Maryland. USA.

- Montserrat, F., Van Colen, C., Provoost, P., Milla, M., Ponti, M., Van den Meersche, K., Ysebaert, T., Herman, P.M.J., 2009. Sediment segregation by bioturbating bivalves. *Estuarine, Coastal and Shelf Science* 83, 379–391. DOI: 10.1016/j.ecss.2009.04.010
- Mumby, P.J., Green, E.P., Edwards, A.J., Clark, C.D., 1997. Coral reef habitat mapping: how much detail can remote sensing provide? *Marine Biology* 130, 193–202. DOI: 10.1007/s002270050238
- Mumby, P.J., Skirving, W., Strong, A.E., Hardy, J.T., LeDrew, E.F., Hochberg, E.J., Stumpf, R.P., David, L.T., 2004. Remote sensing of coral reefs and their physical environment. *Marine Pollution Bulletin* 48, 219–228. DOI: 10.1016/j.marpolbul.2003.10.031
- Mundy, C.N., Babcock, R.C., 1998. Role of light intensity and spectral quality in coral settlement: Implications for depth-dependent settlement? *Journal of Experimental Marine Biology and Ecology* 223, 235–255. DOI: 10.1016/S0022-0981(97)00167-6
- Nakashima, E., Isobe, A., Magome, S., Kako, S., Deki, N., 2011. Using aerial photography and *in situ* measurements to estimate the quantity of macro-litter on beaches. *Marine Pollution Bulletin* 62, 762–769. DOI: 10.1016/j.marpolbul.2011.01.006
- OBIS, 2015. Observations of the polychaete *Lanice conchilega* from the Ocean Biogeographic Information System. Intergovernmental Oceanographic Commission of UNESCO [WWW Document]. URL <http://www.iobis.org> (accessed 6.26.15).
- Olivier, F., Desroy, N., Retière, C., 1996. Habitat selection and adult-recruit interactions in *Pectinaria koreni* (Malmgren) (*Annelida: Polychaeta*) post-larval populations: Results of flume experiments. *Journal of Sea Research* 36, 217–226. DOI: 10.1016/S1385-1101(96)90791-1
- Olsford, F., Schaanning, M.T., Widdicombe, S., Kendall, M.A., Austen, M.C., 2008. Effects of bottom trawling on ecosystem functioning. *Journal of Experimental Marine Biology and Ecology* 366, 123–133. DOI: 10.1016/j.jembe.2008.07.036

- O'Malley, R., 2015. Ocean Productivity: Online VGPM Data [WWW Document].
 Ocean Productivity. URL
<http://orca.science.oregonstate.edu/2160.by.4320.monthly.hdf.vgpm.m.chl.m.sst.php> (accessed 4.6.16).
- O'Shea, O.R., Thums, M., Keulen, M. van, Meekan, M., 2012. Bioturbation by stingrays at Ningaloo Reef, Western Australia. *Mar. Freshwater Res.* 63, 189–197. DOI: 10.1071/MF11180
- Paine, R.T., 1969. A Note on Trophic Complexity and Community Stability. *The American Naturalist* 103, 91–93. DOI: 10.1086/282586
- Pallas, P.S., 1766. *Miscellanea zoologica: quibus novae imprimis atque obscurae animalium species describuntur et observationibus iconibusque illustrantur. apud Petrum van Cleef.*
- Paneque-Gálvez, J., McCall, M.K., Napoletano, B.M., Wich, S.A., Koh, L.P., 2014. Small Drones for Community-Based Forest Monitoring: An Assessment of Their Feasibility and Potential in Tropical Areas. *Forests* 5, 1481–1507. DOI: 10.3390/f5061481
- Passarelli, C., Meziane, T., Thiney, N., Boeuf, D., Jesus, B., Ruivo, M., Jeanthon, C., Hubas, C., 2015. Seasonal variations of the composition of microbial biofilms in sandy tidal flats: Focus of fatty acids, pigments and exopolymers. *Estuarine, Coastal and Shelf Science* 153, 29–37. DOI: 10.1016/j.ecss.2014.11.013
- Passarelli, C., Olivier, F., Paterson, D.M., Hubas, C., 2012. Impacts of biogenic structures on benthic assemblages: microbes, meiofauna, macrofauna and related ecosystem functions. *Mar Ecol Prog Ser* 465, 85–97. DOI: 10.3354/meps09915
- Pauly, D., Caddy, J., 1985. A modification of Bhattachaty's method for the separation of normal distributions. *FAO Fish. Circo* 781(16), pp1987.
- Pauly, K., De Clerk, O., 2011. Low-cost very high resolution intertidal vegetation monitoring enabled by near-infrared kite aerial photography, in: *GIS-Based Environmental Analysis, Remote Sensing and Niche Modeling of Seaweed Communities.* pp. 169–186.

- Pawlik, J.R., 1988. Larval settlement and metamorphosis of two gregarious sabellariid polychaetes: *Sabellaria alveolata* compared with *Phragmatopoma californica*. Journal of the Marine Biological Association of the United Kingdom 68, 101–124. DOI: 10.1017/S002531540005013X
- Perkins, R.G., Honeywill, C., Consalvey, M., Austin, H.A., Tolhurst, T.J., Paterson, D.M., 2003. Changes in microphytobenthic chlorophyll a and EPS resulting from sediment compaction due to de-watering: opposing patterns in concentration and content. Cont. Shelf Res. 23, 575–586. DOI: 10.1016/S0278-4343(03)00006-2
- Petersen, B., Exo, K., 1999. Predation of waders and gulls on *Lanice conchilega* tidal flats in the Wadden Sea. Mar Ecol Prog Ser 178, 229–240. DOI: 10.3354/meps178229
- Pillay, D., Branch, G.M., Dawson, J., Henry, D., 2011. Contrasting effects of ecosystem engineering by the cordgrass *Spartina maritima* and the sandprawn *Callianassa kraussi* in a marine-dominated lagoon. Estuarine, Coastal and Shelf Science 91, 169–176. DOI: 10.1016/j.ecss.2010.10.010
- Pillay, D., Branch, G.M., Forbes, A.T., 2008. Habitat change in an estuarine embayment: anthropogenic influences and a regime shift in biotic interactions. Marine Ecology Progress Series 370, 19–31. DOI: 10.3354/meps07631
- Pillay, D., Branch, G.M., Forbes, A.T., 2007. Effects of *Callianassa kraussi* on microbial biofilms and recruitment of macrofauna: a novel hypothesis for adult–juvenile interactions. Marine Ecology Progress Series 347, 1–14. DOI: 10.3354/meps07054
- Pillay, D., Williams, C., Whitfield, A.K., 2012. Indirect effects of bioturbation by the burrowing sandprawn *Callichirus kraussi* on a benthic foraging fish, *Liza richardsonii*. Marine Ecology Progress Series 453, 151–158. DOI: 10.3354/meps09642
- Polgar, G., Nishi, E., Idris, I., Glasby, C.J., 2015. Tropical polychaete community and reef dynamics: insights from a Malayan *Sabellaria* reef. Raffles Bulletin of Zoology 63, 401–417.

- Poore, G., 2010. *Callianassa kraussi* Stebbing, 1900. Accessed through: World Register of Marine Species [WWW Document]. World Register of Marine Species (WoRMS). URL <http://www.marinespecies.org/aphia.php?p=taxdetails&id=246238> (accessed 7.6.17).
- Price, N., 2010. Habitat selection, facilitation, and biotic settlement cues affect distribution and performance of coral recruits in French Polynesia. *Oecologia* 163, 747–758. DOI: 10.1007/s00442-010-1578-4
- Qian, P.-Y., 1994. Effect of food quantity on growth and reproductive characteristics of *Capitella* sp. (Annelids: *Polychaeta*). *Invertebrate Reproduction & Development* 26, 175–185. DOI: 10.1080/07924259.1994.9672416
- Qian, P.-Y., 1999. Larval settlement of polychaetes. *Hydrobiologia* 402, 239–253. DOI: 10.1023/A:100370492866
- Rabaut, M., Braeckman, U., Hendrickx, F., Vincx, M., Degraer, S., 2008. Experimental beam-trawling in *Lanice conchilega* reefs. *Fisheries Research* 90, 209–216. DOI: 10.1016/j.fishres.2007.10.009
- Rabaut, M., Guilini, K., Van Hoey, G., Vincx, M., Degraer, S., 2007. A bio-engineered soft-bottom environment: The impact of *Lanice conchilega* on the benthic species-specific densities and community structure. *Estuarine, Coastal and Shelf Science* 75, 525–536. DOI: 10.1016/j.ecss.2007.05.041
- Rabaut, M., Van de Moortel, L., Vincx, M., Degraer, S., 2010. Biogenic reefs as structuring factor in *Pleuronectes platessa* (Plaice) nursery. *Journal of Sea Research* 64, 102–106. DOI: 10.1016/j.seares.2009.10.009
- Rabaut, M., Vincx, M., Degraer, S., 2009. Do *Lanice conchilega* (sandmason) aggregations classify as reefs? Quantifying habitat modifying effects. *Helgol Mar Res* 63, 37–46. DOI: 10.1007/s10152-008-0137-4
- R Core Team, 2015. R: A Language and Environment for Statistical Computing. R Foundation for Statistical Computing, Vienna, Austria.
- Read, G., Bellan, G., 2012. *Lanice conchilega* (Pallas, 1766). In: Read, G.; Fauchald, K. (Ed.) (2017). World Polychaeta database. Accessed through: World Register of Marine Species. [WWW Document]. URL

<http://www.marinespecies.org/aphia.php?p=taxdetails&id=131495>
(accessed 7.7.17).

- Rees, E.I.S., Bergmann, M., Galanidi, M., Hinz, H., Shucksmith, R., Kaiser, M.J., 2005. An enriched *Chaetopterus* tube mat biotope in the eastern English Channel. *Journal of the Marine Biological Association of the United Kingdom* 85, 323–326. DOI: 10.1017/S0025315405011215h
- Regnaud, H., Pirazzoli, P.A., Morvan, G., Ruz, M., 2004. Impacts of storms and evolution of the coastline in western France. *Mar. Geol., Storms and their significance in coastal morpho-sedimentary dynamics* 210, 325–337. DOI: 10.1016/j.margeo.2004.05.014
- Reichert, K., Buchholz, F., Giménez, L., 2008. Community composition of the rocky intertidal at Helgoland (German Bight, North Sea). *Helgol Mar Res* 62, 357–366. DOI: 10.1007/s10152-008-0123-x
- Rietkerk, M., Dekker, S.C., Ruiters, P.C. de, Koppel, J. van de, 2004. Self-Organized Patchiness and Catastrophic Shifts in Ecosystems. *Science* 305, 1926–1929. DOI: 10.1126/science.1101867
- Rietkerk, M., van de Koppel, J., 2008. Regular pattern formation in real ecosystems. *Trends in Ecology & Evolution* 23, 169–175. DOI: 10.1016/j.tree.2007.10.013
- Rijnsdorp, A.D., Berghahn, R., Miller, J.M., Van Der Veer, H.W., 1995. Recruitment mechanisms in flatfish: What did we learn and where do we go? *Netherlands Journal of Sea Research* 34, 237–242. DOI: 10.1016/0077-7579(95)90031-4
- Rogers, A., Blanchard, J.L., Mumby, P.J., 2014. Vulnerability of Coral Reef Fisheries to a Loss of Structural Complexity. *Current Biology* 24, 1000–1005. DOI: 10.1016/j.cub.2014.03.026
- Romero, G.Q., Gonçalves-Souza, T., Vieira, C., Koricheva, J., 2015. Ecosystem engineering effects on species diversity across ecosystems: a meta-analysis. *Biol Rev* 90, 877–890. DOI: 10.1111/brv.12138
- Repert, M., 1999. Caractérisation et déterminisme du développement d'une population de l'annélide tubicole *Lanice conchilega* (Pallas 1766) (Polychète

Térébellidé) associé à la conchyliculture en Baie des Veys (Baie de Seine Occidentale) (PhD). Muséum National d'Histoire Naturelle, Paris, France.

- Ropert, M., Dauvin, J.-C., 2000. Renewal and accumulation of a *Lanice conchilega* (Pallas) population in the baie des Veys, western Bay of Seine. *Oceanologica Acta* 23, 529–546. DOI: 10.1016/S0399-1784(00)00143-2
- Ropert, M., Gouletquer, P., 2000. Comparative physiological energetics of two suspension feeders: polychaete annelid *Lanice conchilega* (Pallas 1766) and Pacific cupped oyster *Crassostrea gigas* (Thunberg 1795). *Aquaculture* 181, 171–189. DOI: 10.1016/S0044-8486(99)00216-1
- Sanchez-Hernandez, C., Boyd, D.S., Foody, G.M., 2007. Mapping specific habitats from remotely sensed imagery: Support vector machine and support vector data description based classification of coastal saltmarsh habitats. *Ecological Informatics* 2, 83–88. DOI: 10.1016/j.ecoinf.2007.04.003
- Scilab Enterprises, 2015. ode - Ordinary differential equation solver [WWW Document]. URL https://help.scilab.org/docs/5.5.2/en_US/ode.html (accessed 5.4.17).
- Scilab Enterprises, 2012. Scilab: Free and Open Source software for numerical computation. Scilab Enterprises, France.
- Service Hydrographique et Océanographique de la Marine - SHOM, 2015. Tide gauge Boulogne-sur-Mer at SHOM. [WWW Document]. Marégraphe de Boulogne-Sur-Mer (SHOM - Service Hydrographique et Océanographique de la Marine). URL <http://data.shom.fr/#donnees/refmar/111> (accessed 3.16.16).
- Shipley, B., 2000. Cause and correlation in biology a user's guide to path analysis, structural equations, and causal inference. Cambridge University Press, Cambridge, UK; New York, NY. USA.
- Shuanggen, J., Cardellach, E., Xie, F., 2013. GNSS Remote Sensing: Theory, Methods and Applications, Remote Sensing and Digital Image Processing. Springer Netherlands, Dordrecht, Netherlands.

- Smart, T.I., 2008. Reproductive and Larval Biology of the Northeastern Pacific Polychaete *Owenia collaris* (*Oweniidae*) in Coos Bay, OR. University of Oregon, Oregon, USA.
- Smith, D.J., Underwood, G.J.C., 2000. The production of extracellular carbohydrates by estuarine benthic diatoms: the effects of growth phase and light and dark treatment. *J. Phycol.* 36, 321–333. DOI: 10.1046/j.1529-8817.2000.99148.x
- Smith, M.J., Chandler, J.H., Rose, J., 2009. High spatial resolution data acquisition for the geosciences: kite aerial photography. *Earth Surface Processes and Landforms* 34, 155–161. DOI: 10.1002/esp.1702
- Smith, R.I., 1989. Observations on Spawning Behavior of *Eupolymnia nebulosa*, and Comparisons with *Lanice conchilega* (*Annelida, Polychaeta, Terebellidae*). *Bulletin of Marine Science* 45, 406–414.
- Speybroeck, J., Bonte, D., Courtens, W., Gheschiere, T., Grootaert, P., Maelfait, J.-P., Mathys, M., Provoost, S., Sabbe, K., Stienen, E.W.M., Lancker, V.V., Vincx, M., Degraer, S., 2006. Beach nourishment: an ecologically sound coastal defence alternative? A review. *Aquatic Conserv: Mar. Freshw. Ecosyst.* 16, 419–435. DOI: 10.1002/aqc.733
- StatSoft.Inc, 2004. *Statistica*. StatSoft.Inc, Oklahoma, USA.
- Strasser, M., Pieloth, U., 2001. Recolonization pattern of the polychaete *Lanice conchilega* on an intertidal sand flat following the severe winter of 1995/96. *Helgol Mar Res* 55, 176–181. DOI: 10.1007/s101520100081
- Süli, E., Mayers, D.F., 2003. *An Introduction to Numerical Analysis*. Cambridge University Press.
- Taghon, G.L., Greene, R.R., 1990. Effects of sediment-protein concentration on feeding and growth rates of *Abarenicola pacifica* Healy et Wells (*Polychaeta: Arenicolidae*). *Journal of Experimental Marine Biology and Ecology* 136, 197–216. DOI: 10.1016/0022-0981(90)90161-5
- Teixidó, N., Garrabou, J., Gutt, J., Arntz, W.E., 2007. Iceberg Disturbance and Successional Spatial Patterns: The Case of the Shelf Antarctic Benthic Communities. *Ecosystems* 10, 143–158. DOI: 10.1007/s10021-006-9012-9

- The Council of The European Communities, 2009. Directive 2009/147/EC of the European Parliament and of the Council of 30 November 2009 on the conservation of wild birds.
- The Council of The European Communities, 2007. Council Directive 92/43/EEC of 21 May 1992 on the conservation of natural habitats and of wild fauna and flora (consolidated version 1. 1. 2007).
- Thiébaud, E., Dauvin, J.-C., Lagadeuc, Y., 1994. Horizontal distribution and retention of *Owenia fusiformis* larvae (*Annelida: Polychaeta*) in the Bay of Seine. *Journal of the Marine Biological Association of the United Kingdom* 74, 129–142. DOI: 10.1017/S0025315400035712
- Thiébaud, E., Lagadeuc, Y., Olivier, F., Dauvin, J.C., Retière, C., 1998. Do hydrodynamic factors affect the recruitment of marine invertebrates in a macrotidal area? The case study of *Pectinaria koreni* (*Polychaeta*) in the Bay of Seine (English Channel). *Hydrobiologia* 375–376, 165–176. DOI: 10.1023/A:1017092518829
- Thomson, D.P., Babcock, R.C., Vanderklift, M.A., Symonds, G., Gunson, J.R., 2012. Evidence for persistent patch structure on temperate reefs and multiple hypotheses for their creation and maintenance. *Estuarine, Coastal and Shelf Science* 96, 105–113. DOI: 10.1016/j.ecss.2011.10.014
- Tolhurst, T.J., Jesus, B., Brotas, V., Paterson, D.M., 2003. Diatom migration and sediment armouring – an example from the Tagus Estuary, Portugal. *Hydrobiologia* 503, 183–193. DOI: 10.1023/B:HYDR.0000008474.33782.8d
- Turner, M.G., 2005. Landscape Ecology: What Is the State of the Science? *Annual Review of Ecology, Evolution, and Systematics* 36, 319–344. DOI: 10.1146/annurev.ecolsys.36.102003.152614
- Turner, W., 2014. Sensing biodiversity. *Science* 346, 301–302. DOI: 10.1126/science.1256014
- Ubertini, M., Lefebvre, S., Rakotomalala, C., Orvain, F., 2015. Impact of sediment grain-size and biofilm age on epipelagic microphytobenthos resuspension. *J. Exp. Mar. Biol. Ecol.* 467, 52–64. DOI: 10.1016/j.jembe.2015.02.007

- Underwood, G.J.C., Boulcott, M., Raines, C.A., Waldron, K., 2004. Environmental Effects on Exopolymer Production by Marine Benthic Diatoms: Dynamics, Changes in Composition, and Pathways of Production1. *J. Phycol.* 40, 293–304. DOI: 10.1111/j.1529-8817.2004.03076.x
- Van Colen, C., Lenoir, J., Backer, A.D., Vanellander, B., Vincx, M., Degraer, S., Ysebaert, T., 2009. Settlement of *Macoma balthica* larvae in response to benthic diatom films. *Mar Biol* 156, 2161–2171. DOI: 10.1007/s00227-009-1246-6
- Van Colen, C., Underwood, G.J.C., Serôdio, J., Paterson, D.M., 2014. Ecology of intertidal microbial biofilms: Mechanisms, patterns and future research needs. *J. Sea Res.*, Trophic significance of microbial biofilm in tidal flats 92, 2–5. DOI: 10.1016/j.seares.2014.07.003
- van de Koppel, J., Altieri, A.H., Silliman, B.R., Bruno, J.F., Bertness, M.D., 2006. Scale-dependent interactions and community structure on cobble beaches. *Ecology Letters* 9, 45–50. DOI: 10.1111/j.1461-0248.2005.00843.x
- van de Koppel, J., Bouma, T.J., Herman, P.M.J., 2012. The influence of local- and landscape-scale processes on spatial self-organization in estuarine ecosystems. *Journal of Experimental Biology* 215, 962–967. DOI: 10.1242/jeb.060467
- van de Koppel, J., Gascoigne, J.C., Theraulaz, G., Rietkerk, M., Mooij, W.M., Herman, P.M.J., 2008. Experimental Evidence for Spatial Self-Organization and Its Emergent Effects in Mussel Bed Ecosystems. *Science* 322, 739–742. DOI: 10.1126/science.1163952
- van de Koppel, J., Rietkerk, M., Dankers, N., Herman, P.M.J., 2005. Scale-dependent feedback and regular spatial patterns in young mussel beds. *Am. Nat.* 165, E66-77. DOI: 10.1086/428362
- van der Veer, H.W., Pihl, L., Bergman, M.J.N., 1990. Recruitment mechanisms in North Sea plaice *Pleuronectes platessa*. *Marine Ecology Progress Series* 64, 1–12.
- van der Veer, V.D., Berghahn, R., Miller, J.M., Rijnsdorp, A.D., 2000. Recruitment in flatfish, with special emphasis on North Atlantic species: Progress made by

the Flatfish Symposia. ICES J Mar Sci 57, 202–215. DOI: 10.1006/jmsc.1999.0523

- Van Hoey, G., Guilini, K., Rabaut, M., Vincx, M., Degraer, S., 2008. Ecological implications of the presence of the tube-building polychaete *Lanice conchilega* on soft-bottom benthic ecosystems. Mar Biol 154, 1009–1019. DOI: 10.1007/s00227-008-0992-1
- Van Hoey, G., Vincx, M., Degraer, S., 2006a. Some recommendations for an accurate estimation of *Lanice conchilega* density based on tube counts. Helgol Mar Res 60, 317–321. DOI: 10.1007/s10152-006-0041-8
- Van Hoey, G., Vincx, M., Degraer, S., 2006b. Population dynamics of subtidal *Lanice conchilega* (Pallas, 1766) populations at the Belgian Continental Shelf.
- van Wesenbeeck, B.K., Van De Koppel, J., Herman, P.M.J., Bouma, T.J., 2008. Does scale-dependent feedback explain spatial complexity in salt-marsh ecosystems? Oikos 117, 152–159. DOI: 10.1111/j.2007.0030-1299.16245.x
- Verhoeven, G., 2011. Taking computer vision aloft – archaeological three-dimensional reconstructions from aerial photographs with photostan. Archaeol. Prospect. 18, 67–73. DOI: 10.1002/arp.399
- Volkenborn, N., Hedtkamp, S.I.C., van Beusekom, J.E.E., Reise, K., 2007. Effects of bioturbation and bioirrigation by lugworms (*Arenicola marina*) on physical and chemical sediment properties and implications for intertidal habitat succession. Estuarine, Coastal and Shelf Science 74, 331–343. DOI: 10.1016/j.ecss.2007.05.001
- Volkenborn, N., Polerecky, L., Wetthey, D.S., Woodin, S.A., 2010. Oscillatory porewater bioadvection in marine sediments induced by hydraulic activities of *Arenicola marina*. Limnol. Oceanogr. 55, 1231–1247. DOI: 10.4319/lo.2010.55.3.1231
- Volkenborn, N., Robertson, D.M., Reise, K., 2008. Sediment destabilizing and stabilizing bio-engineers on tidal flats: cascading effects of experimental exclusion. Helgol Mar Res 63, 27–35. DOI: 10.1007/s10152-008-0140-9
- Wang, A., Wang, Y., Chen, J., 2008. Role of *Spartina alterniflora* on sediment dynamics of coastal salt marshes — case study from central Jiangsu and

- middle Fujian coasts. *Front. Earth Sci. China* 2, 269–275. DOI: 10.1007/s11707-008-0021-1
- Wang, K., Franklin, S.E., Guo, X., Cattet, M., 2010. Remote Sensing of Ecology, Biodiversity and Conservation: A Review from the Perspective of Remote Sensing Specialists. *Sensors* 10, 9647–9667. DOI: 10.3390/s101109647
- Weerman, E.J., van de Koppel, J., Eppinga, M.B., Montserrat, F., Liu, Q., Herman, P.M.J., Klausmeier, A.E.C.A., DeAngelis, E.D.L., 2010. Spatial Self-Organization on Intertidal Mudflats through Biophysical Stress Divergence. *The American Naturalist* 176, E15–E32. doi:10.1086/652991
- White, J.-S.S., O'Donnell, J.L., 2010. Indirect effects of a key ecosystem engineer alter survival and growth of foundation coral species. *Ecology* 91, 3538–3548. DOI: 10.1890/09-2322.1
- Widdows, J., Pope, N.D., Brinsley, M.D., 2008a. Effect of *Spartina anglica* stems on near-bed hydrodynamics, sediment erodability and morphological changes on an intertidal mudflat. *Mar Ecol Prog Ser* 362, 45–57. DOI: 10.3354/meps07448
- Widdows, J., Pope, N.D., Brinsley, M.D., Asmus, H., Asmus, R.M., 2008b. Effects of seagrass beds (*Zostera noltii* and *Z. marina*) on near-bed hydrodynamics and sediment resuspension. *Mar Ecol Prog Ser* 358, 125–136. DOI: 10.3354/meps07338
- Wild, C., Hoegh-Guldberg, O., Naumann, M.S., Colombo-Pallotta, M.F., Ateweberhan, M., Fitt, W.K., Iglesias-Prieto, R., Palmer, C., Bythell, J.C., Ortiz, J.-C., Loya, Y., van Woesik, R., 2011. Climate change impedes scleractinian corals as primary reef ecosystem engineers. *Mar. Freshwater Res.* 62, 205–215. DOI: 10.1071/MF10254
- Wildish, D.J., Kristmanson, D.D., Robinson, S.M.C., 2008. Does skimming flow reduce population growth in horse mussels? *J. Exp. Mar. Biol. Ecol.* 1, 33–38. DOI: 10.1016/j.jembe.2008.01.017
- Wilkie, L., O'Hare, M.T., Davidson, I., Dudley, B., Paterson, D.M., 2012. Particle trapping and retention by *Zostera noltii*: A flume and field study. *Aquatic Botany* 102, 15–22. DOI: 10.1016/j.aquabot.2012.04.004

- Willems, W., Goethals, P., Van den Eynde, D., Van Hoey, G., Van Lancker, V., Verfaillie, E., Vincx, M., Degraer, S., 2008. Where is the worm? Predictive modelling of the habitat preferences of the tube-building polychaete *Lanice conchilega*. *Ecological Modelling* 212, 74–79. DOI: 10.1016/j.ecolmodel.2007.10.017
- Wright, J.P., Jones, C.G., Flecker, A.S., 2002. An ecosystem engineer, the beaver, increases species richness at the landscape scale. *Oecologia* 132, 96–101. DOI: 10.1007/s00442-002-0929-1
- Wright, S.W., Jeffrey, S.W., 1997. High-resolution HPLC system for chlorophylls and carotenoids of marine phytoplankton, in: *Phytoplankton Pigments in Oceanography: Guidelines to Modern Methods*. UNESCO, Paris, France, pp. 327–341.
- Wundram, D., Löffler, J., 2008. High-resolution spatial analysis of mountain landscapes using a low-altitude remote sensing approach. *International Journal of Remote Sensing* 29, 961–974. DOI: 10.1080/01431160701352113
- Yeo, R.K., Risk, M.J., 1979. Intertidal Catastrophes: Effect of Storms and Hurricanes on Intertidal Benthos of the Minas Basin, Bay of Fundy. *J. Fish. Res. Board Can.* 36, 667–669. DOI: 10.1139/f79-096
- Zajac, R.N., 2007. Challenges in marine, soft-sediment benthoscape ecology. *Landscape Ecol* 23, 7–18. DOI: 10.1007/s10980-007-9140-4
- Ziegelmeir, E., 1952. Beobachtungen über den Röhrenbau von *Lanice conchilega* (Pallas) im Experiment und am natürlichen Standort. *Helgolander Wiss. Meeresunters* 4, 107–129. DOI: 10.1007/BF02178540
- Zühlke, R., 2001. Polychaete tubes create ephemeral community patterns: *Lanice conchilega* (Pallas, 1766) associations studied over six years. *Journal of Sea Research* 46, 261–272. DOI: 10.1016/S1385-1101(01)00091-0



Publications List

A1 peer reviewed articles

Alves, R.M.S., Van Colen, C., Vincx, M., Vanaverbeke, J., De Smet, B., Guarini, J.-M., Rabaut, M., Bouma, T.J., 2017a. A case study on the growth of *Lanice conchilega* (Pallas, 1766) aggregations and their ecosystem engineering impact on sedimentary processes. *Journal of Experimental Marine Biology and Ecology* 489, 15–23. DOI: 10.1016/j.jembe.2017.01.005

Alves, R.M.S., Vanaverbeke, J., Bouma, T.J., Guarini, J.-M., Vincx, M., Van Colen, C., 2017b. Effects of temporal fluctuation in population processes of intertidal *Lanice conchilega* (Pallas, 1766) aggregations on its ecosystem engineering. *Estuarine, Coastal and Shelf Science* 188, 88–98. DOI: 10.1016/j.ecss.2017.02.012

Lins, L., Guilini, K., Veit-Köhler, G., Hauquier, F., Alves, R.M.S., Esteves, A.M., Vanreusel, A., 2014. The link between meiofauna and surface productivity in the Southern Ocean. *Deep Sea Research Part II: Topical Studies in Oceanography, SI: Southern Ocean Deep Sea--A Benthic View to Pelagic Processes* 108, 60–68. DOI: 10.1016/j.dsr2.2014.05.003

Oral presentations

Alves R. M. S., Van Colen, C., Vincx, M., Vanaverbeke, J., De Smet, B., Guarini, J., Bouma, T. J. (2015-09). Interactions between population dynamics of *Lanice conchilega* and sediment consolidation. Oral presentation at the 50th European Marine Biology Symposium (EMBS 50), Helgoland, Germany.

Alves R. M. S., Van Colen, C., Vincx, M., Vanaverbeke, J., De Smet, B., Guarini, J., Bouma, T. J. (2015-09). The growth of biogenic reefs: a case study on interactions between population dynamics of a tube-building polychaete and sediment consolidation in a wave-dominated intertidal zone. Oral presentation at ECSA 55, London, United Kingdom.

Alves R. M. S., Stal, C., De Wulf, A., Rabaut, M. (2015-07). Assessing the use of cost-efficient kite aerial photography for detection of intertidal biogenic structures in ultra-high spatial resolution: a case study on the *Lanice conchilega* reefs. Oral presentation at the VII International Sandy Beach Symposium, Ilhabela/SP, Brazil.

Alves, R. M. S., Vincx, M., Bouma, T. J., Guarini, J., Rabaut, M. (2014-02). Spatial ecology and population dynamics of *Lanice conchilega* reefs. Oral presentation at the 12th Marine Biology Section Symposium (DuodeceMBSS), Gent, Belgium.

Alves, R. M. S.; Reigada, A. L. D.; Toyama, M. H.; Caetano, F. H.; Zara, F. J. (2006). Morfo-histologia do sistema reprodutor masculino do "siri fedido" *Callinectes bocourti* A. Milne Edwards, 1879 (*Brachyura: Portunidae*). Oral presentation at the IV Brazilian Crustacean Congress, Guarapari/ES, Brazil.

Reigada, A. L. D.; Toyama, M. H.; Serrano, J. S.; Alves, R. M. S.; Zara, F. J. (2006). Prevalência e intensidade de infestação de *Myzobdella lugubris* (*Hirudinida: Piscicolidae*) em *Callinectes bocourti* (*Decapoda: Portunidae*) no estuário de São Vicente, SP, Brasil. Oral presentation at the IV Brazilian Crustacean Congress, Guarapari/ES, Brazil.

Poster presentations

Alves R. M. S., Stal, C., De Wulf, A., Rabaut, M. (2015-07). Assessing the use of cost-efficient kite aerial photography for detection of intertidal biogenic structures in ultra-high spatial resolution: a case study on the *Lanice conchilega* reefs. Poster presentation at the VII International Sandy Beach Symposium, Ilhabela/SP, Brazil.